

# Estimation Method for the Thermochemical Properties of Polycyclic Aromatic Molecules

by

Joanna Yu

Bachelor of Science in Engineering, Escola Politécnica-USP, São Paulo, Brazil, 2001

Submitted to the Department of Chemical Engineering  
in partial fulfillment of the requirements for the degree of

Doctor of Philosophy in Chemical Engineering Practice


at the

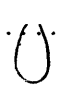
MASSACHUSETTS INSTITUTE OF TECHNOLOGY


September 2004

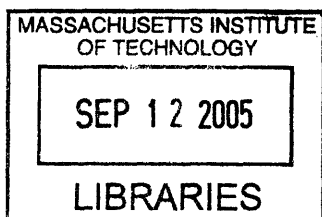
[2005]

© Massachusetts Institute of Technology 2004. All rights reserved.

Author  .....  
Department of Chemical Engineering  
September 1, 2004

Certified by  .....  
William H. Green, Jr.  
Texaco-Mangelsdorf Associate Professor  
Thesis Supervisor

Accepted by  .....  
Daniel Blankschtein  
Professor of Chemical Engineering  
Chairman, Committee for Graduate Students



ARCHIVES



# **Estimation Method for the Thermochemical Properties of Polycyclic Aromatic Molecules**

by

Joanna Yu

Bachelor of Science in Engineering, Escola Politécnica-USP, São Paulo, Brazil, 2001

Submitted to the Department of Chemical Engineering  
on September 1, 2004, in partial fulfillment of the  
requirements for the degree of  
Doctor of Philosophy in Chemical Engineering Practice

## **Abstract**

Polycyclic aromatic molecules, including polycyclic aromatic hydrocarbons (PAHs) have attracted considerable attention in the past few decades. They are formed during the incomplete combustion of hydrocarbon fuels and are precursors of soot. Some PAHs are known carcinogens, and control of their emissions is an important issue. These molecules are found in many materials, including coal, fuel oils, lubricants, and carbon black. They are also implicated in the formation of fullerenes, one of the most chemically versatile class of molecules known. Clearly, models that provide predictive capability for their formation and growth are highly desirable. Thermochemical properties of the species in the model are often the most important parameter, particularly for high temperature processes such as the formation of PAH and other aromatic molecules. Thermodynamic consistency requires that reverse rate constants be calculated from the forward rate constants and from the equilibrium constants. The later are obtained from the thermochemical properties of reactants and products. The predictive ability of current kinetic models is significantly limited by the scarcity of available thermochemical data.

In this work we present the development of a Bond-Centered Group Additivity method for the estimation of the thermochemical properties of polycyclic aromatic molecules, including PAHs, molecules with the furan substructure, molecules with

triple bonds, substituted PAHs, and radicals. This method is based on thermochemical values of about two hundred polycyclic aromatic molecules and radicals obtained from quantum chemical calculations at the B3LYP/6-31G(d) level. A consistent set of homodesmotic reactions has been developed to accurately calculate the heat of formation from the absolute energy. The entropies calculated from the B3LYP/6-31G(d) vibrational frequencies are shown to be at least as reliable as the few available experimental values. This new Bond-Centered Group Additivity method predicts the thermochemistry of C<sub>60</sub> and C<sub>70</sub> fullerenes, as well as smaller aromatic molecules, with accuracy comparable to both experiments and the best quantum calculations. This Bond-Centered Group Additivity method is shown to extrapolate reasonably to infinite graphene sheets.

The Bond-Centered Group Additivity method has been implemented into a computer code within the automatic Reaction Mechanism Generation software (RMG) developed in our group. The database has been organized as a tree structure, making its maintenance and possible extension very straightforward. This computer code allows the fast and easy use of this estimation method by non-expert users. Moreover, since it is incorporated into RMG, it will allow users to generate reaction mechanisms that include aromatic molecules whose thermochemical properties are calculated using the Bond-Centered Group Additivity method.

Exploratory equilibrium studies were performed. Equilibrium concentrations of individual species depend strongly on the thermochemistry of the individual species, emphasizing the importance of consistent thermochemistry for all the species involved in the calculations. Equilibrium calculations can provide many interesting insights into the relationship between PAH and fullerenes in combustion.

Thesis Supervisor: William H. Green, Jr.

Title: Texaco-Mangelsdorf Associate Professor

## Acknowledgments

Many people provided help and support that allowed the completion of this work in such a short time frame. First, I would like to thank my advisor Prof. Bill Green. He provided me with the freedom to explore and to learn to find my own path, while also pointing to the right direction when I was at a lost. His insights improved this work considerably. I am also grateful to the other members of my thesis committee, Prof. Jack Howard and Prof. Larry Scott, for their time, interest, and suggestions.

Dr. Sumathy Raman patiently explained to me almost everything that I know about quantum chemistry and supplied a code for the calculation of the thermochemical contributions of hindered rotors. She also gave valuable advice, both research related and otherwise. Dr. Henning Richter provided the ultimate incentive for this work by being a user in need of thermochemical data. He gave me guidance and filled me in the relevant combustion work. Dr. Richter also performed some of the equilibrium calculations and provided me the thermochemistry in Chemkin format used for other equilibrium calculations. Dr. Jing Song introduced me to object oriented programming, UML, and Java. Her RMG program is the backbone without which the BCGA thermo estimator program would not stand. Sally Petway developed and implemented in RMG the algorithm for the calculation of the symmetry number of ring compounds.

I have been extremely fortunate with the company that I have had in the past three years, both inside and outside the lab. Susan Lanza took care of every administrative hurdle and also of the well-being of the members of the Green Group. Paul Yelvington was a great lab companion and was always very helpful in Unix and other matters. Bryan Wong answered many of my questions about physical chemistry, and together with Oluwayemisi “Luwi” Oluwole, was the source of lively discussions about topics ranging from space trips to Mars to pageant contests. All other members of the Green Group, past and present, are acknowledged for their camaraderie and discussions during group seminar. Many others were also key to making these years a great time, and although the list is long, I am especially grateful to Pia Kohler, Thierry Savin,

Alexander Mitsos, Eva Lambidoni, Anna Pisania, and Yuhua Hu.

Finally, I would like to thank my parents for their unwavering support in every matter.

This work was supported by the National Science Foundation through research grant CTS-0123345. Support from the National Center for Supercomputing Applications through the allocation of supercomputer resources is acknowledged.

# Contents

<b>1</b>	<b>Introduction</b>	<b>21</b>
1.1	Thesis Overview by Chapter . . . . .	23
1.1.1	Chapter 2: Thermochemical Data for PAHs . . . . .	23
1.1.2	Chapter 3: Bond-Centered Group Additivity Method . . . . .	24
1.1.3	Chapter 4: BCGA for Other Aromatic Molecules . . . . .	24
1.1.4	Chapter 5: BCGA for Radicals . . . . .	25
1.1.5	Chapter 6: Resonance Energy . . . . .	25
1.1.6	Chapter 7: Thermochemistry for Non-Aromatic Molecules and Radicals . . . . .	25
1.1.7	Chapter 8: BCGA in RMG . . . . .	26
1.1.8	Chapter 9: Equilibrium Calculations . . . . .	26
	Bibliography . . . . .	26
<b>2</b>	<b>Thermochemical Data for Estimation Method for PAHs with Five- and Six-Membered Rings</b>	<b>29</b>
2.1	Introduction . . . . .	29
2.2	Experimental Thermochemical Properties . . . . .	29
2.2.1	Experimental Enthalpy of Formation Values . . . . .	30
2.2.2	Experimental Entropy Values . . . . .	40
2.3	Computational Methods . . . . .	41
2.4	Results and Discussion . . . . .	51
	Bibliography . . . . .	51

<b>3</b>	<b>Bond-Centered Group Additivity Estimation Method</b>	<b>61</b>
3.1	Existing Estimation Methods . . . . .	61
3.2	Bond-Centered Estimation Method . . . . .	68
3.2.1	Definition of Bond-Centered Groups . . . . .	69
3.2.2	Statistical Validation of the Model . . . . .	75
3.2.3	Coefficients for the Bond-Centered Group Additivity Method . . . . .	78
3.3	Results and Discussion . . . . .	79
3.4	Conclusions . . . . .	89
	Bibliography . . . . .	90
<b>4</b>	<b>Other Polycyclic Aromatic Molecules</b>	<b>93</b>
4.1	Introduction . . . . .	93
4.2	Furans . . . . .	93
4.2.1	Introduction . . . . .	93
4.2.2	Previous Estimation Methods . . . . .	94
4.2.3	Computational Methods . . . . .	94
4.2.4	Estimation Method . . . . .	95
4.2.5	Results and Discussion . . . . .	98
4.3	Arynes . . . . .	100
4.3.1	Introduction . . . . .	100
4.3.2	Experimental Values . . . . .	101
4.3.3	Computational Methods . . . . .	102
4.3.4	Estimation Method . . . . .	103
4.3.5	Results and Discussion . . . . .	107
4.4	Substituted PAHs . . . . .	108
4.4.1	Introduction . . . . .	108
4.4.2	Experimental Thermochemical Properties . . . . .	109
4.4.3	Computational Methods . . . . .	109
4.4.4	Estimation Method . . . . .	114
4.4.5	Conclusions . . . . .	120



Bibliography . . . . .	121
<b>5 Polycyclic Aromatic Hydrocarbon Radicals</b>	<b>127</b>
5.1 $\sigma$ -radicals . . . . .	127
5.1.1 Introduction . . . . .	127
5.1.2 Experimental Values . . . . .	128
5.1.3 Computational Methods . . . . .	129
5.1.4 Estimation Method . . . . .	135
5.1.5 Conclusions . . . . .	140
5.2 $\pi$ -radicals . . . . .	142
5.2.1 Introduction . . . . .	142
5.2.2 Experimental Values . . . . .	143
5.2.3 Previous Estimation Methods . . . . .	144
5.2.4 Computational Methods . . . . .	144
5.2.5 Estimation Method . . . . .	147
5.2.6 Conclusions . . . . .	154
Bibliography . . . . .	157
<b>6 Resonance Energy</b>	<b>163</b>
6.1 Introduction . . . . .	163
6.2 Quantifying Resonance Stabilization . . . . .	164
6.2.1 Hückel Resonance Energy . . . . .	164
6.2.2 Dewar Resonance Energy . . . . .	165
6.2.3 Hess-Schaad Reference Structure . . . . .	165
6.2.4 Number of Kekulé Structures . . . . .	166
6.2.5 Resonance-Structure Theory . . . . .	167
6.2.6 Conjugated Circuits . . . . .	169
6.3 Resonance Energy in the BCGA Method . . . . .	169
6.4 Counting the Number of Kekulé Structures . . . . .	170
6.4.1 Method for Alternant Molecules . . . . .	170
6.4.2 More General Methods . . . . .	171

6.5	Algorithm for Kekulé Structure Counting . . . . .	172
6.5.1	Idea and Implementation . . . . .	172
6.5.2	$\pi$ -Radicals with an Odd Number of Carbons . . . . .	175
6.5.3	Heterocyclic PAHs and PAHs with a Triple Bond . . . . .	175
6.5.4	Performance of the Algorithm . . . . .	177
6.6	Conclusions . . . . .	178
	Bibliography . . . . .	178
<b>7</b>	<b>Estimation of Thermochemical Properties for Non-Aromatic Molecules and Radicals</b>	<b>181</b>
7.1	Introduction . . . . .	181
7.2	Estimation Method . . . . .	183
7.3	The Thermochemistry Database . . . . .	185
7.3.1	Data Structure . . . . .	186
7.3.2	Dictionary . . . . .	192
7.3.3	Library . . . . .	194
7.4	Symmetry and Optical Isomers . . . . .	195
7.5	Conclusions . . . . .	196
	Bibliography . . . . .	196
<b>8</b>	<b>BCGA in RMG</b>	<b>201</b>
8.1	Introduction . . . . .	201
8.2	RMG- Chemical Reaction Mechanism Generator Software . . . . .	201
8.2.1	RMG Packages Relevant to this Work . . . . .	202
8.3	GATP . . . . .	204
8.4	The bondGroups Package . . . . .	205
8.4.1	New Functional Group Elements . . . . .	207
8.4.2	Organization of the Database . . . . .	208
8.5	Identification of Aromaticity . . . . .	209
8.6	Conclusions . . . . .	211
	Bibliography . . . . .	211

<b>9</b>	<b>Equilibrium Calculations</b>	<b>215</b>
9.1	Introduction . . . . .	215
9.2	Global Equilibrium Calculations . . . . .	215
9.3	Results and Discussion . . . . .	216
9.3.1	Sensitivity to the Thermochemical Properties . . . . .	216
9.3.2	Sooting Limits . . . . .	217
9.3.3	Fullerenes versus PAHs . . . . .	221
9.3.4	Concentrations of the Different Fullerenes . . . . .	224
9.4	Conclusions . . . . .	224
	Bibliography . . . . .	226
<b>10</b>	<b>Conclusions and Recommendations</b>	<b>229</b>
10.1	Conclusions . . . . .	229
10.1.1	Assessment of the Available Experimental Data . . . . .	229
10.1.2	Computational Methods . . . . .	230
10.1.3	Bond-Centered Group Additivity Method . . . . .	231
10.1.4	Organization of Thermochemical Database . . . . .	232
10.1.5	Implementation of the BCGA Method into RMG . . . . .	232
10.1.6	Equilibrium Calculations . . . . .	233
10.2	Recommendations for Future Work . . . . .	234
10.2.1	Determination of More Experimental Data . . . . .	234
10.2.2	Expansion of the Method . . . . .	234
10.2.3	Kekulé Structure Count . . . . .	235
10.2.4	Equilibrium Calculations . . . . .	235
10.2.5	Generation of Reaction Mechanisms for Soot Formation . . . . .	236
	Bibliography . . . . .	237
<b>A</b>	<b>Symmetry Numbers</b>	<b>239</b>
A.1	Aliphatic Molecules . . . . .	239
A.2	Cyclic Molecules . . . . .	242
A.3	Algorithm for Symmetry Calculation . . . . .	244

A.4	Examples	244
A.5	Discussion	247
A.6	Conclusions	248
	Bibliography	249
<b>B</b>	<b>Polycyclic Aromatic Molecules Included in this Study</b>	<b>251</b>
<b>C</b>	<b>Examples of Thermochemical Properties Estimation Using BCGA</b>	<b>285</b>
C.1	PAHs with Five-and Six-Membered Rings	285
C.2	Furans	288
C.3	Arynes	297
<b>D</b>	<b>Statistical Analysis</b>	<b>301</b>
D.1	Ring Corrections Method	301
D.2	Collinearity Diagnosis for BCGA for PAHs with Five-and Six-Membered Rings	302
D.3	Principal Component Regression	307
<b>E</b>	<b>Equilibrium Calculation</b>	<b>311</b>
E.1	Thermochemical Properties of Species Included	311
<b>F</b>	<b>Ph.D.CEP Capstone Paper – An Analysis of the Carbon Nanotubes Industry and Strategy for Nano-C</b>	<b>319</b>

# List of Figures

2-1	Some typical PAHs included in this work. . . . .	45
2-2	Example of each of the reaction schemes tested for the calculation of the $\Delta H_f^\circ$ from the absolute energy. . . . .	47
3-1	Existing additivity methods for benzenoid PAHs. . . . .	64
3-2	Existing additivity methods for PAHs containing both five- and six-membered rings. . . . .	67
3-3	Atom-centered groups definition . . . . .	70
3-4	Bond-centered groups defined in this work . . . . .	72
3-5	All the possible CC66 structures . . . . .	73
3-6	Error per carbon atom between $\Delta H_{f,\text{homo}}^\circ$ and $\Delta H_{f,\text{est}}^\circ$ versus the $\Delta H_{f,\text{homo}}^\circ$ . . . . .	85
4-1	Aromatic Bonds Defined for PAHs with a Furan Structure . . . . .	99
4-2	Thermolysis of benzo[c]phenanthrene . . . . .	101
4-3	Aromatic bonds defined for PAHs with triple bonds . . . . .	105
4-4	Arynes used for the derivation of the bond-centered group contributions . . . . .	105
4-5	4-Phenanthrenol should be less stable than 2-Phenanthrenol . . . . .	115
4-6	New Atom-Centered Groups for the Estimation of Thermochemistry of Substituted PAHs . . . . .	116
4-7	Corrections introduced for disubstituted PAHs. . . . .	116
4-8	Proposed tree structure for the groups centered on Cb for substituted PAHs. . . . .	119
5-1	Schematic of each of the groups defined for $\sigma$ -radicals in PAHs . . . . .	138

5-2	Role of odd $\pi$ -radicals on PAH growth. . . . .	143
5-3	Resonance isomers for benzo[ <i>a</i> ]phenalene . . . . .	150
5-4	Benz[ <i>fg</i> ]acenaphthylene has four different resonance isomers with the maximum number of Kekulé structures . . . . .	150
5-5	New Ring Corrections and HBI Groups . . . . .	151
5-6	HBI Groups Defined for Phenoxy Radicals . . . . .	154
6-1	$\ln(K)$ versus DRE plot from Herndon et al. . . . .	168
6-2	Permutations of Pairs of Electrons in Resonance Theory . . . . .	168
6-3	Example of the Algorithm for the Calculation of the Number of Kekulé Structures . . . . .	176
7-1	Example of the incremental specification of a group. . . . .	187
7-2	Partial representation of the thermochemical database tree. . . . .	188
7-3	Partial representation of the HBI database tree . . . . .	191
8-1	UML design diagram for the thermo estimator in RMG . . . . .	206
8-2	Difference between the CC6 and the DD6666 Group . . . . .	210
8-3	Adjacency List Representation for the CC6 and DD6666 Groups . . . . .	210
8-4	Adjacency List Representations for the ‘CC66’ Group . . . . .	210
8-5	ChemGraphs that are actually aromatic . . . . .	212
9-1	PAHs larger than ovalene included in the equilibrium study. . . . .	216
9-2	Effect of different values of $\Delta H_f^\circ$ of $C_{60}$ on the equilibrium concentra- tions of fullerenes . . . . .	218
9-3	Sooting limit predictions . . . . .	220
9-4	Equilibrium concentrations of PAHs and fullerenes . . . . .	222
9-5	Equilibrium constant for $C_{70} + \frac{77}{8} H_2 \longleftrightarrow \frac{7}{8} C_{80}H_{22}$ . . . . .	223
9-6	Equilibrium concentrations of overall PAHs and individual fullerenes . . . . .	225
A-1	Symmetry of methanol . . . . .	240
A-2	Symmetry of methane . . . . .	240
A-3	Subgraphs included in the symmetry correction library . . . . .	243

# List of Tables

2.1	Group values for the estimation of $C_{p,(cr)}^{est}(298.15K)$ . . . . .	32
2.2	Available experimental $\Delta H_{f,(cr)}^\circ$ , $\Delta H_{subl}^\circ$ , and $\Delta H_f^\circ$ of PAHs . . . . .	34
2.3	Available experimental $\Delta H_{f,(cr)}^\circ$ , $\Delta H_{subl}^\circ$ , and $\Delta H_f^\circ$ of fullerenes . . . . .	38
2.4	Uncertainties in $\Delta H_f^\circ$ assigned to each grade. . . . .	39
2.5	Experimental and computed (B3LYP/6-31G(d)) entropies of PAH at 298.15 K. The $S_{(cr)}^\circ$ were determined by calorimetric measurements. The $S_{(g)}^\circ$ in <i>italics</i> were calculated in this work from the vapor pressure measurements reported in the reference listed. . . . .	42
2.6	Comparison of the $\Delta H_f^\circ$ predicted by each of the reaction schemes to the experimental $\Delta H_f^\circ$ for the 16 PAH for which these values are available. In (kcal mol <sup>-1</sup> ). . . . .	49
3.1	Cross-validation of the bond-centered group additivity method . . . . .	77
3.2	$\Delta H_f^\circ$ and $S_{298}^\circ$ values for bond-groups and the $\ln(K)$ term for the estimation of thermochemical properties. . . . .	80
3.3	$C_p^\circ$ values for bond-groups for the estimation of thermochemical properties. . . . .	81
3.4	$\Delta H_f^\circ$ and $S_{298}^\circ$ statistics for the estimation method . . . . .	82
3.5	$C_p^\circ$ statistics for the estimation method . . . . .	82
3.6	Comparison between previous methods the BCGA method for the PAHs with known $\Delta H_{f,exp}^\circ$ . . . . .	86
3.7	Comparison between previous methods the BCGA method for some PAHs whose $\Delta H_{f,exp}^\circ$ are not known . . . . .	87

4.1	Comparison between the experimental geometry of furan the geometry calculated at different levels. . . . .	96
4.2	Comparison between $\Delta H_{f,\text{exp}}^\circ$ and $\Delta H_{f,\text{homo}}^\circ$ for PAHs Containing Furan Structures . . . . .	96
4.3	Comparison between Experimental and B3LYP/6-31G(d) $S_{298}^\circ$ and $C_p^\circ$ for PAHs Containing Furan Structures . . . . .	97
4.4	Group values obtained for $\Delta H_f^\circ$ if bond groups ‘AO5’, ‘BO5’, and ‘CO5’ are considered. . . . .	98
4.5	Coefficients for the estimation of $\Delta H_f^\circ$ and $S_{298}^\circ$ of PAHs with Furan Rings . . . . .	99
4.6	Coefficients for the estimation of $C_p^\circ$ of PAHs with Furan Rings . . . . .	100
4.7	Comparison between the geometry of benzyne calculated at different levels. . . . .	103
4.8	Comparison between the $\Delta H_f^\circ$ calculated from the proposed homodesmic reaction scheme for arynes and $\Delta H_{f,\text{exp}}^\circ$ values. As a reference the $\Delta H_{f,\text{atom}}^\circ$ calculated from atomization reactions are also given. . . . .	104
4.9	Contributions to the $\Delta H_f^\circ$ and $S_{298}^\circ$ from each of the bond-centered group values that describe aryne PAHs. . . . .	106
4.10	Contributions to the $C_p^\circ$ ’s from each of the bond-centered group values that describe aryne PAHs. . . . .	106
4.11	$\Delta H_f^\circ$ , $S_{298}^\circ$ , and $C_p^\circ$ Contributions of the OI5 Group . . . . .	107
4.12	Comparison between the $\Delta H_{f,\text{exp}}^\circ$ and the $\Delta H_f^\circ$ calculated from the proposed homodesmic reaction scheme. . . . .	110
4.13	Experimental and B3LYP/6-31G(d) $S_{298}^\circ$ and $C_{p,300}^\circ$ for some substituted PAHs . . . . .	110
4.14	Experimental and Calculated Frequencies for Phenylacetylene . . . . .	113
4.15	Group values obtained if each of the different carbon functional groups are considered separately. . . . .	118
4.16	Proposed group values for the $\Delta H_f^\circ$ of groups in substituted PAHs. . . . .	118
4.17	Proposed group values for the $S_{298}^\circ$ of groups in substituted PAHs. . . . .	118



4.18	Proposed group values for the $C_p^\circ$ of groups in substituted PAHs. . . .	120
5.1	Experimental values for the BDE of aromatic molecules . . . . .	130
5.2	Experimental values for the singlet-triplet gap of benzyne and the $\Delta H_f^\circ$ of the triplet states . . . . .	130
5.3	CASPT2 $\Delta H_f^\circ$ of didehydronaphthalenes . . . . .	133
5.4	Comparison between experimental and calculated BDE . . . . .	134
5.5	HBI contributions to the $\Delta H_f^\circ$ and $S_{298}^\circ$ . . . . .	138
5.6	HBI contributions to the $C_p^\circ$ 's . . . . .	139
5.7	Bond Dissociation Energy for Didehydroarenes . . . . .	139
5.8	Corrections for BDE of biradicals . . . . .	140
5.9	BDE for Ethynyl Substituted PAHs . . . . .	141
5.10	Experimental $\Delta H_f^\circ$ and (BDE) for the stable parents of $\pi$ -radicals. . .	145
5.11	Experimental BDE for Substituted $\pi$ -Radicals . . . . .	145
5.12	$\Delta H_{f,exp}^\circ$ , $\Delta H_{f,atom}^\circ$ , and $\Delta H_{f,homo}^\circ$ for $\pi$ -Radicals . . . . .	146
5.13	Calculated BDE for Substituted $\pi$ -Radicals . . . . .	148
5.14	$\Delta H_f^\circ$ and $S_{298}^\circ$ Coefficients for the HBI and Ring Correction Groups Developed in the Context of $\pi$ -Radicals . . . . .	151
5.15	$C_p^\circ$ Coefficients for the HBI and Ring Correction Groups Developed in the Context of $\pi$ -Radicals . . . . .	152
5.16	HBI Coefficients and Tree Structure for the Benzylic Groups . . . . .	153
5.17	HBI Coefficients for the $C_p^\circ$ of Benzylic Groups . . . . .	153
5.18	HBI Coefficients and Tree Structure for the Phenoxy Groups . . . . .	155
5.19	HBI Coefficients for the $C_p^\circ$ of Phenoxy Groups . . . . .	155
7.1	Rules for value assignment for "missing" thermochemical groups. . . .	189
7.2	Functional Group Elements defined in RMG . . . . .	193
8.1	New Functional Group Elements defined in RMG . . . . .	207
9.1	Relation between $\phi$ and C/O for benzene . . . . .	218
A.1	Symmetry rules for atoms . . . . .	241

A.2	Symmetry rules for single, double and triple bonds . . . . .	242
A.3	Symmetry rules for symmetry axis . . . . .	243
A.4	Examples of symmetry number for some molecules . . . . .	245
B.1	Benzenoid PAHs included in the development of the BCGA method .	251
B.2	PAHs with five- and six-membered rings included in the development of the BCGA method . . . . .	255
B.3	PAHs with the furan substructure included in the development of the BCGA method . . . . .	262
B.4	PAHs with the furan substructure and with triple bonds included in the development of the BCGA method . . . . .	264
B.5	PAHs with triple bonds included in the development of the BCGA method . . . . .	265
B.6	Acetylene substituted PAHs included in the development of the BCGA method . . . . .	266
B.7	Hydroxyl substituted PAHs included in the development of the BCGA method . . . . .	268
B.8	Methyl substituted PAHs included in the development of the BCGA method . . . . .	269
B.9	Ethylene substituted PAHs included in the development of the BCGA method . . . . .	270
B.10	Aldehyde substituted PAHs included in the development of the BCGA method . . . . .	271
B.11	Biarenes included in the development of the BCGA method . . . . .	272
B.12	$\sigma$ -radicals included in the development of the BCGA method . . . . .	273
B.13	Acetylene substituted $\sigma$ -radicals included in the development of the BCGA method . . . . .	281
B.14	Unsubstituted $\pi$ -radicals included in the development of the BCGA method . . . . .	282

B.15 Oxyl substituted $\pi$ -radicals included in the development of the BCGA method . . . . .	284
B.16 Methyl substituted $\pi$ -radicals included in the development of the BCGA method . . . . .	284
C.1 Estimation of the thermochemical properties using BCGA for the PAHs in Figure 2-1 . . . . .	286
D.1 Regression coefficients for $\Delta H_f^\circ$ based on ring corrections method . . .	301
D.2 Regression coefficient for $\Delta H_f^\circ$ calculated from ordinary least square (OLS) regression . . . . .	302
D.3 Regression coefficient for $S_{int}^\circ$ and $C_p^\circ$ calculated from ordinary least square (OLS) regression . . . . .	303
D.4 Correlation matrix for the standardized and centered matrix of the independent variables . . . . .	305
D.5 Eigenvalues and condition indices for the standardized and centered matrix of independent variables . . . . .	306
D.6 Statistics for the principal component regression . . . . .	308
D.7 Comparison of principal component regressions eliminating the least important principal components . . . . .	309
D.8 Matrix $\mathbf{V}$ . The columns are the eigenvectors corresponding to each principal component . . . . .	310



# Chapter 1

## Introduction

Polycyclic aromatic hydrocarbons (PAHs) and polycyclic aromatic molecules have attracted considerable attention in the past few decades. They are formed during the incomplete combustion of hydrocarbon fuels and are precursors of soot. Some PAHs are known carcinogens, and control of their emissions is an important issue. PAH molecules are found in many materials, including coal, fuel oils, lubricants, and carbon black. They are also implicated in the formation of fullerenes [7], one of the most chemically versatile class of molecules known. Clearly, predictive capability for the formation and growth of PAHs and other polycyclic aromatic molecules is highly desirable, either in order to minimize their formation or to steer their chemistry towards the generation of fullerenes and other desirable carbon nanostructures. The attainment of such a predictive capability involves many aspects, including the enumeration of the important reactions and species in the reaction mechanism, solution of the model's differential equations, and the comparison of the model with experiments.

Thermochemical properties of the species in the model are often the most important parameter, particularly for high temperature processes such as PAH formation. Thermodynamic consistency requires that reverse rate constants be calculated from the forward rate constants and from the equilibrium constants. The latter are obtained from the thermochemical properties of reactants and products. Consequently, low temperature model predictions depend heavily on barrier heights and enthalpy

changes of the reactions, while the model predictions at high temperature rely sensitively on entropy change (as  $\Delta S$  is multiplied by  $T$ ). Conventional methods for estimating thermochemical properties [1] rely heavily on experimental data, but very few such data are available. The predictive ability of current kinetic models is significantly limited by the scarcity of thermochemical data.

Recently, automatic reaction mechanism generation software packages have been developed that accomplish the monumental task of enumerating important reactions involved in combustion (see [10] and references therein). However, the applicability and reliability of such automated mechanism generators still rely on the accuracy of the numerical values employed for thermochemical and kinetic data. Moreover, the increase in computing power will allow these automatically generated mechanisms to encompass a previously unimagined number of different molecules, as long as their thermochemical properties and the kinetic rate constants related to their formation and consumption can be accurately estimated. The ability to accurately and consistently estimate thermochemical values for any PAH is an essential step towards building accurate combustion chemistry models that will allow the prediction of soot and/or fullerene formation using various fuels and various reactor designs.

Unfortunately experimental thermochemical data is only available for 16 of the hundreds of Isolated Pentagon Rule (IPR) PAHs with 24 or fewer carbon atoms. No experimental data is available for any larger PAH species (except for the  $C_{60}$  and  $C_{70}$  fullerenes). Only a very small fraction of other polycyclic aromatic molecules and radicals have had their thermochemical properties determined. In the last decade quantum chemical methods were made robust enough to provide accurate thermochemical data for polyatomic molecules. As a result, quantum chemical methods have been used to fill the void for species that are experimentally difficult to synthesize or hard to detect. However, PAHs are in general too large for accurate, but computationally intensive, quantum calculations such as the G<sub>n</sub> or CBS-*n* methods. Lower level quantum chemical calculations for PAHs have been performed by various groups. In the beginning of the '90s Schulman et al. did SCF calculations with various basis sets for many PAHs up to circumcoronene ( $C_{54}H_{18}$ ) to obtain their heats

of formation [9, 5, 3]. More recently density functional theory (DFT) calculations mostly at the B3LYP/6-31G(d) level of theory have been used for the calculation of  $\Delta H_f^\circ$  of PAHs [4, 6] and fullerenes [2] as well as  $S_{298}^\circ$  and  $C_p^\circ$  of PAHs [8]. However, many issues remain to be resolved: no general method for the determination of accurate  $\Delta H_f^\circ$  of PAHs from the total energies obtained from density functional calculations has been proposed, and computed low vibrational frequencies are thought to have considerable uncertainties, affecting the calculation of the entropy. More importantly, it is not feasible to do even DFT calculations for the myriad of possible PAH isomers. Thus a rapid, self-consistent and accurate estimation method for their thermochemical properties is needed.

## 1.1 Thesis Overview by Chapter

### 1.1.1 Chapter 2: Thermochemical Data for PAHs

An estimation method can at best only be as good as the values used to derive it. Thus the determination of a sound set of thermochemical properties of PAHs is crucial to the success of the estimation method. In Chapter 2 we describe how the thermochemical data were obtained for a set of 139 PAHs with five- and six-membered rings.

A critical assessment of the scarce experimental data is presented. Entropies provided by the B3LYP/6-31G(d) DFT method are shown to agree with the experimental data. Available  $\Delta H_{f,\text{exp}}^\circ$  are used to derive and judge the quality of isodesmic and homodesmic reaction schemes that enable the calculation of  $\Delta H_f^\circ$  from absolute energies given by quantum chemical calculations. A homodesmic reaction scheme that uses benzene, naphthalene, acenaphthalene, phenanthrene, and  $C_{60}$  is shown to predict all the available experimental  $\Delta H_f^\circ$  of PAHs (except for benzo[k]fluoranthene) with a mean average deviation of  $1.4 \text{ kcal mol}^{-1}$ . The  $\Delta H_{f,\text{exp}}^\circ$  for the latter is believed to be too low.

### 1.1.2 Chapter 3: Bond-Centered Group Additivity Method

Chapter 3 begins with a description of current estimation methods for PAHs. Each of these methods have been developed for a particular type of PAHs, and are based on very few experimental  $\Delta H_f^\circ$ .

The idea of a thermochemical properties estimation method based on bond-centered group additivity in conjunction with the  $\ln(K)$  term to describe the resonance energy is introduced.  $K$  is the number of Kekulé structures of the PAH. This method is shown to extrapolate reasonably to infinite gas-phase graphene sheets.

A thorough principal components analysis was performed on the regression model. Collinearity problems were identified. These problems are associated to be inherent to the X-space described by PAHs. To the extent that the set of PAHs used for the derivation of the model is representative, the partial collinearity should not cause problems in the prediction of the thermochemical properties of PAHs not included in the training set. Cross-validation procedures, including the “leave one out” procedure indicated that the proposed bond-centered group additivity method (BCGA) has good predictive capabilities.

### 1.1.3 Chapter 4: BCGA for Other Aromatic Molecules

PAHs with five- and six-membered rings are not the only polycyclic aromatic molecules. The BCGA method proposed in Chapter 3 is extended in Chapter 4 to encompass polycyclic aromatic molecules containing furan substructures, triple bonds, and non-aromatic substitutions.

We propose homodesmotic reactions for the calculation of  $\Delta H_f^\circ$  from the absolute energies calculated from quantum chemistry for these classes of molecules. Group values for polycyclic aromatic molecules containing furan substructures and triple bonds are derived. A method for the estimation of the thermochemical properties of substituted aromatics is proposed, allowing the estimation of species such as phenols, biarenes, and others. This method provides the linking between the BCGA and Benson’s method.



### 1.1.4 Chapter 5: BCGA for Radicals

Chapter 5 is dedicated to the description of the estimation of the thermochemical properties of polycyclic aromatic radicals.  $\sigma$ -radicals are treated through the hydrogen bond increment (HBI) method. New, more specific HBI values are derived for aromatic molecules. These HBI values depend of the environment around the radical site.

Molecules in which the free electron is delocalized over a  $\pi$ -electron network are called  $\pi$ -radicals. We have divided them into two classes. The first are the PAHs with an odd number of carbons, such as indenyl. The second are substituted aromatic radicals, such as benzyl or phenoxy. The difficulty with the estimation of the thermochemical properties of  $\pi$ -radicals is that it is not possible to unequivocally determine the position of the radical, since it is delocalized. We propose the use of the resonance structure with the largest number of Kekulé structures for the calculation of the thermochemical properties of the  $\pi$ -radical.

### 1.1.5 Chapter 6: Resonance Energy

Resonance stabilization is one of the characteristic properties of aromatic molecules. Being a non-local property, it is not amenable to being captured by group additivity methods. Chapter 6 describes methods for easily quantifying resonance energy. The natural logarithm of the number of Kekulé structures ( $\ln(K)$ ) is chosen to account for resonance energy in the BCGA method. An algorithm for the counting of the Kekulé structures of aromatic molecules with any sized-rings is presented.

### 1.1.6 Chapter 7: Thermochemistry for Non-Aromatic Molecules and Radicals

Chapter 7 describes the organization of the thermochemistry database for non-aromatic molecules in the Automatic Reaction Mechanism Generation software (RMG) developed by Dr. Jing Song. The thermochemistry database consists of the groups from

Benson’s Group Additivity method, hydrogen bond increment (HBI) values for radicals, and other corrections for non-nearest neighbor interactions.

Traditionally thermochemical databases have been organized as unordered lists of the groups. Such lists don’t capture any of the information regarding the relationship amongst the groups. In Chapter 7 we describe how the database was organized as a tree structure. The idea of organizing chemical information in a tree structure had already been implemented by Dr. Sumathy Raman, Dr. Jing Song and Catherina Wijaya for reaction families. A tree structure is easily maintained and extended.

Values are not available for all the possible Benson’s atom-centered groups. There are fewer than 300 hundred group values involving carbon, oxygen and hydrogen atoms, whereas the corresponding thermochemical database tree has more than 1000 nodes. We propose in Chapter 7 assigning “missing” groups values from other similar groups. This assignment is unique and allows the estimation of the thermochemical properties of any molecule.

Some basic concepts and terminology used in RMG are also introduced in this Chapter.

### **1.1.7 Chapter 8: BCGA in RMG**

Chapter 8 describes the implementation of the bond-centered group additivity method presented in Chapters 3 to 5 into a computer program. This program is completely integrated to RMG, meaning that if an aromatic molecule is input into RMG, its thermochemical properties can be estimated using the BCGA method proposed in this work. On the other hand, RMG can work as a thermo estimator, independent from its reaction mechanism generation capabilities.

### **1.1.8 Chapter 9: Equilibrium Calculations**

The results of some exploratory equilibrium studies are reported in Chapter 9. Interesting insight on the relationship between PAH and fullerenes in combustion system are gained.

# Bibliography

- [1] S. W. Benson. *Thermochemical Kinetics*. John Wiley & Sons, New York, 2nd edition, 1976.
- [2] J. Cioslowski, N. Rao, and D. Moncrieff. Standard enthalpies of formation of fullerenes and their dependence on structural motifs. *Journal of the American Chemical Society*, 122:8265–8270, 2000.
- [3] R. L. Disch, J. M. Schulman, and R. C. Peck. Ab initio heats of formation of medium-sized hydrocarbons. 13. studies of benzo[e]pyrene, benzo[ghi]perylene, coronene, and circumcoronene. *Journal of Physical Chemistry*, 96:3998–4002, 1992.
- [4] W. C. Herndon, P. U. Biedermann, and I. Agranat. Molecular structure parameters and predictions of enthalpies of formation for catacondensed and peri-condensed polycyclic aromatic hydrocarbons. *Journal of Organic Chemistry*, 63:7445–7448, 1998.
- [5] R. C. Peck, J. M. Schulman, and R. L. Disch. Ab initio heats of formation of medium-sized hydrocarbons. 12. 6-31g\* studies of the benzenoid aromatics. *Journal of Physical Chemistry*, 94:6637–6641, 1990.
- [6] S. Pogodin and I. Agranat. Overcrowding motifs in large pahs. an ab initio study. *Journal of Organic Chemistry*, 67:265–270, 2002.
- [7] H. Richter, W. J. Grieco, and J. B. Howard. Formation mechanism of polycyclic aromatic hydrocarbons and fullerenes in premixed benzene flames. *Combustion and Flame*, 119:1–22, 1999.
- [8] L. Rutz, H. Bockhorn, and J. W. Bozzelli. Thermodynamic properties of unsaturated and polycyclic aromatic hydrocarbons. *Proceeding of the Third Joint Meeting of the U.S. Sections of the Combustion Institute*, 2003.
- [9] J. M. Schulman, R. C. Peck, and R. L. Disch. Ab initio heats of formation of medium-sized hydrocarbons. 11. the benzenoid aromatics. *Journal of the American Chemical Society*, 111:5675–5680, 1989.
- [10] J. Song. *Building Robust Chemical Reaction Mechanisms: Next Generation of Automatic Model Construction Software*. Phd thesis, Massachusetts Institute of Technology, 2004.



## Chapter 2

# Thermochemical Data for Estimation Method for PAHs with Five- and Six-Membered Rings

### 2.1 Introduction

The basis of an estimation method are the values used to derive the model. Section 2.2 in this Chapter presents a critical assessment of the available experimental enthalpies and entropies of formation of PAHs. Unfortunately there are not enough experimental data for the development of a comprehensive and statistically significant method for the estimation of the thermochemical properties of PAHs. Thus Section 2.3 describes the computational methods used to obtain reliable thermochemical data for a large set of PAHs.

### 2.2 Experimental Thermochemical Properties

The quality of an estimation method can be assessed only by comparison of its prediction with measured data. Undoubtedly experimental values are the “gold standard”. Unfortunately, there are not many of them available and in many cases it is not even clear how reliable an experimental value is. This section is a critical survey of the

experimental enthalpies and entropies of formation of PAH that can be found in the literature. Values for the  $\Delta H_f^\circ$  of PAHs have been adopted among the experimental values and uncertainties have been assigned to them.

### 2.2.1 Experimental Enthalpy of Formation Values

Gas phase  $\Delta H_f^\circ$  of PAH are usually obtained by adding the heat of formation of the solid state,  $\Delta H_{f,(cr)}^\circ$ , and the heat of sublimation,  $\Delta H_{subl}^\circ$ . For benzene, which is liquid at ambient temperature, the heat of formation of the liquid,  $\Delta H_{f,(lq)}^\circ$ , and the heat of vaporization,  $\Delta H_{vap}^\circ$ , are used. From the heat released by the combustion of the solid PAH, the  $\Delta H_{f,(cr)}^\circ$  is calculated, taking into account reduction to the standard state. Usually complete combustion to  $\text{CO}_2$  and  $\text{H}_2\text{O}$  is verified by visual inspection (no formation of soot) or by measurement of the  $\text{CO}_2$  formed. Some authors base the results of their combustion experiments on the amount of  $\text{CO}_2$  recovered, to minimize the errors arising due to incomplete combustion and impurities in the sample [14]. When soot is formed, its massic energy of combustion also has to be taken into account, as done by Nagano for the combustion of naphthacene [50].

Enthalpies of sublimation are usually determined either calorimetrically or by vapor-pressure measurements. Since PAHs have very low volatility, torsion-effusion and the Knudsen-effusion methods are most frequently used for their vapor-pressure measurements. When effusion methods are used, the  $\Delta H_{subl}^\circ$  is calculated from the Clayperon equation:

$$\Delta H_{subl,T_1}^\circ = T_1 \left( \frac{dp}{dT} \right) [V_g - V_{cr}] \quad (2.1)$$

Usually the gas phase is considered to be ideal and  $V_{cr}$  is assumed to be negligible in comparison to  $V_g$ , in which case Eq. 2.1 becomes:

$$\Delta H_{subl,T_1}^\circ = -R \left( \frac{d \ln p}{d(1/T)} \right) \quad (2.2)$$

When the empirical relation

$$\log p = A - B/T \quad (2.3)$$

is fitted to the vapor pressure data, the  $\Delta H_{subl}^\circ$  is given by:

$$\Delta H_{subl}^\circ = 2.303 \times R \times B \quad (2.4)$$

where  $R$  is the gas constant. Due to the low volatility of PAH, vapor pressure measurements are usually done at higher temperatures and should be corrected to 298.15 K.

Kirchhoff's equation is used to adjust the heat of sublimation to the desired temperature:

$$\Delta H_{subl}^\circ(298.15K) = \Delta H_{subl}^\circ(T_m) + \int_{298.15}^{T_m} (C_{p,(cr)} - C_{p,(g)}) dT \quad (2.5)$$

$$\approx \Delta H_{subl}^\circ(T_m) + (C_{p,(cr)} - C_{p,(g)}) (T_m - 298.15) \quad (2.6)$$

Since heat capacities are not always available, many methods have been proposed to account for the second term in Eq. 2.6. Some authors adjusted their experimental heat of sublimation and report the value at 298.15 K. When the original authors have not applied any temperature correction to their experimental work, we adjusted the literature enthalpies of sublimation to 298.15 K using the equation proposed by Chickos et al [10]:

$$(C_{p,(cr)} - C_{p,(g)}) = [0.75(\text{JK}^{-1}\text{mol}^{-1}) + 0.15C_{p,(cr)}^{est}(298.15)] \quad (2.7)$$

where  $T_m$  is the middle of the temperature interval where the vapor pressure measurements were carried out. The  $\Delta H_{subl}^\circ$  from Wakayama and Inokuchi [74] were corrected using the average temperatures cited by Chickos and Acree [8]. The  $C_{p,(cr)}^{est}$  are evaluated by group additivity. For the PAHs in this study, the group values recommended by Chickos et al. [9, 8] are used (Table 2.1). Eq 2.7 has been applied successfully to temperatures up to 500 K [7]. The temperature correction to  $\Delta H_{subl}^\circ$  is of the order of 1 kcal mol<sup>-1</sup>, except for C<sub>60</sub> and C<sub>70</sub>. For these large molecules,  $T_m$  is very high (above 800 K), and the assumption of constant heat capacity is not adequate. However, for the smaller PAHs, since temperature correction of the  $\Delta H_{subl}^\circ$  is comparable to the experimental error, some authors, especially from earlier works (e.g. Boyd et al. [5]),

considered the heat of sublimation to be constant with temperature, introducing small systematic errors to the enthalpies of sublimation.

The compilation of experimental  $\Delta H_{f,(cr)}^\circ$ ,  $\Delta H_{subl}^\circ$  and  $\Delta H_{f,(g)}^\circ$  is found in Tables 2.2 and 2.3. This compilation is not meant to be complete. Rather, this table offers a list of the values that have been most widely cited and should give a good idea of the dispersion among the data. Cox & Pilcher in 1970 published a very careful compilation of  $\Delta H_{f,(cr)}^\circ$  and of  $\Delta H_{subl}^\circ$  of organic and organometallic compounds available at that time [15]. When more than one value was available, they made a selection of the “best” value based on the experimental quality of the reported work. Pedley et al. made a later compilation in 1986, following mainly the recommendations made by Cox & Pilcher and adding some new values [55]. The most recent review of the thermochemistry of PAHs was done by Slayden and Liebman [66]. The values from Cox & Pilcher and from Pedley et al. are now widely cited and, in general, accepted. It is appropriate to mention that both references did not apply temperature corrections to the values they compiled. Thus, in some cases, they recommend enthalpies of formation at 298.15 K based on enthalpies of sublimation measured at higher temperature ranges. More recently Chickos and Acree collected most of the published enthalpies of sublimation in an extensive review of the literature from 1910 to 2001 [8].

For many of the PAHs, only one value of  $\Delta H_{f,(cr)}^\circ$  or of  $\Delta H_{subl}^\circ$  has been reported, making it difficult to assess the reliability of the experimental value. When more than one value is available in the literature, it is not uncommon that the values reported by different authors differ by a couple of kcal mol<sup>-1</sup>. We do not report here the uncertainties associated with each individual value because often those uncertainties

Table 2.1: Group values for the estimation of  $C_{p,(cr)}^{est}(298.15K)$ .

Benson's notation	J K <sup>-1</sup> mol <sup>-1</sup>
$C_{B^-(H)}$	17.5
$C_{BF^-(C_B)_2(C_{BF})}$ or $C_{BF^-(C_B)(C_{BF})_2}$	8.5
$C_{BF^-(C_{BF})_3}$	9.1



refer to a particular experimental setup. Rather, we assign levels of confidence to each of the  $\Delta H_f^\circ$  that we adopted. Grade ‘A’ refers to values that are well known and widely used. Their uncertainty should be less than 0.5 kcal mol<sup>-1</sup>. Grade ‘B’ was assigned to values for which many independent experiments have been performed, giving results which are close to each other. The uncertainties for these  $\Delta H_f^\circ$  should be within 2.0 kcal mol<sup>-1</sup>. Grade ‘C’ was given to values that are based on a single measurement or when the measured values (of the  $\Delta H_{f,(cr)}^\circ$  or of the  $\Delta H_{subl}^\circ$ ) have a large spread. The uncertainties associated with these values might be as large as 5.0 kcal mol<sup>-1</sup>. Finally grade ‘D’ was assigned to a  $\Delta H_f^\circ$  that is suspected to be in error and to the  $\Delta H_f^\circ$  of C<sub>60</sub> and C<sub>70</sub> fullerenes. The experimental  $\Delta H_f^\circ$  for these molecules have uncertainties of 10 kcal mol<sup>-1</sup> or more. The uncertainty associated with each grade are summarized in Table 2.4.

Table 2.2: Available experimental  $\Delta H_{f,(cr)}^\circ$ ,  $\Delta H_{subl}^\circ$ , and  $\Delta H_f^\circ$  of PAHs. All values are reported at 298.15 K. The values in *italics* were cited in the reference listed under the last column. The original source are given in superscript. The  $\Delta H_f^\circ$  adopted in this work are in bold.

Substance	$\Delta H_{f,(cr)}^\circ$ (kcal mol <sup>-1</sup> )	$\Delta H_{subl}^\circ$ (kcal mol <sup>-1</sup> )	$\Delta H_{f,(g)}^\circ$ (kcal mol <sup>-1</sup> )	Ref.
Benzene <sup>a</sup>	11.72	8.1 <sup>b</sup>	<b>19.8</b>	A [60]
	-	-	<i>19.7</i>	[55]
	-	8.3 <sup>c</sup>	20.0	[30]
Naphthalene	-	15.9	-	[31]
	18.58	-	-	[14]
	-	17.22	-	[47]
	-	17.4	-	[39]
	<i>18.6</i> <sup>d</sup>	<i>17.3</i> <sup>e</sup>	<i>35.9</i>	[55]
	<i>18.6</i> <sup>[55]</sup>	17.4	<b>36.0</b>	A [12]
-	17.6	-	[51]	
Acenaphthalene	44.70	17.0 <sup>f</sup>	61.7	[5]
	-	17.44	-	[47]
	<i>44.70</i> <sup>[5]</sup>	<i>17.44</i> <sup>[47]</sup>	<b>62.1</b>	C [55]
	-	19.0	-	[51]
Phenanthrene	26.59	<i>20.1</i> <sup>[75]</sup>	-	[41]
	-	21.8	-	[34]
	-	22.2	-	[31]
	27.77	-	-	[14]
	-	21.72	-	[47]
	-	22.1	-	[39]
	<i>27.77</i> <sup>[14]</sup>	<i>21.82</i> <sup>e</sup>	<i>49.6</i>	[55]
	26.23	21.85 <sup>g</sup>	48.1	[69]
	-	21.9	-	[51]
	-	22.86	-	[52]
	-	21.8	-	[61]
	<i>27.1</i> <sup>h</sup>	<i>21.8</i> <sup>[55]</sup>	<i>48.9</i>	[66]
26.39	<i>21.8</i> <sup>[61]</sup>	<b>48.2</b>	B [50]	
-	21.8	-	[11]	

*continued*

<sup>a</sup>Values listed for benzene refer to the liquid phase, and not to the solid crystal.

<sup>b</sup>From unpublished data by D. D. Wagman, W. J. Taylor, J. Pignocco, and F. D. Rossini, National Bureau of Standards.

<sup>c</sup>From personal communication of W. C. Herndon with J. Chickos.

<sup>d</sup>Assessed to be the “best value” by [55].

<sup>e</sup>Based on values by [47] and [39].

<sup>f</sup>Vapor pressure measurements were done in a temperature range from 290 to 333K.

<sup>g</sup>From heat of fusion and heat of vaporization measurements.

<sup>h</sup>Average of values of Coleman [14] and Steele [69]

Table 2.2: *continued*

Substance	$\Delta H_{f,(cr)}^\circ$ (kcal mol <sup>-1</sup> )	$\Delta H_{subl}^\circ$ (kcal mol <sup>-1</sup> )	$\Delta H_{f,(g)}^\circ$ (kcal mol <sup>-1</sup> )	Ref.
Anthracene	31.46	22.3 <sup>[75]</sup>	-	[41]
	-	22.5	-	[34]
	-	24.6	-	[31]
	30.88	-	-	[14]
	-	24.6 <sup>i</sup>	-	[43]
	-	24.9 <sup>j</sup>	-	[43]
	-	25.0	-	[39]
	30.00	-	-	[46]
	30.88 <sup>[14]</sup>	24.3 <sup>k,l</sup>	55.2	[55]
	-	24.5	-	[51]
	-	24.23	-	[52]
	-	24.71	-	[61]
	30.5 <sup>m</sup>	24.3 <sup>[55]</sup>	54.8	[66]
	30.28	24.71 <sup>[61]</sup>	<b>55.0</b>	B [49]
Pyrene	-	24.4	-	[34]
	-	23.6	-	[31]
	27.44 <sup>[76]</sup>	-	-	[67]
	-	24.09 <sup>j</sup>	-	[42]
	-	24.14 <sup>i</sup>	-	[42]
	29.99	23.95	<b>53.9<sup>n</sup></b>	C [67]
	-	24.1	-	[51]
	-	25.10	-	[52]
Fluoranthene	-	24.1	-	[31]
	46.00	24.40 <sup>o, k</sup>	70.4	[5]
	-	23.7	-	[47]
	45.4 <sup>p</sup>	23.7 <sup>[47]</sup>	<b>69.1</b>	B [55]
	-	24.2	-	[51]

*continued*<sup>a</sup>Calorimetric measurement.<sup>b</sup>Mass effusion measurement.<sup>k</sup>Based on values by [43] and [39].<sup>l</sup>Not corrected to 298.15K.<sup>m</sup>Average of values of Coleman [14] and Metzger [46]<sup>n</sup>This is the value recommended by [55].<sup>o</sup>This value was measured in a temperature range from 338 to 353 K.<sup>p</sup>From E. F. Westrum, Jr., W.-K. Wong, S.-W. Wong, Presented at the ACS Meeting, Miami Beach, April, 1967.

Table 2.2: *continued*

Substance	$\Delta H_{f,(cr)}^\circ$ (kcal mol <sup>-1</sup> )	$\Delta H_{subl}^\circ$ (kcal mol <sup>-1</sup> )	$\Delta H_{f,(g)}^\circ$ (kcal mol <sup>-1</sup> )	Ref.
Triphenylene	35.30	26.3 <sup>q</sup>	-	[41]
	-	28.3	-	[31]
	-	26.8	-	[74]
	36.28	-	-	[26]
	-	30.23	-	[39]
	36.28 <sup>[26]</sup>	29.25 <sup>r</sup>	<b>65.5</b> C	[55]
	-	28.2	-	[51]
	35.02 <sup>s</sup>	28.45 <sup>t</sup>	63.5	[66]
Chrysene	34.82	28.1 <sup>q</sup>	-	[41]
	-	29.2	-	[31]
	-	29.1	-	[74]
	-	31.31	-	[39]
	34.73 <sup>[41]</sup>	29.76 <sup>u, k</sup>	64.5	[55]
	-	29.2	-	[51]
	34.73 <sup>[55]</sup>	28.25 <sup>v, k</sup>	<b>63.0</b> C	[66]
Benz[a]anthracene	40.93	26.1 <sup>v</sup>	-	[41]
	-	28.5	-	[31]
	-	29.8	-	[74]
	40.83 <sup>[41]</sup>	25.14	65.97	[29]
	-	29.47	-	[39]
	40.82 <sup>[41]</sup>	29.2 <sup>k, u</sup>	70.0	[55]
	-	28.4	-	[51]
	40.82 <sup>[55]</sup>	28.06 <sup>t</sup>	<b>68.9</b> C	[66]
Benz[c]phenanthrene	44.3	25.4 <sup>q</sup>	-	[41]
	-	25.4 <sup>[41]</sup>	-	[74]
	44.2 <sup>[41]</sup>	25.4 <sup>[74]</sup>	<b>69.6</b> C	[55]

*continued*<sup>q</sup>From estimated solvation energy and measured heat of solution.<sup>r</sup>Based on [31] and [39].<sup>s</sup>Average of values of Westrum (see footnote *p*) and Good [26]<sup>t</sup>From personal communication of S. W. Slayden with J. S. Chickos.<sup>u</sup>Based on values by [74] and [39].<sup>v</sup>Based on values by [74] and [51].

Table 2.2: *continued*

Substance	$\Delta H_{f,(cr)}^\circ$ (kcal mol <sup>-1</sup> )	$\Delta H_{subl}^\circ$ (kcal mol <sup>-1</sup> )	$\Delta H_{f,(g)}^\circ$ (kcal mol <sup>-1</sup> )	Ref.
Naphthalene	38.1	29.7 <sup>q</sup>	-	[41]
	-	29.6	-	[34]
	-	31.0	-	[74]
	-	34.35	-	[39]
	38.0 <sup>[41]</sup>	31.7 <sup>u</sup>	69.7	[55]
	-	31.0	-	[51]
	-	31.39	-	[52]
	49.45	29.8 <sup>[74], k</sup>	<b>79.3</b>	C [50]
Corannulene	81.81	-	-	[36]
	81.81 <sup>[36]</sup>	28.27	<b>110.1</b>	C [11]
Perylene	-	32.2	-	[34]
	43.66	-	-	[71]
	-	34.7	-	[25]
	43.69 <sup>p</sup>	-	-	[55]
	-	30.3	-	[51]
	-	32.80	-	[52]
	43.69 <sup>[55]</sup>	32.65 <sup>w</sup>	<b>76.3</b>	C [11]
Benzo[k]fluoranthene	41.20	29.68	<b>70.9</b>	D [21]
Coronene	-	37.6	-	[34]
	-	36.8	-	[31]
	-	33.2	-	[74]
	-	35.2	-	[51]
	-	33.70	-	[52]
	35.01	37.17 <sup>[7]</sup>	72.2	[48]
	36.45 <sup>[35]</sup>	37.05 <sup>x</sup>	<b>73.5</b>	C [11]

<sup>w</sup>Based on values by [34], [52] and [11].

<sup>x</sup>Estimated from [34] and [31].

The most widely cited value for the  $\Delta H_f^\circ$  of benzene (19.8 kcal mol<sup>-1</sup>) was reported by Prosen et al. [60]. Herndon et al. [30] suggest a value that is 0.2 kcal mol<sup>-1</sup> higher, based on an unpublished heat of vaporization value. We chose to use the most widely accepted value. In the case of naphthalene, although Cox & Pilcher [15] cite many  $\Delta H_{f,(cr)}^\circ$ , ranging from 15.5 to 19.6 kcal mol<sup>-1</sup>, the value that they recommend (18.6 kcal mol<sup>-1</sup>) is widely used without much controversy. Naphthalene has been classified as a primary reference material for calorimetry and differential thermal analysis with a recommended  $\Delta H_{subl}^\circ$  of 17.35 kcal mol<sup>-1</sup> [61].

The value of  $\Delta H_f^\circ$  of phenanthrene from Nagano [50] was chosen over the value

Table 2.3: Available experimental  $\Delta H_{f,(cr)}^\circ$ ,  $\Delta H_{subl}^\circ$ , and  $\Delta H_f^\circ$  of fullerenes. All values are reported at 298.15 K. The values in *italics* were cited in the reference listed under the last column. The original source are given in superscript. The  $\Delta H_f^\circ$  adopted in this work are in bold.

Substance	$\Delta H_{f,(cr)}^\circ$ (kcal mol <sup>-1</sup> )	$\Delta H_{subl}^\circ$ (kcal mol <sup>-1</sup> )	$\Delta H_{f,(g)}^\circ$ (kcal mol <sup>-1</sup> )	Ref.
C <sub>60</sub>	-	34.15 <sup>a</sup>	-	[73]
	-	44.36 <sup>a</sup>	-	[44]
	-	39.15 <sup>a</sup>	-	[1]
	578.94	<i>55.93</i> <sup>b</sup>	634.9	[70]
	545.0	-	-	[3]
	543.26	-	-	[37]
	544.48	<i>54.66</i> <sup>c</sup>	599.1	[20]
	556.17	-	-	[4]
	563.95	<i>54.66</i> <sup>c</sup>	618.6	[79]
	562.86	-	-	[38]
	<i>556.17</i> <sup>[4]</sup>	43.26	599.4	[58]
	<i>560.71</i> <sup>d</sup>	<i>43.91</i> <sup>e</sup>	<b>604.6</b> D	[17]
C <sub>70</sub>	-	48.0 <sup>f</sup>	-	[1]
	-	52.3 <sup>g</sup>	-	[1]
	567.6	-	-	[37]
	-	49.5 <sup>g</sup>	-	[62]
	-	53.3 <sup>g</sup>	-	[62]
	610.7	-	-	[4]
	<i>610.7</i> <sup>[4]</sup>	47.8 <sup>h</sup>	<b>658.5</b> D	[57]
	616.1	<i>50.2</i> <sup>i</sup>	666.3	[19]
586.0	<i>47.8</i> <sup>[57]</sup>	633.8	[59]	

<sup>a</sup>Extrapolated to 298K by [58].

<sup>b</sup>Value from [54], extrapolated to 298K by [70]. [54] worked with mixtures of C<sub>60</sub> and C<sub>70</sub>.

<sup>c</sup>Value from [44], extrapolated to 298K by [20].

<sup>d</sup>Average of values from [79] and [38].

<sup>e</sup>From measurements of [58].

<sup>f</sup>Extrapolation to 298K by [57] using 2<sup>nd</sup> law.

<sup>g</sup>Extrapolation to 298K by [19] using 2<sup>nd</sup> law.

<sup>h</sup>Value proposed based on vapor pressure measurements by many workers, and extrapolation to 298K with 2<sup>nd</sup> and 3<sup>rd</sup> law.

<sup>i</sup>Derived from vapor pressure measurements of [1] and [62]. Extrapolated to 298K with 2<sup>nd</sup> and 3<sup>rd</sup> law.

Table 2.4: Uncertainties in  $\Delta H_f^\circ$  assigned to each grade.

Grade	Uncertainty (kcal mol <sup>-1</sup> )
A	0.5
B	2.0
C	5.0
D	10.0

suggested by Pedley et al. [55]. While studying the equilibrium of a system with phenanthrene, hydrogen and 9,10-dihydrophenanthrene, Steele et al. noted that the enthalpy of formation of phenanthrene failed to predict the correct equilibrium constant [69]. They then measured the combustion energy of phenanthrene obtaining a value about 1.5 kcal mol<sup>-1</sup> lower than the one suggested by Pedley et al. This new value predicts a more accurate equilibrium constant for the aforementioned system. More recently Nagano also measured  $\Delta H_f^\circ$  of solid phenanthrene [50], obtaining a value in accordance with the value obtained by Steele et al. [69]. Phenanthrene is evaluated as a tertiary reference material, with a recommended  $\Delta H_{subl}^\circ$  of 21.82 kcal mol<sup>-1</sup> [61].

The large spread on the earlier heat of sublimation of anthracene has been attributed to the difficulty of ensuring a high level of purity of this substance. Nevertheless, anthracene is evaluated as a primary reference material for calorimetry and differential thermal analysis, with a recommended  $\Delta H_{subl}^\circ$  of 24.7 kcal mol<sup>-1</sup> [61].

For the larger PAH, the data becomes more scarce, and the dispersions among them are also large. We have as a rule adopted the most recently recommended value. It is worthwhile to mention the debate over the  $\Delta H_f^\circ$  of naphthacene. Many authors, comparing the experimental enthalpy of formation of this PAH accepted at the time with values predicted by semi-empirical [16] and quantum chemical calculations [65, 30] have noticed that the experimental  $\Delta H_f^\circ$  of naphthacene was about 10 kcal mol<sup>-1</sup> too low. Recently Nagano measured again the energy of combustion for this PAH obtaining a value about 10 kcal mol<sup>-1</sup> higher than the previously accepted value [50]. Nagano conjectured that the sample for the measurement by Magnus et al. [41] might have been oxidized before the calorimetric measurements. This finding

shows that theoretical predictions are now very powerful and can aid experimentalists to determine the quality of a calorimetric measurement.

Experimental values for  $C_{60}$  and  $C_{70}$  fullerenes are very abundant due to the interest that these molecules have generated. However, large dispersions among the experimental values are found. The presence of impurities, such as solvents and adsorbed gases, and the use of small samples are commonly cited as the main cause for the discrepancy between the experimental  $\Delta H_{f,(cr)}^\circ$  values [18, 59]. Comparison of results from different groups has led to the conclusion that the history of the samples affect the calorimetric experiments considerably [18], however no standard procedure for the preparation and handling of fullerene samples for thermochemical measurement exists yet. For large molecules such as the fullerenes, the correction of the enthalpy of sublimation from the temperature at which the vapor pressure was measured to 298.15 K is significant.  $\Delta H_{subl}^\circ$  values extrapolated to 298.15 K by different authors using the same experimental vapor pressure measurements can vary by as much as 4 kcal mol<sup>-1</sup>.

## 2.2.2 Experimental Entropy Values

Unfortunately, PAH entropy and heat capacity data are even more rare in the literature than heats of formation. In principle, gas phase entropies can be calculated from the vibrational frequencies (usually of the solid phase) obtained spectroscopically. However, sufficiently reliable vibrational assignments are not available for PAHs, even for those with abundant spectroscopic data such as naphthalene, phenanthrene and anthracene [22]. Gas phase entropy can also be obtained by the third-law approach, adding the entropy of the crystal, the entropy of sublimation and the decrease of entropy due to compression, as given by Eq. 2.8:

$$S_{(g)}^\circ = S_{(cr)} + \Delta S_{subl} + S_{comp} \quad (2.8)$$

$$= S_{(cr)} + \frac{\Delta H_{subl}}{T} + R \ln \left( \frac{p}{p^\circ} \right) \quad (2.9)$$



The entropy of the crystal is obtained by measurement of  $C_p^\circ$  from 0 K to the temperature of interest. Heat capacity measurements are difficult at temperatures near 0 K, and often the Debye extrapolation for the  $C_p^\circ$  is used. In Table 2.5 we present experimental gas phase entropies that are available in the literature as well as entropies that we calculated from published experimental data. If equations of the form of Eq. 2.3 are used to relate the dependence of the vapor pressure to the temperature, then Eq. 2.9 is simplified to:

$$S_{(g)}^\circ = S_{(cr)} + 2.303 \times R \times A \quad (2.10)$$

The parameters ‘A’ available in the literature were used in conjunction with experimental  $S_{(cr)}$  to calculate  $S_{(g)}^\circ$ . The entropy of the crystal was taken at the average temperature ( $T_m$ ) at which the parameter ‘A’ was obtained, and thus the  $S_{(g)}^\circ$  obtained is at  $T_m$ . It was corrected back to 298.15 K by using gas phase heat capacities obtained from quantum chemical calculations (B3LYP/6-31G(d)). These  $C_p^\circ$  are expected to be much more accurate than the entropies, because entropies are quite sensitive to uncertainties in low frequency modes. Gas-imperfection corrections have been assumed negligible for the vapor-solid equilibrium since the vapor pressure is low. Entropies calculated in this manner are shown in *italics*. Some of the entropies obtained from vibrational assignments are also listed in Table 2.5. We note that there is a very wide spread in the entropy values for some of the PAHs. This spread is due to differences in the values of vapor pressure over solid PAH reported by different authors, leading to large differences in the ‘A’ parameter. The last column in Table 2.5 was calculated from density functional theory (see Section 2.3).

## 2.3 Computational Methods

137 PAHs containing both five- and six-membered rings and the C<sub>60</sub> and C<sub>70</sub> fullerenes were considered for the present study. This set of molecules was chosen ensuring that a broad range of structural characteristics in PAHs was represented. 43 of

Table 2.5: Experimental and computed (B3LYP/6-31G(d)) entropies of PAH at 298.15 K. The  $S_{(cr)}^\circ$  were determined by calorimetric measurements. The  $S_{(g)}^\circ$  in *italics* were calculated in this work from the vapor pressure measurements reported in the reference listed.

Substance	$S_{(cr)}^\circ$ (cal K <sup>-1</sup> mol <sup>-1</sup> )	$S_{(g)}^\circ$ (cal K <sup>-1</sup> mol <sup>-1</sup> )	Ref.	$S_{B3LYP,(g)}^\circ$ (cal K <sup>-1</sup> mol <sup>-1</sup> )
Benzene <sup>a</sup>	41.9	-	[33]	64.5±0.2
	41.411	64.457	[53]	
Naphthalene	39.9	-	[33]	80.1±0.8
	38.89	-	[68]	
	40.01	-	[45]	
	-	80.22 <sup>b</sup>	[71]	
	-	79.67 <sup>c</sup>	[6]	
	-	80.10 <sup>c</sup>	[12]	
Phenanthrene	50.6	-	[32]	95.2±1.7
	51.40	-	[23]	
	-	93.52 <sup>c</sup>	[40]	
	-	<i>97.2</i>	[34]	
	-	<i>111.6</i>	[31]	
Anthracene	49.6	-	[32]	93.6±1.7
	49.51	-	[27]	
	-	93.95 <sup>c</sup>	[40]	
	-	<i>89.9</i>	[34]	
	-	<i>88.1</i>	[31]	
Pyrene	53.75	-	[77]	96.0±1.7
	-	94.03 <sup>b</sup>	[42]	
	-	96.3 <sup>b</sup>	[67]	
	-	<i>100.9</i>	[34]	
	-	<i>96.2</i>	[31]	
	-	<i>96.4</i>	[42]	
Fluoranthene	55.11	-	[77]	99.1±1.8
	-	<i>100.5</i>	[31]	
	-	<i>88.6</i>	[5]	

*continued*

<sup>a</sup>Values for benzene refer to the liquid, not to the solid crystal

<sup>b</sup>From vibrational assignment.

<sup>c</sup>From vapor pressure measurements.

Table 2.5: *continued*

Substance	$S_{(\text{cr})}^{\circ}$ (cal K <sup>-1</sup> mol <sup>-1</sup> )	$S_{(\text{g})}^{\circ}$ (cal K <sup>-1</sup> mol <sup>-1</sup> )	Ref.	$S_{\text{B3LYP},(\text{g})}^{\circ}$ (cal K <sup>-1</sup> mol <sup>-1</sup> )
Triphenylene	60.87	-	[77]	108.5±3.7
	-	107.9	[31]	
	-	97.1	[74]	
Naphthacene	51.48	-	[78]	107.0±2.8
	-	91.0	[34]	
	-	95.0	[74]	
Perylene	-	117.9	[25]	112.0±6.0
	63.23	-	[78]	
	-	117.5	[34]	
	-	115.7	[31]	
	-	116.0	[25]	
Coronene	67.13	-	[78]	112.6±2.8
	-	115.3	[31]	
	-	109.0	[74]	
C <sub>60</sub>	102.1	-	[17]	128.8±3.2
	-	162.0	[44]	
	-	127.6	[1]	
	-	133.8	[57]	
C <sub>70</sub>	108.2	-	[17]	147.8±3.9
	-	144.6	[1]	
	-	171.4	[62]	
	-	143.8	[57]	

the PAHs contain only six-membered rings, and the largest PAH studied contains 11 rings. All the PAHs considered in this study follow the Isolated Pentagon Rule (IPR), that is, none have fused five-membered rings. Figure 2-1 shows some typical PAHs included in this work. Quantum chemical calculations were carried out using the Gaussian 98 suite of programs [24]. The geometries were fully optimized at the B3LYP level using 6-31G(d) basis set and the stationary points were characterized by computing the second derivatives, namely the force constant matrix, at the same level. B3LYP/6-31G(d) provides accurate geometries and it has been shown that larger basis sets do not improve the geometries [2]. For C<sub>60</sub> and C<sub>70</sub> fullerenes, the B3LYP/6-31G(d) geometries from Cioslowski [13] and the frequencies calculated at this same level by Schettino et al. were used [64, 63]. A frequency scaling factor of 0.9613 has been employed for the calculation of the vibrational partition function, the zero point energy, entropy and heat capacities. The scaling factor used for the frequencies of C<sub>60</sub> and C<sub>70</sub> fullerenes was 0.98, as recommended by Schettino et al. [64, 63]. Uncertainties were assigned to the calculated entropies by assuming an uncertainty of  $\pm 20$  cm<sup>-1</sup> in all the computed frequencies and making the worst case assumption that all the frequencies are either too high or too low. This assumption is a very conservative estimation of the error in the quantum calculations.

Atomization, isodesmic and homodesmic reactions were tested for the calculation of the  $\Delta H_f^\circ$  from the absolute energy. It is known in the literature that the use of such reaction schemes helps in the cancellation of systematic errors that arise in quantum chemical calculations due to the incomplete capture of the electron correlation energy [56, 28]. Since the set of species that can be included in the isodesmic/homodesmic reactions may vary, these reactions do not lead to unique values for the enthalpy of formation. Given that the aim of this work is to provide a *consistent* method for the estimation of thermochemical properties of PAHs, it is important to establish one standard reaction scheme, through which the  $\Delta H_f^\circ$  of all the PAH should be calculated. We evaluate the quality of a reaction scheme by comparing its prediction of the  $\Delta H_f^\circ$  of a PAH with known experimental data.

In atomization reactions, the absolute energy of the PAH is compared to the

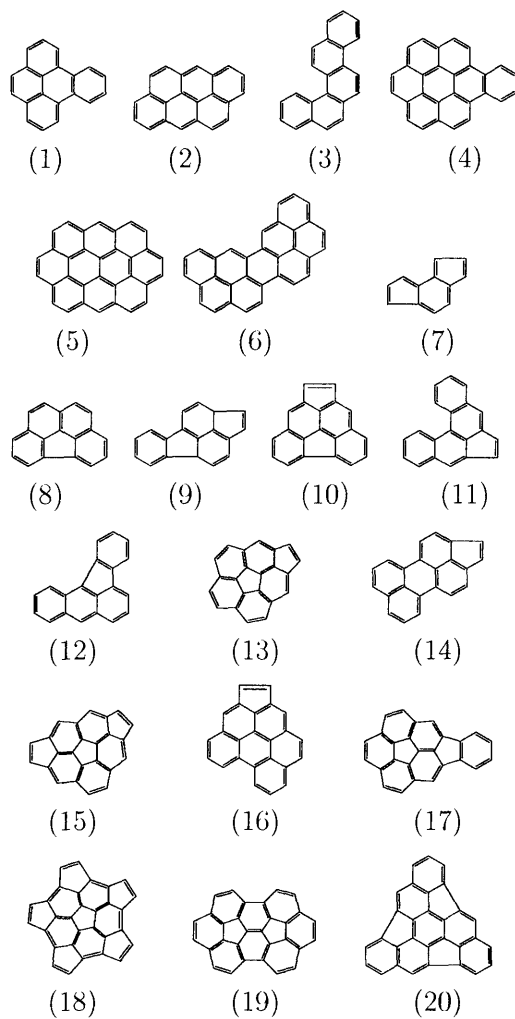


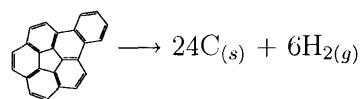
Figure 2-1: Some typical PAHs included in this work.

absolute energy of carbon and hydrogen atoms, which have known  $\Delta H_f^\circ$ . We included bond additivity corrections and spin-orbit corrections [56]. It is expected that if species that are more similar to the molecule whose  $\Delta H_f^\circ$  needs to be calculated were employed in the reaction scheme, a better cancellation of errors would occur. The reason is that the amount of electron correlation energy that is recovered in a quantum calculation should be similar for molecules with similar bonding characteristics.

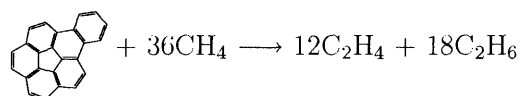
Isodesmic reactions conserve the number of types of bonds, and should thus be an improvement on a simple atomization reaction. In using isodesmic reactions, we treat the PAH as a non-delocalized molecule. Ethane accounts for the C-C single bonds, ethylene for the double bonds and methane for the C-H bonds. Further enhancement in the calculation of  $\Delta H_f^\circ$  should be provided by homodesmic reactions, which in addition to the types of bonds, also conserve the hybridization of the atoms in the bond (in PAHs all the carbons are  $sp^2$ ). The first set of homodesmic reactions studied (Homodesmic1) uses 1,3-butadiene to account for the single bonds and ethylene for the double bonds. The second set of homodesmic reactions (Homodesmic2) tries to capture the effect of electron delocalization and involves only aromatic molecules, using benzene to account for the carbon atoms that are bonded to a hydrogen, naphthalene to account for the carbons that belong to two or three aromatic rings, and acenaphthalene to account for the carbons that belong to five-membered rings. The third set of homodesmic reactions tested (Homodesmic3) employs phenanthrene and corannulene in addition to the molecules used in Homodesmic2. Phenanthrene accounts for rings that make up the bay region of a PAH, while corannulene accounts for the structure where a five-membered ring is completely surrounded by six-membered rings. Finally, the fourth homodesmic reaction scheme tested employs the same reference molecules as the Homodesmic3 scheme, but uses  $1/12C_{60}$  instead of corannulene to account for five-membered rings completely surrounded by six-membered rings. Figure 2-2 exemplifies the isodesmic and homodesmic reactions used.

The comparison between the  $\Delta H_f^\circ$  calculated from total energies by the various reaction schemes and the available experimental data is shown in Table 2.6, along with the mean average deviation (MAD) and root mean square error (RMS) for each reac-

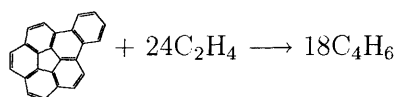
Atomization reaction



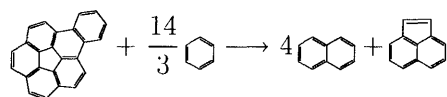
Isodesmic reaction



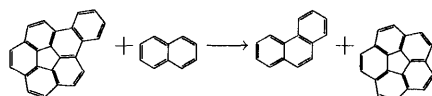
Homodesmic1 reaction



Homodesmic2 reaction



Homodesmic3 reaction



Homodesmic4 reaction

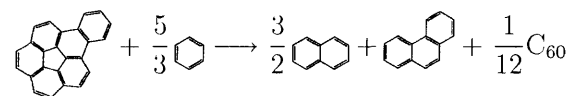


Figure 2-2: Example of each of the reaction schemes tested for the calculation of the  $\Delta H_f^\circ$  from the absolute energy.

tion scheme. The MAD and RMS do not include the errors of benzo[k]fluoranthene. The atomization reaction scheme provided enthalpies of formation that are remarkably close to the experimental values, except for the C<sub>60</sub> and C<sub>70</sub> fullerenes. We believe that this performance is fortuitous, since previous studies with other delocalized systems showed that atomization reactions do not perform reliably [72]. Among the other reaction schemes, the performance generally improved as the similarity between the molecules involved in the reaction scheme and the PAH with unknown  $\Delta H_f^\circ$  increased. As expected, the  $\Delta H_f^\circ$  calculated through the homodesmic reaction scheme involving only aromatic molecules (Homodesmic2) provided a more extensive error cancellation compared to the isodesmic and the Homodesmic1 reaction scheme. However, Homodesmic2 was not able to capture the stabilization provided by bay areas. It systematically overpredicts the  $\Delta H_f^\circ$  for the benzenoid ring PAHs that contain bay area(s). Moreover, this scheme overpredicts the  $\Delta H_f^\circ$  of corannulene by 10 kcal mol<sup>-1</sup>.

Homodesmic3 and Homodesmic4 reaction schemes both correct for the systematic overprediction of the  $\Delta H_f^\circ$  of PAHs with bay areas by including phenanthrene as a reference molecule. They differ in their handling of structures in which a five-membered ring is completely surrounded by six-membered rings. The  $\Delta H_f^\circ$  for both C<sub>60</sub> and C<sub>70</sub> predicted by Homodesmic3 are almost 100 kcal mol<sup>-1</sup> too low, indicating that the use of corannulene as a reference structure is not adequate. The use of C<sub>60</sub> rather than corannulene as a reference structure in Homodesmic4 leads to a  $\Delta H_f^\circ$  of C<sub>70</sub> that agrees very well with the experimental value. However, the  $\Delta H_f^\circ$  of corannulene is overpredicted by 7 kcal mol<sup>-1</sup>. We note that there is only one experimental value for the  $\Delta H_f^\circ$  of corannulene and all the tested reaction schemes (with the exception of the isodesmic scheme) consistently lead to a  $\Delta H_f^\circ$  that is higher than this experimental value (by 7 to 10 kcal mol<sup>-1</sup>). Unfortunately there are no other  $\Delta H_{f,\text{exp}}^\circ$  for PAHs similar to corannulene for us to make a definitive judgement of whether the  $\Delta H_{f,\text{exp}}^\circ$  for the latter is in error or not. On the other hand, there are a couple of consistent experimental measurements of the  $\Delta H_f^\circ$  of C<sub>60</sub>. We chose to use the Homodesmic4 reaction scheme to consistently calculate  $\Delta H_f^\circ$  of all



Table 2.6: Comparison of the  $\Delta H_f^\circ$  predicted by each of the reaction schemes to the experimental  $\Delta H_f^\circ$  for the 16 PAH for which these values are available. In (kcal mol<sup>-1</sup>).

	Formula	$\Delta H_{f,\text{exp}}^\circ$	$\Delta H_{f,\text{rxn scheme}}^\circ - \Delta H_{f,\text{exp}}^\circ$					
			A <sup>a</sup>	I <sup>b</sup>	H1 <sup>c</sup>	H2 <sup>d</sup>	H3 <sup>e</sup>	H4 <sup>f</sup>
Benzene	C <sub>6</sub> H <sub>6</sub>	19.8	1.1	-4.3	-2.0	0 <sup>g</sup>	0 <sup>g</sup>	0 <sup>g</sup>
Naphthalene	C <sub>10</sub> H <sub>8</sub>	36.0	-0.3	-7.6	-2.9	0 <sup>g</sup>	0 <sup>g</sup>	0 <sup>g</sup>
Phenanthrene	C <sub>14</sub> H <sub>10</sub>	48.1	2.3	-7.9	-0.8	3.0	0 <sup>g</sup>	0 <sup>g</sup>
Anthracene	C <sub>14</sub> H <sub>10</sub>	55.2	-0.3	-10.1	-3.0	0.8	0.8	0.8
Pyrene	C <sub>16</sub> H <sub>10</sub>	53.9	-0.4	-10.6	-1.9	2.1	2.1	2.1
Triphenylene	C <sub>18</sub> H <sub>12</sub>	65.5	1.7	-11.1	-1.7	3.0	-0.1	-0.1
Benzo[c]phenanthrene	C <sub>18</sub> H <sub>12</sub>	69.6	2.9	-9.9	0.5	4.3	-1.7	-1.7
Benz[a]anthracene	C <sub>18</sub> H <sub>12</sub>	69.6	-0.7	-14.2	-4.7	0.0	-3.0	-3.0
Chrysene	C <sub>18</sub> H <sub>12</sub>	63.0	3.4	-9.5	0.0	4.7	-1.2	-1.2
Naphthacene	C <sub>18</sub> H <sub>12</sub>	79.3	-3.1	-15.9	-6.5	-1.8	-1.8	-1.8
Perylene	C <sub>20</sub> H <sub>12</sub>	76.4	-0.5	-13.1	-2.0	2.9	-0.1	-0.1
Coronene	C <sub>24</sub> H <sub>12</sub>	73.6	-3.4	-18.2	-4.0	1.4	1.4	1.4
Acenaphthalene	C <sub>12</sub> H <sub>8</sub>	61.7	2.1	-6.0	0.3	0 <sup>g</sup>	0 <sup>g</sup>	0 <sup>g</sup>
Fluoranthene	C <sub>16</sub> H <sub>10</sub>	69.8	-0.6	-12.2	-3.6	-2.9	-2.9	-2.9
Corannulene	C <sub>20</sub> H <sub>10</sub>	110.2	9.5	-2.8	9.0	10.2	0 <sup>g</sup>	7.3
Benzo[k]fluoranthene	C <sub>20</sub> H <sub>12</sub>	(71.0)	(12.0)	(-1.5)	(9.6)	(11.1)	(11.1)	(11.1)
C <sub>60</sub>	C <sub>60</sub>	604.6	40.2	31.5	68.2	40.3	-87.8	0 <sup>g</sup>
C <sub>70</sub>	C <sub>70</sub>	658.5	31.3	21.3	64.0	37.5	-90.5	-2.7
Errors excluding the C <sub>60</sub> and C <sub>70</sub> fullerenes								
MAD <sup>h</sup>			2.1	10.2	2.8	2.4	0.9	1.4
RMS <sup>h</sup>			3.1	11.0	3.7	3.6	1.2	1.2
Errors including the C <sub>60</sub> and C <sub>70</sub> fullerenes								
MAD <sup>h</sup>			6.1	12.1	10.2	6.8	11.3	1.4
RMS <sup>h</sup>			12.7	13.8	22.9	13.7	30.6	2.2

<sup>a</sup>Atomization reaction

<sup>b</sup>Isodesmic reaction

<sup>c</sup>Homodesmic1 reaction

<sup>d</sup>Homodesmic2 reaction

<sup>e</sup>Homodesmic3 reaction

<sup>f</sup>Homodesmic4 reaction

<sup>g</sup>This PAH is a reference molecule for this homodesmic scheme

<sup>h</sup>Does not include errors for benzo[k]fluoranthene

the PAHs included in this study.

The reported experimental  $\Delta H_f^\circ$  of benzo[k]fluoranthene is 71.0 kcal mol<sup>-1</sup> [21]. However, all the reaction schemes (again, with the exception of the isodesmic scheme) consistently predict its  $\Delta H_f^\circ$  to be about 10 kcal mol<sup>-1</sup> higher. Furthermore, examination of the experimental enthalpies of formation of the other PAHs made us skeptical of the  $\Delta H_{f,\text{exp}}^\circ$  of benzo[k]fluoranthene. For instance, it is only 1.8 kcal mol<sup>-1</sup> higher than the  $\Delta H_f^\circ$  of fluoranthene, which has one less benzene ring. By comparison, fluoranthene’s  $\Delta H_f^\circ$  is in turn 7 kcal mol<sup>-1</sup> higher than the  $\Delta H_f^\circ$  of acenaphthalene, which has one benzene ring less than fluoranthene. This led us to suspect that the experimental  $\Delta H_f^\circ$  of benzo[k]fluoranthene is too low and to label it with a ‘D’ (see Table 2.2).

The choice of the appropriate reaction scheme is crucial, since the  $\Delta H_f^\circ$  calculated using different reference species can disagree considerably. Since high-level quantum chemical calculations for systems containing more than 10 heavy atoms are still very computationally expensive, we must rely on the very scarce experimental data to determine the quality of the homodesmic reaction schemes. By comparisons with the available experimental  $\Delta H_f^\circ$  for PAHs and fullerenes, we determined that, given the currently available experimental data, Homodesmic4 is the most accurate reaction scheme.

The biggest discrepancies between the experimental  $\Delta H_f^\circ$  and the heats of formation calculated through the Homodesmic4 reaction scheme are for corannulene and for benzo[k]fluoranthene. The  $\Delta H_{f,\text{exp}}^\circ$  are considerably lower than the  $\Delta H_{f,\text{homo}}^\circ$ . Kobayashi et al. measured the experimental  $\Delta H_f^\circ$  of corannulene [36]. They also measured the  $\Delta H_{f,(\text{cr})}^\circ$  of C<sub>60</sub> and of C<sub>70</sub> [37], and both values are also lower (by  $\sim 10$  kcal mol<sup>-1</sup> and  $\sim 40$  kcal mol<sup>-1</sup> respectively) than currently accepted values. As discussed previously, we have reasons to suspect the value of the  $\Delta H_{f,\text{exp}}^\circ$  of benzo[k]fluoranthene, which was measured by Diogo et al. [21]. Their group also measured the  $\Delta H_{f,(\text{cr})}^\circ$  of C<sub>60</sub> [20] and of C<sub>70</sub> [19]. Their value for the  $\Delta H_{f,(\text{cr})}^\circ$  of C<sub>60</sub> is  $\sim 10$  kcal mol<sup>-1</sup> than the currently accepted value, whereas their  $\Delta H_{f,(\text{cr})}^\circ$  for C<sub>70</sub> is close to the currently accepted value. Although these comparisons are in no way a proof that the  $\Delta H_{f,\text{exp}}^\circ$  for

corannulene and for benzo[k]fluoranthene are wrong, they strengthen the case for re-measuring these experimental values, and give us confidence to use our Homodesmic4 reaction scheme to obtain the  $\Delta H_f^\circ$  of other PAHs.

From now on we will refer to the Homodesmic4 reaction scheme as simply the Homodesmic reaction scheme, and  $\Delta H_{f,\text{homo}}^\circ$  refers to the enthalpy of formation calculated through this homodesmic reaction scheme from absolute energies obtained at the B3LYP/6-31G(d) level of theory.

## 2.4 Results and Discussion

An extensive assessment of the available experimental data was performed. Unfortunately there are very few experimental data for polycyclic aromatic molecules. Heats of formation in the gas phase are calculated from the heats of formation of the crystal ( $\Delta H_{f,(\text{cr})}^\circ$ ) measured through combustion experiments and from heats of sublimation ( $\Delta H_{\text{subl}}^\circ$ ) calculated from vapor pressure measurements. For many of the PAHs only one experimental value for  $\Delta H_{f,(\text{cr})}^\circ$  and/or  $\Delta H_{\text{subl}}^\circ$  is available. When more than one  $\Delta H_{f,(\text{cr})}^\circ$  or  $\Delta H_{\text{subl}}^\circ$  are available, it is not uncommon for them to differ from each other by a couple of kcal mol<sup>-1</sup>.

We developed a homodesmic reaction scheme that closely emulates the experimental  $\Delta H_f^\circ$  of the PAHs. The estimation method for the enthalpy of formation that we propose can at best be as good as the  $\Delta H_{f,\text{homo}}^\circ$  given by the homodesmic reaction scheme.

“Experimental” values for the entropies were calculated from the third law method based on experimental heat capacity and vapor pressure data. As a comparison with the experimental values, the entropies calculated from the B3LYP/6-31G(d) are listed in the last column of Table 2.5. Except for naphthalene, the entropy calculated from quantum chemistry is within the uncertainty of the experimental entropy. We conclude that the  $S_{298}^\circ$  calculated at the B3LYP/6-31G(d) level are at least as reliable as the available experimental values.



# Bibliography

- [1] J. Abrefah, D. R. Olander, M. Balooch, and W. J. Siekhaus. Vapor-pressure of buckminsterfullerene. *Applied Physics Letters*, 60(11):1313–1314, 1992.
- [2] C. W. Bauschlicher. A comparison of the accuracy of different functionals. *Chemical Physics Letters*, 246:40–44, 1995.
- [3] H. D. Beckhaus, C. Ruechardt, M. Kao, F. Diederich, and C. S. Foote. Stability of buckminsterfullerene C<sub>60</sub>: experimental determination of the heat of formation. *Angewandte Chemie*, 104(1):69–70 (See also *Angew. Chem., Int. Ed. Engl.*, 1992, 31(1), 63–4), 1992.
- [4] H. D. Beckhaus, S. Verevkin, C. Ruechardt, F. Diederich, C. Thilgen, H. U. ter Meer, H. Mohn, and W. Mueller. C<sub>70</sub> is as stable as C<sub>60</sub>: experimental determination of the heat of formation of C<sub>70</sub>. *Angewandte Chemie*, 106(9):1033–5 (See also *Angew. Chem., Int. Ed. Engl.*, 1994, 33(9), 996–8), 1994.
- [5] R. H. Boyd, R. L. Christensen, and R. Pua. The heats of combustion of acenaphthalene, acenaphthylene, and fluoranthene. Strain and delocalization in bridged naphthalenes. *Journal of the American Chemical Society*, 87(16):3554–3559, 1965.
- [6] S. S. Chen, S. A. Kudchadker, and R. C. Wilhoit. Thermodynamic properties of normal and deuterated naphthalene. *Journal of Physical and Chemical Reference Data*, 8(2):527–535, 1979.
- [7] J. Chickos, G. Nichols, J. Wilson, J. Orf, P. Webb, and J. Wang. A protocol for deriving values for  $\Delta_{fus}H_m(298.15K)$  and  $\Delta_{vap}H_m(298.15K)$ . Applications in obtaining  $\Delta_{subl}H_m(298.15K)$ . In M. E. Minas da Piedade, editor, *Energetics of Stable Molecules and Reactive Intermediates*, volume 535 of *Series C: Mathematical and Physical Sciences*, pages 177–202. Kluwer Academic Publishers, Dordrecht, 1998.
- [8] J. S. Chickos and W. E. Acree. Enthalpies of sublimation of organic and organometallic compounds. 1910–2001. *Journal of Physical and Chemical Reference Data*, 31(2):537–698, 2002.
- [9] J. S. Chickos, D. G. Hesse, and J. F. Liebman. A group additivity approach for the estimation of heat capacities of organic liquids and solids at 298K. *Structural Chemistry*, 4(4):261–269, 1993.

- [10] J. S. Chickos, S. Hosseini, D. G. Hesse, and J. F. Liebman. Heat capacity corrections to a standard state: A comparison of new and some literature methods for organic liquids and solids. *Structural Chemistry*, 4(4):271–278, 1993.
- [11] J. S. Chickos, P. Webb, G. Nichols, T. Kiyobayashi, P.-C. Cheng, and L. Scott. The enthalpy of vaporization and sublimation of corannulene, coronene, and perylene at  $t=298.15\text{k}$ . *Journal of Chemical Thermodynamics*, 34:1195–2006, 2002.
- [12] R. D. Chirico, S. E. Knipmeyer, A. Nguyen, and W. V. Steele. The thermodynamic properties to the temperature 700 K of naphthalene and of 2,7-dimethylnaphthalene. *Journal of Chemical Thermodynamics*, 25(12):1461–94, 1993.
- [13] J. Cioslowski, N. Rao, and D. Moncrieff. Standard enthalpies of formation of fullerenes and their dependence on structural motifs. *Journal of the American Chemical Society*, 122:8265–8270, 2000.
- [14] D. J. Coleman and G. Pilcher. Heats of combustion of biphenyl, bibenzyl, naphthalene, anthracene and phenanthrene. *Transactions of the Faraday Society*, 62(4):821–827, 1966.
- [15] J. D. Cox and G. Pilcher. *Thermochemistry of organic and organometallic compounds*. Academic Press, London, 1970.
- [16] M. J. S. Dewar and C. Llano. Ground states of conjugated molecules. XI. Improved treatment of hydrocarbons. *Journal of the American Chemical Society*, 91(4):789–795, 1969.
- [17] V. V. Diky and G. J. Kabo. Thermodynamic properties of  $\text{C}_{60}$  and  $\text{C}_{70}$  fullerenes. *Russian Chemical Reviews*, 69(2):95–104, 2000.
- [18] H. P. Diogo and M. E. M. Da Piedade. Enthalpies of formation of  $\text{C}_{60}$  and  $\text{C}_{70}$  in the crystalline state: an unfinished tale? *Proceedings - Electrochemical Society*, 98-8(Recent Advances in the Chemistry and Physics of Fullerenes and Related Materials):627–635, 1998.
- [19] H. P. Diogo, M. E. Minas Da Piedade, A. D. Darwish, and T. J. S. Dennis. Enthalpy of formation of  $\text{C}_{70}$ . *Journal of Physics and Chemistry of Solids*, 58(11):1965–1971, 1997.
- [20] H. P. Diogo, M. E. Minas da Piedade, T. J. S. Dennis, J. P. Hare, H. W. Kroto, R. Taylor, and D. R. M. Walton. Enthalpies of formation of buckminsterfullerene ( $\text{C}_{60}$ ) and of the parent ions  $\text{C}_{60}^+$ ,  $\text{C}_{60}^{2+}$ ,  $\text{C}_{60}^{3+}$  and  $\text{C}_{60}$ . *Journal of the Chemical Society, Faraday Transactions*, 89(19):3541–4, 1993.
- [21] H. P. Diogo and M. E. M. Piedade. Enthalpy of formation of benzo[k]fluoranthene. *Journal of Chemical Thermodynamics*, 34:173–184, 2002.

- [22] O. V. Dorofeeva, L. V. Gurvich, and S. J. Cyvin. On calculation of thermodynamic properties of polycyclic aromatic hydrocarbons. *Thermochimica Acta*, 102:59-66, 1986.
- [23] H. L. Finke, J. F. Messerly, S. H. Lee, A. G. Osborn, and D. R. Douslin. Comprehensive thermodynamic studies of seven aromatic hydrocarbons. *Journal of Chemical Thermodynamics*, 9:937-956, 1977.
- [24] M. J. Frisch, G. W. Trucks, H. B. Schlegel, G. E. Scuseria, M. A. Robb, J. R. Cheeseman, V. G. Zakrzewski, J. A. Montgomery, J., R. E. Stratmann, J. C. Burant, S. Dapprich, J. M. Millam, A. D. Daniels, K. N. Kudin, M. C. Strain, O. Farkas, J. Tomasi, V. Barone, M. Cossi, R. Cammi, B. Mennucci, C. Pomelli, C. Adamo, S. Clifford, J. Ochterski, G. A. Petersson, P. Y. Ayala, Q. Cui, K. Morokuma, N. Rega, P. Salvador, J. J. Dannenberg, D. K. Malick, A. D. Rabuck, K. Raghavachari, J. B. Foresman, J. Cioslowski, J. V. Ortiz, A. G. Baboul, B. B. Stefanov, G. Liu, A. Liashenko, P. Piskorz, I. Komaromi, R. Gomperts, R. L. Martin, D. J. Fox, T. Keith, M. A. Al-Laham, C. Y. Peng, A. Nanayakkara, M. Challacombe, P. M. W. Gill, B. Johnson, W. Chen, M. W. Wong, J. L. Andres, C. Gonzalez, M. Head-Gordon, E. S. Replogle, and J. A. Pople. *Gaussian 98*, 2002.
- [25] R. Gigli, L. Malaspina, and G. Bardi. Vapor-pressure and sublimation enthalpy of perylene. *Annali Di Chimica*, 63(9-10):627-633, 1973.
- [26] W. D. Good. The enthalpies of formation of some bridged-ring polynuclear aromatic hydrocarbons. *Journal of Chemical Thermodynamics*, 10:553-558, 1978.
- [27] P. Goursot, H. L. Girdhar, and Jr. Westrum, E. F. Thermodynamics of polynuclear aromatic molecules. III. Heat capacities and enthalpies of fusion of anthracene. *Journal of Physical Chemistry*, 74(12):2538-41, 1970.
- [28] W. J. Hehre, R. Ditchfield, L. Radom, and J. A. Pople. Molecular orbital theory of the electronic structure of organic compounds. V. Molecular theory of bond separation. *Journal of the American Chemical Society*, 92(16):4796-4801, 1970.
- [29] W. C. Herndon. Thermochemical parameters for benzenoid hydrocarbons. *Thermochimica Acta*, 8:225-237, 1974.
- [30] W. C. Herndon, P. U. Biedermann, and I. Agranat. Molecular structure parameters and predictions of enthalpies of formation for catacondensed and peri-condensed polycyclic aromatic hydrocarbons. *Journal of Organic Chemistry*, 63:7445-7448, 1998.
- [31] H. Hoyer and W. Peperle. Dampfdruckmessungen an organischen substanzen und ihre sublimationswärmen. *Berichte der Bunsen-Gesellschaft für Physikalische Chemie*, 62(1):61-66, 1958.

- [32] H. M. Huffman, G. S. Parks, and M. Barmore. Thermal data on organic compounds. X. Further studies on the heat capacities, entropies and free energies of hydrocarbons. *Journal of the American Chemical Society*, 53:3876–3888, 1931.
- [33] H. M. Huffman, G. S. Parks, and A. D. Daniels. Thermal data on organic compounds. VII. The heat capacities, entropies and free energies of twelve aromatic hydrocarbons. *Journal of the American Chemical Society*, 52:1547, 1930.
- [34] H. Inokuchi, S. Shiba, T. Handa, and H. Akamatu. Heats of sublimation of condensed polynuclear aromatic hydrocarbons. *Bulletin of the Chemical Society of Japan*, 25(5):299–302, 1952.
- [35] T. Kiyobayashi. *PhD Dissertation*. Phd, Osaka University, 1996.
- [36] T. Kiyobayashi, Y. Nagano, M. Sakiyama, K. Yamamoto, P.-C. Cheng, and L. T. Scott. Formation enthalpy of corannulene: Microbomb combustion calorimetry. *Journal of the American Chemical Society*, 117(11):3270–1, 1995.
- [37] T. Kiyobayashi and M. Sakiyama. Combustion calorimetric studies on C<sub>60</sub> and C<sub>70</sub>. *Fullerene Science and Technology*, 1(3):269–73, 1993.
- [38] V. P. Kolesov, S. M. Pimenova, V. K. Pavlovich, N. B. Tamm, and A. A. Kurskaya. Enthalpies of combustion and formation of fullerene C<sub>60</sub>. *Journal of Chemical Thermodynamics*, 28:1121–1125, 1996.
- [39] C. G. Kruif. Enthalpies of sublimation and vapour pressures of 11 polycyclic hydrocarbons. *Journal of Chemical Thermodynamics*, 12(3):243–248, 1980.
- [40] S. A. Kudchadker, A. P. Kudchaker, and B. J. Zwolinski. Chemical thermodynamic properties of anthracene and phenanthrene. *Journal of Chemical Thermodynamics*, 11:1051–1059, 1979.
- [41] A. Magnus, H. Hartmann, and F. Becker. Verbrennungswärmen und Resonanzenergien von mehrkernigen aromatischen Kohlenwasserstoffen. *Zeitschrift fr Physikalische Chemie*, 197:75–91, 1951.
- [42] L. Malaspina, G. Bardi, and R. Gigli. Simultaneous determination by Knudsen-effusion microcalorimetric technique of vapor-pressure and enthalpy of vaporization of pyrene and 1,3,5-triphenylbenzene. *Journal of Chemical Thermodynamics*, 6(11):1053–1064, 1974.
- [43] L. Malaspina, R. Gigli, and G. Bardi. Microcalorimetric determination of the enthalpy of sublimation of benzoic acid and anthracene. *The Journal of Chemical Physics*, 59(1):387–394, 1973.
- [44] C. K. Mathews, M. Sai Baba, T. S. L. Narasimhan, R. Balasubramanian, N. Sivaraman, T. G. Srinivasan, and P. R. V. Rao. Vaporization studies on buckminsterfullerene. *Journal of Physical Chemistry*, 96:3566–3568, 1992.



- [45] J. P. McCullough, H. L. Finke, J. F. Messerly, S. S. Todd, T. C. Kincheloe, and G. Waddington. The low-temperature thermodynamic properties of naphthalene, 1-methylnaphthalene, 2-methylnaphthalene, 1,2,3,4-tetrahydronaphthalene, trans-decahydronaphthalene, and cis-decahydronaphthalene. *Journal of Physical Chemistry*, 61:1105–1116, 1957.
- [46] R. M. Metzger, C. S. Kuo, and E. S. Arafat. A semi-micro rotating-bomb combustion calorimeter. *Journal of Chemical Thermodynamics*, 15:841–851, 1983.
- [47] E. Morawetz. Enthalpies of vaporization for a number of aromatic compounds. *Journal of Chemical Thermodynamics*, 4:455–460, 1972.
- [48] Y. Nagano. Micro-combustion calorimetry of coronene. *Journal of Chemical Thermodynamics*, 32(8):973–977, 2000.
- [49] Y. Nagano. High-precision micro-combustion calorimetry of anthracene. *Journal of Chemical Thermodynamics*, 33(4):377–388, 2001.
- [50] Y. Nagano. Standard enthalpies of formation of phenanthrene and naphthacene. *Journal of Chemical Thermodynamics*, 34:377–383, 2002.
- [51] K. Nass, D. Lenoir, and A. Kettrup. Calculation of the thermodynamic properties of polycyclic aromatic hydrocarbons by an incremental procedure. *Angewandte Chemie- International Edition*, 34(16):1735–1736, 1995.
- [52] V. Oja and E. M. Suuberg. Vapor pressures and enthalpies of sublimation of polycyclic aromatic hydrocarbons and their derivatives. *Journal of Chemical and Engineering Data*, 43(3):486–492, 1998.
- [53] G. D. Oliver, M. Eaton, and H. M. Huffman. The heat capacity, heat of fusion, and entropy of benzene. *Journal of the American Chemical Society*, 70:1502–5, 1948.
- [54] C. Pan, M. P. Sampson, Y. Chai, R. H. Hauge, and J. L. Margrave. Heats of sublimation from a polycrystalline mixture of C<sub>60</sub> and C<sub>70</sub>. *Journal of Physical Chemistry*, 95:2944–2946, 1991.
- [55] J. B. Pedley, R. D. Naylor, and S. P. Kirby. *Thermochemical data of organic compounds*. Chapman and Hall, London, 2nd edition, 1986.
- [56] G. A. Petersson, D. K. Malick, W. G. Wilson, J. W. Ochterski, J. A. Montgomery, and M. J. Frisch. Calibration and comparison of the Gaussian-2, complete basis set, and density functional methods for computational thermochemistry. *Journal of Chemical Physics*, 109(24):10570–10579, 1998.
- [57] V. Piacente, G. Gigli, P. Scardala, A. Giustini, and G. Bardi. Vapor pressure of C<sub>70</sub> fullerene. *Journal of Physical Chemistry*, 100:9815–9819, 1996.

- [58] V. Piacente, G. Gigli, P. Scardala, A. Giustini, and D. Ferro. Vapor pressure of  $C_{60}$  buckminsterfullerene. *Journal of Physical Chemistry*, 99:14052–14057, 1995.
- [59] S. M. Pimenova, S. V. Melkhanova, and V. P. Kolesov. Thermochemical determination of the enthalpies of combustion and formation of fullerene  $C_{70}$ . *Journal of Chemical Thermodynamics*, 35(1):189–193, 2003.
- [60] E. J. Prosen, W. H. Johnson, and F. D. Rossini. Heats of combustion and formation at 25 °C of the alkylbenzenes through  $C_{10}H_{14}$ , and of the higher normal monoalkylbenzenes. *Journal of Research of the National Bureau of Standards*, 36:455–461, 1946.
- [61] R. Sabbah, X. W. An, J. S. Chickos, M. L. P. Leitao, M. V. Roux, and L. A. Torres. Reference materials for calorimetry and differential thermal analysis. *Thermochimica Acta*, 331(2):93–204, 1999.
- [62] M. Sai Baba, T. S. Lakshmi Narasimhan, R. Balasubramanian, N. Sivaraman, and C. K. Mathews. Studies on the thermodynamics of the fullerene  $C_{60}$ - $C_{70}$  binary system. *Journal of Physical Chemistry*, 98(4):1333–40, 1994.
- [63] V. Schettino, M. Pagliai, and G. Cardini. The infrared and raman spectra of fullerene  $C_{70}$ . dft calculations and correlations with  $C_{60}$ . *Journal of Physical Chemistry A*, 106(9):1815–1823, 2002.
- [64] V. Schettino, M. Pagliai, L. Ciabini, and G. Cardini. The vibrational spectrum of fullerene  $C_{60}$ . *Journal of Physical Chemistry A*, 105(50):11192–11196, 2001.
- [65] J. M. Schulman, R. C. Peck, and R. L. Disch. Ab initio heats of formation of medium-sized hydrocarbons. 11. the benzenoid aromatics. *Journal of the American Chemical Society*, 111:5675–5680, 1989.
- [66] S. W. Slayden and J. F. Liebman. The energetics of aromatic hydrocarbons: An experimental thermochemical perspective. *Chemical Reviews*, 101:1541–1566, 2001.
- [67] N. K. Smith, Jr. Stewart, R. C., A. G. Osborn, and D. W. Scott. Pyrene: Vapor pressure, enthalpy of combustion, and chemical thermodynamic properties. *Journal of Chemical Thermodynamics*, 12:919–926, 1980.
- [68] J. C. Southard and F. G. Brickwedde. Low temperature specific heats. i. an improved calorimeter for use from 14 to 300 k. the heat capacity and entropy of naphthalene. *Journal of the American Chemical Society*, 55:4378–4384, 1933.
- [69] W. V. Steele, R. D. Chirico, A. Nguyen, I. A. Hossenlopp, and N. K. Smith. Determination of ideal-gas enthalpies of formation for key compounds. *AIChE Symposium Series*, 86:138–154, 1990.

- [70] W. V. Steele, R. D. Chirico, N. K. Smith, W. E. Billups, P. R. Elmore, and A. E. Wheeler. Standard enthalpy of formation of buckminsterfullerene. *Journal of Physical Chemistry*, 96(12):4731–3, 1992.
- [71] D. R. Stull, E. F. Westrum, J., and G. C. Sinke. *The Chemical Thermodynamics of Organic Compounds*. John Wiley & Sons, New York, 1969.
- [72] R. Sumathi and W. H. Green Jr. Thermodynamic properties of ketenes: Group additivity values from quantum chemical calculations. *Journal of Physical Chemistry A*, 106:7937–7949, 2002.
- [73] A. Tokmakoff, D. R. Haynes, and S. M. George. Desorption kinetics of multilayers of C<sub>60</sub> fullerene from aluminum oxide(0001). *Chemical Physics Letters*, 186(4-5):450–5, 1991.
- [74] N. Wakayama and H. Inokuchi. Heats of sublimation of polycyclic aromatic hydrocarbons and their molecular packings. *Bulletin of the Chemical Society of Japan*, 40:2267–2271, 1967.
- [75] K. L. Wolf and H. Weghofer. Heat of sublimation. *Zeitschrift für Physikalische Chemie*, B39:194–208, 1938.
- [76] S.-W. S. Wong. *Enthalpies of combustion of selected compounds composed of globular or polynuclear aromatic molecules*. Phd thesis, University of Michigan, 1967.
- [77] W.-K. Wong and E. F. Westrum. Thermodynamics of polynuclear aromatic molecules I. Heat capacities and enthalpies of fusion of pyrene, fluoranthene, and triphenylenes. *Journal of Chemical Thermodynamics*, 3:106–124, 1971.
- [78] W.-K. Wong and Jr. Westrum, E. F. Thermodynamics of polynuclear aromatic molecules. II. Low-temperature thermal properties of perylene, coronene, and naphthacene. *Molecular Crystals and Liquid Crystals*, 61(3-4):207–28, 1980.
- [79] A. Xu-wu, H. Jun, and B. Zheng. Standard molar enthalpies of combustion and formation of C<sub>60</sub>. *Journal of Chemical Thermodynamics*, 28(10):1115–1119, 1996.



# Chapter 3

## Bond-Centered Group Additivity Estimation Method

### 3.1 Existing Estimation Methods

Before we describe the proposed Bond-Centered Group Additivity method, we will provide an overview to the currently existing estimation methods for polycyclic aromatic molecules. This overview will give the reader a background of the field and an idea of the shortcomings of each of the existing methods.

The most widely used estimation method for the thermochemical properties of PAHs is the one proposed by Stein et al. [18, 17], who extended Benson's group additivity method [2, 3, 4]. In this method, the  $[C_{B-(H)}]$  group defined previously by Benson was retained and three new groups were introduced to describe carbons that belong to two or three aromatic rings:  $[C_{BF-(C_B)_2(C_{BF})}]$ ,  $[C_{BF-(C_B)(C_{BF})_2}]$ , and  $[C_{BF-(C_{BF})_3}]$ . These groups are illustrated in Figure 3-1(a), where an abbreviated notation is used, in which the groups are named A, B, C, and D respectively. The  $\Delta H_f^\circ$ ,  $S_{298}^\circ$ , and  $C_p^\circ$  values for the A group had been derived from the corresponding experimental values of benzene. The  $\Delta H_f^\circ$  values for groups B and C were derived from experimental values of other benzenoid PAHs available at that time. The  $S_{298}^\circ$  and  $C_p^\circ$  contributions of groups B and C were assumed to be equivalent. Values for the entropy of these groups were derived from entropies calculated using the third-

law method from experimental values of naphthalene, phenanthrene, anthracene and pyrene. The heat capacities for these groups were obtained from the experimental heat capacities of naphthalene. The  $\Delta H_f^\circ$  for the D group was derived from the  $\Delta H_{f,\text{subl}}^\circ$  of pyrene (see further discussion at the end of Section 3.3).  $S_{298}^\circ$  values for group D were derived from graphite, although the inter-layer interactions which are so important in graphite are absent in gas-phase PAHs.

Moiseeva and Dorofeeva [12] noted that entropy values estimated using the group values from Stein et al. and values calculated from vibrational assignment differed by  $2.6 \text{ cal K}^{-1} \text{ mol}^{-1}$  on average for PAHs with more than two D groups. Based on this finding, they proposed dividing the D group from the estimation method of Stein et al. into  $D_1$  and  $D_2$  groups. The  $D_1$  and  $D_2$  groups are defined by Moiseeva et al. as carbon atoms common to three aromatic rings. The  $D_1$  group is attached to two or three B or C groups, whereas the  $D_2$  group is attached to at most one B or C group (see Figure 3-1(b)). Moiseeva et al. do not mention the D groups from Stein et al. that belong to only two rings. In Figure 3-1(b) these ambiguous and undefined groups are denoted simply as D. The group contributions to  $\Delta H_f^\circ$  were derived based on the experimental enthalpies of formation available in the compilation by Pedley et al. [13], except for naphthacene, triphenylene and benzo[c]phenanthrene, because the discrepancies between the experimental values and the  $\Delta H_f^\circ$  predicted by the additivity scheme were much larger than the experimental uncertainties. The  $S_{298}^\circ$  and  $C_p^\circ$  contributions for each of the new groups were obtained from statistical mechanics, using the vibrational frequencies calculated from a simple approximate force field.

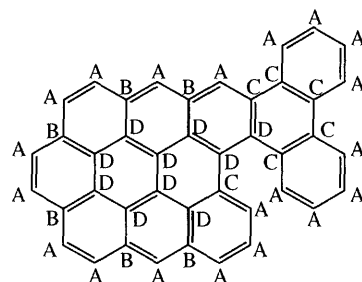
Herndon et al. proposed a bond-additivity method to estimate the heat of formation of benzenoid PAHs [8], where the parameters are the number of C-H and C-C bonds and the number of bay regions with 3 (S3) or 4 rings (S4). They showed this method to be equivalent to the group additivity method proposed by Stein et al. if the D group is differentiated when it belongs to three ( $D_{int}$ ) or to two rings ( $D_{per}$ ). Recognizing that non-planarity effects increase with the number of rings in the same bay region, they also introduced the groups S5 and S6, for bay regions with 5 and 6

rings, respectively (see Figure 3-1(c) for an example of the S5 group). Herndon et al. introduced two additional parameters: T, which accounts for pairs of S3 structures that share a common central ring, and the natural logarithm of the Kekulé structure count  $\ln(K)$  to quantify the resonance energy. Herndon et al.'s estimation method was parameterized against  $\Delta H_f^\circ$  of 153 benzenoid PAHs calculated from molecular mechanics. The proposed method matches the  $\Delta H_f^\circ$  calculated from molecular mechanics very well, and the  $\ln(K)$  term greatly improves its accuracy. Of course, the accuracy of the molecular mechanics calculation on which these parameters are based is not known; it was probably parameterized to data from a few small PAHs.

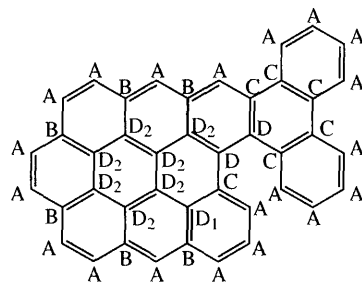
All the methods mentioned so far apply only to benzenoid PAHs. However, most of the PAHs, including those involved in the formation of fullerenes, have both five- and six-membered rings. When five-membered rings are taken into account, the complexity of the problem increases considerably. Since five-membered rings introduce strain and curvature to the molecule, the groups in five-membered rings have to be treated differently than those in six-membered rings.

Stein et al. tackled this problem by considering each ring as a group [16, 17]. They proposed ring-group values for the benzene ring and for the cyclopentadiene ring in structures such as indene and acenaphthalene. They acknowledged that this method is not very accurate, but said that the estimations should be suitable for rough equilibrium calculations, and suggested that this method could serve as a foundation on which to build more accurate estimation methods as more and more data become available.

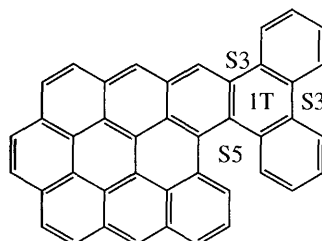
The ring-additivity method proposed by Stein et al. has not been pursued further. Instead, researchers have turned to developing specialized groups for carbon atoms that belong to five-membered rings. Moiseeva and Dorofeeva [11] extended their group additivity method for benzenoid PAHs [12] by introducing three new groups for the carbons in five-membered rings of unsaturated PAHs, as shown in Figure 3-2(a). The E group is a  $[C_{\beta}-(H)]$  group on a five-membered ring. Analogously, the J group is similar to the six-membered ring C group and K is similar to the D group as defined by Stein et al. The contribution of the E group to  $\Delta H_f^\circ$  was derived from



(a) Groups defined by Stein et al. [18, 17]



(b) Groups defined by Moiseeva and Dorofeeva [12]



(c) Bond additivity method for benzenoid PAHs from Herndon et al. [8]

Figure 3-1: Existing additivity methods for benzenoid PAHs.



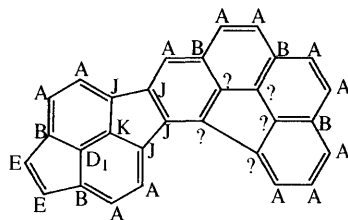
the experimental values of acenaphthalene, by considering that the five-membered ring is joined to the naphthalene by two B and one D<sub>1</sub> groups, as shown in Figure 3-2(a). The contribution of the J group to  $\Delta H_f^\circ$  was assumed to be the same as the C group, and the value of the enthalpy of formation of the K group was obtained from fluoranthene. The contributions from these groups to  $S_{298}^\circ$  and  $C_p^\circ$  were obtained from molecules with the acenaphthalene and fluoranthene fragments whose thermodynamic properties were calculated by statistical mechanics. Since the J and K group values were derived solely based on fluoranthene fragments, which are all planar, they cannot describe structures where the five-membered ring is surrounded by three or more consecutive benzene rings, as shown in Figure 3-2(a).

Pope and Howard [14] noting that the method from Moiseeva and Dorofeeva [11] does not capture the curvature introduced by five-membered rings, included one more term, which they called KC, that should account for all the curvature. They systematically listed the groups that can be formed with the C<sub>B</sub> atom in a six-membered ring, C<sub>B</sub> atom in a five-membered ring, C<sub>BF</sub> atom that belongs only to six-membered rings, C<sub>BF</sub> atom that belongs to one six-membered and one five-membered ring and C<sub>BF</sub> atom that belongs to two six-membered and one five-membered ring. Due to the lack of experimental values of the thermochemical properties of the PAHs, they lumped all the possible groups into eight groups (see Figure 3-2(b)): A, B, C and D as defined by Stein et al. [18], E as defined by Moiseeva and Dorofeeva [11], J as all the carbon atoms that belong to one five-membered ring and one six-membered ring, K as all the carbon atoms that belong to two six-membered rings and one five-membered ring and that are bonded to two J groups (this group should not introduce curvature in the PAH), and KC as all the other carbon atoms at the junction of two six-membered rings and one five-membered ring. Notice the difference in the definition of the J and the K groups between Moiseeva and Dorofeeva [11] and Pope and Howard [14]. The group values for benzenoid PAHs (groups A, B, C and D) were taken from Stein et al. [18, 17]. The values for the groups E, J and K that Moiseeva derived [11] are used, despite the different definition of the J and K groups. The contribution of the KC value to the  $\Delta H_f^\circ$  was derived from the experimental value of C<sub>60</sub>, and the  $S_{298}^\circ$

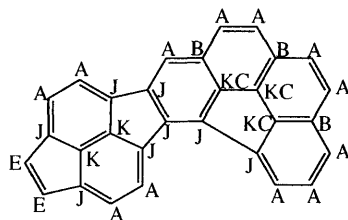
and  $C_p^\circ$  groups values for KC were derived from statistical mechanics calculations of  $C_{60}$ . Pope and Howard acknowledge that their method still suffers limitations when capturing H-H repulsion or any curvature effects different than the one present in  $C_{60}$  fullerenes.

Armitage and Bird derived the value for the  $[C_{BF}-(C_{BF})_3]$  group that belongs to one five-membered ring in a different way [1]. They named the group that connects the naphthalene fragment to the benzene fragment in fluoranthene as F (see Figure 3-2(c)). Instead of considering its contribution to the  $\Delta H_f^\circ$  to be equivalent to a C group, as done by Moiseeva [11] with their J group, they assumed the contribution of this group to the  $\Delta H_f^\circ$  to be equivalent to the contribution of the  $C_B-C_B$  group in biphenyl. This assumption is based on the fact that the F-F bond length is close to the bond length of a single bond. The group E, defined as a group that belongs to two six-membered and one five-membered rings, was derived from the experimental  $\Delta H_f^\circ$  of fluoranthene. The resulting method gives good estimates for the  $\Delta H_f^\circ$  of corannulene and  $C_{70}$  fullerene.

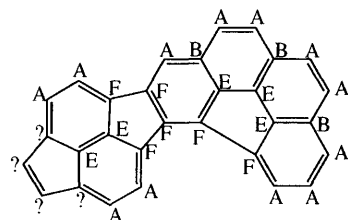
Each of the methods described in this section aimed to solve one specific weakness of the original method proposed by Stein et al. [18], such as strain caused by non-planarity arising from steric interactions [8] and strain caused by planar five-membered ring systems [11]. The development of these methods highlighted the difficulties in establishing a comprehensive estimation method for the thermochemical properties of PAHs. First of all, it is evident from the previous works that the thermochemistry of PAH is heavily dependent on its topology. However, the existing definitions of groups in PAHs with five- and six-membered rings are confusing. Since each of the previous methods dealt only with specific topological characteristics of these PAHs, it is sometimes not clear how wide the definition of a group really is. Another serious difficulty is the insufficient number of experimental values of the thermochemical properties of PAHs. This scarcity hinders the identification of structures that affect the  $\Delta H_f^\circ$ ,  $S_{298}^\circ$  and  $C_p^\circ$  of PAHs. Even when these structures are identified, it is difficult to assess the quality of the estimation method, because there are no values to compare the predictions with. Finally, it has been shown that resonance



(a) Groups defined by Moiseeva and Dorofeeva [11]



(b) Groups defined by Pope and Howard [14]



(c) Groups defined by Armitage and Bird [1]

Figure 3-2: Existing additivity methods for PAHs containing both five- and six-membered rings.

energy plays an important role in determining the  $\Delta H_f^\circ$  of PAHs. The inclusion of a term to capture resonance energy improved the performance of the method proposed by Herndon et al. considerably [8]. From these considerations it is concluded that an estimation method for PAHs with five- and six-membered rings can be developed based on the topology of these molecules. The definition of groups in this method should be unambiguous and comprehensive. The method should be based on sound values of the thermochemical properties, and finally, it should be able to capture the effects of resonance energy in PAHs with both five- and six-membered rings.

### 3.2 Bond-Centered Estimation Method

Benson justified the use of additivity laws to estimate properties of molecules due to the empirical finding that forces between atoms are very “short range” [2]. In these additivity estimation methods, a molecule is divided into parts, and each part is assigned a portion of the molecular property. The estimation of the property for a new molecule simply requires the addition of the properties of each of its constituent parts, assuming that these have been previously defined. Benson and Buss [3] established a hierarchical system for such additivity laws, in which the “zeroth”-order law would be the additivity of atom properties. This simplest additivity law estimates the molecular weight precisely, but presents obvious limitations for the estimation of the thermochemical properties of the molecule. Augmenting each part into which the molecule is divided allows the additivity scheme to better capture the short range interactions that occur in the molecule. Thus the first- and second-order approximation are respectively the additivity of bond and of group properties, where a group is defined as a “polyvalent atom in a molecule together with all of its ligands”. We will call this group an atom-centered group. The atom-centered group method performs very well for aliphatic molecules, especially those that are not heavily substituted.  $S_{298}^\circ$  and  $C_p^\circ$  estimated by this atom-centered group additivity method are on typically within  $\pm 0.3 \text{ cal K}^{-1} \text{ mol}^{-1}$  of the measured values, whereas the estimated  $\Delta H_f^\circ$  are typically within  $\pm 1 \text{ kcal mol}^{-1}$ . However, this atom-centered group additivity

scheme is not enough to capture all the peculiarities of a PAH molecule. The concept of group additivity is based on the assumption that non-nearest neighbors interactions do not affect significantly the thermochemistry of the molecule. However PAHs are characterized by their delocalized resonance and aromaticity. Moreover, although Benson introduced ring-corrections, they are not able to properly account for the strain caused by the presence of five-membered rings in PAHs. As discussed in Section 3.1, previous researchers have tried to capture the effect of five-membered rings by introducing new atom-centered groups but still had difficulties capturing all the nuances of these effects.

### 3.2.1 Definition of Bond-Centered Groups

We propose a different approach. Instead of introducing more atom-centered groups, we go back and consider the hierarchical system proposed by Benson and Buss [3], which starts by dividing a molecule first into atoms, then bonds and finally into atom-centered groups. If we want to capture properties that are not as local as in aliphatic molecules, the natural extension of Benson and Buss' hierarchical system is to divide the molecule into bond-centered groups. We define a bond-centered group as a bond connecting two of Benson's atom-centered groups. For simplicity, we rename Benson's groups: 'A' is defined as the  $C_B$ -(H) atom-centered group of Benson [2] and 'B' is the  $C_{BF}$ -( $C_B$ )<sub>2</sub>( $C_{BF}$ ) atom-centered group. 'C' is defined either as a  $C_{BF}$ -( $C_B$ )( $C_{BF}$ )<sub>2</sub> or  $C_{BF}$ -( $C_{BF}$ )<sub>3</sub> atom-centered group with a further restriction that it belongs to only two rings, i.e., it is on the periphery of the PAH. 'D' is defined as a  $C_{BF}$ -( $C_{BF}$ )<sub>3</sub> atom-centered group in which the center  $C_{BF}$  atom belongs to three rings. Our definition of the 'C' and 'D' groups is slightly different from Benson's definition (compare Figures 3-1(a) and 3-3). The definition of these atom-centered groups is irrespective of the size of the rings to which these atoms belong. A depiction of these groups for an arbitrary PAH is shown in Figure 3-3. Possible bond-centered groups between these types of atom-centered groups are: AA, AB, AC, BB, BC, BD, CC, CD and DD.

Although the bond-centered groups span a larger structure than the atom-centered

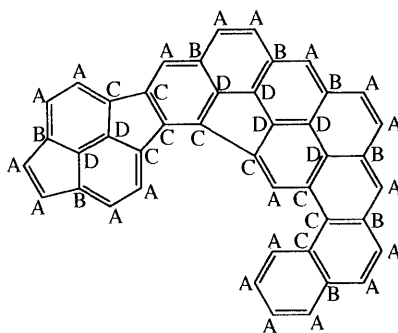


Figure 3-3: Atom-centered groups used for the definition of the bond-centered groups. These atom-centered groups follow basically the definition established by Benson [2], with a small difference in the definition of the ‘C’ and ‘D’ groups. ‘A’ corresponds to the  $[C_B-(H)]$  group, ‘B’ corresponds to the  $[C_{BF}-(C_B)_2(C_{BF})]$  group, ‘C’ corresponds to a group that is in a bay region. It can be either a  $[C_{BF}-(C_B)(C_{BF})_2]$  group or a  $[C_{BF}-(C_{BF})_3]$  group, and ‘D’ corresponds to the  $[C_{BF}-(C_{BF})_3]$  group that is internal to the PAH.

groups, they still do not completely capture non-neighbor effects, such as the electron delocalization characteristic of aromatic molecules. Carter in 1949 had already recognized that the resonance energy is a function of the logarithm of the number of Kekulé structures in aromatic molecules [5]. We developed an algorithm to count the number of Kekulé structures of PAHs containing both five- and six-membered rings. This algorithm will be described in detail in a subsequent publication.

One notes that five-membered rings introduce strain to the system and that five-membered rings completely surrounded by six-membered rings introduce non-planarity to the PAH. From these observations one could be inclined to propose a method in which the bond-groups would not be differentiated according to the size of the rings. Instead, in such a method, five-membered ring corrections should be included. In the case of IPR PAHs, two ring corrections could be included: one for five-membered rings that are not completely surrounded by six-membered rings and another for five-membered rings that are completely surrounded by six-membered rings. Such a method would have 11 parameters:  $\ln(K)$ , AAx, ABx, ACx, CCx, BB6x, BC6x, CC6x, DD6x, R5 and R5o. The ‘6’ after the name of the bond-group indicate the size of the ring to which it belongs, the ‘x’ indicates a ring with either 5

or 6 carbons and ‘R5’ and ‘R5o’ are the ring corrections. The BD6x and CD6x are linearly dependent to the previous bond-groups (see subsequent discussion). However, the errors arising from such a method are unacceptable: RMS is 14.4 kcal mol<sup>-1</sup> and MAD is 9.0 kcal mol<sup>-1</sup>. The statistics for this method can be found in Appendix D.1. Moreover, it is not clear how further ring corrections should be introduced either to improve the performance of this method or to describe non-IPR PAHs.

It is clear that the simple solution of including two ring corrections is not adequate, and a more detailed definition of the bond-groups is necessary. We define bond-centered groups that specify explicitly the size of the ring(s) to which the bond belongs. The diagrams in Figures 3-4 and 3-5 should aid in the understanding of these bond-group. The numbers in the bond-group’s nomenclature refer to the size of the ring(s) to which the bond belongs. Bonds on the boundary between fused five-membered rings (BB55, BC55, CC55, BD55, CD55 and DD55) were not included, since PAHs with two fused 5-membered rings were not included in the model development. The bond-group DD66 was further subdivided to capture the different energetic contributions arising when the rings above and below it are six- or five-membered rings. The resulting bonds are DD6666, DD6665 and DD6655. The last two digits in the name of these bonds refer to the size of the rings above and below the bond-group. Additionally, the DD6665 and DD6655 bonds were further subdivided according to whether the five-membered ring(s) above the DD bond are completely surrounded by six-membered rings or not. The DD6665 bond was subdivided into the DD6665- and DD6665o, whereas the DD6655 was subdivided into DD6655-, DD6655o and DD6655oo. A dash (-) at the end of the name of the bond indicates that the five-membered ring(s) is(are) not completely surrounded by six-membered rings, whereas one ‘o’ at the end indicates that one five-membered ring is completely surrounded by six-membered rings. DD6655oo represents the case where both five-membered rings above and below the bond are completely surrounded by six-membered rings.

The contributions of each of the bond-groups and of the  $\ln(K)$  term to the  $\Delta H_f^\circ$  was derived through a weighted least square regression. The weight for each PAH is assigned as the inverse of the uncertainty in the value of the  $\Delta H_{f,\text{homo}}^\circ$ . This uncer-

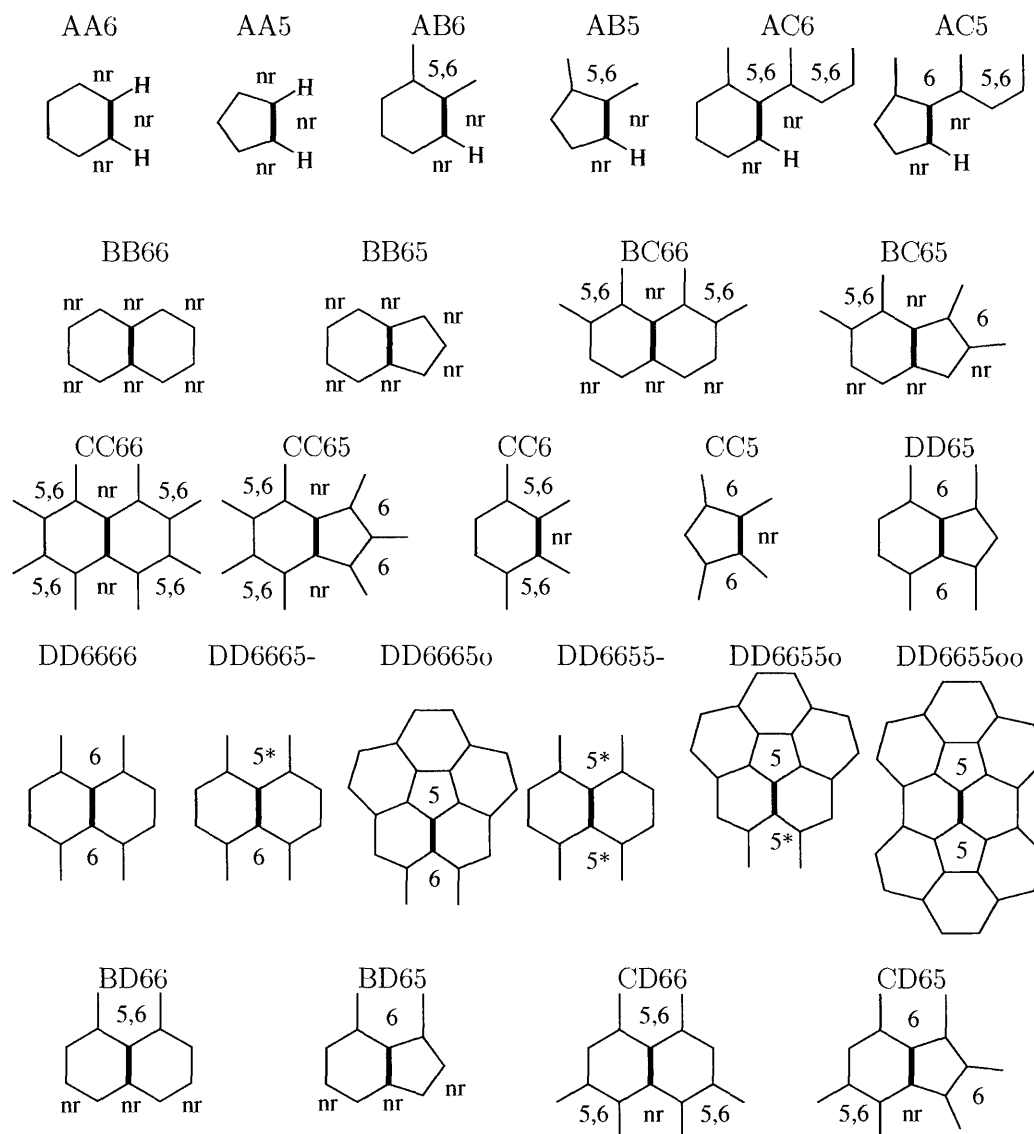


Figure 3-4: Bond-centered groups defined in this work. Each of the bond-centered group connects two atom-centered groups as defined in Figure 3-3. In the nomenclature, the numbers following the two letters correspond to the size of the ring that the bond-centered group belong to. In the case of DD66 groups, the two last numbers define the size of the rings that are above and below the DD66 bond-centered group. In each scheme, the bond-centered groups are shown in bold. The numbers in each ring corresponds to its size. A ring that can be either five-membered or six-membered is represented by a '5,6'. Positions marked by a '5\*' cannot be completely surrounded by other rings. Positions where no ring is allowed are marked with 'nr'. Positions that are not marked might or might not have a ring.



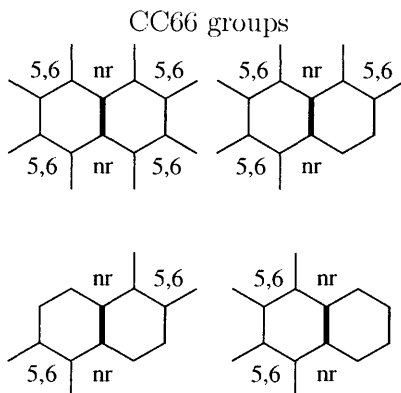


Figure 3-5: All the possible CC66 structures. Figure S1 in the Supporting Information of reference [20] shows all the possible structures for bond-groups BC66, BC65, CC66, CC65, CD66, and CD65. For the sake of conciseness, in Figure 3-4 only the structures with all the possible rings are shown.

tainty arises from the uncertainty in the experimental  $\Delta H_f^\circ$  of the reference molecules used in the homodesmic reaction scheme and the uncertainty in the quantum chemical calculation of the heat of reaction ( $\Delta H_{rxn}$ ) of the homodesmic reaction, as given by Eq. 3.1:

$$\varepsilon = \varepsilon_{\text{exptl}} \Delta H_f^\circ + \varepsilon_{\text{quantum}} \Delta H_{rxn} \quad (3.1)$$

For example, for the molecule in Figure 2-2, for which the Homodesmic4 scheme uses 5/3 of benzene, 3/2 of naphthalene, one phenanthrene and one 1/12 of C<sub>60</sub>,

$$\varepsilon_{\text{exptl}} \Delta H_f^\circ = \frac{5}{3} \varepsilon_{\text{benzene}} + \frac{3}{2} \varepsilon_{\text{naphthalene}} + \varepsilon_{\text{phenanthrene}} + \frac{1}{12} \varepsilon_{\text{C}_{60}} \quad (3.2)$$

The uncertainties of the reference molecules are given by our grading of the experimental values (Tables 2.2 to 2.4). The error in the quantum chemical calculation of  $\Delta H_{rxn}$  is expected to increase with molecular size, and was taken to be:

$$\varepsilon_{\text{quantum}} \Delta H_{rxn} = (\text{number of C atoms}) \times (0.2 \text{ kcal mol}^{-1}) \quad (3.3)$$

The  $\varepsilon$ 's computed using Eq. 3.1 are reasonably consistent with the deviations shown in

Table 2.6. For the molecules that form the base of the Homodesmic4 reaction scheme (i.e. benzene, naphthalene, phenanthrene, acenaphthalene and C<sub>60</sub>),  $\varepsilon_{\text{experimental}} \Delta H_f^\circ$  is considered to be equivalent to the uncertainty that we assigned to its experimental value and  $\varepsilon_{\text{quantum}} \Delta H_{\text{rxn}}$  is defined as zero.

Of the 25 bond-groups that describe five- and six-membered ring PAHs, only 21 are linearly independent. For example, the number of BD65, BD66, CD65 and CD66 in a PAH is given by:

$$\text{BD65} = \text{AB5} - 2 \times \text{BB65} - \text{BC65} \quad (3.4)$$

$$\text{BD66} = -0.5 \times \text{AB5} + 0.5 \times \text{AB6} - 2 \times \text{BB66} - \text{BC66} \quad (3.5)$$

$$\text{CD65} = \text{AC5} + 2 \times \text{CC5} - \text{BC65} - 2 \times \text{CC65} \quad (3.6)$$

$$\text{CD66} = -0.5 \times \text{AC5} + 0.5 \times \text{AC6} - \text{CC5} + \text{CC6} - \text{BC66} - 2 \times \text{CC66} \quad (3.7)$$

Similar linear-dependency issues arise in other group additivity schemes, as often discussed in the literature [2, 6, 19]. The enthalpy contributions of the BD65, BD66, CD65, and CD66 bond-groups were assigned to be 4.0 kcal mol<sup>-1</sup>. The entropy and heat capacities contributions from these four groups were assigned to be zero.

When the regression is performed with the  $\ln(K)$  term and all the linearly independent bond-groups, it is found that not all the bond-groups are statistically significant. In order to ensure that all the parameters of the model are statistically significant, the bond-group values for BB66 and BB65 were set to be equal. The same was done for the bond-groups BC66 and BC65 and for the bond-groups CC66 and CC65. Since only six of the PAHs studied have the bond-groups DD6665o and/or DD6655oo, we first obtained the contributions of the  $\ln(K)$  term and of the remaining bond-groups by performing a regression without those six PAHs. Next the contributions of the DD6665o and DD6655oo bond-groups were determined through a weighted regression of the  $\Delta H_f^\circ$  of the six PAHs that contain these groups, holding the other group values fixed.

### 3.2.2 Statistical Validation of the Model

A regression diagnostics of the proposed model revealed some collinearity problems. The matrix of the independent variables for the 133 PAHs that do not contain the bonds DD6665o and DD6655oo has a condition number of 33 (see Table D.5 in Appendix D), which is an indication of moderate dependencies among the variables [15]. Variance inflation factors (VIF) larger than 10 for some of the regression coefficients are also a symptom of collinearity (see Table D.2). Principal component analysis [15] was performed, and determined that the last four principal components each accounted for less than 1% of the total dispersion of the X-space (see Table D.6). Most of the collinearity problem is due to the last principal component, as attested by its condition index. However its relatively large  $t$ -value indicates that this principal component might be significant. Indeed, when principal component #17 is eliminated from the regression, both the mean average deviation (MAD) and the root mean square error (RMS) increase significantly (see Table D.7). On the other hand, principal components #16 and #15 have very small  $t$ -values, and elimination of these principal components increases MAD and RMS only slightly. However, the elimination of these two principal components does not alleviate the collinearity problem significantly, as indicated by the small change in the largest VIFs (see Appendix D.7). Since the exclusion of these principal components does not alleviate the collinearity problem while causing the MAD and RMS to increase slightly (for the elimination of principal components #16 and #15, the MAD and RMS increase from 2.54 to 3.17 kcal mol<sup>-1</sup> and from 3.64 to 4.60 kcal mol<sup>-1</sup> respectively), we chose to adopt the coefficients obtained by the ordinary least square regression. The collinearity present in this model is a reflection of the structure of the X-space. For example, PAHs with five-membered rings usually have fewer resonance structures than PAHs of the same size that only have six-membered rings. To the extent that the training set of 133 PAHs is representative, the partial collinearity should not cause problems in the prediction of the thermochemical properties of PAHs not included in the training set. The coefficients involved in the collinearity are identified by their large VIF, and the

most prominent is the  $\ln(K)$  term. Other terms that show strong correlation are the AA6, AB6, AC6, CC6, BB65, and BB66 bonds.

A cross-validation of the proposed estimation method was performed in order to test its predictive capability. The set of 133 PAHs (the original 139 excluding the 6 PAHs containing DD6665o and/or DD6655oo bond-groups) was divided into two subsets, the first with 67 PAHs and the second with the remaining 66 PAHs. The coefficients for the  $\ln(K)$  term and for the bond-groups were obtained for each of the subsets, and are shown in Table 3.1. One notices that the coefficients obtained from both subsets of PAHs are very close to the coefficients obtained from the entire set. The differences in the values of each of the coefficients are comparable to their standard errors, indicating that the latter are good estimates of the uncertainty of the coefficients. The RMS and MAD obtained when the coefficients derived from Set 1 are used to predict the  $\Delta H_f^\circ$  of the PAHs contained in Set 2 and vice-versa are also shown in Table 3.1. These errors are comparable to the errors obtained from the complete set, indicating that the proposed bond-centered group additivity method has very good predictive capabilities. Since only 6 of the PAHs studied contain the DD6665o and/or DD6655oo bond-groups, no cross-validation was performed for these bond-groups. The uncertainty in these group values may be considerably higher than in the others.

Additionally, the model for the 133 PAHs was also validated by the “leave one out” procedure. The discrepancy between the  $\Delta H_f^\circ$  for each observation and its prediction from the regression equation obtained by leaving that observation out was calculated. The MAD and RMS for these residuals are 2.95 and 4.35 kcal mol<sup>-1</sup> respectively. These values are only slightly higher than the MAD and RMS for the Complete Set, as reported in Table 3.1. No anomalous outliers were found.

Table 3.1: Cross-validation of the proposed bond-centered group additivity method. The coefficients obtained by regressing  $\Delta H_f^\circ$  over the entire set of 133 PAHs are shown (in kcal mol<sup>-1</sup>), along with the coefficients from the regression over two distinct sets of PAHs. The RMS and MAD given for Set 1 refer to the errors obtained by using the coefficients obtained through Set 1 to predict the  $\Delta H_f^\circ$  of the PAHs in Set 2, and vice-versa. The DD6665o and DD6655oo bond-groups were omitted in the cross-validation.

	Complete Set	Set 1	Set 2
$\ln(K)$	-19.59 ± 1.1	-16.54	-17.74
AA5	10.39 ± 0.7	8.93	10.30
AA6	5.54 ± 0.1	5.21	5.90
AB5	8.72 ± 0.4	9.15	8.65
AB6	5.10 ± 0.2	4.60	5.25
AC5	4.70 ± 0.6	4.48	5.17
AC6	2.32 ± 0.3	1.42	2.15
CC5	11.87 ± 0.8	11.64	12.49
CC6	9.15 ± 0.7	9.39	9.29
BB65	4.10 ± 0.5	6.16	3.96
BB66	4.10 ± 0.5	6.16	3.96
BC65	3.26 ± 0.3	3.78	2.56
BC66	3.26 ± 0.3	3.78	2.56
CC65	5.71 ± 0.5	5.82	5.72
CC66	5.71 ± 0.5	5.82	5.72
DD65	13.24 ± 0.4	14.15	12.40
DD6666	2.71 ± 0.3	2.68	1.88
DD6665-	7.20 ± 0.7	7.98	5.32
DD6655-	20.43 ± 1.2	22.21	18.95
DD6655o	16.40 ± 1.0	13.76	16.19
BD65 <sup>a</sup>	4.00 ± -	4.00	4.00
BD66 <sup>a</sup>	4.00 ± -	4.00	4.00
CD65 <sup>a</sup>	4.00 ± -	4.00	4.00
CD66 <sup>a</sup>	4.00 ± -	4.00	4.00
MAD	2.54	3.16	2.75
RMS	3.64	5.53	4.30

<sup>a</sup>Values for these bonds were assigned (see text)

### 3.2.3 Coefficients for the Bond-Centered Group Additivity Method

The intrinsic entropy ( $S_{int}^\circ$ ) was used to derive the bond-groups, as in Benson’s method [2]. These bond-group values do not contain information about the symmetry of the molecule, so that in order to calculate the  $S_{298}^\circ$  of a PAH, a correction due to the symmetry has to be added to  $S_{int}^\circ$  calculated from the bond-group values:

$$S_{298}^\circ = S_{int}^\circ - R \ln(\sigma) \quad (3.8)$$

The  $S_{int}^\circ$  and  $C_p^\circ$  at 300, 400, 500, 600, 800, 1000 and 1500 K calculated at the B3LYP/6-31G(d) level for all the PAHs included in this study can be found in the Supporting Information of [20]. They were fitted through a weighted linear regression to the same bond-groups used for the  $\Delta H_f^\circ$ . Stein et al. arrived at a value of 1.82 cal K<sup>-1</sup> mol<sup>-1</sup> for the  $S_{298}^\circ$  contribution of the ‘C<sub>BF</sub>-(C<sub>BF</sub>)<sub>3</sub>’ group from the entropy of bulk graphite, the entropy gain due to cleavage of the graphite to become a surface layer and evaporation of this layer to form a graphitic layer in the gas phase [18]. The contribution of the DD6666 group to the  $S_{298}^\circ$  was fixed to match the  $S_{298}^\circ$  for an infinite graphene sheet proposed by Stein et al. This assignment of the value of the DD6666  $S_{298}^\circ$  ensures the correct extrapolation of the entropy to infinitely large benzenoid PAHs.

The inclusion of the  $\ln(K)$  term did not improve the estimation method for  $S_{int}^\circ$  or the  $C_p^\circ$  and thus the estimation method for these thermochemical properties does not include the  $\ln(K)$  term. The  $\ln(K)$  was the term that was causing most of the collinearity problem in the regression of the  $\Delta H_f^\circ$ , thus the models for  $S_{int}^\circ$  and  $C_p^\circ$  show virtually no collinearity as attested by the VIF values of their coefficients (see Table D.3 in Appendix D). The weights used were the same as the ones used for the derivation of the bond-group values of  $\Delta H_f^\circ$ .

The contributions from each bond-group and the  $\ln(K)$  term to the  $\Delta H_f^\circ$ ,  $S_{298}^\circ$ , and  $C_p^\circ$  are listed in Tables 3.2 and 3.3 along with their standard deviations. The standard deviations for the  $C_p^\circ$  were less than 0.1 cal K<sup>-1</sup> mol<sup>-1</sup>. Since the level of

confidence on the values for the bond-groups DD6665o and DD6655oo is not as high as for the other bond-groups, the values for these groups are given in parentheses. The statistics for the regression can be found in Tables 3.4 and 3.5 and were calculated considering the complete set of 139 PAHs. The statistics for  $\Delta H_f^\circ$  and  $S_{298}^\circ$  related to the set of 133 PAHs that do not contain the DD6665o and the DD6655oo bond-groups are given in parenthesis. All the mean average deviation (MAD) and root mean square errors (RMS) are in relation to the homodesmic B3LYP/6-31G(d) values and have not been weighted.

The thermochemical properties of PAHs are estimated by summing the contribution of each of its bonds, as given in Tables 3.2 and 3.3.  $\Delta H_{f,est}^\circ$  has an additional term related to the resonance energy ( $-16.95\ln(K)$ ). Sample calculations were made for the PAHs in Figure 2-1 and are found in Table C.1. The number of each of the bond-groups for all the PAHs included in this study can be found in the Supporting Information of [20].

### 3.3 Results and Discussion

The estimation method for the thermochemical properties developed in this work was based on the  $\Delta H_{f,homo}^\circ$ ,  $S_{298}^\circ$  and  $C_p^\circ$  obtained from DFT calculations. As a comparison with the experimental values, the entropies calculated from the B3LYP/6-31G(d) are listed in the last column of Table 2.5. Except for naphthacene, the entropy calculated from quantum chemistry is within the uncertainty of the entropy calculated from the third law method based on experimental heat capacity and vapor pressure data. We conclude that the  $S_{298}^\circ$  calculated at the B3LYP/6-31G(d) level and with our bond-centered group additivity method are at least as reliable as the available experimental values. We developed a homodesmic reaction scheme that closely emulates the experimental  $\Delta H_f^\circ$  of the PAHs. The estimation method for the enthalpy of formation that we propose can at best be as good as the  $\Delta H_{f,homo}^\circ$  given by the homodesmic reaction scheme.

The bond-centered group values reported in Tables 3.2 and 3.3 allow the esti-

Table 3.2:  $\Delta H_f^\circ$  and  $S_{298}^\circ$  values for bond-groups and the  $\ln(K)$  term for the estimation of thermochemical properties.

	$\Delta H_f^\circ$ (kcal mol <sup>-1</sup> )	$S_{298}^\circ$ (cal K <sup>-1</sup> mol <sup>-1</sup> )
$\ln(K)$	-19.59 ± 1.1	-
AA5	10.39 ± 0.7	13.03 ± 0.2
AA6	5.54 ± 0.1	11.58 ± < 0.1
AB5	8.72 ± 0.4	6.57 ± 0.1
AB6	5.10 ± 0.2	3.50 ± < 0.1
AC5	4.70 ± 0.6	6.98 ± 0.2
AC6	2.32 ± 0.3	4.31 ± 0.1
CC5	11.87 ± 0.8	-1.87 ± 0.2
CC6	9.15 ± 0.7	-5.23 ± 0.2
BB65	4.10 ± 0.5	-0.58 ± 0.1
BB66	4.10 ± 0.5	-0.58 ± 0.1
BC65	3.26 ± 0.3	-0.94 ± 0.1
BC66	3.26 ± 0.3	-0.94 ± 0.1
CC65	5.71 ± 0.5	-1.10 ± 0.2
CC66	5.71 ± 0.5	-1.10 ± 0.2
DD65	13.24 ± 0.4	2.58 ± 0.1
DD6666	2.71 ± 0.3	1.21 <sup>a</sup> ± -
DD6665-	7.20 ± 0.7	1.45 ± 0.2
DD6665o <sup>b</sup>	(3.44 ± 0.7)	(0.12 ± 0.2)
DD6655-	20.43 ± 1.2	1.70 ± 0.4
DD6655o	16.40 ± 1.0	0.51 ± 0.3
DD6655oo <sup>b</sup>	(-0.24 ± 0.7)	(-0.54 ± < 0.1)
BD66 <sup>c</sup>	4.00 ± -	0.0 ± -
BD65 <sup>c</sup>	4.00 ± -	0.0 ± -
CD66 <sup>c</sup>	4.00 ± -	0.0 ± -
CD65 <sup>c</sup>	4.00 ± -	0.0 ± -

<sup>a</sup>Derived to match the entropy of graphene proposed by Stein et al. [18]

<sup>b</sup>Values for these two bonds were derived from only 6 PAHs

<sup>c</sup>Values for these bonds were assigned (see text)



Table 3.3:  $C_p^\circ$  values for bond-groups for the estimation of thermochemical properties.

	$C_{p,T}$ (cal K <sup>-1</sup> mol <sup>-1</sup> )						
	300 K	400 K	500 K	600 K	800 K	1000 K	1500 K
ln( $K$ )	-	-	-	-	-	-	-
AA5	3.4	4.6	5.6	6.4	7.5	8.3	9.3
AA6	3.4	4.6	5.6	6.4	7.6	8.3	9.5
AB5	3.4	4.6	5.5	6.2	7.2	7.8	8.6
AB6	3.4	4.6	5.5	6.2	7.3	7.9	8.8
AC5	3.5	4.6	5.5	6.2	7.1	7.7	8.6
AC6	3.5	4.6	5.5	6.2	7.2	7.9	8.8
CC5	3.3	4.4	5.2	5.9	6.8	7.3	7.9
CC6	3.4	4.5	5.4	6.1	7.0	7.6	8.4
BB65	-1.3	-1.9	-2.3	-2.6	-3.1	-3.3	-3.6
BB66	-1.3	-1.9	-2.3	-2.6	-3.1	-3.3	-3.6
BC65	-1.4	-1.9	-2.3	-2.7	-3.1	-3.4	-3.7
BC66	-1.4	-1.9	-2.3	-2.7	-3.1	-3.4	-3.7
CC65	-1.4	-1.9	-2.4	-2.7	-3.1	-3.4	-3.7
CC66	-1.4	-1.9	-2.4	-2.7	-3.1	-3.4	-3.7
DD65	1.4	1.9	2.4	2.7	3.1	3.4	3.7
DD6666	1.5	2.0	2.4	2.7	3.2	3.4	3.8
DD6665-	1.4	1.9	2.3	2.7	3.1	3.3	3.6
DD6665o <sup>a</sup>	(1.3)	(1.8)	(2.3)	(2.6)	(3.1)	(3.3)	(3.6)
DD6655-	1.3	1.9	2.3	2.7	3.1	3.4	3.7
DD6655o	1.2	1.8	2.2	2.6	3.1	3.3	3.6
DD6655oo <sup>a</sup>	(1.3)	(1.8)	(2.3)	(2.6)	(3.1)	(3.3)	(3.5)
BD66 <sup>b</sup>	0.0	0.0	0.0	0.0	0.0	0.0	0.0
BD65 <sup>b</sup>	0.0	0.0	0.0	0.0	0.0	0.0	0.0
CD66 <sup>b</sup>	0.0	0.0	0.0	0.0	0.0	0.0	0.0
CD65 <sup>b</sup>	0.0	0.0	0.0	0.0	0.0	0.0	0.0

<sup>a</sup>Values for these two bonds were derived from only 6 PAHs

<sup>b</sup>Values for these bonds were assigned (see text)

Table 3.4:  $\Delta H_f^\circ$  and  $S_{298}^\circ$  statistics for the estimation method. The errors were calculated for the complete set of 139 PAHs and were not weighted. The statistics related to the set of 133 molecules that do not contain the DD6665o and the DD6655oo bond-groups are given in parenthesis

	$\Delta H_f^\circ$ (kcal mol <sup>-1</sup> )	$S_{298}^\circ$ (cal K <sup>-1</sup> mol <sup>-1</sup> )
N	139 (133)	139 (133)
Parameters	19 (17)	18 (16)
MAD	2.78 (2.54)	0.71 (0.67)
RMS	4.25 (3.64)	1.04 (1.02)

Table 3.5:  $C_p^\circ$  statistics for the estimation method

	$C_{p,T},$ (cal K <sup>-1</sup> mol <sup>-1</sup> )						
	300 K	400 K	500 K	600 K	800 K	1000 K	1500 K
N							139
Parameters							18
MAD	0.33	0.73	0.31	0.20	0.49	0.50	0.31
RMS	0.45	1.18	0.62	0.30	0.58	0.63	0.45

mation of the thermochemical properties of any PAH containing both five- and six-membered rings that follows the Isolated Pentagon Rule. The deliberate subdivision of certain groups into more specific substructures is a straightforward and powerful way to improve group additivity methods to meet the needs of a specific application, as done by Bozzelli and co-workers in defining Hydrogen-Bond Increment (HBI) groups for radicals [10], and Sumathi and Green [19] for ketene species. In this bond-centered group additivity scheme for the estimation of the thermochemical properties of PAHs, it was verified that in order to estimate accurately the  $\Delta H_f^\circ$  of PAHs up to C<sub>60</sub> and C<sub>70</sub> fullerenes, it was necessary to subdivide the DD66 group into DD6666, DD6665, and DD6655, according to the size of the ring that is above and below the DD bond. Proceeding in this manner, the further subdivision of the DD6665 group into the DD6665- and DD6665o groups and of the DD6655 group into the DD6655-, DD6655o, and DD6655oo groups, according to whether the five-membered rings above and below the DD bond are completely surrounded by six-membered rings or not, improves the estimation method significantly for the PAHs studied. Each of these bond-groups indeed describe different environments as evidenced by the very different

contributions to the  $\Delta H_f^\circ$  from each of these groups. The DD6655- bond, as it occurs in pyracylene introduces considerable strain to the molecule, and thus its contribution to the  $\Delta H_f^\circ$  of a PAH is very high (20.43 kcal mol<sup>-1</sup>). Incidentally the  $\Delta H_{f,est}^\circ$  for pyracylene estimated by the bond-centered group additivity method (96.4 kcal mol<sup>-1</sup>) agrees very well with the value obtained by Diogo et al. [7] (97.8 kcal mol<sup>-1</sup>) from a measured energy of combustion and an estimated  $\Delta H_{f,subl}^\circ$ . Completely surrounding a five-membered ring with six-membered rings provides stability to the PAH, as is attested by the contributions of the DD6655o and DD6655oo bonds to the  $\Delta H_f^\circ$ . Also the comparison of bond-groups DD6665- and DD6665o shows this trend. If the  $\Delta H_f^\circ$  of larger fullerenes is to be estimated with more accuracy, then the DD6655 and DD6665 bond-groups may need to be subdivided even further. A method similar to the “structural motifs scheme” developed by Cioslowski [6] for the estimation of the  $\Delta H_f^\circ$  fullerenes would result.

In Figure 3-6 the difference between the  $\Delta H_{f,homo}^\circ$  and the estimated enthalpy of formation ( $\Delta H_{f,est}^\circ$ ) per carbon atom is plotted against  $\Delta H_{f,homo}^\circ$ . For the majority of the  $\Delta H_{f,est}^\circ$ , including the estimated  $\Delta H_{f,est}^\circ$  for C<sub>60</sub> and C<sub>70</sub>, the error per carbon atom is less than 0.2 kcal mol<sup>-1</sup>. The errors of the PAHs that contain the bond-group(s) DD6665o and DD6655oo are shown with a filled circle. The most obvious outlier, with an absolute error of more than 1 kcal mol<sup>-1</sup> per carbon is as-indacene (PAH (7) in Figure 2-1). This is the only PAH in which the rings above and below the CC6 bond are both five-membered. The current bond-centered group model is not able to capture the strain that this relatively unstable structure has. Perhaps in the future the CC6 group should be subdivided as we have done with the DD66 group. The three filled circles that are below the -0.2 kcal mol<sup>-1</sup> per carbon error line correspond to PAHs that contain the DD6665o bond-group. The only other PAH that contain this bond-group is C<sub>70</sub>. Since C<sub>70</sub> contains 20 of this group, the value of DD6665o is strongly influenced by this molecule. As of now it is not possible to conclude whether: 1) inclusion of more PAHs containing the DD6665o group would lead to a value of DD6665o that would give acceptable errors for C<sub>70</sub> and the other PAHs with this bond-group, 2) the DD6665o bond-group needs to be sub-divided, or

3) the homodesmic reaction scheme used to obtain the  $\Delta H_{f,\text{homo}}^\circ$  is not adequate for PAHs with the structural feature described by the DD6665o group.

The inclusion of the term that describes the resonance energy does not improve the estimation of the  $S_{int}^\circ$  nor of the  $C_p^\circ$  and thus the method proposed here for the estimation of these thermochemical properties does not include the  $\ln(K)$  term. Examining the contributions of each of the bond-groups to  $C_p^\circ$ , one concludes that the groups can be divided into three categories. The first category includes the bond-groups that are in the periphery of the PAH (they include always an ‘A’ group). The second is composed of the bond-groups that link two atom-groups that are in the periphery of the PAH, but that belong to two rings. Finally the last category is composed of the bond-groups that link two D groups. Entropies and heat capacities are much more amenable to a description by additivity methods than  $\Delta H_f^\circ$ .

Differences between the experimental  $\Delta H_f^\circ$  and values estimated by some of the previous methods and by the bond-centered group additivity method (BCGA) presented in this paper are given in Table 3.6. The difference between  $\Delta H_{f,\text{est}}^\circ$  and  $\Delta H_{f,\text{homo}}^\circ$  for some PAHs whose experimental  $\Delta H_f^\circ$  are not available are shown in Table 3.7. Benson’s group additivity method [18] applies to PAHs with six-membered rings only. The other two atom-centered group additivity methods are extensions of Benson’s method to include five-membered rings. Moiseeva and Dorofeeva [12] derived new groups for benzenoid PAHs, while Armitage and Bird [1] use essentially the same values suggested by Benson for the six-membered rings in their PAHs. The new bond-centered group additivity method is much in better agreement with the experimental and quantum chemical  $\Delta H_f^\circ$ ’s, and also is applicable to a broader range of PAHs, than any existing method.

The previous atom-centered group additivity methods for PAHs with five-membered rings describe only specific structures, as shown in Figure 3-2. In order to enrich the comparison of the performance of the bond-centered group additivity method, the method proposed by Armitage and Bird was extended to describe acenaphthalene structures. The value for the missing group was derived from the experimental  $\Delta H_f^\circ$  of acenaphthalene. The  $\Delta H_f^\circ$  calculated from this extended Armitage and Bird

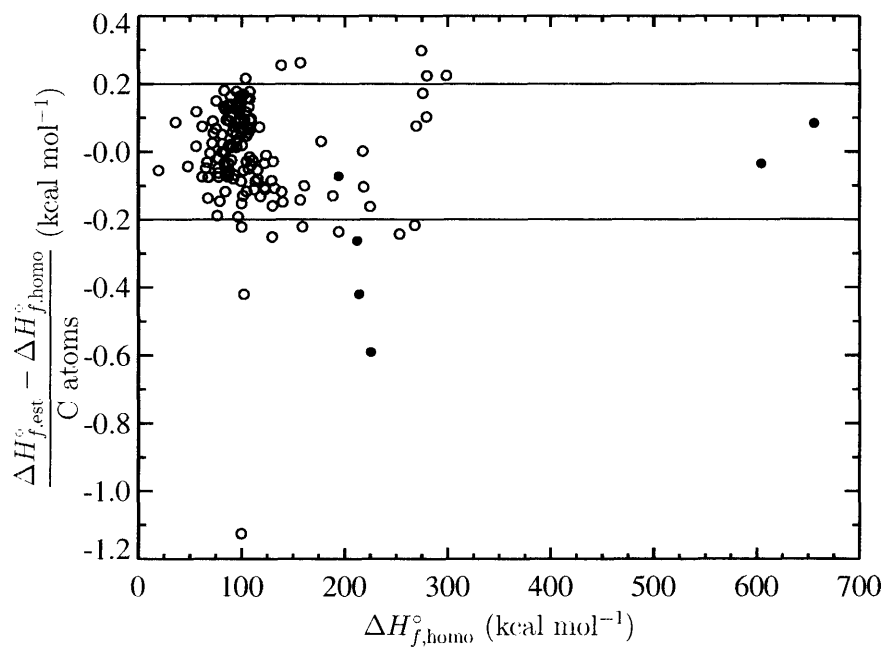


Figure 3-6: Error per carbon atom between  $\Delta H_{f,\text{homo}}^\circ$  and  $\Delta H_{f,\text{est}}^\circ$  versus the  $\Delta H_{f,\text{homo}}^\circ$ . The filled circles correspond to PAHs that contain the bond-group(s) DD6665o and/or DD6655oo.

Table 3.6: Comparison between the atom-centered group additivity methods and the bond-centered group additivity method (BCGA) presented in this work for the PAHs with known experimental  $\Delta H_f^\circ$ . In (kcal mol<sup>-1</sup>).

PAH		$\Delta H_{f,\text{exp}}^\circ$	$\Delta H_{f,\text{homo}}^\circ$	$\Delta H_{f,\text{est}}^\circ - \Delta H_{f,\text{exp}}^\circ$			
				B <sup>a</sup>	M <sup>b</sup>	A <sup>c</sup>	BCGA <sup>d</sup>
Benzene	C <sub>6</sub> H <sub>6</sub>	19.8	19.8	0.0	-3.2	0.0	-0.1
Naphthalene	C <sub>10</sub> H <sub>8</sub>	36.0	36.0	0.0	-0.1	0.0	0.2
Phenanthrene	C <sub>14</sub> H <sub>10</sub>	48.1	48.1	1.9	1.5	1.9	-0.1
Anthracene	C <sub>14</sub> H <sub>10</sub>	55.2	56.1	-3.0	0.0	-3.0	-0.1
Pyrene	C <sub>16</sub> H <sub>10</sub>	53.9	56.2	1.3	8.2	1.2	3.7
Triphenylene	C <sub>18</sub> H <sub>12</sub>	65.5	65.7	-3.7	-7.8	-3.7	-0.2
Benzo[c]phenanthrene	C <sub>18</sub> H <sub>12</sub>	69.6	68.0	-4.5	-3.5	-4.5	-2.7
Benz[a]anthracene	C <sub>18</sub> H <sub>12</sub>	69.6	66.7	-3.4	-0.7	-3.4	-3.7
Chrysene	C <sub>18</sub> H <sub>12</sub>	63.0	61.9	1.0	-0.3	1.0	0.8
Naphthacene	C <sub>18</sub> H <sub>12</sub>	79.3	77.6	-10.9	-4.8	-10.9	-4.1
Perylene	C <sub>18</sub> H <sub>12</sub>	76.4	76.5	-9.4	-6.2	-9.5	-3.1
Coronene	C <sub>24</sub> H <sub>12</sub>	73.6	75.2	3.8	-2.9	3.5	2.4
Acenaphthalene	C <sub>12</sub> H <sub>8</sub>	62.1	62.1	-	4.1	-	-1.2
Fluoranthene	C <sub>16</sub> H <sub>10</sub>	69.8	67.3	-	-0.7	-0.7	-5.2
Corannulene	C <sub>20</sub> H <sub>10</sub>	110.1	117.4	-	-	-0.3	7.7
Benzo[k]fluoranthene <sup>e</sup>	C <sub>20</sub> H <sub>12</sub>	(71.0)	82.6	-	(17.4)	(14.3)	(10.2)
C <sub>60</sub>	C <sub>60</sub>	604.6	604.6	-	-	29.5	-2.2
C <sub>70</sub>	C <sub>70</sub>	658.5	655.8	-	-	-9.9	0.7
MAD				3.6	3.1	5.5	2.7

<sup>a</sup>Benson's Method

<sup>b</sup>Moiseeva's Method

<sup>c</sup>Armitages's Method

<sup>d</sup>Bond-Centered Group Additivity Method

<sup>e</sup>The experimental  $\Delta H_f^\circ$  of benzo[k]fluoranthene is suspected to be in error. Values not included in the calculation of the MAD.

Table 3.7: Comparison between the atom-centered group additivity methods and the bond-centered group additivity method (BCGA) presented in this work for some PAHs whose experimental  $\Delta H_f^\circ$  are not known. These PAHs are the ones shown in Figure 2-1. In (kcal mol<sup>-1</sup>).

PAH	$\Delta H_{f,\text{homo}}^\circ$	$\Delta H_{f,\text{est}}^\circ - \Delta H_{f,\text{homo}}^\circ$				
		Benson	Moiseeva	Armitage <sup>a</sup>	BCGA	
(1)	C <sub>20</sub> H <sub>12</sub>	69.7	-2.7	0.5	-2.8	0.0
(2)	C <sub>22</sub> H <sub>12</sub>	81.5	-7.1	-1.4	-7.3	0.0
(3)	C <sub>22</sub> H <sub>14</sub>	81.5	-2.4	-	-2.4	0.9
(4)	C <sub>28</sub> H <sub>14</sub>	90.4	-1.2	-11.6	-1.5	-0.8
(5)	C <sub>32</sub> H <sub>14</sub>	102.2	-2.6	-12.2	-3.1	-2.2
(6)	C <sub>32</sub> H <sub>16</sub>	116.0	-10.6	-1.6	-10.9	-2.3
(8)	C <sub>18</sub> H <sub>10</sub>	87.4	-	-	2.1	-1.3
(9)	C <sub>18</sub> H <sub>10</sub>	104.7	-	-5.4	-9.5	-1.9
(10)	C <sub>20</sub> H <sub>10</sub>	130.0	-	-	-14.4	-2.7
(11)	C <sub>20</sub> H <sub>12</sub>	89.4	-	7.0	1.8	3.0
(12)	C <sub>20</sub> H <sub>12</sub>	85.4	-	0.2	-1.2	1.7
(13)	C <sub>22</sub> H <sub>10</sub>	156.8	-	-	-13.5	-3.4
(14)	C <sub>22</sub> H <sub>12</sub>	100.6	-	-0.2	-7.6	0.6
(15)	C <sub>24</sub> H <sub>10</sub>	194.3	-	-	-24.9	-5.3
(16)	C <sub>24</sub> H <sub>12</sub>	99.1	-	6.3	-1.0	2.7
(17)	C <sub>26</sub> H <sub>12</sub>	161.0	-	-	-10.7	-3.1
(18)	C <sub>30</sub> H <sub>10</sub>	269.5	-	-	-	2.8
(19)	C <sub>30</sub> H <sub>12</sub>	194.3	-	-	-7.0	-2.7
(20)	C <sub>30</sub> H <sub>12</sub>	217.7	-	-	-37.5	2.8
MAD			5.3	5.1	11.5	2.1

<sup>a</sup>Extended to include PAHs with acenaphthalene structures (see text).

method are listed in Table 3.7. The bond-centered group additivity scheme presented here is able to provide thermochemical properties for any IPR PAH. The  $\Delta H_f^\circ$  of corannulene and  $C_{70}$  fullerene estimated by the Bird and Armitage method agrees well with the  $\Delta H_{f,\text{exp}}^\circ$ . However, it is not uncommon for the  $\Delta H_f^\circ$  estimated by this method to deviate by 10 kcal mol<sup>-1</sup> or more from the  $\Delta H_{f,\text{homo}}^\circ$  for smaller PAHs. The group additivity method of Armitage and Bird usually underestimates  $\Delta H_f^\circ$ . The bond-centered group additivity method has a considerably smaller MAD for the PAHs listed in Table 3.7 than the other methods. All the group additivity methods estimate the  $\Delta H_f^\circ$  of benzo[k]fluoranthene to be about 10 kcal mol<sup>-1</sup> higher than the available experimental value. The unusually large discrepancies between literature values and the present calculations suggest that the  $\Delta H_f^\circ$  of benzo[k]fluoranthene and the  $S_{298}^\circ$  of naphthacene should be remeasured.

For an infinite hexagon lattice, the number of Kekulé structures per node is 0.161532 [9]. Since the contribution of the ‘DD6666’ bond to the  $\Delta H_f^\circ$  is 2.71 kcal mol<sup>-1</sup>, it is straightforward to calculate the prediction of the BCGA method for an infinite graphene sheet:

$$\frac{\Delta H_{f,\text{graphene}}^\circ}{\#C} = \frac{3}{2} \times 2.71 - 19.59 \times 0.161532 = 0.90 \text{ kcal mol}^{-1} \quad (3.9)$$

This seems to be a reasonable limit. Stein et al. proposed a value for the ‘Cbf’ group of 1.45 kcal mol<sup>-1</sup> based on the  $\Delta H_{f,\text{subl}}^\circ$  of pyrene [18]. Since the  $\Delta H_f^\circ$  of solid graphite is zero, it is reasonable to assume that the  $\Delta H_f^\circ$  of a hypothetical “gaseous” graphite corresponds to the  $\Delta H_{f,\text{subl}}^\circ$  of large benzenoid PAHs. For large PAHs the  $\Delta H_{f,\text{subl}}^\circ$  per carbon atom is expected to decrease, since ratio of carbons at the edge of the PAH to the carbons in the interior decreases. Carbons at the edge of the PAH contribute more to the  $\Delta H_f^\circ$  than carbons in the interior of the PAH. For example, compare the values for the ‘AA6’ and ‘DD6666’ groups. The  $\Delta H_{f,\text{subl}}^\circ$  for coronene is 1.4 kcal mol<sup>-1</sup> per carbon (see Table 2.2). The contribution of the DD6666 group was derived so as to match the entropy proposed by Stein et al. for an infinite graphene in the gaseous phase. The DD6666  $C_p^\circ$  values derived here naturally match the  $C_p^\circ$



values proposed by Stein et al. for graphene in the gaseous phase, which were taken to be equal to the  $C_p^\circ$  of graphite, since the surface heat capacity is negligible.

Finally, a word of caution is due. As in any method of additivity of molecular substructures, the independent variables of the bond centered group additivity method are mildly correlated. For example, the presence of an AB6 bond will usually (but not always) mean the presence of an AA6 bond. The resulting collinearity is inherent to the X-space, and should not present a serious problem, since a wide variety of PAHs structures (up to the C<sub>60</sub> and C<sub>70</sub> fullerenes) has been included in this study, encompassing most of the X-space spanned by PAHs of practical interest.

### 3.4 Conclusions

A bond-centered group additivity method for the estimation of the thermochemical properties of PAHs has been derived based on thermochemical properties calculated at the B3LYP/6-31G(d) level.  $\Delta H_f^\circ$  were obtained through a set of homodesmotic reactions that uses only aromatic molecules. This carefully chosen set of reference molecules corrects for effects that were not completely captured by the quantum chemical calculations. Resonance energy is described through the natural logarithm of the number of Kekulé structures. An algorithm has been developed to count the number of Kekulé structures in PAHs with both six- and five-membered rings (see Chapter 6). The new bond-centered group additivity method can be easily coupled with Benson's atom-centered group additivity method for aliphatic molecules. All the bond-centered groups are clearly defined and extendable. Extendability means that if the thermochemical properties of a certain class of species need to be estimated with more accuracy, the bond-groups can be differentiated and more specific values derived for them. The bond-centered group additivity method for the estimation of the thermochemical properties of PAHs described in this paper captures the structural particularities that determine the  $\Delta H_f^\circ$  of PAHs up to fullerenes. It extrapolates to reasonable values for an infinite graphene sheet. This new method allows the rapid estimation of  $\Delta H_f^\circ$ ,  $S_{298}^\circ$  and  $C_p^\circ$  values that are practically as good as B3LYP

calculations or experimental measurements.

# Bibliography

- [1] D. A. Armitage and C. W. Bird. Enthalpies of formation of fullerenes by the group additivity method. *Tetrahedron Letters*, 34(36):5811–5812, 1993.
- [2] S. W. Benson. *Thermochemical Kinetics*. John Wiley & Sons, New York, 2<sup>nd</sup> edition, 1976.
- [3] S. W. Benson and J. H. Buss. Additivity rules for the estimation of molecular properties. thermodynamic properties. *The Journal of Chemical Physics*, 29(3):546–572, 1958.
- [4] S. W. Benson, F. R. Cruickshank, D. M. Golden, G. R. Haugen, H. E. O’Neal, A. S. Rodgers, R. Shaw, and W. R. Additivity rules for the estimation of thermochemical properties. *Chemical Reviews*, 69:279–294, 1969.
- [5] P. G. Carter. An empirical equation for the resonance energy of polycyclic aromatic hydrocarbons. *Trans. Faraday Soc.*, 45:597–602, 1949.
- [6] J. Cioslowski, N. Rao, and D. Moncrieff. Standard enthalpies of formation of fullerenes and their dependence on structural motifs. *Journal of the American Chemical Society*, 122:8265–8270, 2000.
- [7] H. P. Diogo, G. Persy, M. E. M. Piedade, and J. Wirz. The enthalpy of formation of pyracylene. *Journal of Organic Chemistry*, 61:6733–6734, 1996.
- [8] W. C. Herndon, P. C. Nowak, D. A. Connor, and P. Lin. Empirical model calculations for thermodynamic and structural properties of condensed polycyclic aromatic hydrocarbons. *Journal of the American Chemical Society*, 114:41–47, 1992.
- [9] D. J. Klein, H. Zhu, R. Valenti, and M. A. Garcia-Bach. Many-body valence-bond theory. *International Journal of Quantum Chemistry*, 65:421–438, 1997.
- [10] T. H. Lay, J. W. Bozzelli, A. M. Dean, and E. R. Ritter. Hydrogen atom bond increments for calculation of thermodynamic properties of hydrocarbon radical species. *Journal of Physical Chemistry*, 99(39):14514–14527, 1995.
- [11] N. F. Moiseeva and O. V. Dorofeeva. Group additivity scheme for calculating the chemical thermodynamic properties of gaseous polycyclic aromatic hydrocarbons containing five-membered rings. *Thermochimica Acta*, 168:179–186, 1990.

- [12] N. F. Moiseeva, O. V. Dorofeeva, and V. S. Jorish. Development of Benson group additivity methods for estimation of ideal gas thermodynamic properties of polycyclic aromatic hydrocarbons. *Thermochimica Acta*, 153:77–85, 1989.
- [13] J. B. Pedley, R. D. Naylor, and S. P. Kirby. *Thermochemical data of organic compounds*. Chapman and Hall, London, 2<sup>nd</sup> edition, 1986.
- [14] C. J. Pope and J. B. Howard. Thermochemical properties of curved PAH and fullerenes: A group additivity method compared with MM3(92) and MOPAC predictions. *The Journal of Chemical Physics*, 99:4306–4316, 1995.
- [15] J. O. Rawlings. *Applied Regression Analysis*. Statistics/Probability Series. Wadsworth & Brooks, Pacific Grove, California, 1988.
- [16] S. E. Stein and B. D. Barton. Chemical thermodynamics of polyaromatic compounds containing heteroatoms and five-membered rings. *Thermochimica Acta*, 44:265–281, 1981.
- [17] S. E. Stein and A. Fahr. High-temperature stabilities of hydrocarbons. *Journal of Physical Chemistry*, 89:3714–3725, 1985.
- [18] S. E. Stein, D. M. Golden, and S. W. Benson. Predictive scheme for thermochemical properties of polycyclic aromatic hydrocarbons. *Journal of Physical Chemistry*, 81(4):314–317, 1977.
- [19] R. Sumathi and W. H. Green Jr. Thermodynamic properties of ketenes: Group additivity values from quantum chemical calculations. *Journal of Physical Chemistry A*, 106:7937–7949, 2002.
- [20] J. Yu, R. Sumathi, and W. H. Green Jr. Accurate and efficient method for predicting thermochemistry of polycyclic aromatic hydrocarbons – Bond-Centered Group Additivity. *Journal of the American Chemical Society*, accepted for publication, 2004.

# Chapter 4

## Other Polycyclic Aromatic Molecules

### 4.1 Introduction

In the previous chapters we have proposed a Bond-Centered Group Additivity method for the estimation of the thermochemical properties of PAHs with both five- and six-membered rings. However, these are not the only classes of molecules that are formed in a combustion system. In this chapter we show that the BCGA method can be extended to other polycyclic aromatic molecules as well. We propose group values for aromatic molecules containing a furan ring, triple bonds, and for substituted aromatic rings, extending considerably the applicability of the BCGA method.

### 4.2 Furans

#### 4.2.1 Introduction

According to the simple Hückel ( $4N + 2$ ) rule furan should be considered an aromatic ring. This rule states that cyclic (planar) systems with  $(4N + 2)$   $\pi$ -electrons are more stable than their open chain analogues. Other measures of aromaticity also confirm that furan is aromatic. For example, its NICS index is -12.3, compared to benzene's

-9.7 value. NICS (nucleus-independent chemical shift) is defined as a negative value of the absolute shielding computed at a ring center. Rings with negative NICS values are considered as aromatic, and the more negative the NICS, the more aromatic are the rings.

The kinetics of formation and consumption during combustion of PAHs containing furan rings (especially dibenzofuran) has attracted considerable attention [31], because the polychlorinated form of these species are very carcinogenic. Polychlorinated dibenzodioxins and dibenzofurans (PCDD/F) are a major problem in waste incineration (e.g. [3]). On another note, heterocyclic PAHs have attracted attention due to the possibility of tailoring the curvature and rigidity of buckybowls by the introduction of heteroatoms at strategic positions [30].

#### **4.2.2 Previous Estimation Methods**

A few estimation methods for PAHs containing a furan ring have been proposed [1, 32, 2, 21]. These works were all based on ring corrections for the entire furan ring. The proposed ring corrections were derived from the thermochemical properties of furan only or of furan and benzofuran. There are no guaranties on how the ring correction estimate will perform for larger PAHs or for furan rings in other environments.

#### **4.2.3 Computational Methods**

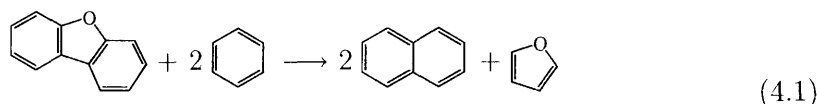
##### **Quantum Chemical Calculations**

The optimized geometries and vibrational frequencies for 29 PAHs containing the furan structure were calculated at the B3LYP/6-31G(d) level using the Gaussian 98 suite of programs [13]. El-Azhary and Suter [8] compared the performance of various methods (HF, MP2, LDA, BVWN, BLYP, and B3LYP) and basis sets (*cc*-pVDZ, *cc*-pVTZ, and 6-31G\*\*) in the calculation of the geometry and vibrational frequencies of furan. In Table 4.1 the experimental geometry of this molecule is compared with the geometry obtained at different levels of computation. We can conclude that the B3LYP/6-31G(d) method can obtain accurate geometries for furan structures. El-

Azhary and Suter found that among the methods that they tested, the geometry from the B3LYP method provides the best agreement with experimental geometry. The effect of the basis set of the calculated bond angles and frequencies was very small.

### Homodesmic Reactions

We used the same homodesmic reaction scheme used for five- and six-membered ring PAHs to calculate the  $\Delta H_f^\circ$  of PAHs that contain the furan substructure. Furan was added as reference molecule to account for the furan ring in these PAHs.



The agreement between the  $\Delta H_f^\circ$  calculated from this homodesmic reaction scheme with the available experimental values is very good, as shown in Table 4.2. The calculation of the errors related to  $\Delta H_{f,\text{homo}}^\circ$  was done as described in Section 2.3. The error bars reported for  $\Delta H_{f,\text{exp}}^\circ$  often refer to a particular experimental setup, and are not a realistic indication of the uncertainty in the experimental value. Thus the uncertainty in the  $\Delta H_{f,\text{exp}}^\circ$  of furan was assigned to be 2 kcal mol<sup>-1</sup> (which corresponds to a grade of ‘C’ as discussed in Section 2.2.1).

### Entropy and Heat Capacities

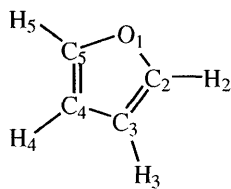
Experimental values for entropy and heat capacities for this class of PAHs are only available for furan. The values listed in Table 4.3 are the ones cited by Stull et al. [34]. The experimental values are compared to the values calculated at the B3LYP/6-31G(d) level.

#### 4.2.4 Estimation Method

We introduced the new atom-centered group ‘O’, corresponding to the oxygen in PAHs with a furan structure. The introduction of the ‘O’ atom-centered group leads to three new bond-centered groups: ‘AO5’, ‘BO5’, and ‘CO5’. These three bonds

Table 4.1: Comparison between the experimental geometry of furan the geometry calculated at different levels.

	Exp. <sup>a</sup>	MP2	B3LYP	B3LYP
		6-31G** <sup>b</sup>		6-31G(d)
Bond Lengths (Å)				
O <sub>1</sub> -C <sub>2</sub>	1.362	1.364	1.364	1.364
C <sub>2</sub> -C <sub>3</sub>	1.361	1.365	1.361	1.361
C <sub>3</sub> -C <sub>4</sub>	1.431	1.426	1.444	1.436
C <sub>2</sub> -H <sub>2</sub>	1.075	1.074	1.079	1.079
C <sub>3</sub> -H <sub>3</sub>	1.077	1.075	1.087	1.081
Bond Angles				
C <sub>2</sub> -O <sub>1</sub> -C <sub>5</sub>	106.5	107.2	106.4	106.8
O <sub>1</sub> -C <sub>2</sub> -C <sub>3</sub>	110.7	110.8	110.5	110.5
C <sub>2</sub> -C <sub>3</sub> -C <sub>4</sub>	106.0	105.6	106.0	106.1
O <sub>1</sub> -C <sub>2</sub> -H <sub>2</sub>	115.9	116.2	115.8	115.6
C <sub>2</sub> -C <sub>3</sub> -H <sub>3</sub>	126.1	126.8	126.5	126.6



<sup>a</sup>As cited by [8]

<sup>b</sup>Reference [8]

Table 4.2: Comparison between  $\Delta H_{f,\text{exp}}^\circ$  values and  $\Delta H_f^\circ$  calculated from the proposed homodesmic reaction scheme for PAHs containing furan structures. As a reference the  $\Delta H_{f,\text{atom}}^\circ$  calculated from atomization reactions are also given.

		$\Delta H_{f,\text{exp}}^\circ$ (kcal mol <sup>-1</sup> )	$\Delta H_{f,\text{atom}}^\circ$ (kcal mol <sup>-1</sup> )	$\Delta H_{f,\text{homo}}^\circ$ (kcal mol <sup>-1</sup> )
Furan	C <sub>4</sub> H <sub>4</sub> O	-8.3±0.2 <sup>a</sup>	-6.5±0.4	-8.3±2
2,3-Benzofuran	C <sub>8</sub> H <sub>6</sub> O	3.3±0.2 <sup>b</sup>	5.1±0.9	4.1±3
Dibenzofuran	C <sub>12</sub> H <sub>8</sub> O	11.3±1.1 <sup>b</sup> , 13.2±0.1 <sup>c</sup>	13.2±1.3	13.1±4

<sup>a</sup>Reference [16]

<sup>b</sup>As cited in [23]

<sup>c</sup>Reference [5]



Table 4.3: Comparison between experimental and B3LYP/6-31G(d)  $S_{298}^{\circ}$  and  $C_p^{\circ}$  for PAHs containing furan structures. In (cal K<sup>-1</sup> mol<sup>-1</sup>).

	Furan	
	Exp. <sup>a</sup>	Calc.
$S_{298}^{\circ}$	63.86	64.0
$C_{p,300}^{\circ}$	15.75	16.1
$C_{p,400}^{\circ}$	21.20	21.6
$C_{p,500}^{\circ}$	25.73	26.1
$C_{p,600}^{\circ}$	29.31	29.6
$C_{p,800}^{\circ}$	34.41	34.6
$C_{p,1000}^{\circ}$	37.89	38.0
$C_{p,1500}^{\circ}$	-	43.0

<sup>a</sup>As cited by [34]

describe the two bonds in the furan ring that are bonded to the oxygen atom. Their difference lies on the environment of the carbon adjacent to the oxygen. For example, in ‘AO5’ the carbon has two benzene bonds and one single bond, and in ‘CO5’ the carbon is in a bay region. The other bonds in the furan ring are treated as normal bonds in a PAH.

To calculate the contributions of these furan bonds, we subtracted the values corresponding to the contributions of the bonds of five- and six-membered rings (whose values were derived in Chapter 3) from the thermochemical properties of these furan-PAHs. In the calculation of the structure count of the PAHs containing the furan structure, we counted the number of different ways the double and single bonds can be drawn in the molecule. For example, furan has a Kekulé structure count of 1, and dibenzofuran has a structure count of 4. The contributions from each of such bonds to the  $\Delta H_f^{\circ}$  is shown in Table 4.4. Given the relatively high MAD and RMS obtained from this method, we conclude that the ‘AO5’, ‘BO5’, and ‘CO5’ bonds are not specific enough to capture the characteristics of PAHs containing the furan structure. Thus these bonds have been further subdivided depending on the neighbor of the carbon atom. For example, the ‘AO5’ bond has been subdivided into ‘AO5(A)’, ‘AO5(B)’, and ‘AO5(C)’. Figure 4-1 should help in the understanding of these new bonds. It is not necessary that both of the rings marked with \* in ‘BO5(C)’ and

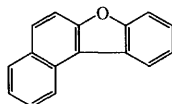
Table 4.4: Group values obtained for  $\Delta H_f^\circ$  if bond groups ‘AO5’, ‘BO5’, and ‘CO5’ are considered.

	$\Delta H_f^\circ$ (kcal mol <sup>-1</sup> )
AO5	-17.65 ± 0.7
BO5	-13.11 ± 0.9
CO5	-18.88 ± 2.0
MAD	3.70
RMS	5.22

‘CO5(C)’ be present, but at least one must be. The coefficients obtained for the new bonds are shown in Tables 4.5 and 4.6. The standard deviations for the  $C_p^\circ$  coefficients was 0.1 cal K<sup>-1</sup> mol<sup>-1</sup> or smaller.

## 4.2.5 Results and Discussion

The differentiation of the ‘AO5’, ‘BO5’, and ‘CO5’ according to the neighbor of the carbon atom improves the estimation method. Both the MAD and the RMS decrease by almost 2 kcal mol<sup>-1</sup>. The predictive capability of this estimation method can be assessed through the “leave one out” procedure. The discrepancy between the  $\Delta H_f^\circ$  for each observation and its prediction from the regression equation obtained by leaving that observation out was calculated. The MAD and RMS for these residuals are 2.37 and 3.98 kcal mol<sup>-1</sup>. These values are not significantly larger than the values for the ordinary least square regression presented in Table 4.5, indicating that the method has good predictive capabilities. The maximum residual  $y_i - \hat{y}_{i(i)}$ , where  $y_i$  is  $\Delta H_{f,\text{homo}}^\circ$  and  $\hat{y}_{i(i)}$  is the predicted  $\Delta H_f^\circ$  from coefficients derived without including the  $i$ th observation in the regression, was -10.99 kcal mol<sup>-1</sup> for



This is the only furan ring in which the ‘C’ carbon of the ‘BO5(C)’ group is bonded to two other ‘C’ carbons. This is maybe an indication that if the bond-centered groups are to be refined further, the ‘BO5(C)’ (and probably the ‘CO5(C)’ group should be subdivided according to the atoms that are bonded to the ‘C’ carbon.

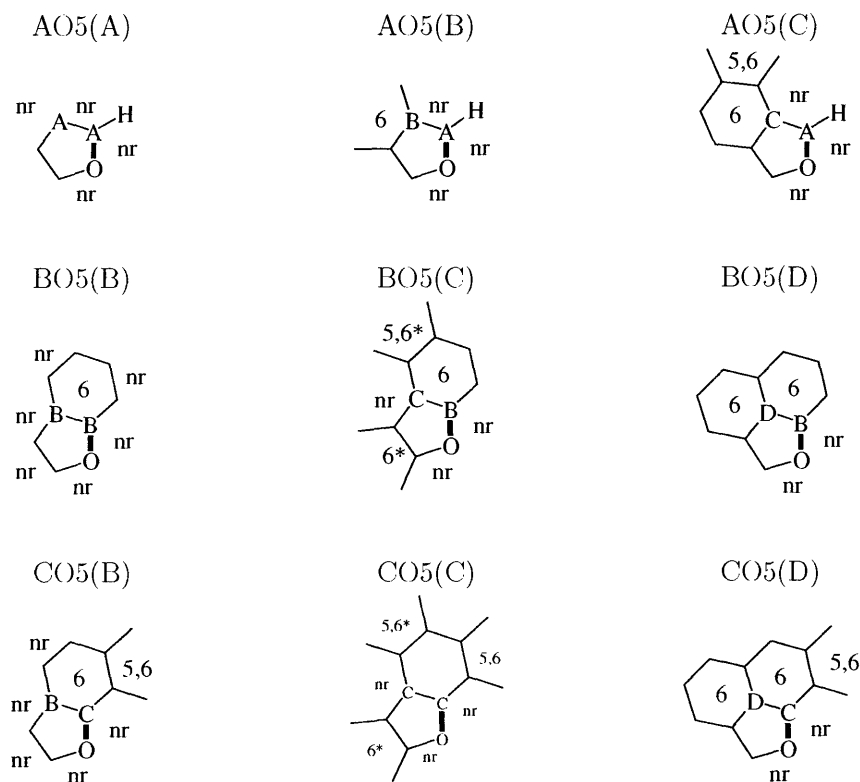


Figure 4-1: Aromatic bonds defined for PAHs with a furan structure. The rings marked with a \* in the ‘BO5(C)’ and ‘CO5(C)’ bond-groups don’t have to necessary be both present, but at least one must be.

Table 4.5: Coefficients for the estimation of  $\Delta H_f^\circ$  and  $S_{298}^\circ$  of PAHs with Furan Rings.

	$\Delta H_f^\circ$ (kcal mol <sup>-1</sup> )	$S_{298}^\circ$ (cal K <sup>-1</sup> mol <sup>-1</sup> )
AO5(A)	-19.74 ± 0.5	13.2 ± 0.1
AO5(B)	-15.02 ± 0.7	12.6 ± 0.1
AO5(C)	-14.84 ± 1.3	12.4 ± 0.2
BO5(B)	-12.56 ± 1.2	5.2 ± 0.2
BO5(C)	-14.48 ± 0.6	5.6 ± 0.1
BO5(D)	-9.33 ± 1.0	6.7 ± 0.2
CO5(B)	-17.69 ± 1.7	5.9 ± 0.3
CO5(C)	-19.37 ± 1.8	5.0 ± 0.3
CO5(D)	-17.97 ± 2.0	6.8 ± 0.3
MAD	1.76	0.32
RMS	3.05	0.53

Table 4.6: Coefficients for the estimation of  $C_p^\circ$  of PAHs with Furan Rings. The standard error of each  $C_p^\circ$  coefficient is smaller than  $0.1 \text{ cal K}^{-1} \text{ mol}^{-1}$ .

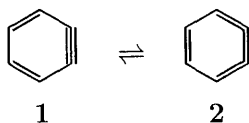
	$C_{p,T}$ ( $\text{cal K}^{-1} \text{ mol}^{-1}$ )						
	300 K	400 K	500 K	600 K	800 K	1000 K	1500 K
AO5(A)	2.9	3.9	4.6	5.2	6.1	6.6	7.5
AO5(B)	3.0	3.8	4.6	5.2	5.9	6.7	7.5
AO5(C)	2.8	3.7	4.5	5.1	5.9	6.8	7.3
BO5(B)	2.8	3.4	4.2	4.9	5.3	6.3	6.8
BO5(C)	2.8	3.6	4.3	5.0	5.5	6.4	6.8
BO5(D)	3.0	3.6	4.4	5.0	5.4	6.3	6.8
CO5(B)	2.8	3.3	4.1	4.9	5.1	6.3	6.7
CO5(C)	2.6	3.4	4.3	4.9	5.4	6.4	6.4
CO5(D)	2.9	3.5	4.3	4.9	5.3	6.3	6.5
MAD	0.07	0.06	0.06	0.06	0.09	0.07	0.09
RMS	0.10	0.10	0.09	0.09	0.12	0.12	0.13

Bond centered groups are more flexible than ring corrections. As exemplified in the previous paragraph, it is easy to refine the method to exactly capture the important factors that determine the thermochemistry of furan rings. The nine bonds presented in this work can describe any furan ring occurring in PAHs.

## 4.3 Arynes

### 4.3.1 Introduction

Arynes are formed through didehydrogenation of the parent arene at the *ortho* position. They can be viewed as a delocalized structure in which the second  $\pi$ -orbital from the triple bond is perpendicular to the first. The electrons in this second  $\pi$ -orbital are not free to move around the aromatic ring. MO results have shown that both resonance structures **1** and **2** contribute to benzyne [17].



Arynes are believed to be important intermediates in the formation of five-membered rings from benzenoid PAHs. One proposed mechanism suggests that after 1,2-didehydrogenation of the parent arene, the resulting aryne will be in equilibration with its carbene isomer. The latter is then trapped intramolecularly to form a five membered ring [29]. The thermolysis of benzo[*c*]phenanthrene [19] is shown in Figure 4-2 as an example.

In the literature, didehydroarenes (not necessarily at the *ortho* position) are in general called arynes. In this work we use the term aryne only for PAHs in which the dehydrogenation occurs at neighboring carbons, allowing the formation of a triple bond.

### 4.3.2 Experimental Values

The  $\Delta H_{f,\text{exp}}^\circ$  of benzyne has been measured by many groups using different methods, and the values have ranged from 98 to 113 kcal mol<sup>-1</sup> [37]. The  $\Delta H_f^\circ$  of 1,2- and 2,3-didehydronaphthalenes have been estimated through the study of bromine elimination reactions with bromonaphthalenes [22]. The  $\Delta H_f^\circ$  of 9,10-didehydrophenanthrene has been estimated through the study of the thermal decomposition of 9,10-disubstituted derivatives of phenanthrene [15]. A list of these scarce experimental  $\Delta H_f^\circ$  is found in Table 4.8.

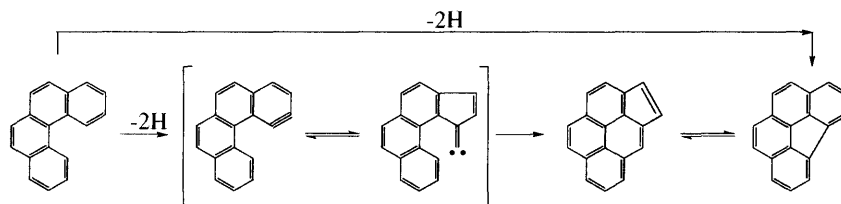


Figure 4-2: Arynes have been proposed to be intermediates in the formation of five-membered rings, as shown here in the thermolysis of benzo[*c*]phenanthrene [19]

### 4.3.3 Computational Methods

#### Quantum Chemical Calculations

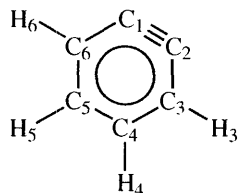
Cioslowski [6] tested many quantum chemical methods for aryne compounds. He found that the B3LYP/6-311G(d,p) method provided a geometry of benzyne comparable to higher level, benchmark calculations such as MP2/6-311G\*\*, QCISD/6-311G\*\*, and CCSD(T)/6-311G\*\*. A comparison between the benzyne geometry from these benchmark calculations and the geometry from B3LYP/6-311G\*\* and B3LYP/6-31G(d) is given in Table 4.7. The geometry for benzyne, the prototype aryne compound, calculated with the B3LYP/6-31G(d) method also agrees well with the geometries from the higher level calculations. However, B3LYP/6-31G(d) does not provide good absolute energy for benzyne. While the MP2/6-311G\*\*, QCISD/6-311G\*\*, and B3LYP/6-311G\*\* methods give heats of 1,2-didehydrogenation of benzene of 86.1, 91.2, and 82.8 kcal mol<sup>-1</sup> at 0K, compared to the experimental value of 86.6 ± 3.0 kcal mol<sup>-1</sup> (at 298K) [6], the value calculated from B3LYP/6-31G(d) (at 0K) is ca. 7 kcal mol<sup>-1</sup> higher, 93.5 kcal mol<sup>-1</sup>. However, we would still like to use the B3LYP/6-31G(d) method for the calculation of arynes, so that we can profit from the values already calculated at this level for the other PAHs. The calculations for 10 arynes were done at the B3LYP/6-31G(d) level with a judicious choice of homodesmic reactions to calculate sound values for the  $\Delta H_f^\circ$  from the B3LYP/6-31G(d) absolute energies.

#### Homodesmic Reactions

We used the same homodesmic reaction scheme adopted for five- and six-membered rings to calculate the  $\Delta H_f^\circ$  of arynes from the absolute energies. In order to correct for the discrepancy in the total energy of aryne compounds at the B3LYP/6-31G(d) level, we added benzyne as a reference molecule in the homodesmic reaction scheme to account for the triple bond in these PAHs. For example, the  $\Delta H_f^\circ$  of 1,2-didehydro-

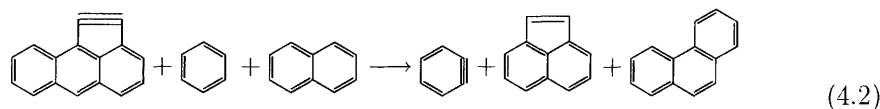
Table 4.7: Comparison between the geometry of benzyne calculated at different levels.

	QCISD	MP2	B3LYP	B3LYP
	6-311G** <sup>a</sup>			6-31G(d)
Bond Lengths (Å)				
C <sub>1</sub> -C <sub>2</sub>	1.256	1.268	1.256	1.251
C <sub>2</sub> -C <sub>3</sub>	1.395	1.393	1.391	1.385
C <sub>3</sub> -C <sub>4</sub>	1.409	1.410	1.422	1.413
C <sub>4</sub> -C <sub>5</sub>	1.417	1.414	1.412	1.407
C <sub>3</sub> -H <sub>3</sub>	1.085	1.085	1.089	1.085
C <sub>4</sub> -H <sub>4</sub>	1.088	1.088	1.092	1.088
Bond Angles				
C <sub>1</sub> -C <sub>2</sub> -C <sub>3</sub>	126.9	126.8	127.1	126.9
C <sub>1</sub> -C <sub>6</sub> -C <sub>5</sub>	110.5	110.6	110.7	110.3
C <sub>1</sub> -C <sub>6</sub> -H <sub>6</sub>	126.7	127.0	127.1	127.2
C <sub>3</sub> -C <sub>4</sub> -C <sub>5</sub>	122.5	122.7	122.4	122.4
C <sub>3</sub> -C <sub>4</sub> -H <sub>4</sub>	118.9	118.6	118.5	118.7



<sup>a</sup>Reference [6]

aceanthrylene is calculated through:



The  $\Delta H_{f,\text{homo}}^\circ$  values for the 1,2- and for 2,3-didehydronaphthalenes agree well with the  $\Delta H_f^\circ$  values estimated for these molecules by Linnert and Riveros [22] from experimental results of bromine elimination reactions with bromonaphthalenes. As shown in Table 4.8, the  $\Delta H_f^\circ$  calculated through the proposed homodesmotic reaction scheme agrees very well with the available  $\Delta H_{f,\text{exp}}^\circ$ . On the other hand, the  $\Delta H_{f,\text{atom}}^\circ$  for benzyne is ca. 7 kcal mol<sup>-1</sup> higher than its  $\Delta H_{f,\text{exp}}^\circ$ , as was expected, knowing that the heat of 1,2-didehydrogenation of benzene is overestimated by the same amount by the B3LYP/6-31G(d) method.

#### 4.3.4 Estimation Method

The bond-centered groups for five- and six-membered ring PAHs derived in Chapter 3 were used for the benzene bonds in the arynes. The  $\ln(K)$  term was also used.

Table 4.8: Comparison between the  $\Delta H_f^\circ$  calculated from the proposed homodesmic reaction scheme for arynes and  $\Delta H_{f,\text{exp}}^\circ$  values. As a reference the  $\Delta H_{f,\text{atom}}^\circ$  calculated from atomization reactions are also given.

		$\Delta H_{f,\text{exp}}^\circ$ (kcal mol <sup>-1</sup> )	$\Delta H_{f,\text{atom}}^\circ$ (kcal mol <sup>-1</sup> )	$\Delta H_{f,\text{homo}}^\circ$ (kcal mol <sup>-1</sup> )
Benzyne	C <sub>6</sub> H <sub>4</sub>	106.6 ± 3 <sup>a</sup>	113.9 ± 0.7	106.6 ± 2
1,2-didehydronaphthalene	C <sub>10</sub> H <sub>6</sub>	122 ± 6 <sup>b</sup>	131.9 ± 1.1	121.6 ± 3
2,3-didehydronaphthalene	C <sub>10</sub> H <sub>6</sub>	124 ± 6 <sup>b</sup>	134.4 ± 1.1	124.1 ± 3
Acenaphthylene	C <sub>12</sub> H <sub>6</sub>	160 ± 4 <sup>c</sup>	182.5 ± 1.3	173.1 ± 7.5
9,10-didehydrophenanthrene	C <sub>14</sub> H <sub>8</sub>	143 ± 9 <sup>d</sup>	141.7 ± 1.6	132.0 ± 4.5

<sup>a</sup>Reference [22]

<sup>b</sup>Reference [36]

<sup>c</sup>Reference [4]

<sup>d</sup>Reference [15]

The number of Kekulé structures was counted in the same way as for the five- and six-membered ring PAHs. For example, benzyne is considered to have 2 Kekulé structures, and the didehydronaphthalenes each have 3. We introduced one new atom-centered group ‘I’, corresponding to the carbons that belong to a triple bond in benzyne structures. The ‘I’ atom-centered group leads to the following new bond-centered groups: ‘AI6’, ‘BI6’, ‘CI6’, ‘II6’, ‘AI5’, ‘BI5’, ‘CI5’, and ‘II5’. Figure 4-3 should help in the understanding of these new bonds. Of these 8 new bond-centered groups, only six are linearly independent. For example, the number of bonds ‘II5’ and ‘II6’ are related to the number of their remaining bonds through:

$$\text{II5} = 0.5 \times \text{AI5} + 0.5 \times \text{BI5} + 0.5 \times \text{CI5} \quad (4.3)$$

$$\text{II6} = 0.5 \times \text{AI6} + 0.5 \times \text{BI6} + 0.5 \times \text{CI6} \quad (4.4)$$

The values for these groups were derived from the thermochemical properties of the 10 arynes (shown in Figure 4-4) for which B3LYP/6-31G(d) calculations were performed. The contributions of bonds ‘II5’ and ‘II6’ to the  $\Delta H_f^\circ$  were assigned to be 70.0 and 50.0 kcal mol<sup>-1</sup>, respectively. Their contributions to  $S_{298}^\circ$  and  $C_p^\circ$  was set to zero. The coefficients obtained from a weighted least square regression are shown in Tables 4.9 and 4.10.



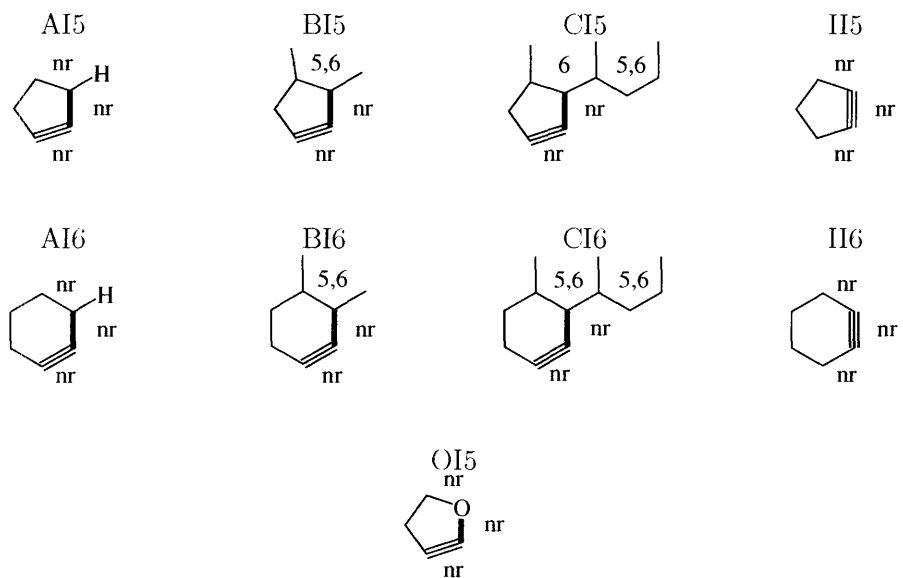


Figure 4-3: Aromatic bonds defined for PAHs with triple bonds

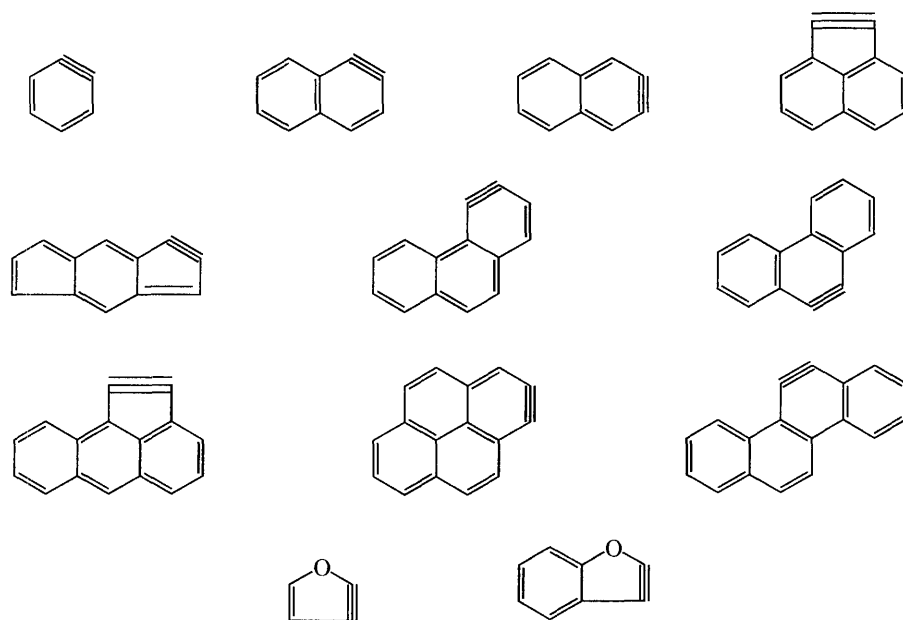


Figure 4-4: Arynes used for the derivation of the bond-centered group contributions

Table 4.9: Contributions to the  $\Delta H_f^\circ$  and  $S_{298}^\circ$  from each of the bond-centered group values that describe aryne PAHs.

	$\Delta H_f^\circ$ (kcal mol <sup>-1</sup> )	$S_{298}^\circ$ (cal K <sup>-1</sup> mol <sup>-1</sup> )
AI5	41.44 ± 2.8	21.3 ± 0.7
BI5	35.02 ± 0.8	13.9 ± 0.2
CI5	29.12 ± 1.9	14.7 ± 0.4
II5	70.00 ± -	0.0 ± -
AI6	26.94 ± 0.2	17.4 ± 0.0
BI6	24.66 ± 0.3	9.5 ± 0.1
CI6	19.57 ± 0.8	9.9 ± 0.2
II6	50.00 ± -	0.0 ± -
MAD	0.423	0.092
RMS	1.038	0.200

Table 4.10: Contributions to the  $C_p^\circ$ 's from each of the bond-centered group values that describe aryne PAHs.

	$C_{p,T} (cal K^{-1} mol^{-1})$						
	300 K	400 K	500 K	600 K	800 K	1000 K	1500 K
AI5	5.6±0.2	6.3±0.4	7.1±0.1	7.6±0.3	8.5±0.4	8.9±1.3	10.2±2.5
BI5	4.9±0.1	5.7±0.1	6.5±0.1	7.1±0.1	7.7±0.1	8.5±0.3	9.1±0.7
CI5	5.0±0.1	5.7±0.3	6.4±0.1	7.2±0.2	7.6±0.3	8.6±0.8	9.0±1.7
II5	0.0	0.0	0.0	0.0	0.0	0.0	0.0
AI6	4.7±0.1	5.8±0.1	6.7±0.1	7.3±0.1	8.2±0.1	9.0±0.1	9.7±0.1
BI6	4.7±0.1	5.7±0.1	6.5±0.1	7.2±0.1	7.8±0.1	8.7±0.2	9.2±0.3
CI6	4.7±0.1	5.5±0.1	6.4±0.1	7.2±0.1	7.8±0.1	9.0±0.4	9.6±0.7
II6	0.0	0.0	0.0	0.0	0.0	0.0	0.0
MAD	0.019	0.048	0.020	0.035	0.054	0.142	0.281
RMS	0.056	0.112	0.052	0.091	0.122	0.316	0.608

The contribution of the OI5 group was determined separately, from the thermochemical properties of the two smallest PAHs with this group, which are shown in Figure 4-4. The values derived for this group are listed in Table 4.11.

### 4.3.5 Results and Discussion

The triple bond introduces considerable strain to aryne PAHs, as is attested by the high values of the  $\Delta H_f^\circ$  coefficients for each of the bonds.

Ford and Biehl [10] studied the relative stability of polycyclic arynes using semiempirical (AM1) molecular orbital calculations. They concluded that two factors affected the stability of arynes: the first is the relief of steric strain that accompanies the removal of the hydrogen atoms from the parent arene, and the second is the ability of the carbon skeleton to accommodate the shorter dehydro-bond. The bond-centered groups proposed here for arynes are directly related to the relief of steric strain provided by the removal of the hydrogens from the parent arene. When a dehydro-bond has a ‘C’ atom-centered group as a neighbor, it means that it is adjacent to a bay region. Thus the contribution of the ‘CI’ bonds to the  $\Delta H_f^\circ$  are significantly lower than the contribution of the other aryne bonds. The second factor affecting the stability of arynes is related to the bond order at the position of the dehydro-bond in the parent arene. Thus the triple bond that is formed in a bond that has high bond order in the parent arene is more stable than a triple bond that is formed in a bond that has lower bond order in the parent arene. The bond-centered group additivity method indirectly captures this effect through the  $\ln(K)$  term. The  $\ln(K)$  term is non-local property of the molecule, unlike the bond order, which is a property of each bond.

Since only ten arynes were used to derive six bond-groups values, it was not possible to perform a cross-validation of the method. It is expected however, based

Table 4.11:  $\Delta H_f^\circ$ ,  $S_{298}^\circ$ , and  $C_p^\circ$  contributions of the OI5 group.  $\Delta H_f^\circ$  in (kcal mol<sup>-1</sup>),  $S_{298}^\circ$  and  $C_p^\circ$  in (cal K<sup>-1</sup> mol<sup>-1</sup>).

	$\Delta H_f^\circ$	$S_{298}^\circ$	$C_{p,T}$						
			300 K	400 K	500 K	600 K	800 K	1000 K	1500 K
OI5	27.54	20.8	4.4	5.4	5.9	6.2	6.9	7.0	7.0

on the success of the bond-centered additivity method for PAHs with five- and six-membered rings and for PAHs with the furan substructure, that a bond-centered group additivity method should also be applicable to arynes.

The ‘XI5’ group values might not be very accurate, with uncertainties higher than those reported in Table 4.9. These possible higher uncertainties derive from the fact that we cannot affirm that the proposed homodesmic reaction provides accurate  $\Delta H_{f,\text{homo}}^\circ$  for arynes in which the triple bond is in a five-membered ring. This conclusion is arrived at by the comparison between the available  $\Delta H_{f,\text{exp}}^\circ$  and the calculated  $\Delta H_{f,\text{homo}}^\circ$  for acenaphthylene, the only such PAH with an  $\Delta H_{f,\text{exp}}^\circ$  (see Table 4.8).

## 4.4 Substituted PAHs

### 4.4.1 Introduction

A variety of substituted PAHs have been detected in flames. Hydroxyl substituted PAHs are formed during the early stages of fuel oxidation [18, 7]. Vinyl and ethynyl substituted PAHs are formed from the reaction of acetylene with PAHs and PAH radicals, respectively, and have been proposed to be important intermediates in the PAH growth mechanism [35, 11, 12]. A variety of biarenes have been detected in the pyrolysis of aromatic fuels [27, 25, 14]. Under some pyrolytic conditions, it is believed that polymerization of PAHs forming biarenes is a more important channel for molecular weight growth than acetylene addition [38, 27]. Biarenes are highly reactive intermediates that can undergo intramolecular cyclodehydrogenation forming new five- and six-membered rings.

Even when one considers only substitutions consisting of carbon and oxygen atoms, the number of possible combinations between position of substitution in the PAH and the nature of substitute is very large. This number grows even more when one considers disubstituted (and polysubstituted!) PAHs. It is not the goal of this work to provide group values for all the possible combinations of substituted PAHs. Rather, we want to provide the framework for an estimation method, that is a tree

structure with sound values in the higher nodes. The more specific nodes, down in the tree, can be filled in later, as the importance of each node is determined from the use of the thermochemical properties propose here.

We have included in this work PAHs substituted with acetyl, alcohol, methyl, vinyl, aldehyde, and phenyl groups. A few disubstituted PAHs were also studied.

## 4.4.2 Experimental Thermochemical Properties

There are a few experimental  $\Delta H_f^\circ$  for substituted PAHs. Some of these values from the NIST Webbook [23] are listed in Table 4.12. Experimental  $S_{298}^\circ$  and  $C_p^\circ$  are listed as cited by Stull et al. [34] in Table 4.13. In general the B3LYP/6-31G(d) calculated  $S_{298}^\circ$  and  $C_p^\circ$  agree well with experimental data. The discrepancy between the experimental and calculated  $S_{298}^\circ$  for phenylacetylene is discussed in Section 4.4.3.

## 4.4.3 Computational Methods

### Quantum Chemical Calculations

B3LYP/6-31G(d) calculations were performed for a set of 70 substituted PAHs. All torsional motions around the single bonds for the alcohol, methyl, vinyl, aldehyde and phenyl substituted groups were treated as hindered internal rotations. The dihedral angle corresponding to the internal rotation was varied from  $0^\circ$  to  $360^\circ$  in increments of  $30^\circ$  while the remaining 3N-7 internal coordinates were optimized at the B3LYP/6-31G(d) level. The resulting potential energy surface was fitted to a Fourier series  $\sum_m [A_m \cos(m\phi) + B_m \sin(m\phi)]$  with  $m = 5$ . The partition function for the hindered rotation was obtained by solving the one-dimensional Schrödinger equation

$$-\frac{h^2}{8\pi^2 I_{hir}} \frac{d^2 \Psi(\Phi)}{d\Phi^2} + V(\Phi) \Psi(\Phi) = E(\Phi) \Psi(\Phi) \quad (4.5)$$

for the energy eigenvalues. The reduced moment of inertia for rotation,  $I_{hir}$ , was taken as the reduced moment of the two groups about an axis passing through the

Table 4.12: Comparison between the  $\Delta H_{f,\text{exp}}^\circ$  and the  $\Delta H_f^\circ$  calculated from the proposed homodesmotic reaction scheme.

	Formula	$\Delta H_{f,\text{exp}}^\circ$ (kcal mol <sup>-1</sup> ) <sup>a</sup>	$\Delta H_{f,\text{homo}}^\circ$ (kcal mol <sup>-1</sup> )	$\Delta H_{f,\text{homo}}^\circ - \Delta H_{f,\text{exp}}^\circ$ (kcal mol <sup>-1</sup> )
Phenol	C <sub>6</sub> H <sub>6</sub> O	-23.0 ± 0.1	-23.0 ± 0.5	0 <sup>b</sup>
1,2-Benzenediol	C <sub>6</sub> H <sub>6</sub> O <sub>2</sub>	-65.7 ± 0.3	-66.8 ± 1.5	-1.1
1,3-Benzenediol	C <sub>6</sub> H <sub>6</sub> O <sub>2</sub>	-68.0 ± 0.3	-66.5 ± 1.5	1.6
1,4-Benzenediol	C <sub>6</sub> H <sub>6</sub> O <sub>2</sub>	-66.2 ± 0.3	-64.2 ± 1.5	2.0
Benzaldehyde	C <sub>7</sub> H <sub>6</sub> O	-8.8 ± 0.7	-8.8 ± 1.0	0 <sup>b</sup>
Toluene	C <sub>7</sub> H <sub>8</sub>	12.0 ± 0.2	12.0 ± 0.5	0 <sup>b</sup>
Phenylacetylene	C <sub>8</sub> H <sub>6</sub>	73.3 ± 0.4	73.3 ± 0.5	0 <sup>b</sup>
Styrene	C <sub>8</sub> H <sub>8</sub>	35.1 ± 0.2	35.1 ± 0.5	0 <sup>b</sup>
o-Xylene	C <sub>8</sub> H <sub>10</sub>	4.5 ± 0.3	5.2 ± 1.5	0.7
m-Xylene	C <sub>8</sub> H <sub>10</sub>	4.1 ± 0.2	4.1 ± 1.5	-0.1
p-Xylene	C <sub>8</sub> H <sub>10</sub>	4.3 ± 0.2	4.1 ± 1.5	-0.2
1-Naphthalenol	C <sub>10</sub> H <sub>8</sub> O	-7.4 ± 0.4	-7.0 ± 1.5	0.4
2-Naphthalenol	C <sub>10</sub> H <sub>8</sub> O	-7.2 ± 0.4	-7.2 ± 1.5	0 <sup>b</sup>
1-methyl-Naphthalene	C <sub>11</sub> H <sub>10</sub>	27.9 ± 0.6	29.3 ± 1.5	1.4
2-methyl-Naphthalene	C <sub>11</sub> H <sub>10</sub>	27.8 ± 0.6	27.9 ± 1.5	0.1
Biphenyl	C <sub>12</sub> H <sub>10</sub>	43.5 ± 0.2	43.5 ± 0.5	0 <sup>b</sup>
1,8-dimethyl-Naphthalene	C <sub>12</sub> H <sub>12</sub>	26.0 ± 0.7	29.1 ± 2.5	3.1
Diphenylmethane	C <sub>13</sub> H <sub>12</sub>	39.4 ± 0.4	39.4 ± 1.1	0 <sup>b</sup>
4-methyl-Phenanthrene	C <sub>15</sub> H <sub>12</sub>	46.8 ± 0.3	47.7 ± 3.0	0.9

<sup>a</sup>From ref. [23]

<sup>b</sup>Used in the homodesmotic reaction scheme

Table 4.13: Comparison between the experimental and B3LYP/6-31G(d)  $S_{298}^\circ$  and  $C_{p,300}^\circ$  for some substituted PAHs. The experimental values are listed as cited in [34]. The difference between the calculated value and the experimental value is given in the columns under the header  $\Delta$ . All values in (cal K<sup>-1</sup> mol<sup>-1</sup>).

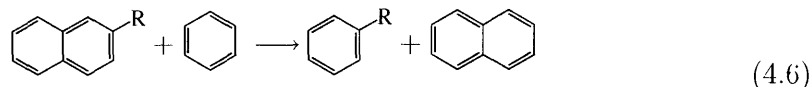
	Formula	$S_{298}^\circ$			$C_{p,300}^\circ$		
		Exp.	Calc.	$\Delta$	Exp.	Calc.	$\Delta$
Phenol	C <sub>6</sub> H <sub>6</sub> O	75.43	75.48	0.05	24.90	25.15	0.25
Toluene	C <sub>7</sub> H <sub>8</sub>	76.64	76.90	0.26	24.94	25.33	0.39
Phenylacetylene	C <sub>8</sub> H <sub>6</sub>	76.88	79.06	2.18	27.63	28.59	0.96
Styrene	C <sub>8</sub> H <sub>8</sub>	82.48	82.08	-0.40	29.35	29.17	-0.18
o-Xylene	C <sub>8</sub> H <sub>10</sub>	84.31	84.26	-0.05	32.02	32.02	0.00
m-Xylene	C <sub>8</sub> H <sub>10</sub>	85.49	85.65	0.16	30.66	30.53	-0.13
p-Xylene	C <sub>8</sub> H <sub>10</sub>	84.23	84.37	0.14	30.49	30.52	0.03
1-methyl-Naphthalene	C <sub>11</sub> H <sub>10</sub>	90.21	90.43	0.22	38.37	38.78	0.41
2-methyl-Naphthalene	C <sub>11</sub> H <sub>10</sub>	90.83	91.62	0.79	38.42	37.63	-0.79
Biphenyl	C <sub>12</sub> H <sub>10</sub>	93.85	93.24	-0.61	39.05	40.90	1.85

center of gravity of both groups. Some disubstituted PAHs were studied and in this case the potential energy scan was done on only one of the rotors. The geometry optimization was done for the optimum dihedral angle of the other rotor.

## Homodesmic Reactions

Mó et al. tested several reaction schemes to obtain the  $\Delta H_f^\circ$  for substituted PAHs from absolute energies calculated with the B3LYP method at various basis set expansions, including 6-31G(d) [26]. As expected, they found that simple atomization and isodesmic reactions do not perform satisfactorily, whereas an isodesmic reaction that uses the unsubstituted parent compound performs very well.

We propose a homodesmic reaction scheme that uses, in addition to the unsubstituted parent PAH, also the simplest benzene substituted species as reference molecules. The  $\Delta H_f^\circ$  of the unsubstituted PAHs are calculated using the homodesmic reaction scheme described in Section 2.3. For example, for the calculation of the  $\Delta H_f^\circ$  of a substituted naphthalene, naphthalene and the corresponding substituted benzene would be used:



The  $\Delta H_f^\circ$  calculated from the proposed homodesmic reaction scheme are compared to some available  $\Delta H_{f,\text{exp}}^\circ$  in Table 4.12. In this table, the errors listed for the  $\Delta H_{f,\text{exp}}^\circ$  are the ones reported in the corresponding reference. For the purpose of calculating the errors in the  $\Delta H_{f,\text{homo}}^\circ$  and the weights of the calculated values of each PAH, we assigned a grade ‘A’ for all the  $\Delta H_f^\circ$  of the substituted benzenes, except for benzaldehyde. A grade ‘A’ corresponds to an uncertainty in the  $\Delta H_{f,\text{exp}}^\circ$  of 0.5 kcal mol<sup>-1</sup>. Benzaldehyde was assigned an uncertainty of 1 kcal mol<sup>-1</sup>.

The errors for  $\Delta H_{f,\text{homo}}^\circ$  were calculated as described in Section 2.3. The difference between  $\Delta H_{f,\text{homo}}^\circ$  and  $\Delta H_{f,\text{exp}}^\circ$  are shown in the last column of Table 4.12. In general the errors are small.

## Entropies and Heat Capacities

The vibrational frequencies were scaled by a factor of 0.9613, and the  $S_{298}^{\circ}$  take into account the symmetry of the molecules. The B3LYP/6-31G(d) entropies and heat capacities agree reasonably well with the corresponding experimental values. Exceptions are phenylacetylene and the  $C_p^{\circ}$  of biphenyl.

The experimental  $S_{298}^{\circ}$  of phenylacetylene has been calculated by Evans and Nyquist [9] from their vibrational frequencies assignment. They studied the Raman spectra of the liquid phase corrected for depolarization and the infrared absorption spectra in the 3800-450  $\text{cm}^{-1}$  and in the 450-300  $\text{cm}^{-1}$  range. Phenylacetylene has  $C_{2v}$  symmetry and its 36 normal modes are distributed as  $13a_1 + 12b_1 + 3a_2 + 8b_2$ . Of the last two  $b_2$  modes, one is assigned to the 165  $\text{cm}^{-1}$  Raman band. However, as no unassigned band remain in the region in which the last mode is expected, Evans and Nyquist took it to be coincident with a  $b_1$  mode at 353  $\text{cm}^{-1}$ . In the B3LYP calculations, two frequency modes are found around the mid-100  $\text{cm}^{-1}$  and only one in the mid-300  $\text{cm}^{-1}$  range, as shown in Table 4.14. It is known that calculated vibrational frequencies of carbon-carbon multiple bonds are very sensitive to the basis set used [24, 20]. Kwon et al. performed B3LYP calculations for phenylacetylene at increasingly larger basis set until the basis set dependence disappeared [20]. We see that although slightly different frequencies are obtained at larger basis sets, even at the largest basis set that they used, 6-311++G(2df,2pd), the general behavior is the same as that obtained with the 6-31G(d) basis set. It is possible that the last  $b_2$  mode, which Evans and Nyquist assigned to be coincident with the 353  $\text{cm}^{-1}$  mode, should actually be assigned to be coincident with the 165  $\text{cm}^{-1}$  mode. In this case, the discrepancy between the experimental and B3LYP/6-31G(d) would decrease by 1.3  $\text{cal K}^{-1} \text{mol}^{-1}$ . Kwon et al. also measured the spectra of phenylacetylene cations, and found that the two lowest modes were at 110 and 145  $\text{cm}^{-1}$ , while the third lowest mode was at 311  $\text{cm}^{-1}$  [20], supporting the idea that phenylacetylene should have two frequency modes between 100 and 200  $\text{cm}^{-1}$ .

From the discussion in the previous paragraph, nothing conclusive can be said



Table 4.14: Comparison between lowest 20 experimental and calculated frequencies for phenylacetylene. The calculated frequencies were not corrected by a scale factor. In ( $\text{cm}^{-1}$ ).

Experimental <sup>a</sup>	B3LYP	
	6-31G(d)	6-311++G(2df,2pd) <sup>b</sup>
165	146	142
353	159	161
353 <sup>c</sup>	377	371
418	413	413
467	472	474
517	531	539
531	546	558
621	578	638
621	626	645
657	637	689
691	705	708
756	776	777
763	778	782
842	858	860
918	931	946
971	969	998
986	998	1014
1001	1017	1018
1029	1056	1050
1070	1110	1102

<sup>a</sup>From [9].

<sup>b</sup>From [20].

<sup>c</sup>A missing normal mode is assigned to be coincident to the 353  $\text{cm}^{-1}$  band.

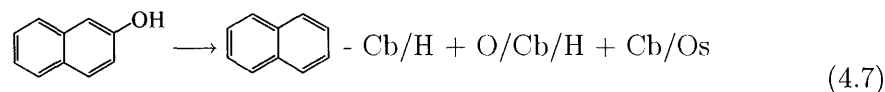
about what the correct vibrational assignment is. However, there is strong evidence that the vibrational assignment of phenylacetylene used to calculate its experimental  $S_{298}^{\circ}$  is not absolute. In view of all this discussion, we chose to use, for the sake of consistency, the  $S_{298}^{\circ}$  calculated at the B3LYP/6-31G(d) level for all the acetylene substituted PAHs to derive groups for all estimation method.

The discrepancy between experimental and the B3LYP/6-31G(d) of  $C_p^{\circ}$  for biphenyl is less worrisome, since the discrepancy decreases at higher temperatures. At 1000K the B3LYP/6-31G(d) is the same as the experimental value (96 cal K<sup>-1</sup> mol<sup>-1</sup>).

#### 4.4.4 Estimation Method

In addition to the 70 substituted PAHs for which we did quantum chemical calculations, we also used the experimental  $\Delta H_f^{\circ}$  for 20 disubstituted PAHs in the derivation of the coefficients of the estimation method.

The thermochemical properties of the substituted PAHs can be calculated from the thermo of the corresponding unsubstituted PAH and appropriate Benson's atom-centered group values. For example, 2-Naphthalenol is given by:



The thermo of the unsubstituted PAH can be calculated from the bond-centered group additivity method proposed in Chapter 3, taking the group values from Benson for the remaining atom-centered groups.

Benson and Stein and Fahr provided atom-centered group values for the calculation of the thermochemical properties of substituted PAHs [1, 33]. In Benson's method the Cb's are not differentiated, although it is known, for example, that a substituent near a bay region should lead to a higher energy than a substituent in another position (see Figure 4-5). In this work we want to be able to capture these differences, therefore we will refine Benson's groups, making them more specific. The groups for substituted PAHs can be divided into two classes. The first class consist



Figure 4-5: Benson’s method does not differentiate the groups according to where in the PAH the substituent is located, although it is known, for example, that a substituent at a bay region leads to a higher energy than a substituent in another position, due to steric interactions.

of groups centered at a Cb (e.g. Cb/Os), and the second class are those groups in which Cb is one of the neighbors (e.g. O/Cb/H). We chose to differentiate the groups that are centered at a Cb according to the environment of the Cb. The new group values differentiate whether the substitution is bonded to a six- or to a five-membered ring. For substitution on six-membered rings we also have different group values depending on whether the substituted site is bonded to a ‘C’, to a ‘B’ or only to ‘A’ atom-centered groups (see Section 3.2.1 for definition of atom-centered groups). The groups proposed for the estimation of the thermo of substituted PAHs are shown in Figure 4-6.

With the exception of 9-phenyl-Anthracene and 9-Anthracenol, all the molecules with A6(BX) groups used to obtain the group values had X = ‘A’. All the molecules used to derive the A6(CX) group also had X = ‘A’. Non-nearest neighbor corrections for *ortho*, *meta*, and *para* substitutions on the same aromatic ring, as well as a correction for a substitution on both ‘A’ atom-centered groups connected to the same ‘B’ group were introduced. This last correction was named ‘18’, which refers to the positions in naphthalene that correspond to this correction, as shown in Figure 4-7. Due to the lack of data for disubstituted PAHs, the corrections for the disubstitution was assigned to each substitution. That is, a non-nearest neighbor correction was assigned to R<sub>1</sub> independently of the nature of R<sub>2</sub>, and vice-versa.

The groups for  $\Delta H_f^\circ$  derived in this manner and also differentiating the type of functional group connected to the central Cb can be found in Table 4.15. The mean

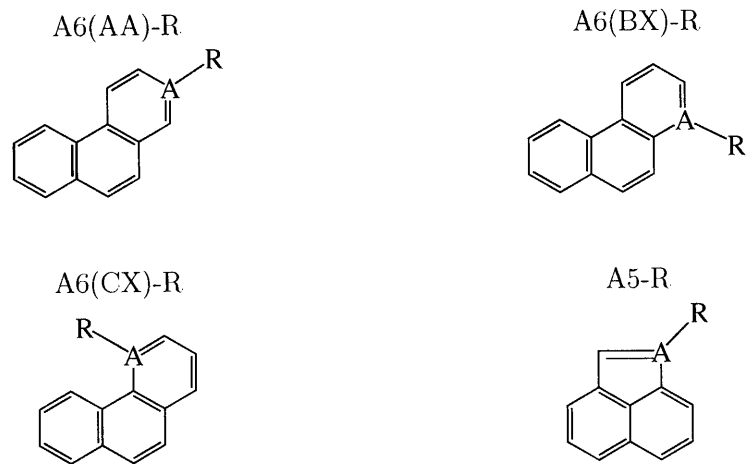


Figure 4-6: New groups introduced in this work. The groups are differentiated according to the environment in the PAH where they are bonded. The '6' and the '5' in the name of the group determines the size of the ring, and the two letters in parenthesis refer to the atom-centered groups in the PAH that are bonded to the central Cb. An 'X' stands for any atom-centered group ('A', 'B', or 'C').

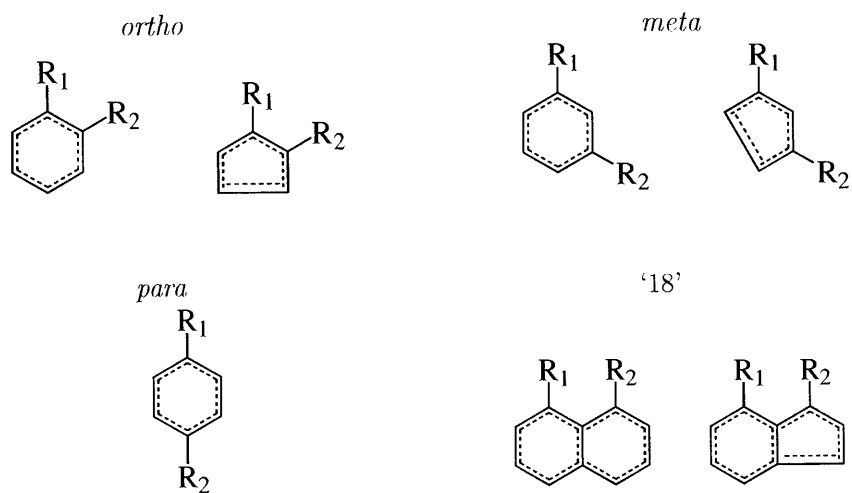


Figure 4-7: Corrections introduced for disubstituted PAHs.

average deviation (MAD) of the  $\Delta H_f^\circ$  of the PAHs included in this study calculated using these coefficients is  $0.49 \text{ kcal mol}^{-1}$ , and the root mean square error (RMS) is  $1.42 \text{ kcal mol}^{-1}$ . As seen in Table 4.15, two factors affect the groups values the most: 1) whether the substituent is a carbon or an oxygen and 2) the environment to which the central Cb atom is bonded in the PAH. The functional group of the substituted carbon plays only a secondary role. This leads to the conclusion that in a tree structure for the Cb-R group values, the groups should first be differentiated according to whether the substitution is a carbon or an oxygen. The next differentiation should be according to the environment in the PAH of the central Cb. We first differentiate according to whether the Cb group belongs to a six- or to a five-membered ring. Finally, the groups can be differentiated according to the functional group of the substitution. This proposed tree structure for the Cb-R groups is shown in Figure 4-8. Given the small number of PAHs included in this study relative to the number of parameters being estimated, many of the standard errors for the coefficients are comparable to the coefficients themselves (see Table 4.15). In order to increase the statistical significance of the coefficients we lumped the groups in level L4 in which  $R = \text{Cs, Cd, Cb, or CO}$ . Since the values for the  $R = \text{Ct}$  groups are systematically lower than for the other carbon substituents, the values for the  $\Delta H_f^\circ$  of these groups were not lumped. A weighted least square regression was performed to determine the contributions of each of the groups for the monosubstituted PAHs. The contributions of the polysubstituted corrections were then derived from the thermochemistry of the PAHs with more than one substitution. The *meta* and *para* corrections for all the substituent were set to zero, with the exception of the corrections for the Os and CO substituents. The standard deviations for this new set of coefficients decreased in comparison to the coefficients shown in Table 4.15, whereas the MAD and RMS increased only slightly, to 0.61 and 1.22 respectively.

The  $S_{298}^\circ$  and  $C_p^\circ$  group values were derived from the thermochemistry of the 70 substituted PAHs for which quantum chemical calculations were performed. Groups values for these properties were derived only up to the L3 level, and are shown in Tables 4.17 and 4.18. All non-nearest neighbor corrections for  $S_{298}^\circ$  and  $C_p^\circ$  were set

Table 4.15: Group values obtained if each of the different carbon functional groups are considered separately.

	$\Delta H_f^\circ$ (kcal mol <sup>-1</sup> ) for each R					
	Cs	Cds	Cb	Ct	CO	Os
A6(AA)-R	5.3 ± 0.3	5.5 ± 0.2	5.3 ± 0.2	5.1 ± 0.3	5.6 ± 0.4	-1.5 ± 0.3
A6(BX)-R	6.8 ± 1.1	8.2 ± 0.9	7.3 ± 0.6	5.1 ± 0.7	5.8 ± 1.1	-1.9 ± 0.6
A6(CX)-R	13.0 ± 2.2	12.3 ± 2.0	13.3 ± 2.2	10.0 ± 2.1	14.7 ± 2.2	0.6 ± 2.2
A5-R	4.5 ± 4.3	4.0 ± 4.3	3.6 ± 4.3	2.8 ± 4.3	4.2 ± 4.3	-2.0 ± 4.3
<i>ortho</i>	0.3 ± 0.5	1.6 ± 0.4	1.8 ± 0.6	0.7 ± 0.5	-1.9 ± 0.7	0.5 ± 0.5
<i>meta</i>	0.2 ± 0.6	0.1 ± 0.4	0.5 ± 0.6	0.3 ± 0.5	-2.8 ± 0.7	0.4 ± 0.5
<i>para</i>	0.0 ± 0.6	-0.1 ± 0.4	0.3 ± 0.6	0.1 ± 0.5	-2.7 ± 0.7	1.7 ± 0.5
18	2.6 ± 1.1	1.7 ± 1.2	0.0 ± 0.0	3.4 ± 1.1	4.1 ± 1.2	-1.1 ± 1.1

Table 4.16: Proposed group values for the  $\Delta H_f^\circ$  of groups in substituted PAHs.

	$\Delta H_f^\circ$ (kcal mol <sup>-1</sup> ) for each R						
	C	Cs	Cds	Cb	Ct	CO	Os
A6(AA)	5.19±0.1	f <sup>a</sup>	f	f	5.18±0.3	f	-1.67±0.4
A6(BX)	7.83±0.5	f	f	f	5.06±0.9	f	-1.44±1.1
A6(CX)	13.27±1.4	f	f	f	10.04±2.7	f	0.64±2.7
A5	4.09±2.7	f	f	f	2.76±5.2	f	-1.97±5.2
<i>ortho</i>	-	-0.92±1.0	1.96±0.9	0.83±0.4	0.63±0.9	-1.53±1.5	0.76±0.7
<i>meta</i>	-	-	-	-	-	-2.35±1.5	0.54±0.7
<i>para</i>	-	-	-	-	-	-2.26±1.5	1.75±0.7
18	1.62±0.6	f	f	3.43±1.5	3.44±1.5	f	-1.49±1.5

<sup>a</sup>All the nodes labelled with an 'f' get the value of its father

Table 4.17: Proposed group values for the  $S_{298}^\circ$  of groups in substituted PAHs.

	$S_{298}^\circ$ (cal K <sup>-1</sup> mol <sup>-1</sup> )
A6(AA)-C	-6.0 ± 0.2
A6(BX)-C	-7.5 ± 0.7
A6(CX)-C	-10.9 ± 2.3
A5-C	-7.0 ± 4.5
A6(AA)-O	-7.9 ± 0.5
A6(BX)-O	-11.0 ± 1.5
A6(CX)-O	-11.1 ± 4.9
A5-O	-10.3 ± 9.9
MAD	1.86
RMS	2.78

**L1:** A-H  
**L1:** A-O  
     **L2:** A6-Os  
         **L3:** A6(AA)-Os  
         **L3:** A6(BX)-Os  
         **L3:** A6(CX)-Os  
     **L2:** A5-Os  
**L1:** A-C  
     **L2:** A6-C  
         **L3:** A6(AA)-C  
             **L4:** A6(AA)-Cs  
             **L4:** A6(AA)-Cds  
             **L4:** A6(AA)-Cb  
             **L4:** A6(AA)-Ct  
             **L4:** A6(AA)-CO  
         **L3:** A6(BX)-C  
             **L4:** A6(BX)-Cs  
             **L4:** A6(BX)-Cds  
             **L4:** A6(BX)-Cb  
             **L4:** A6(BX)-Ct  
             **L4:** A6(BX)-CO  
         **L3:** A6(CX)-C  
             **L4:** A6(CX)-Cs  
             **L4:** A6(CX)-Cds  
             **L4:** A6(CX)-Cb  
             **L4:** A6(CX)-Ct  
             **L4:** A6(CX)-CO  
     **L2:** A5-C  
         **L3:** A5-Cs  
         **L3:** A5-Cds  
         **L3:** A5-Cb  
         **L3:** A5-Ct  
         **L3:** A5-CO

Figure 4-8: Proposed tree structure for the groups centered on Cb for substituted PAHs.

Table 4.18: Proposed group values for the  $C_p^\circ$  of groups in substituted PAHs.

	$C_{p,T}^\circ(\text{cal K}^{-1} \text{mol}^{-1})$						
	300 K	400 K	500 K	600 K	800 K	1000 K	1500 K
A6(AA)-C	3.2±0.1	3.8±0.1	4.3±0.1	4.8±0.1	5.5±0.1	6.0±0.1	6.8±0.1
A6(BX)-C	3.6±0.3	4.1±0.3	4.5±0.3	4.9±0.3	5.4±0.4	5.8±0.4	6.6±0.4
A6(CX)-C	3.4±1.0	4.3±1.0	5.0±1.0	5.5±1.1	6.2±1.2	6.7±1.3	7.5±1.5
A5-C	2.7±2.0	3.1±2.0	3.5±2.1	3.9±2.2	4.5±2.3	4.9±2.5	5.7±2.9
A6(AA)-O	4.0±0.2	5.4±0.2	6.3±0.2	6.8±0.2	7.2±0.2	7.3±0.3	7.6±0.3
A6(BX)-O	3.8±0.6	5.3±0.7	6.3±0.7	6.8±0.7	7.5±0.8	7.9±0.8	8.2±0.9
A6(CX)-O	3.9±2.2	5.6±2.2	6.5±2.3	6.9±2.4	7.2±2.6	7.3±2.7	7.5±3.2
A5-O	4.6±4.3	6.2±4.4	7.0±4.5	7.4±4.8	7.5±5.1	7.6±5.4	7.7±6.3
MAD	0.73	0.70	0.73	0.78	0.79	0.86	1.12
RMS	1.14	1.23	1.31	1.41	1.54	1.64	1.95

to zero.

The uncertainties in the group values corresponding to substitution on a five-membered ring are very high. The reason for that is the assigned 5 kcal mol<sup>-1</sup> uncertainty in the  $\Delta H_{f,\text{exp}}^\circ$  of acenaphthalene (see Section 2.2.1). This high uncertainty leads high uncertainties in the  $\Delta H_{f,\text{homo}}^\circ$  of PAHs with five-membered rings. Consequently these PAHs receive a very small weight in the least square regression, resulting in very high standard deviations for their group values.

#### 4.4.5 Conclusions

We note that Benson’s group values centered on Cb differentiate according to the functional group of the atom to which the Cb is bonded but not according to the environment in the PAH of the Cb. We found that the environment around the substituted Cb influences the thermochemistry more than the functional groups to which the Cb is bonded.

Given the many possible substituted PAH structures, we provided here a framework to approach the problem. The values for the higher nodes in the tree have been provided, but there is still plenty of room for development. Future work would include derivation of values for the (BB), (BC) and (CC) groups, if needed. Currently



these groups receive the corresponding value of the (BX) and (CX) groups, which were derived mostly using  $X = 'A'$  (see Section 4.4.4).

For example, Mulholland studied the relative stability of bianthryls, and found that as expected, 9,9'-bianthryls are less stable than 2,9'-bianthryls [28]. Although currently we do not have enough values to distinguish between these two isomers, the proposed tree structure allows for this differentiation.

Slightly more accurate predictions would also be obtained by deriving different group values according to the functional group of the carbon to which the central Cb is bonded.



# Bibliography

- [1] S. W. Benson. *Thermochemical Kinetics*. John Wiley & Sons, New York, 2<sup>nd</sup> edition, 1976.
- [2] C. W. Bird. The application of group additivity parameters to the prediction of the enthalpies of formation of heteroaromatic compounds. *Tetrahedron*, 52(45):14335-14340, 1996.
- [3] M. Blumenstock, R. Zimmermann, K. W. Schramm, and A. Kettrup. Influence of combustion conditions on the PCDD/F-, PCB-, PCBz- and PAH-concentrations in the post-combustion chamber of a waste incineration pilot plant. *Chemosphere*, 40(9-11):987-993, 2000.
- [4] K. M. Broadus and S. R. Kass. The electron as a protecting group. 3. Generation of acenaphthylene radical anion and the determination of the heat of formation of a strained cycloalkyne. *Journal of the American Chemical Society*, 123(18):4189-4196, 2001.
- [5] R. D. Chirico, B. E. Gammon, S. E. Knipmeyer, A. Nguyen, M. M. Strube, C. Tsionopoulos, and W. V. Steele. The thermodynamic properties of dibenzofuran. *Journal of Chemical Thermodynamics*, 22:1075-1096, 1990.
- [6] J. Cioslowski, P. Piskorz, and D. Moncrieff. Electronic structure studies of 1,2-didehydrogenation of arenes and rearrangement of arynes to annelated cyclopentadienylidene-carbenes. *Journal of the American Chemical Society*, 120(8):1695-1700, 1998.
- [7] I. Da Costa, R. Fournet, F. Billaud, and F. Battin-Leclerc. Experimental and modeling study of the oxidation of benzene. *International Journal of Chemical Kinetics*, 35(10):503-524, 2003.
- [8] A. A. El-Azhary and H. U. Suter. Comparison between optimized geometries and vibrational frequencies calculated by the DFT methods. *Journal of Physical Chemistry*, 100(37):15056-15063, 1996.
- [9] J. C. Evans and R. A. Nyquist. Vibrational spectra of ethynyl benzene and ethynyl benzene-d. *Spectrochimica Acta*, 16:918-928, 1960.

- [10] G. P. Ford and E. R. Biehl. Computed (AM1) relative stabilities of polycyclic arynes are simply related to the steric and electronic properties of the parent hydrocarbons. *Tetrahedron Letters*, 36(21):3663–3666, 1995.
- [11] M. Frenklach, D. W. Clary, W. C. J. Gardiner, and S. E. Stein. Detailed kinetic modeling of soot formation in shock-tube pyrolysis of acetylene. *The Combustion Institute*, 20:887–901, 1984.
- [12] M. Frenklach, D. W. Clary, T. Yuan, W. C. J. Gardiner, and S. E. Stein. Mechanism of soot formation in acetylene-oxygen mixtures. *Combustion Science and Technology*, 50:79–115, 1986.
- [13] M. J. Frisch, G. W. Trucks, H. B. Schlegel, G. E. Scuseria, M. A. Robb, J. R. Cheeseman, V. G. Zakrzewski, J. A. Montgomery, J., R. E. Stratmann, J. C. Burant, S. Dapprich, J. M. Millam, A. D. Daniels, K. N. Kudin, M. C. Strain, O. Farkas, J. Tomasi, V. Barone, M. Cossi, R. Cammi, B. Mennucci, C. Pomelli, C. Adamo, S. Clifford, J. Ochterski, G. A. Petersson, P. Y. Ayala, Q. Cui, K. Morokuma, N. Rega, P. Salvador, J. J. Dannenberg, D. K. Malick, A. D. Rabuck, K. Raghavachari, J. B. Foresman, J. Cioslowski, J. V. Ortiz, A. G. Baboul, B. B. Stefanov, G. Liu, A. Liashenko, P. Piskorz, I. Komaromi, R. Gomperts, R. L. Martin, D. J. Fox, T. Keith, M. A. Al-Laham, C. Y. Peng, A. Nanayakkara, M. Challacombe, P. M. W. Gill, B. Johnson, W. Chen, M. W. Wong, J. L. Andres, C. Gonzalez, M. Head-Gordon, E. S. Replogle, and J. A. Pople. *Gaussian 98*, 2002.
- [14] J. Griesheimer and K. H. Homann. Large molecules, radical ions, and small soot particles in fuel-rich hydrocarbon flames. part ii. aromatic radicals and intermediate pahn in a premixed low-pressure naphthalene/oxygen/argon flame. *The Combustion Institute*, 27:1753–1759, 1998.
- [15] H.-F. Grutzmacher and J. Lohmann. Nachweis von 9,10-dehydro-phenanthren durch pyrolyse-massenspektrometrie. *Liebigs Ann. Chem.*, 726:47–56, 1969.
- [16] G. B. Guthrie, D. W. Scott, W. N. Hubbard, C. Katz, J. P. McCullough, M. E. Gross, K. D. Williamson, and G. Waddington. Thermodynamic properties of furan. *Journal of the American Chemical Society*, 74(18):4477–4730, 1952.
- [17] R. Hoffmann, A. Imamura, and W. J. Hehre. Benzyne, dehydroconjugated molecules, and the interaction of orbitals separated by a number of intervening sigma bonds. *Journal of the American Chemical Society*, 90(6):1499–1059, 1968.
- [18] K. H. Homann. Fullerenes and soot formation- new pathways to large particles in flames. *Angewandte Chemie- International Edition*, 37:2434–2451, 1998.
- [19] L. W. Jenneskens, M. Sarobe, and J. W. Zwikker. Thermal generation and (inter)conversion of (multi)cyclopenta-fused polycyclic aromatic hydrocarbons. *Pure & Applied Chemistry*, 68(2):219–224, 1996.

- [20] C. H. Kwon, H. L. Kim, and M. S. Kim. Vibrational analysis of vacuum ultraviolet mass-analyzed threshold ionization spectra of phenylacetylene and benzonitrile. *Journal of Physical Chemistry A*, 107:10969–10975, 2003.
- [21] T. H. Lay, T. Yamada, P. L. Tsai, and J. W. Bozzelli. Thermodynamic parameters and group additivity ring corrections for three- to six-membered oxygen heterocyclic hydrocarbons. *Journal of Physical Chemistry A*, 101(13):2471–2477, 1997.
- [22] H. V. Linnert and J. M. Riveros. Benzyne-related mechanisms in the gas phase ion/molecule reactions of haloarenes. *Int. J. Mass. Spectrom. Ion. Processes*, 140(1):163–176, 1994.
- [23] P. J. Linstrom and W. G. Mallard, editors. *NIST Chemistry WebBook*, volume Number 69 of *NIST Standard Reference Database*. National Institute of Standards and Technology, Gaithersburg MD, 20899 (<http://webbook.nist.gov>), March 2003.
- [24] J. M. L. Martin, T. J. Lee, and P. R. Taylor. A purely ab initio spectroscopic quality quartic force field for acetylene. *Journal of Chemical Physics*, 108(2):676–691, 1998.
- [25] M. C. Masonjones, A. R. Lafleur, and A. F. Sarofim. Biarene formation during pyrolysis of a mixture of anthracene and naphthalene. *Combustion Science and Technology*, 109:273–285, 1995.
- [26] O. Mo, M. Yanez, J. Elguero, M. V. Roux, P. Jimenez, J. Z. Davalos, M. A. V. Ribeiro da Silva, M. D. M. C. Ribeiro da Silva, P. Cabildo, and R. Claranunt. Substituent effects on enthalpies of formation: Benzene derivatives. *Journal of Physical Chemistry A*, 107(3):366–371, 2003.
- [27] J. Mukherjee, A. F. Sarofim, and J. P. Longwell. Polycyclic aromatic hydrocarbons from the high-temperature pyrolysis of pyrene. *Combustion and Flame*, 96:191–200, 1994.
- [28] J. A. Mulholland, J. Mukherjee, M. J. Wornat, A. F. Sarofim, and G. C. Rutledge. Semiempirical molecular orbital estimation of the relative stability of bianthryls produced by anthracene pyrolysis. *Combustion and Flame*, 94(3):233–43, 1993.
- [29] M. Sarobe, L. W. Jennekens, and U. E. Wiersum. Thermolysis of benzo[c]phenanthrene: Conversion of an alternant  $C_{18}H_{12}$  PAH into non-alternant  $C_{18}H_{10}$  PAHs. *Tetrahedron Letters*, 37(7):1121–1122, 1996.
- [30] G. N. Sastry and U. D. Priyakumar. The role of heteroatom substitution in the rigidity and curvature of buckybowls. A theoretical study. *Journal of the Chemical Society, Perkin Transactions 2*, (1):30–40, 2001.

- [31] K. Sendt, G. B. Bacskay, and J. C. Mackie. Pyrolysis of furan: Ab initio quantum chemical and kinetic modeling studies. *Journal of Physical Chemistry A*, 104:1861–1875, 2000.
- [32] S. E. Stein and B. D. Barton. Chemical thermodynamics of polyaromatic compounds containing heteroatoms and five-membered rings. *Thermochimica Acta*, 44:265–281, 1981.
- [33] S. E. Stein and A. Fahr. High-temperature stabilities of hydrocarbons. *Journal of Physical Chemistry*, 89:3714–3725, 1985.
- [34] D. R. Stull, E. F. Westrum, J., and G. C. Sinke. *The Chemical Thermodynamics of Organic Compounds*. John Wiley & Sons, New York, 1969.
- [35] P. Weilmunster, A. Keller, and K. H. Homann. Large molecules, radicals, ions, and small soot particles in fuel-rich hydrocarbon flames. part i: Positive ions of polycyclic aromatic hydrocarbons (PAH) in low-pressure premixed flames of acetylene and oxygen. *Combustion and Flame*, 116(1/2):62–83, 1999.
- [36] P. G. Wenthold and R. R. Squires. Biradical thermochemistry from collision-induced dissociation threshold energy measurements. absolute heats of formation of *ortho*-, *meta*-, and *para*-benzyne. *Journal of the American Chemical Society*, 116:6401–6412, 1994.
- [37] P. G. Wenthold, R. R. Squires, and W. C. Lineberger. Ultraviolet photoelectron spectroscopy of the *o*-, *m*-, and *p*-benzyne negative ions. Electron affinities and singlet-triplet splittings for *o*-, *m*-, and *p*-benzyne. *Journal of the American Chemical Society*, 120(21):5279–5290, 1998.
- [38] M. J. Wornat, A. F. Sarofim, and A. R. Laffleur. The pyrolysis of anthracene as a model coal-derived aromatic compound. *The Combustion Institute*, 24th:955–963, 1992.

# Chapter 5

## Polycyclic Aromatic Hydrocarbon Radicals

### 5.1 $\sigma$ -radicals

#### 5.1.1 Introduction

It is known that the bond dissociation energy (BDE) for PAHs depends on the position at which the  $\sigma$ -radical is formed. For example, Wang and Frenklach noted that the C-H bond in PAHs depends on the neighboring geometry of the C-H bond [41]. In particular, they found that C-H bonds located at the edge of a bay region are 1 to 2 kcal mol<sup>-1</sup> weaker than those that are not at a bay region, due to steric repulsion of the hydrogens. Moreover, they found that the steric repulsion is further increased when a bay region hydrogen is replaced by an ethynyl group. For example, the BDE for the C-H bond in the 5 position of 4-ethynyl-phenanthrene was about 3 kcal mol<sup>-1</sup> weaker than the BDE of the C-H's in normal bay regions [41]. They also noted that the strength of the C-H bond in PAHs is essentially independent of molecular size [41]. Wang and Frenklach do not mention the effect on entropy and heat capacities.

This knowledge has not been systematized and incorporated into estimation methods for the thermochemical properties of PAHs. A database from 1997 [33] for the THERM computer program for estimation of the thermochemical properties of

molecules [32] includes BDE values for phenyl, 1-naphthalenyl and 2-naphthalenyl only. The NIST Positive Ion Energetics-Structures and Properties computer program includes only one group phenyl radicals, not differentiating according to the environment around the  $\sigma$ -radical [26].

Aromatic biradicals have received considerable attention in the recent years. These didehydroarenes show different degrees of biradical character depending on the number of  $\sigma$  bonds separating the radical site and on the relative orientation of the nonbonding  $\sigma$  radicals [18]. However, the structure and reactivity of these species is still not very well known.

Although  $\sigma$ -radical species are ubiquitous within combustion mechanisms, there are conspicuously few biradicals present [14]. Richter and Howard [31] in their review of PAH formation and growth pathways list some mechanisms in which biradicals are intermediates to the formation of the first aromatic ring. One of the reasons for the general absence of didehydroarenes in combustion mechanisms is the lack of knowledge about their thermochemistry and reactivity.

Radicals of ethynyl substituted PAHs were also studied, since these species are intermediates in the hydrogen-abstraction-acetylene-addition (HACA) mechanism for PAH formation and growth [42, 21].

### 5.1.2 Experimental Values

There are not many experimental measurements of the BDE of aromatic molecules. The available BDE and  $\Delta H_{f,\text{exp}}^\circ$  are listed in Table 5.1, as well as  $\Delta H_f^\circ$  calculated from the available BDE and vice-versa (given in *italics*). Until the early '90s, a value of  $110.9 \pm 2$  kcal mol<sup>-1</sup> was recommended for the C-H bond energy of benzene. Recently, Davico et al. studied the kinetics of the proton transfer between amide ion and benzene ( $\text{C}_6\text{H}_6 + \text{NH}_2^- \rightleftharpoons \text{C}_6\text{H}_5^- + \text{NH}_3$ ) to determine a value of  $113.5 \pm 0.5$  kcal mol<sup>-1</sup> [8]. This value for the BDE of the benzene C-H bond is currently widely accepted [2, 30, 22] and used. More recently, Ervin and DeTuri evaluated the gas-phase acidities of 12 reference species, including that of ammonia [11]. Combining their new  $\Delta_{\text{acid}}H_{0K}(\text{NH}_3)$  with the kinetics measurements by Davico et al., they



obtained a value for the BDE of benzene of  $112.9\pm 0.5$  kcal mol<sup>-1</sup>.

In the past few years, a couple of experimental measurements of the BDE of the C-H bonds in naphthalene were carried out [30, 12, 22]. In general, it is concluded that the energies for the 1- and 2-positions are, within experimental error, indistinguishable and approximately equal to the BDE of benzene.

The  $\Delta H_f^\circ$  of a few biradicals have been measured, and their value is also reported in Table 5.1. It is a consensus that all benzynes have singlet ground states [45], and thus the values reported in Table 5.1 refer to the singlet state. The singlet-triplet gap ( $\Delta E_{ST}$ ) for the benzynes has been measured [45], allowing the calculation of the  $\Delta H_f^\circ$  for the triplet states of these species (see Table 5.2).

One could estimate the  $\Delta H_f^\circ$  for benzynes by treating them as biradicals consisting of two independent phenyl radicals. In this case, the C-H bond energy of the second radical site is assumed to be the same as the bond energy of the first radical site. Using the BDE for phenyl measured by Davico et al. [8] and corrected by Ervin and DeTuri [11], one obtains the value of  $141.9\pm 1$  kcal mol<sup>-1</sup>. The  $\Delta H_f^\circ$  obtained for the triplet state of benzyne are all the same, within experimental uncertainties, as this estimated value, indicating that the benzyne triplet states can be viewed as biradicals containing two independent radical sites.

### 5.1.3 Computational Methods

#### Quantum Chemical Calculations

Barckholtz et al. [2] surveyed many computational methods to calculate the bond dissociation energies of PAHs. They found that B3LYP/6-31G(d) had the smallest average error compared to the experimental BDE values available for small PAHs. DFT methods usually do not suffer from serious spin-contamination problems, and are thus adequate for the calculation of open-shell systems [4]. We performed B3LYP/6-31G(d) calculations for radicals at different positions for IPR PAHs up to C<sub>26</sub>H<sub>9</sub>. Frequencies were calculated at the same level of theory and scaled by a factor of 0.9613 to obtain zero point energies (ZPE) and thermal correction to the enthalpy.

Table 5.1: Experimental values for the BDE of aromatic molecules. The  $\Delta H_f^\circ$  values for the didydroarenes correspond to the singlet. BDE for the didydroarenes correspond to the removal of the second H, and were only given molecules in which the radical sites are symmetrical. Values in *italics* were calculated from the  $\Delta H_f^\circ$  of the corresponding stable molecule and  $\Delta H_{f,\text{exp}}^\circ$  or  $\text{BDE}_{\text{exp}}$ . The uncertainties given in this case are the sum of the uncertainties of the  $\Delta H_f^\circ$  of the stable molecule (as given by our grading system, see Section 2.3) and the uncertainty in the experimental value of the measured property of the radical.

		$\Delta H_{f,\text{exp}}^\circ$ (kcal mol <sup>-1</sup> )	$\text{BDE}_{\text{exp}}$ (kcal mol <sup>-1</sup> )	Reference
<i>ortho</i> -Benzynes	C <sub>6</sub> H <sub>4</sub>	106.6 ± 3.0	<i>78.2 ± 4<sup>a</sup></i>	[44]
<i>meta</i> -Benzynes	C <sub>6</sub> H <sub>4</sub>	122.0 ± 3.1	<i>93.6 ± 4<sup>a</sup></i>	[44]
<i>para</i> -Benzynes	C <sub>6</sub> H <sub>4</sub>	137.3 ± 3.3	<i>108.9 ± 4<sup>a</sup></i>	[44]
Phenyl	C <sub>6</sub> H <sub>5</sub>	<i>81.2 ± 1</i>	113.5 ± 0.5	[8]
		<i>80.5 ± 1</i>	112.9 ± 0.5	[11]
1,2-Didehydronaphthalene	C <sub>10</sub> H <sub>6</sub>	122 ± 6	-	[25]
2,3-Didehydronaphthalene	C <sub>10</sub> H <sub>6</sub>	124 ± 6	<i>76.9 ± 11<sup>b</sup></i>	[25]
1,4-Didehydronaphthalene	C <sub>10</sub> H <sub>6</sub>	152.9 ± 1.4	-	[36]
1-Naphthalenyl	C <sub>10</sub> H <sub>7</sub>	<i>96.0 ± 2</i>	112.2 ± 1.3	[30]
		<i>97.2 ± 6</i>	113.4 ± 5.2	[22]
		<i>96.7 ± 4</i>	112.8 ± 3.3	[12]
2-Naphthalenyl	C <sub>10</sub> H <sub>7</sub>	<i>95.7 ± 2</i>	111.9 ± 1.4	[30]
		<i>99.2 ± 5</i>	115.4 ± 4.9	[22]
Acenaphthylene	C <sub>12</sub> H <sub>6</sub>	160 ± 4	84 ± 2	[3]
1-Acenaphthylenyl	C <sub>12</sub> H <sub>7</sub>	<i>127 ± 9</i>	117 ± 4	[3]
9,10-Didehydrophenanthrene	C <sub>14</sub> H <sub>8</sub>	143 ± 9	-	[17]

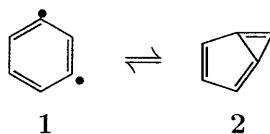
<sup>a</sup>Calculated using the BDE for phenyl given by Ervin and DeTuri [11].

<sup>b</sup>Calculated from the BDE value of 2-Naphthalenyl given by [22].

Table 5.2: Experimental values for the singlet-triplet gap of benzyne and the  $\Delta H_f^\circ$  of the triplet states [45].

	$\Delta E_{ST}$ (kcal mol <sup>-1</sup> )	$\Delta H_f^\circ$ triplet (kcal mol <sup>-1</sup> )
<i>ortho</i> -Benzynes	37.5±0.3	144.1±3.3
<i>meta</i> -Benzynes	21.0±0.3	142.9±3.1
<i>para</i> -Benzynes	3.8±0.5	141.6±2.9

Calculating the thermochemistry of aromatic biradicals is a challenging task for computational chemistry [24]. Density functional theory has been shown to perform poorly for these species. The equilibrium geometries of didydroarenes, such as *meta*-benzynes, depend strongly on the level of theory applied [46]. Since the potential energy surface between the biradical and the bicyclic structure of *meta*-benzynes is very flat, Winkler and Sander found that systematic deviations in ‘secondary’ geometrical parameters might affect the energy considerably. These authors concluded through Natural Bond Orbital (NBO) and topological analysis of the electron density distribution at the B3LYP/cc-pVTZ level that the bicyclic structure is not adequate to describe *meta*-benzynes.



However, our singlet calculations of *meta*-benzynes at the B3LYP/6-31G(d) level leads to the bicyclic species as the optimized geometry.

Squires and Cramer found that DFT singlet energies are unreliable for most didihydroarenes [37], since DFT severely underestimates the singlet stabilities for biradicals with large separation between radical sites. They attributed this underestimation to the failure of DFT methods to capture static electron correlation [6]. Lindh et al. suggest that in addition to adequate treatment of static electron correlation (through multiconfigurational methods), basis set of triple- $\zeta$  quality and the use of isodesmic reactions are indispensable for the treatment of didihydroarenes [24].

In view of all these difficulties, we chose not to base our estimation method for didihydroarenes on values calculated at the B3LYP/6-31G(d) level. Instead, we will rely on the available experimental data and higher level calculations. Squires and Cramer studied the electronic interactions in aryne biradicals [37]. They calculated electronic energies for all the didihydroarenes at the multiconfigurational CASPT2/cc-pVDZ//CAS/cc-pVDZ level. They used a homodesmotic reaction involving naphthalene and naphthyl radical (assuming that the C-H bond energy of naphthalene is equal to that of benzene) for the calculation of the  $\Delta H_f^\circ$  of the didi-

hydronaphthalenes in which the radical sites were separated by two or more  $\sigma$ -bonds. For the species in which the radical sites are adjacent to each other (1,2- and 2,3-didehydronaphthalene) they used an isodesmic equation in which the two hydrogens from naphthalene are transferred to acetylene forming the didehydronaphthalene and ethylene. For 1,3-didehydronaphthalene, which has intermediate biradical character, they calculated the  $\Delta H_f^\circ$  as the average of the values derived from the homodesmic and the isodesmic reaction. The  $\Delta H_f^\circ$  calculated by Squires and Cramer [37] are listed in Table 5.3.

Calculations at the B3LYP/6-31G(d) level were performed for 16 ethynyl substituted radicals in which the radical site was separated from the ethynyl substitution by one  $\sigma$ -bond.

### Homodesmic Reaction Scheme

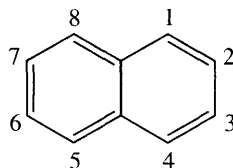
Although the B3LYP/6-31G(d) is one of the computational methods that provide the best agreement with experimental BDE's [2], BDE's calculated from DFT methods are in general underestimated [13]. For example, B3LYP/6-31G(d) gives a value of 109.5 kcal mol<sup>-1</sup> for the BDE of benzene at 298K. This value is at least 2 kcal mol<sup>-1</sup> lower than the accepted experimental values. The direct calculation of the BDE involves the comparison of the absolute energy of the stable molecule with the absolute energies of the radical and of H atom

$$\text{BDE(R-H)} = \text{E(H}^\bullet) + \text{E(R}^\bullet) - \text{E(RH)} \quad (5.1)$$

where the absolute energies E include the zero-point energy and thermal correction to 298K. In Eq. 5.1, the absolute energy of a stable molecule is being compared to the absolute energy of a radical and of the H atom. It is known that the radical site leads to regular changes in the geometry of the molecule [4, 2]. In using Eq. 5.1, the errors in the quantum chemical calculations due to the new geometry in the vicinity of the radical site are not being cancelled out. We thus propose calculating the BDE

Table 5.3:  $\Delta H_f^\circ$  for didehydronaphthalenes calculated at the CASPT2 level by Squires and Crames [37].

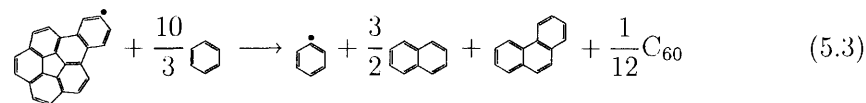
	$\Delta H_f^\circ$ (kcal mol <sup>-1</sup> )	
	singlet	triplet
1,2	122.1	165.2
1,3	138.5	161.1
1,4	154.5	159.9
1,5	152.4	160.1
1,6	158.1	158.8
1,7	157.7	159.1
1,8	158.5	159.2
2,3	124.2	163.8
2,6	157.4	159.0
2,7	156.4	159.1



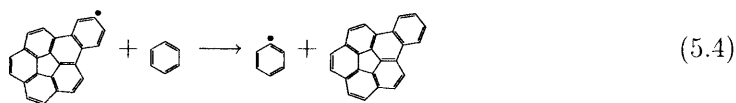
from

$$\text{BDE(R-H)} = \Delta H_{f,\text{exp}}^\circ(\text{H}^\bullet) + \Delta H_{f,\text{homo}}^\circ(\text{R}^\bullet) - \Delta H_{f,\text{homo}}^\circ(\text{RH}) \quad (5.2)$$

where the  $\Delta H_{f,\text{homo}}^\circ(\text{RH})$  are calculated through the homodesmic reaction proposed in Section 2.3. For the calculation of the  $\Delta H_{f,\text{homo}}^\circ(\text{R}^\bullet)$  of the radical, we include phenyl radical to the homodesmic reaction scheme. Thus the errors in the quantum chemical calculation of the geometry in the vicinity of the radical site should be cancelled out with the similar errors arising from the calculation of the radical site in phenyl. For example, the  $\Delta H_f^\circ$  of a benzo[*a*]corannulene radical would be calculated through the following homodesmic reaction:



Since the homodesmic reaction for the calculation of the  $\Delta H_f^\circ$  of the stable benzo[*a*]corannulene is very similar to Eq. 5.3, most of the molecules cancel out, and we are effectively calculating  $\Delta H_{f,\text{homo}}^\circ(\text{R}^\bullet)$  through



where the  $\Delta H_f^\circ$  of the stable benzo[*a*]corannulene is obtained from the homodesmic reaction described in Section 2.3. The BDE calculated through the proposed homodesmic reaction scheme are compared with the available experimental BDE and with the BDE calculated through Eq. 5.1.

By using this homodesmic reaction scheme, we are effectively parameterizing the quantum chemical calculation with the  $\Delta H_{f,\text{exp}}^\circ$  of the reference radical. It is thus imperative that this reference radical and its  $\Delta H_{f,\text{exp}}^\circ$  be chosen judiciously. Two reasons led to the choice of phenyl as the reference radical. Firstly, it is an aromatic structure, and thus it is expected that the changes arising from the abstraction of a hydrogen from benzene will be similar to the changes from the abstraction of the hydrogen of the other PAHs. Secondly, many measurements of the BDE for benzene have been carried out. The two most recent values (113.5 and 112.9 kcal mol<sup>-1</sup>), which have been widely accepted and used, differ from each other by less than 1 kcal mol<sup>-1</sup>. We have adopted the BDE value from Ervin and DeTuri [11], who reevaluated the  $\Delta_{\text{acid}}H_{0K}$  of ammonia and recalculated the BDE from the measurements of Davico et al. [8]. An uncertainty of 1 kcal mol<sup>-1</sup> was assigned to this BDE value.

The uncertainties in the BDE values calculated from Eq. 5.3 are assigned to be equal to the uncertainty of the  $\Delta H_{f,\text{homo}}^\circ$  of the radical species. This uncertainty in turn is the sum of the uncertainties of the species involved in the homodesmic reaction (Eq. 5.4). Consequently, the uncertainties in the BDE values calculated

Table 5.4: Experimental BDE compared to the BDE calculated at the B3LYP/6-31G(d) level and with the value calculated using the proposed homodesmic reaction. The BDE calculated through atomization reactions (i.e., the  $\Delta H_f^\circ$  in Eq. 5.2 are calculated from atomization reactions) are also given. All the values are in kcal mol<sup>-1</sup>.

	experimental	B3LYP/6-31G(d)		
		direct	atomization	homodesmic
Phenyl	112.9 ± 0.5	109.5 ± 0.7	110.8 ± 0.7	112.9 ± 2.0
1-Naphthalenyl	112.2 ± 1.3	109.7 ± 1.1	111.0 ± 1.1	113.1 ± 2.0
2-Naphthalenyl	111.9 ± 1.4	109.6 ± 1.1	110.8 ± 1.1	113.0 ± 2.0
1-Acenaphthylenyl	117 ± 4	113.8 ± 1.3	115.1 ± 1.3	117.2 ± 6.5

from the homodesmotic reaction scheme are larger than the uncertainties of the BDE values calculated directly (vide Table 5.4). The latter involves only the uncertainties in the experimental values of the H atom and of  $C_{(g)}$ . Within the experimental uncertainties, the  $\Delta H_{f,\text{homo}}^\circ(\text{R}^\bullet)$  calculated using the proposed homodesmotic reaction scheme for  $\sigma$ -radicals (Eq. 5.4) agree with the  $\Delta H_{f,\text{exp}}^\circ(\text{R}^\bullet)$ .

The  $\Delta H_f^\circ$  of the ethynyl substituted radicals were calculated using a homodesmotic reaction scheme analogous to Eq. 5.4, in which the stable species is the ethynyl substituted PAH.

### 5.1.4 Estimation Method

We use the HBI method proposed by Lay et al. [23] to estimate the thermochemical properties of radicals from the properties of the stable molecule. For any  $\sigma$ -radical the H abstraction reaction can be written



with  $\Delta H_{rxn,298}^\circ = \text{BDE}$ . The thermochemical properties of the radical are related to the thermochemical properties of the corresponding stable species through:

$$\Delta H_f^\circ(\text{R}^\bullet) = \text{BDE}(\text{R-H}) + \Delta H_f^\circ(\text{RH}) - \Delta H_f^\circ(\text{H}^\bullet) \quad (5.6)$$

$$S_{int,298}^\circ(\text{R}^\bullet) = S_{int,298}^\circ(\text{RH}) + \Delta S_{298}^\circ(\text{HBI}) \quad (5.7)$$

$$C_p(T)(\text{R}^\bullet) = C_p(T)(\text{RH}) + \Delta C_p(T)(\text{HBI}) \quad (5.8)$$

where  $\Delta H_f^\circ(\text{H}^\bullet) = 52.153 \text{ kcal mol}^{-1}$  and  $S_{int}^\circ$  is the intrinsic entropy (excluding symmetry). BDE is the bond dissociation energy and corresponds to the hydrogen bond increment (HBI) for  $\Delta H_f^\circ$ .  $\Delta S_{298}^\circ(\text{HBI})$  and  $\Delta C_p(T)(\text{HBI})$  are the HBI group values for estimating the entropy and the heat capacity of the radical from its parent. Symmetry is not included in the values of  $\Delta S_{298}^\circ(\text{HBI})$ , and thus the calculation of  $S_{298}^\circ$  for radicals should take into account the difference in the symmetry of the radical

and its parent stable molecule:

$$S_{298}^{\circ}(\mathbf{R}^{\bullet}) = S_{298}^{\circ}(\text{RH}) + \Delta S_{298}^{\circ}(\text{HBI}) - R \ln(\sigma_{\text{radical}}/\sigma_{\text{parent}}) \quad (5.9)$$

The contributions of each of the groups to the HBI values of  $\Delta H_f^{\circ}$ ,  $S_{298}^{\circ}$ , and  $C_p^{\circ}$  were derived through a weighted least square regression. The weight for each radical is assigned as the inverse of the uncertainty in the value of the  $\Delta H_{f,\text{homo}}^{\circ}$ .

The HBI value for the  $\Delta H_f^{\circ}$  varies with the position of the radical in the PAH molecule. The groups defined in this work are shown in Figure 5-1. The values derived for each of these groups are listed in Tables 5.5 and 5.6. The BDE for hydrogens that are at the edge of a bay region ('A6(6Bay)J' group) is smaller than the BDE of a radical site whose carbon is only bonded to other 'A' or 'B' atom-centered groups ('A6(notBay)J' group). This lower BDE occurs because the abstraction of that hydrogen relieves some steric strain in the PAH. Similarly, the BDE for hydrogens that are at the edge of a cove (two adjacent bay regions [10]) is even lower ('A6(6Cove)J' group). The abstraction of the hydrogen at this position makes the strained non-planar benzo[c]phenanthrene structure become planar. When the center ring in the bay-region is a five-membered ring ('A6(5Bay)J' group), the hydrogens at the edge of the bay-region are further away from each other, and we found that the values for the HBI of this group are virtually the same as the HBI values for the 'A6(notBay)J' group. Wang and Frenklach noted in their AM1 calculations that the C-H bond at the 5 position in 4-ethynyl-Phenanthrene was about 3 kcal mol<sup>-1</sup> weaker than the C-H bond in non-substituted bay regions. Noting that the difference between the BDE contributions of the 'A6(6Bay)J' and of the 'A6(6Cove)J' is about 4 kcal mol<sup>-1</sup>, we propose to treat bay regions that are substituted with a 'large' substituent as a cove (see Figure 5-1). We consider 'large' substituents to be any of the carbon functional groups: 'Cs', 'Cd', 'Ct', and 'Cb'.

The BDE for radical sites on five-membered rings is more than 3kcal mol<sup>-1</sup> higher than on six-membered rings. Radicals on five-membered rings that are at the edge of a bay region were also included in this study. However, the BDE for these species



does not vary significantly from the BDE of radicals on other five-membered rings. Thus there is no need for further differentiation of the ‘A5J’ group according to whether it is on the edge of a bay region or not. Barckholtz et al. [2] performed B3LYP/6-31G(d) calculations for the radicals of furan and dibenzofuran. We used their results together with our homodesmotic reaction scheme to obtain the HBI value for the  $\Delta H_f^\circ$  of the ‘FuranJ’ group listed in Table 5.5. The HBI contribution for this group is not expected to differ from the HBI contributions of the ‘A5J’ group.

## Biradicals

The *ortho* singlet didehydroarenes are arynes, and the estimation method for them has been developed in Section 4.3. Here we will only deal with the triplet states and with biradicals in which the radical sites are more than one  $\sigma$  bond apart from each other (not in the *ortho* position).

The BDE for the benzyne and didehydronaphthalenes are listed in Table 5.7 along with the position of the radical and the difference between the BDE value calculated through simple HBI approach and the actual BDE (as listed in Tables 5.2 and 5.3). The simple group additivity method for the calculation of the BDE uses the values given in Table 5.5. In the case of benzene and the naphthalenes, only the ‘A6(notBay)J’ group is present. From the data presented in Table 5.7, we introduce corrections for the BDE of singlet *ortho*- and *meta*-didehydroarenes. When the radical sites are at positions other than *ortho* or *meta* from each other, they can be treated as two independent radical sites, and the simple HBI approach provides fairly good BDE estimates. The same is true for the triplet states at all positions.

The corrections for the HBI values obtained in this manner are listed in Table 5.8. We note that the largest contributions to the MAD and RMS of the triplet state are from the *ortho*-didehydronaphthalenes. We feel that at this point it is not worthwhile to introduce a correction to the BDE of didehydroarenes at the *ortho* position, because the BDE values from the *ortho*-didehydronaphthalenes were not derived from experiments.

Entropies and heat capacities for didehydroarenes should be calculated using the

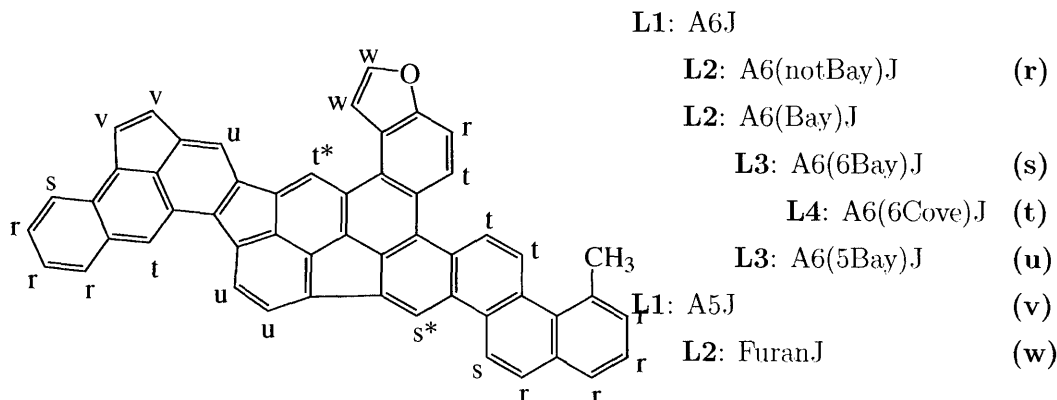


Figure 5-1: Schematic of each of the groups defined for  $\sigma$ -radicals in PAHs. On the right the tree structure for these groups is also shown. The groups marked with a \* fit more than one group definition, since they are at the edge of two bay regions, one in which the ring in the center of the bay region is a five-membered ring and one in which the center ring is a six-membered ring. In these cases, priority is given to the bay region with a six-membered ring.

Table 5.5: HBI contributions to the  $\Delta H_f^\circ$  and  $S_{298}^\circ$  from each of the bond-centered group values that describe PAH  $\sigma$ -radicals.

	$\Delta H_f^\circ$ (kcal mol <sup>-1</sup> )	$S_{298}^\circ$ (cal K <sup>-1</sup> mol <sup>-1</sup> )
A6(notBay)J	113.05 ± 0.04	1.24 ± 0.02
A6(6Bay)J	111.07 ± 0.1	0.73 ± 0.1
A6(6Cove)J	106.07 ± 0.4	2.42 ± 0.2
A6(5Bay)J	112.94 ± 0.3	1.15 ± 0.2
A5J	116.56 ± 0.2	1.27 ± 0.1
FuranJ	120.33 ± 0.3 <sup>a</sup>	f <sup>b</sup>
MAD	0.373	0.104
RMS	0.738	0.204

<sup>a</sup>Derived from calculations by Barckholtz et al. [2] (see text).

<sup>b</sup>This node gets the  $S_{298}^\circ$  values of its father.

Table 5.6: HBI contributions to the  $C_p^\circ$ 's from each of the bond-centered group values that describe  $\sigma$ -radicals.

	$C_{p,T}$ (cal K <sup>-1</sup> mol <sup>-1</sup> )						
	300 K	400 K	500 K	600 K	800 K	1000 K	1500 K
A6(notBay).J	-0.5±0.1	-1.1±0.1	-1.7±0.1	-2.1±0.1	-2.8±0.1	-3.2±0.1	-3.8±0.1
A6(6Bay).J	-0.6±0.1	-1.2±0.1	-1.7±0.1	-2.2±0.1	-2.8±0.1	-3.2±0.1	-3.8±0.1
A6(6Cove).J	-0.3±0.1	-1.0±0.1	-1.6±0.1	-2.0±0.1	-2.7±0.1	-3.1±0.2	-3.6±0.4
A6(5Bay).J	-0.6±0.1	-1.2±0.1	-1.8±0.1	-2.2±0.1	-2.8±0.1	-3.2±0.2	-3.6±0.4
A5.J	-0.5±0.1	-1.2±0.1	-1.8±0.1	-2.3±0.1	-2.9±0.1	-3.3±0.1	-3.9±0.3
Furan.J	f <sup>a</sup>						
MAD	0.050	0.047	0.043	0.044	0.083	0.158	0.340
RMS	0.076	0.072	0.065	0.066	0.119	0.221	0.467

<sup>a</sup>This node gets the  $C_p^\circ$  values of its father.

Table 5.7: Bond Dissociation Energy for didydroarenes.  $\Delta$ BDE refers to the difference between the value calculated through simple HBI approach and the actual BDE. All values in (kcal mol<sup>-1</sup>).

		Position	singlet		triplet	
			BDE	$\Delta$ BDE	BDE	$\Delta$ BDE
<i>ortho</i> -Benzyne	C <sub>6</sub> H <sub>4</sub>	<i>ortho</i>	- <sup>a</sup>		228.59	2.48
<i>meta</i> -Benzyne	C <sub>6</sub> H <sub>4</sub>	<i>meta</i>	206.49	-19.62	227.39	1.28
<i>para</i> -Benzyne	C <sub>6</sub> H <sub>4</sub>	<i>para</i>	221.79	-4.32	226.09	-0.02
1,2-Didehydronaphthalene	C <sub>6</sub> H <sub>4</sub>	<i>ortho</i>	- <sup>a</sup>		233.52	7.41
1,3-Didehydronaphthalene	C <sub>10</sub> H <sub>8</sub>	<i>meta</i>	206.82	-19.29	229.42	3.31
1,4-Didehydronaphthalene	C <sub>10</sub> H <sub>8</sub>	<i>para</i>	222.82	-3.29	228.22	2.11
1,5-Didehydronaphthalene	C <sub>10</sub> H <sub>8</sub>	<i>other</i>	220.72	-5.39	228.42	2.31
1,6-Didehydronaphthalene	C <sub>10</sub> H <sub>8</sub>	<i>other</i>	226.42	0.31	227.12	1.01
1,7-Didehydronaphthalene	C <sub>10</sub> H <sub>8</sub>	<i>other</i>	226.02	-0.09	227.42	1.31
1,8-Didehydronaphthalene	C <sub>10</sub> H <sub>8</sub>	<i>other</i>	226.82	0.71	227.52	1.41
2,3-Didehydronaphthalene	C <sub>10</sub> H <sub>8</sub>	<i>ortho</i>	- <sup>a</sup>		232.12	6.01
2,6-Didehydronaphthalene	C <sub>10</sub> H <sub>8</sub>	<i>other</i>	225.72	-0.39	227.32	1.21
2,7-Didehydronaphthalene	C <sub>10</sub> H <sub>8</sub>	<i>other</i>	224.72	-1.39	227.42	1.31

<sup>a</sup>This is an aryne and the estimation method for its thermochemical properties is described in Section 4.3.

Table 5.8: Corrections for the BDE of biradicals in kcal mol<sup>-1</sup>.

	singlet	triplet
ortho	- <sup>a</sup>	0
meta	-19.45	0
para	-3.80	0
other	0	0
MAD	1.38	2.40
RMS	2.52	3.26

<sup>a</sup>This is an aryne and the estimation method for its thermochemical properties is described in Section 4.3

simple HBI method, with the coefficients listed in Table 5.5 and 5.6.

### Ethynyl-Substituted Radicals

As shown in Table 5.9, the BDE for C-H which have a neighboring ethynyl substitution is ca. 1 kcal mol<sup>-1</sup> higher than the BDE given in Table 5.5.  $\Delta$ BDE refers to the difference between the BDE from the ethynyl substituted radical and the BDE for the corresponding radical group.

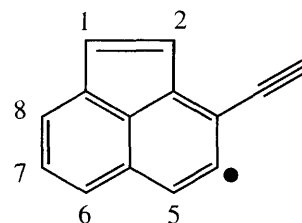
We thus propose adding the average of the  $\Delta$ BDE to the BDE of radicals that have an ethynyl substitution as a neighbor:  $1.22 \pm 0.26$  kcal mol<sup>-1</sup>. The MAD and RMS for the ethynyl substituted PAHs included in this study are 0.22 and 0.27 kcal mol<sup>-1</sup>, respectively. The ethynyl substitution does not affect the entropy and the heat capacity HBIs significantly.

### 5.1.5 Conclusions

We have proposed using homodesmic reactions to calculate the BDE of PAHs with  $\sigma$ -radicals. Calculation using the quantum chemical energies directly (Eq. 5.1) are not always adequate. In using the proposed homodesmic reaction scheme, quantum chemical errors of the geometry in the vicinity of the radical site should be cancelled out.

Table 5.9: BDE for ethynyl Substituted PAHs.  $\Delta$ BDE refers to the difference between the value calculated through simple HBI approach and the actual BDE. All values in (kcal mol<sup>-1</sup>).

		BDE	$\Delta$ BDE
Phenyl,2-ethynyl	C <sub>8</sub> H <sub>5</sub>	114.15	1.10
2-Naphthalenyl,1-ethynyl	C <sub>12</sub> H <sub>7</sub>	114.04	0.99
1-Naphthalenyl,2-ethynyl	C <sub>12</sub> H <sub>7</sub>	114.34	1.29
3-Naphthalenyl,2-ethynyl	C <sub>12</sub> H <sub>7</sub>	114.23	1.18
1-Acenaphthalenyl,2-ethynyl	C <sub>14</sub> H <sub>7</sub>	118.18	1.63
4-Acenaphthalenyl,3-ethynyl	C <sub>14</sub> H <sub>7</sub>	114.70	1.65
3-Acenaphthalenyl,4-ethynyl	C <sub>14</sub> H <sub>7</sub>	114.63	1.58
5-Acenaphthalenyl,4-ethynyl	C <sub>14</sub> H <sub>7</sub>	114.63	1.58
4-Acenaphthalenyl,5-ethynyl	C <sub>14</sub> H <sub>7</sub>	113.90	0.85
2-Phenanthrenyl,1-ethynyl	C <sub>16</sub> H <sub>9</sub>	114.27	1.21
1-Phenanthrenyl,2-ethynyl	C <sub>16</sub> H <sub>9</sub>	114.36	1.31
3-Phenanthrenyl,2-ethynyl	C <sub>16</sub> H <sub>9</sub>	114.19	1.14
9-Antlraceny,1-ethynyl	C <sub>16</sub> H <sub>9</sub>	113.94	0.88
3-Antlraceny,2-ethynyl	C <sub>16</sub> H <sub>9</sub>	114.18	1.13
2-Pirenyl,1-ethynyl	C <sub>18</sub> H <sub>9</sub>	113.99	0.94
5-Pirenyl,4-ethynyl	C <sub>18</sub> H <sub>9</sub>	114.06	1.01



We present in this section the framework of an estimation method for the thermochemical properties of  $\sigma$ -radicals through HBI contributions. The proposed method can estimate the properties radicals on five- and six-membered rings, on the furan ring, and of radical sites neighboring an ethynyl substitution. Moreover, corrections have been provided for the calculation of the singlet state of biradicals on the *meta* and *para* positions. The singlet state of radicals of the *ortho* position is calculated using the method for arynes described in Section 4.3. We found that the treatment of biradicals in the triplet state as two independent radical sites is a reasonable simplification.

To our knowledge, the work presented here is the most complete and detailed method for the estimation of the thermochemical properties of  $\sigma$ -radicals. While this method will certainly meet the needs of current modelers, it does not cover all the possible aryl  $\sigma$ -radicals. For example, we only provided a correction for ethynyl-substituted PAH radicals, whereas there are many other possible substitutions that

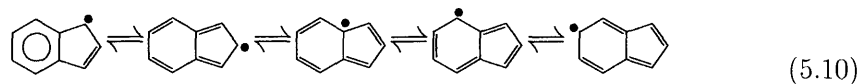
might lead to different corrections. As the importance of these other corrections become apparent, their incorporation into the method should be easy.

## 5.2 $\pi$ -radicals

### 5.2.1 Introduction

We denote as  $\pi$ -radicals those systems in which the free electron is delocalized over a  $\pi$ -electron network. These species are significantly more stable than comparable nondelocalized radicals [34].

Three classes of  $\pi$ -radicals are included in this work: those PAHs with an odd number of carbon atoms, those with a methylene substitution, such as benzyl, and those with a oxyl radical substitution. Examples of the resonance structures in each of these classes of  $\pi$ -radicals are shown in Eq. (5.10) to (5.12).



Homann and co-workers have detected  $\pi$ -radicals with an odd number of carbons in flames, as intermediates in the oxidation zone [19, 43, 16, 1, 20]. Griesheimer and Homann measured the concentration of indenyl radical to be 2.6% of the concentration of indene [16], markedly higher than the ratio of phenyl to benzene (1.6%) that they measured. This higher percentage was attributed to the larger stability of  $\pi$ -radicals compared to  $\sigma$ -radicals. Homann and co-workers pointed out that as the PAHs become larger, the concentration of odd-numbered PAHs becomes higher than the corresponding non-radical, hydrogenated species [19]. They suggest that the

structure of these larger species influence their reactivity more than the fact that it is a radical or not. Odd  $\pi$ -radicals are believed to be formed by unimolecular decomposition of oxyl radicals to the  $\pi$ -radical and CO. The  $\pi$ -radical can then further react with another  $\pi$ -radical to form a stable aromatic molecule [27]. This pathway (shown in Figure 5-2) is believed to be an important channel for PAH growth.

In fuel rich flames or pyrolysis,  $\text{CH}_3$  is a major radical. It can react with aromatic molecules forming methyl substituted PAHs. The C-H bond at the methyl site is about  $15\text{kcal mol}^{-1}$  weaker than at aromatic sites, and thus the abstraction of this hydrogen, forming benzylic radicals, is favored over the abstraction of hydrogens at the aromatic ring.

The reaction of aromatic molecules with O atoms to give oxyl radicals is believed to be one of the main pathways of PAH oxidation [7]. The other pathway goes through H abstraction forming  $\sigma$  radicals. These in turn can react with  $\text{O}_2$  or OH radicals to form oxyl radicals too [7].

## 5.2.2 Experimental Values

Unfortunately very little experimental thermochemical measurements for PAH  $\pi$ -radicals have been made. The reported value for  $\Delta H_{f,\text{exp}}^\circ$  of cyclopentadienyl has ranged from 47 to 63  $\text{kcal mol}^{-1}$  [9]. The higher, more recent value has found confirmation in various theoretical calculations [40, 29] and has been adopted in this work, with a grade of 'C' (which corresponds to an uncertainty of 5  $\text{kcal mol}^{-1}$ ). The  $\Delta H_f^\circ$  of indenyl and fluorenyl can be derived from published values of the  $\Delta H_f^\circ$  and BDE of the parent stable molecules indene and fluorene. These values are given in

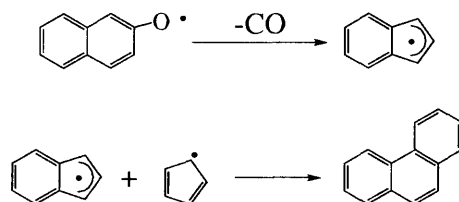


Figure 5-2: Role of odd  $\pi$ -radicals on PAH growth.

Table 5.10. The  $\Delta H_{f,\text{exp}}^\circ$  values for cyclopentadienyl, indenyl and fluorenyl are given in Table 5.12.

McMillen and Golden in their review of the bond dissociation energies list BDE values for a couple of methylene substituted aromatics [28]. Experimental value for the BDE of hydroxy substituted PAHs is only available for the phenoxy radical. From their compilation of data, McMillen and Golden concluded that benzylic radicals in polycyclic aromatic systems are more stable than the benzyl radical itself. Moreover, they noted that, as in allylic systems, a secondary benzyl radical is more stable than the primary radical. However, this stabilization is roughly the same whether the benzyl radical is made secondary by substitution of a methyl group or by a second phenyl group (compare the BDE values of 1-ethylbenzyl and diphenylmethyl radicals). That is, the second phenyl group results in little increase in the resonance stabilization energy.

### 5.2.3 Previous Estimation Methods

No estimation method exists currently for the thermochemical properties of  $\pi$ -radicals with an odd number of carbons.

Lay et al. proposed HBI group values for the estimation of the thermochemistry of benzyl radicals [23]. They derived values for benzyl radicals with zero, one and two alkyl groups substituted at the radical carbon. In their method, no differentiation of the groups according to the size of the aromatic system is made. The BDE values were calculated from experimental  $\Delta H_f^\circ$  for the radicals, and the  $\Delta S_{298}^\circ(\text{HBI})$  and  $\Delta C_p(T)(\text{HBI})$  values were calculated from assigned vibrational frequencies.

### 5.2.4 Computational Methods

#### Quantum Chemical Calculations

The B3LYP/6-31G(d) was used for the calculation of the optimized geometries of 26  $\pi$ -radicals with an odd number of carbons, five benzylic, and six phenoxy radicals. Frequencies were calculated at the same level of theory and scaled by a factor of



Table 5.10: Experimental  $\Delta H_f^\circ$  and (BDE) for the stable parents of  $\pi$ -radicals.

		$\Delta H_{f,\text{exp}}^\circ$ (kcal mol <sup>-1</sup> )	BDE (kcal mol <sup>-1</sup> )
Cyclopentadiene	C <sub>5</sub> H <sub>6</sub>	31.94±0.28 <sup>a</sup>	81.5±2.7 <sup>b</sup> , 82.9±2.2 <sup>c</sup>
Indene	C <sub>9</sub> H <sub>8</sub>	39.08±0.37 <sup>c</sup>	81.1±2.4 <sup>c</sup> , 84±3 <sup>d</sup>
Fluorene	C <sub>13</sub> H <sub>10</sub>	41.83±0.35 <sup>e</sup> , 39.89±0.98 <sup>e</sup>	81.2±2.4 <sup>e</sup> , 81.2 <sup>f</sup>

<sup>a</sup>Reference [5].

<sup>b</sup>Reference [35].

<sup>c</sup>Reference [9].

<sup>d</sup>Reference [38], as cited by [35]

<sup>e</sup>As cited in [26].

<sup>f</sup>Reference [15], as cited by [35].

Table 5.11: Experimental BDE of substituted  $\pi$ -radicals in kcal mol<sup>-1</sup>.

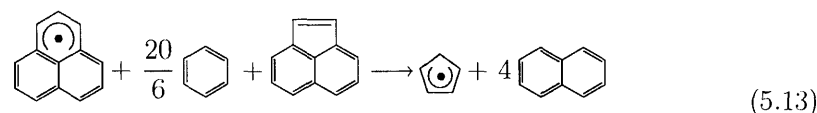
		experimental BDE	Reference
Benzyl	C <sub>7</sub> H <sub>7</sub>	88.0 ± 1	As cited by [28]
		89.7 ± 1	[39] <sup>a</sup>
1-Naphthylmethyl radical	C <sub>11</sub> H <sub>9</sub>	85.1 ± 1.5	As cited by [28]
5-Anthracenylmethyl radical	C <sub>15</sub> H <sub>11</sub>	81.8 ± 1.5	As cited by [28]
9-Phenanthrylmethyl radical	C <sub>15</sub> H <sub>11</sub>	85.1 ± 1.5	As cited by [28]
1-Ethylbenzyl radical	C <sub>8</sub> H <sub>9</sub>	85.4 ± 1.5	As cited by [28]
2-propanylbenzyl radical	C <sub>9</sub> H <sub>11</sub>	84.4 ± 1.5	As cited by [28]
Diphenylmethyl radical	C <sub>13</sub> H <sub>11</sub>	84 ± 2	As cited by [28]
Phenoxy	C <sub>6</sub> H <sub>5</sub> O	88.1 ± 1.4	[39] <sup>a</sup>

<sup>a</sup>Calculated from the  $\Delta H_f^\circ$  of the radical listed in this reference

0.9613 to obtain zero point energies (ZPE) and thermal correction to the enthalpy.

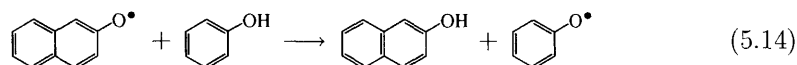
### Homodesmotic Reaction Scheme

It is not possible to assign a unequivocal stable parent to  $\pi$ -radicals with an odd number of carbons, since the odd free electron is free to move throughout the aromatic system. Thus we used the homodesmotic reaction scheme proposed in Section 2.3 with the addition of cyclopentadienyl to account for the delocalized radical. An example of this homodesmotic reaction is given in Eq. (5.13) for the phenalene radical.



A comparison between the  $\Delta H_f^\circ$  calculated through this homodesmotic reaction scheme and the available  $\Delta H_{f,\text{exp}}^\circ$  is provided in Table 5.12. The  $\Delta H_{f,\text{atom}}^\circ$  are also given for comparison.

For the calculation of the  $\Delta H_f^\circ$  of the benzylic and phenoxy radicals, we used a homodesmotic reaction scheme similar to that shown in Eq (5.4). Benzyl and phenoxy are used as reference molecules in place of phenyl. For example, the  $\Delta H_f^\circ$  of 1-naphthalenyloxy is calculated through:



The bond dissociation energies calculated through this homodesmotic reaction scheme

Table 5.12: Comparison between the  $\Delta H_{f,\text{exp}}^\circ$ ,  $\Delta H_{f,\text{atom}}^\circ$ , and  $\Delta H_{f,\text{homo}}^\circ$  for  $\pi$ -radicals.

		$\Delta H_{f,\text{exp}}^\circ$ (kcal mol <sup>-1</sup> )	$\Delta H_{f,\text{atom}}^\circ$ (kcal mol <sup>-1</sup> )	$\Delta H_{f,\text{homo}}^\circ$ (kcal mol <sup>-1</sup> )
Cyclopentadienyl	C <sub>5</sub> H <sub>5</sub>	63.3±2.2 <sup>a</sup>	59.4±0.6	63.2±5
Indenyl	C <sub>9</sub> H <sub>7</sub>	68.03±2.37 <sup>b</sup>	64.9±1.0	65.7±6
Fluorenyl	C <sub>13</sub> H <sub>9</sub>	70.88±2.75 <sup>b</sup> , 68.94±3.38 <sup>b</sup>	72.0±1.4	73.8±8

<sup>a</sup>Reference [9].

<sup>b</sup>Obtained from the  $\Delta H_f^\circ$  and BDE values of the stable molecule given in Table 5.10.

are listed in Table 5.13.

## 5.2.5 Estimation Method

### $\pi$ -Radicals with an Odd Number of Carbons

The difficulty associated with the calculation of the thermochemistry of  $\pi$ -radicals is that it is not possible to determine unequivocally at which position the odd electron is. In  $\pi$ -radicals, the odd electron is free to move throughout the entire aromatic system (see for example Eq. (5.10) to (5.12)). Thus a simple HBI approach is not applicable for this class of radicals. It is expected however, that resonance forms in which the odd electron is in a position that allows a higher number of Kekulé structures contribute more to the properties of the molecule than those in which a lower number of Kekulé structures are possible.

We are proposing the following scheme to estimate the thermochemical properties of  $\pi$ -radicals with an odd number of carbons:

1. Identify all the resonance species of the odd  $\pi$ -radical, with the radical site in any of the carbons of the PAH. Figure 5-3 exemplifies this procedure for Benz[*de*]anthracene.
2. Choose the species that leads to the largest number of Kekulé structures. These species will consist of an aromatic part, where the bonds can delocalize, and a non-aromatic part, in which the double and single bonds are fixed. For Benz[*de*]anthracene species (5) has the largest number of Kekulé structures.
3. Estimate the thermochemical properties considering the contributions of the aromatic and of the non-aromatic part separately. The thermochemical properties of the non-aromatic part will require the atom-centered groups for substituted PAHs developed in Section 4.4, ring corrections, and HBI for the radical.
4. When more than one species lead to the same maximum number of Kekulé structures, the thermochemical properties of the species with the lowest  $\Delta H_f^\circ$  is

Table 5.13: Comparison between available experimental BDE and BDE calculated through the homodesmic reaction scheme for substituted  $\pi$ -radicals.

		BDE (kcal mol <sup>-1</sup> )	
		experimental	homodesmic
Benzyl	C <sub>7</sub> H <sub>7</sub>	89.7 ± 1	89.7 <sup>a</sup> ± 3
1-Naphthylmethyl radical	C <sub>11</sub> H <sub>9</sub>	85.1 ± 1.5	88.1 ± 4
2-Naphthylmethyl radical	C <sub>11</sub> H <sub>9</sub>	-	88.9 ± 4
1-Acenaphthylmethyl radical	C <sub>13</sub> H <sub>11</sub>	-	90.5 ± 9
5-Anthracenylmethyl radical	C <sub>15</sub> H <sub>11</sub>	81.8 ± 1.5	-
9-Phenanthrylmethyl radical	C <sub>15</sub> H <sub>11</sub>	85.1 ± 1.5	-
1-ethylbenzyl radical	C <sub>8</sub> H <sub>9</sub>	85.4 ± 1.5	-
2-propanylbzyl radical	C <sub>9H11</sub>	84.4 ± 1.5	-
Diphenylmethyl radical	C <sub>13</sub> H <sub>11</sub>	84 ± 2	-
4-Phenanthrenylmethyl radical		-	88.4 ± 6
Phenoxy	C <sub>6</sub> H <sub>5</sub> O	88.1 ± 1.4	88.1 <sup>a</sup> ± 3
1-Naphthalenyloxy	C <sub>10</sub> H <sub>7</sub> O	-	81.6 ± 4
2-Naphthalenyloxy	C <sub>10</sub> H <sub>7</sub> O	-	86.1 ± 4
1-Acenaphthalenyloxy	C <sub>12</sub> H <sub>9</sub> O	-	73.6 ± 9
4-Phenanthrenyloxy	C <sub>14</sub> H <sub>9</sub> O	-	82.2 ± 6
5-Anthracenyloxy	C <sub>14</sub> H <sub>9</sub> O	-	70.7 ± 5

<sup>a</sup>Used in the homodesmic reaction scheme.

assigned for the molecule. Benz[*fg*]acenaphthylene is an example in which four different species all have a Kekulé structure count of 3, as shown in Figure 5-4.

This estimation method requires the definition of some new ring corrections and HBI values for non-aromatic groups. Figure 5-5 presents a scheme of each of these new ring corrections and HBI groups. The number in the name of each ring correction indicates the size of the ring, and in parenthesis the functional groups of the carbons belonging to the ring are given, except for the Cb groups. The experimental  $\Delta H_f^\circ$  of indene and fluorene were also included in the regression. The uncertainty in the  $\Delta H_f^\circ$  of these molecules was assigned to be 1 kcal mol<sup>-1</sup>. The value for the  $\Delta H_{f,\text{exp}}^\circ$  of fluorene used was the average of the two available experimental values (Table 5.10). A weighted regression was performed to determine the contributions of the ring corrections and HBI values. The weights were defined as the inverse of the uncertainties of the  $\Delta H_f^\circ$  of each molecule. The uncertainties in the experimental values of the  $\Delta H_f^\circ$  of indene and fluorene were assigned to be 1 kcal mol<sup>-1</sup>.

The contributions of these HBI groups and ring corrections to  $\Delta H_f^\circ$ ,  $S_{298}^\circ$ , and  $C_p^\circ$ , as well as the MAD and RMS for each of them are shown in Tables 5.14 and 5.15. We would like to emphasize that the derivation of the groups presented in this section was based on the current values for the BCGA method for PAHs (see Section 3.2), group values for substituted PAHs (see Section 4.4) and other atom centered groups with Cd or Cs as central atoms and Cs, Cd, Cb, and H as neighbors. If any of the values for these groups were to change significantly, a revision of the values developed in this section would be necessary.

Lastly, a word of caution is due. Although ring corrections were derived here that theoretically allow the calculation of the thermochemistry PAHs with non-aromatic rings, we discourage such practice without prior validation. The ‘5(CdCdCs)’ and ‘5(Cs)’ ring corrections allow an accurate estimation of the thermochemistry of indene and fluorene. However, the ring corrections derived here were based solely those two molecules and  $\pi$ -radicals, and have not been thoroughly tested for other (stable) ring systems with both aromatic and non-aromatic rings.

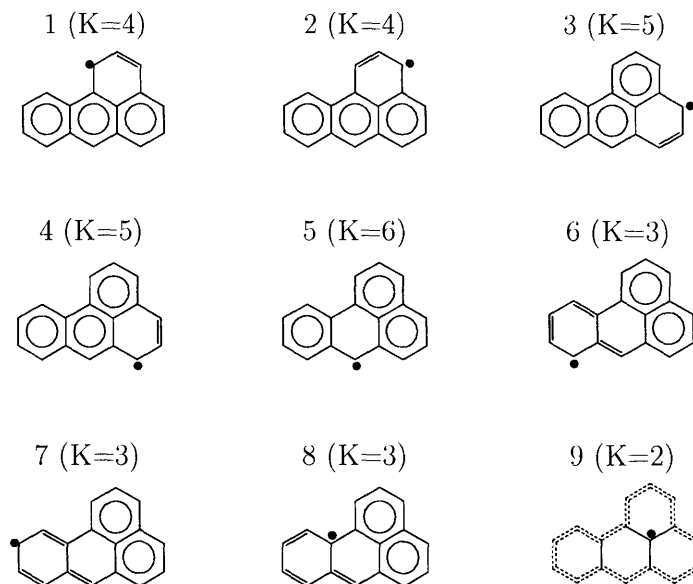


Figure 5-3: Resonance isomers for the benzo[*a*]phenalene odd  $\pi$ -radical. The number in parentheses indicate the number of Kekulé structures for each of the resonance isomer. The thermochemical properties of an odd  $\pi$ -radical are calculated from the resonance isomer that has the largest number of Kekulé structures.

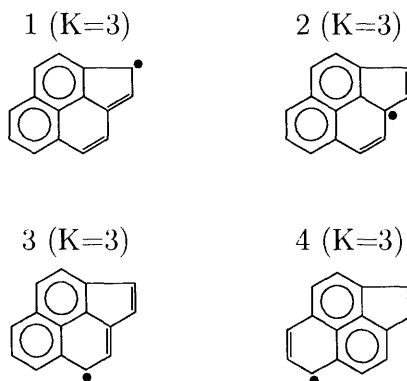
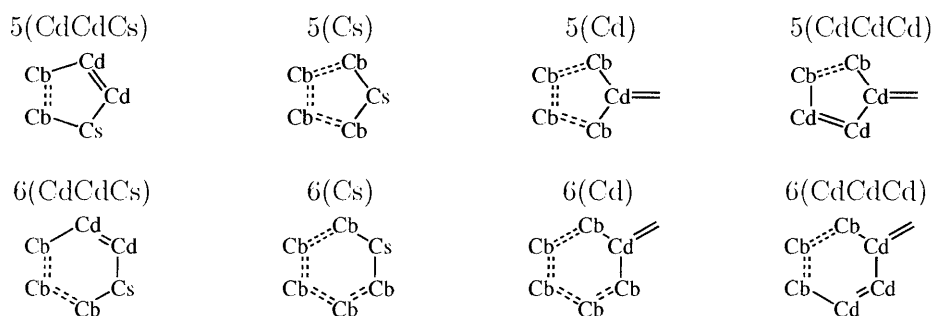


Figure 5-4: Benz[*fg*]acenaphthylene is an example of an odd  $\pi$ -radical that has four different species with the maximum number of Kekulé structures.

### Ring Corrections



### HBI groups

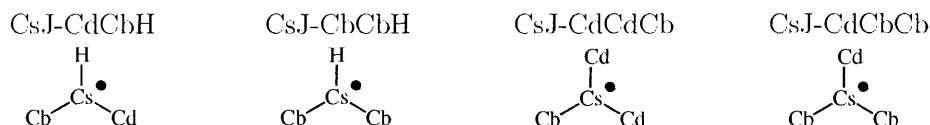


Figure 5-5: New ring corrections and HBI groups introduced for the calculation of the thermochemistry of  $\pi$ -radicals with an odd number of carbons.

Table 5.14:  $\Delta H_f^\circ$  and  $S_{298}^\circ$  coefficients for the HBI and ring correction groups developed in the context of  $\pi$ -radicals with an odd number of carbons.

	$\Delta H_f^\circ$ (kcal mol <sup>-1</sup> )	$S_{298}^\circ$ (cal K <sup>-1</sup> mol <sup>-1</sup> )
HBI groups		
Cs.J-CdCbH	$76.39 \pm 1.1$	$1.63 \pm 1.6$
Cs.J-CbCbH	$81.02 \pm 1.5$	$4.58 \pm 2.1$
Cs.J-CdCdCb	$80.54 \pm 3.4$	$-5.26 \pm 4.8$
Cs.J-CdCbCb	$81.17 \pm 3.7$	$-11.62 \pm 5.2$
Ring Corrections		
5(CdCdCs)	$3.53 \pm 0.7$	$29.43 \pm 1.0$
5(Cs)	$-1.52 \pm 0.7$	$16.62 \pm 1.0$
5(Cd)	$-7.01 \pm 4.9$	$25.04 \pm 6.8$
5(CdCdCd)	$9.80 \pm 2.8$	$33.45 \pm 3.8$
6(CdCdCs)	$-22.36 \pm 2.3$	$28.15 \pm 3.2$
6(Cs)	$-27.96 \pm 2.9$	$32.77 \pm 4.0$
6(Cd)	$-22.61 \pm 4.2$	$27.09 \pm 5.8$
6(CdCdCd)	$-14.17 \pm 2.6$	$32.34 \pm 3.6$
MAD	2.76	2.35
RMS	3.45	5.78

Table 5.15:  $C_p^\circ$  coefficients for the HBI and ring correction groups developed in the context of  $\pi$ -radicals with an odd number of carbons.

	$C_{p,T}^\circ$ (cal K <sup>-1</sup> mol <sup>-1</sup> )						
	300 K	400 K	500 K	600 K	800 K	1000 K	1500 K
HBI groups							
CsJ-CdCbH	-0.4±0.1	-0.9±0.1	-1.3±0.2	-1.7±0.2	-2.8±0.2	-3.3±0.2	-4.4±0.2
CsJ-CbCbH	-0.5±0.1	-1.2±0.2	-1.9±0.2	-2.3±0.2	-3.4±0.3	-4.1±0.3	-5.2±0.3
CsJ-CdCdCb	-0.3±0.2	-1.0±0.4	-1.6±0.5	-1.6±0.5	-2.2±0.6	-2.7±0.7	-2.9±0.8
CsJ-CdCbCb	-0.5±0.2	-0.8±0.4	-1.3±0.5	-1.8±0.6	-2.9±0.7	-4.1±0.8	-5.7±0.8
Ring Corrections							
5(CdCdCs)	-3.4±0.0	-3.3±0.1	-3.0±0.1	-2.7±0.1	-2.7±0.1	-2.0±0.1	-2.1±0.2
5(Cs)	-4.4±0.0	-3.9±0.1	-3.2±0.1	-2.8±0.1	-2.8±0.1	-1.5±0.1	-1.7±0.2
5(Cd)	-3.7±0.2	-3.6±0.5	-3.3±0.7	-2.9±0.7	-2.7±0.9	-1.8±1.0	-2.2±1.1
5(CdCdCd)	-4.2±0.1	-4.7±0.3	-4.7±0.4	-4.3±0.4	-3.6±0.5	-3.0±0.6	-2.7±0.6
6(CdCdCs)	-5.0±0.1	-5.0±0.2	-4.3±0.3	-3.8±0.3	-3.4±0.4	-2.5±0.5	-2.3±0.5
6(Cs)	-4.9±0.1	-5.4±0.3	-4.9±0.4	-4.3±0.4	-4.1±0.5	-2.8±0.6	-2.8±0.6
6(Cd)	-4.9±0.2	-5.0±0.4	-4.5±0.6	-4.0±0.6	-3.6±0.7	-2.7±0.9	-2.8±0.9
6(CdCdCd)	-5.9±0.1	-6.4±0.3	-6.0±0.4	-5.3±0.4	-4.2±0.5	-3.5±0.5	-2.8±0.6
MAD	0.14	0.27	0.38	0.41	0.49	0.60	0.64
RMS	0.18	0.38	0.59	0.64	0.75	0.91	0.95

## Benzylic Radicals

The second class of  $\pi$ -radicals studied are those containing a methyl radical substitution, such as the benzyl radical. The radical site can move through the aromatic rings. The species in which the radical is at the methyl site will always be one of the species that has the largest number of Kekulé structures. We propose estimating the thermochemical properties of such  $\pi$ -radicals by calculating the thermo for this species. We calculated the HBI contribution to the  $\Delta H_f^\circ$  of Benzyl, 1-Naphthylmethyl, 2-Naphthylmethyl, , and 4-Phenanthrylmethyl radicals, and they are all close to the value of 88.5 kcal mol<sup>-1</sup> Lay et al. The BDE for the 1-Acenaphthylmethyl is slightly higher, thus we divided the Benzyl-P HBI group from Lay et al. [23] into ‘Benzyl6-P’ and ‘Benzyl5-P’, depending on the size of the ring to which the methyl group is bonded. The groups for secondary and tertiary benzyl radicals from Lay et al. [23] are kept. The proposed HBI group values are listed in Tables 5.16 and 5.17.



Table 5.16: HBI tree structure and  $\Delta H_f^\circ$  and  $C_p^\circ$  coefficients for the benzylic groups.

	BDE (kcal mol <sup>-1</sup> )	$S_{298}^\circ$ (cal K <sup>-1</sup> mol <sup>-1</sup> )
L1: Benzyl-P		
L2: Benzyl6-P	88.99 ± 0.4	0.2 ± 0.7
L2: Benzyl5-P	90.47 ± 1.6	-1.1 ± 3.1
L1: Benzyl6-S <sup>a</sup>	85.9	-3.81
L1: Benzyl6-T <sup>a</sup>	83.8	-3.69

<sup>a</sup>Values for these groups from Lay et al. [23].

Table 5.17: HBI coefficients for the  $C_p^\circ$  of benzylic groups.

	$C_{p,T}^\circ$ (cal K <sup>-1</sup> mol <sup>-1</sup> )						
	300 K	400 K	500 K	600 K	800 K	1000 K	1500 K
Benzyl6-P	0.3±0.3	0.2±0.3	-0.2±0.3	-0.6±0.2	-1.4±0.2	-2.0±0.2	-2.6±0.1
Benzyl5-P	-0.4±1.4	-0.2±1.3	-0.4±1.2	-0.8±1.1	-1.5±0.9	-2.0±0.7	-2.6±0.4
Benzyl6-S <sup>a</sup>	0.75	0.09	-0.63	-1.21	-2.07	-2.69	-
Benzyl6-T <sup>a</sup>	0.87	-0.78	-1.54	-2.06	-2.74	-3.19	-

<sup>a</sup>Values for these groups from Lay et al. [23].

## Phenoxy Radicals

Similarly to the benzylic radicals, the species in which the free electron is at the hydroxy site will always be one of the species with the largest number of Kekulé structures. Thus we chose to assign the thermochemistry of this resonance species to the phenoxy radicals. The HBI groups were derived from only the few radicals for which we did quantum chemical calculations. A scheme of the HBI groups for the phenoxy radicals is shown in Figure 5-6. These groups were organized in a tree structure, as shown in Table 5.18. The standard deviations in the  $C_p^\circ$  values are  $0.1 \text{ cal K}^{-1} \text{ mol}^{-1}$  or smaller.

### 5.2.6 Conclusions

We have worked with two classes of radicals in which the free electron is delocalized over a  $\pi$ -electron network. The first comprises the PAHs in which not all the  $\pi$ -electrons can be paired. All the PAHs with an odd number of carbons fall into this category. The second class of  $\pi$ -radicals considered are those with a substitution. We have worked with both methylene and oxyl radical substitutions.

In all  $\pi$ -radicals it is not possible to unequivocally establish the radical site, due to the delocalization of the free electron. Thus we chose to always calculate the thermochemistry of the resonance species that has the highest number of Kekulé structures. In case of the first class of  $\pi$ -radicals, the radical is divided into an aromatic and a non-aromatic part. Ring corrections and HBI values are needed to estimate the thermochemistry of the non-aromatic part. To our knowledge, this is

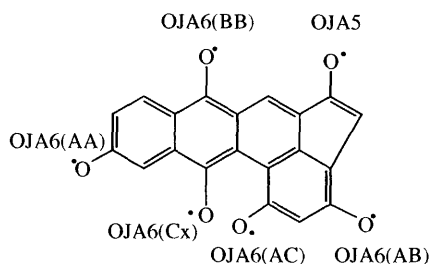


Figure 5-6: Schematic of each of the HBI groups defined for phenoxy radicals.

Table 5.18: HBI tree structure and  $\Delta H_f^\circ$  and  $C_p^\circ$  coefficients for the phenoxy groups.

	BDE (kcal mol <sup>-1</sup> )	$S_{298}^\circ$ (cal K <sup>-1</sup> mol <sup>-1</sup> )	Based on values from
L1: OJA6	OJA6(AA)		
L2: OJA6(AA)	86.82 ± 0.95	-0.4 ± 0.5	Phenoxy and 2-Naphthalenyloxy 1-Naphthalenyloxy 5-Anthracenyloxy 4-Phenanthrenyloxy
L2: OJA6(AB)	81.60 ± 1.19	0.4 ± 0.6	
L2: OJA6(BB)	70.66 ± 0.95	0.8 ± 0.5	
L2: OJA6(AC)	82.17 ± 0.87	1.1 ± 0.5	
L2: OJA6(Cx)	OJA6(BB)		
L1: OJA5	73.57 ± 0.56	0.4 ± 0.3	1-Acenaphthalenyloxy
MAD	0.33	0.18	
RMS	1.46	0.79	

 Table 5.19: HBI coefficients for the  $C_p^\circ$  of phenoxy groups.

	$C_p^\circ$ (cal K <sup>-1</sup> mol <sup>-1</sup> )						
	300 K	400 K	500 K	600 K	800 K	1000 K	1500 K
L1: OJA6	OJA6(AA)						
L2: OJA6(AA)	-1.9	-2.3	-2.6	-2.8	-3.0	-3.1	-3.1
L2: OJA6(AB)	-2.7	-3.3	-3.5	-3.4	-3.3	-3.2	-3.1
L2: OJA6(BB)	-2.1	-2.3	-2.5	-2.6	-2.7	-2.8	-3.0
L2: OJA6(AC)	-1.9	-2.7	-3.0	-3.2	-3.2	-3.2	-3.1
L2: OJA6(Cx)	OJA6(BB)						
L1: OJA5	-2.5	-3.2	-3.5	-3.7	-3.6	-3.5	-3.3
MAD	0.05	0.05	0.05	0.05	0.03	0.03	0.01
RMS	0.23	0.24	0.22	0.20	0.15	0.11	0.06

the first method proposed for the estimation of the thermochemical properties of this class of  $\pi$ -radicals.

Since in the substituted  $\pi$ -radicals the resonance isomer in which the free electron is at the substitution is always one of the isomers with the maximum number of Kekulé structures, the traditional HBI values are used to estimate the thermochemical properties of these species. These values already take into account the resonance stabilization by specifying that its 'O' or 'C' central-atom is bonded to a 'Cb'.

# Bibliography

- [1] J. Ahrens, A. Keller, R. Kovacs, and K. H. Homann. Large molecules, radicals, ions, and small soot particles in fuel-rich hydrocarbon flames. part 3. rempi mass spectrometry of large flame pahn and fullerenes and their quantitative calibration through sublimation. *Berichte der Bunsen-Gesellschaft*, 102(12):1823-1839, 1998.
- [2] C. Barckholtz, T. A. Barckholtz, and C. M. Hadad. C-H and N-H bond dissociation energies of small aromatic hydrocarbons. *Journal of the American Chemical Society*, 121(3):491-500, 1999.
- [3] K. M. Broadus and S. R. Kass. The electron as a protecting group. 3. Generation of acenaphthylene radical anion and the determination of the heat of formation of a strained cycloalkyne. *Journal of the American Chemical Society*, 123(18):4189-4196, 2001.
- [4] J. Cioslowski, G. Liu, M. Martinov, P. Piskorz, and D. Moncrieff. Energetics and site specificity of the homolytic C-H bond cleavage in benzenoid hydrocarbons: An ab initio electronic structure study. *Journal of the American Chemical Society*, 118:5261-5264, 1996.
- [5] J. D. Cox and G. Pilcher. *Thermochemistry of Organic and Organometallic Compounds*. Academic Press, New York, 1970.
- [6] C. J. Cramer and R. R. Squires. Prediction of singlet-triplet splittings for arync biradicals from  $^1\text{H}$  hyperfine interactions in aryl radicals. *Journal of Physical Chemistry A*, 101(49):9191-9194, 1997.
- [7] I. Da Costa, R. Fournet, F. Billaud, and F. Battin-Leclerc. Experimental and modeling study of the oxidation of benzene. *International Journal of Chemical Kinetics*, 35(10):503-524, 2003.
- [8] G. E. Davico, V. M. Bierbaum, C. H. DePuy, G. B. Ellison, and R. R. Squires. The C-H bond energy of benzene. *Journal of the American Chemical Society*, 117:2590-2599, 1995.
- [9] D. J. DeFrees, R. T. McIver, and W. J. Hehre. Heats of formation of gaseous free radicals via ion cyclotron double resonance spectroscopy. *Journal of the American Chemical Society*, 102:3334-3338, 1980.

- [10] J. R. Dias. Benzenoid series having a constant number of isomers. *Journal of Chemical Information and Computer Sciences*, 30(1):61–64, 1990.
- [11] K. M. Ervin and V. F. DeTuri. Anchoring the gas-phase acidity scale. *Journal of Physical Chemistry A*, 106(2):9947–9956, 2002.
- [12] K. M. Ervin, T. M. Ramond, G. E. Davico, R. L. Schwartz, S. M. Casey, and W. C. Lineberger. Naphthyl radical: Negative ion photoelectron spectroscopy, Franck-Condon simulation, and thermochemistry. *Journal of Physical Chemistry A*, 105(48):10822–10831, 2001.
- [13] Y. Feng, L. Liu, J.-T. Wang, H. Huang, and Q.-X. Guo. Assessment of experimental bond dissociation energies using composite ab initio methods and evaluation of the performances of density functional methods in the calculation of bond dissociation energies. *Journal of Chemical Information and Computer Sciences*, 43(6):2005–2013, 2003.
- [14] M. Frenklach, D. W. Clary, T. Yuan, W. C. J. Gardiner, and S. E. Stein. Mechanism of soot formation in acetylene-oxygen mixtures. *Combustion Science and Technology*, 50:79–115, 1986.
- [15] S. Furuyama, D. M. Golden, and S. W. Benson. Kinetics and thermochemistry of the gas-phase reaction of cyclopentadiene and iodine. Relevance to the heat of formation of cyclopentadienyl iodide and cyclopentadienyl radical. *International Journal of Chemical Kinetics*, 3(3):237–248, 1971.
- [16] J. Griesheimer and K. H. Homann. Large molecules, radical ions, and small soot particles in fuel-rich hydrocarbon flames. part ii. aromatic radicals and intermediate paths in a premixed low-pressure naphthalene/oxygen/argon flame. *The Combustion Institute*, 27:1753–1759, 1998.
- [17] H.-F. Grutzmacher and J. Lohmann. Nachweis von 9,10-dehydro-phenanthren durch pyrolyse-massenspektrometric. *Liebigs Ann. Chem.*, 726:47–56, 1969.
- [18] R. Hoffmann, A. Imamura, and W. J. Hehre. Benzynes, dehydroconjugated molecules, and the interaction of orbitals separated by a number of intervening sigma bonds. *Journal of the American Chemical Society*, 90(6):1499–1059, 1968.
- [19] K. H. Homann. Fullerenes and soot formation- new pathways to large particles in flames. *Angewandte Chemie- International Edition*, 37:2434–2451, 1998.
- [20] A. Keller, R. Kovacs, and K. H. Homann. Large molecules, ions, radicals and small soot particles in fuel-rich hydrocarbon flames. part iv. large polycyclic aromatic hydrocarbons and their radicals in a fuel-rich benzene-oxygen flame. *Physical Chemistry Chemical Physics*, 2(8):1667–1675, 2000.
- [21] V. V. Kislov, A. M. Mebel, and L. S. H. Ab initio and dft study of the formation mechanisms of polycyclic aromatic hydrocarbons: The phenanthrene synthesis from biphenyl and naphthalene. *J. Phys. Chem. A*, 106:6171–6182, 2002.

- [22] H. A. Lardin, R. R. Squires, and P. G. Wenthold. Determination of the electron affinities of  $\alpha$ - and  $\beta$ -naphthyl radicals using the kinetic method with full entropy analysis. the C-H bond dissociation energies of naphthalene. *Journal of Mass Spectrometry*, 36(6):607–615, 2001.
- [23] T. H. Lay, J. W. Bozzelli, A. M. Dean, and E. R. Ritter. Hydrogen atom bond increments for calculation of thermodynamic properties of hydrocarbon radical species. *Journal of Physical Chemistry*, 99(39):14514–14527, 1995.
- [24] R. Lindh, A. Bernhardsson, and M. Schuetz. Benzyne thermochemistry: A benchmark ab initio study. *Journal of Physical Chemistry A*, 103(48):9913–9920, 1999.
- [25] H. V. Linnert and J. M. Riveros. Benzyne-related mechanisms in the gas phase ion/molecule reactions of haloarenes. *Int. J. Mass. Spectrom. Ion. Processes*, 140(1):163–176, 1994.
- [26] P. J. Linstrom and W. G. Mallard, editors. *NIST Chemistry WebBook*, volume Number 69 of *NIST Standard Reference Database*. National Institute of Standards and Technology, Gaithersburg MD, 20899 (<http://webbook.nist.gov>), March 2003.
- [27] N. Marinov, W. J. Pitz, C. K. Westbrook, A. M. Vincitore, M. J. Castaldi, S. M. Senkan, and C. F. Melius. Aromatic and polycyclic aromatic hydrocarbon formation in a laminar premixed n-butane flame. *Combustion and Flame*, 114:192–213, 1998.
- [28] D. F. McMillen and D. M. Golden. Hydrocarbon bond dissociation energies. *Annual Review of Physical Chemistry*, 33:493–532, 1982.
- [29] L. V. Moskaleva and M. C. Lin. Unimolecular isomerization/decomposition of cyclopentadienyl and related bimolecular reverse process: Ab initio mo/statistical theory study. *Journal of Computational Chemistry*, 21(6):415–425, 2000.
- [30] D. R. Reed and S. R. Kass. Experimental determination of the  $\alpha$  and  $\beta$  C-H bond dissociation energies in naphthalene. *Journal of Mass Spectrometry*, 35(4):534–539, 2000.
- [31] H. Richter and J. B. Howard. Formation of polycyclic aromatic hydrocarbons and their growth to soot - A review of chemical reaction pathways. *Progress in Energy and Combustion Science*, 26(4-6):565–608, 2000.
- [32] E. R. Ritter and J. W. Bozzelli. Therm: Thermodynamic property estimation for gas phase radicals and molecules. *International Journal of Chemical Kinetics*, 23:767–778, 1991.
- [33] E. R. Ritter and J. W. Bozzelli. Therm: Thermodynamic property estimation for gas phase radicals and molecules, 1997.

- [34] D. A. Robaugh and S. E. Stein. Stabilities of highly conjugated radicals from bonds homolysis rates. *Journal of the American Chemical Society*, 108(3224-3229), 1986.
- [35] B. Römer, G. A. Janaway, and J. I. Brauman. Cyclopentadienyl, indenyl, and fluorenyl anions: Gas-phase and solvation energy contributions to electron detachment energies. *Journal of the American Chemical Society*, 119(9):2249-2254, 1997.
- [36] W. R. Roth, H. Hopf, T. Wasser, H. Zimmermann, and C. Werner. 1,4-didehydronaphthalene. *Liebigs Annalen*, (10):1691-1695, 1996.
- [37] R. R. Squires and C. J. Cramer. Electronic interactions in aryne biradicals. ab initio calculations of the structures, thermochemical properties, and singlet-triplet splittings of the didehydronaphthalenes. *Journal of Physical Chemistry A*, 102(45):9072-9081, 1998.
- [38] S. E. Stein. In B. D. Blaustein, B. C. Bockrath, and S. Friedman, editors, *New Approaches in Coal Chemistry*, volume 169, page 97. American Chemical Society, Washington, DC, 1981.
- [39] W. Tsang. Heats of formation of organic free radicals by kinetic methods. In J. A. Martinho Simoes, A. Greenberg, and J. F. Liebman, editors, *Energetics of Organic Free Radicals*, pages 22-58. Blackie Academic and Professional, London, 1996.
- [40] H. Wang and K. Brezinsky. Computational study on the thermochemistry of cyclopentadiene derivatives and kinetics of cyclopentadienone thermal decomposition. *Journal of Physical Chemistry A*, 102(9):1530-1541, 1998.
- [41] H. Wang and M. Frenklach. Enthalpies of formation of benzenoid aromatic-molecules and radicals. *Journal of Physical Chemistry*, 97(15):3867-3874, 1993.
- [42] H. Wang and M. Frenklach. Calculations of rate coefficients for the chemically activated reactions of acetylene with vinylic and aromatic radicals. *Journal of Physical Chemistry*, 98:11465-11489, 1994.
- [43] P. Weilmunster, A. Keller, and K. H. Homann. Large molecules, radicals, ions, and small soot particles in fuel-rich hydrocarbon flames. part i: Positive ions of polycyclic aromatic hydrocarbons (PAH) in low-pressure premixed flames of acetylene and oxygen. *Combustion and Flame*, 116(1/2):62-83, 1999.
- [44] P. G. Wenthold and R. R. Squires. Biradical thermochemistry from collision-induced dissociation threshold energy measurements. absolute heats of formation of *ortho*-, *meta*-, and *para*-benzynes. *Journal of the American Chemical Society*, 116:6401-6412, 1994.



- [45] P. G. Wenthold, R. R. Squires, and W. C. Lineberger. Ultraviolet photoelectron spectroscopy of the *o*-, *m*-, and *p*-benzyne negative ions. electron affinities and singlet-triplet splittings for *o*-, *m*-, and *p*-benzyne. *Journal of the American Chemical Society*, 120(21):5279–5290, 1998.
- [46] M. Winkler and W. Sander. The structure of *meta*-benzyne revisited – A close look into  $\sigma$ -bond formation. *Journal of Physical Chemistry A*, 105(45):10422–10432, 2001.



# Chapter 6

## Resonance Energy

### 6.1 Introduction

One of the distinctive features of polycyclic aromatic molecules is, as their name suggests, the aromaticity. This property is associated with the cyclic delocalization of electrons, leading to stabilization of the molecule. The aromatic character of PAHs is not a local property, the electrons are free to move throughout the entire system. Thus the stabilization of the PAHs due to electron delocalization cannot be captured by the bond-centered group additivity scheme. In this chapter we present a way to easily quantify this stabilization and to incorporate it in the thermochemical properties estimation method presented in this work.

Several criteria have been proposed to characterize and quantify aromaticity. These criteria basically are divided into four categories: 1) energetic. Aromatic molecules are more stable than their chain analogues; 2) structural. There is a general bond length equalization. The bond lengths in aromatic systems are typically between the length of a single and a double bond; 3) magnetic. Aromatic systems have a  $\pi$ -electron ring current that is induced when the system is exposed to external magnetic fields; and 4) reactivity. Aromatic molecules would like to retain their  $\pi$ -electron structure, and thus prefer substitution to addition.

We are interested in the amount of energy stabilization that electron delocalization brings to PAHs. Thus we will emphasize on the energetic criteria of aromaticity.

Our goal is to provide a method that can estimate qualitatively resonance stabilization from the topological structure of the molecule. After all, the thermochemical properties of the PAHs should be estimated from the knowledge of the connectivity of the atoms only.

## 6.2 Quantifying Resonance Stabilization

Resonance energy is defined as the difference between the energy of the  $\pi$ -electrons of a conjugated molecule ( $E_\pi$ ) and the energy of the  $\pi$ -electrons of a hypothetical reference structure ( $E_\pi(\text{ref})$ ), in which there is no electron delocalization:

$$RE = E_\pi - E_\pi(\text{ref}) \quad (6.1)$$

It is a measure of how much stability the delocalization of the  $\pi$  electrons provide to an aromatic system. However, the choice of the reference structure is rather arbitrary, and varying definitions of the resonance energy have arisen depending on this choice. Schaad and Hess provide a good review of the different reference structures that have been proposed [18]. Here we will discuss briefly some methods that have been proposed to quantify the resonance energy, either using Eq. 6.1 or using other concepts.

### 6.2.1 Hückel Resonance Energy

One of the first proposals for a reference structure is based on carbon-carbon double bonds isolated by conjugation barriers. That is, the reference structure in the Hückel resonance energy (HRE) is ethylene:

$$HRE = E_\pi - nE_\pi(\text{CH}_2 = \text{CH}_2) \quad (6.2)$$

The  $\pi$  energies of the conjugated molecule and of the reference structure (ethylene) are calculated from the Hückel Molecular Orbital Theory (HMO). The aromaticity

predictions of the HRE do not agree very well with experimental observation of the stability of conjugated molecules [18]. It has been shown that the reason for the inadequacy of the HRE is traced to the fact that this resonance energy is roughly proportional to the number of  $\pi$ -electrons in the system [23].

### 6.2.2 Dewar Resonance Energy

Dewar et al. proposed using acyclic polyene-like reference structures [2]. This type of resonance energy is named after Dewar (DRE), and is defined as:

$$DRE = E_{\pi} - \sum_{i=1} n_i E_i \quad (6.3)$$

where  $n_i$  is the number of a particular bond polyene type (C-C, C=C, C-H, and so on) and  $E_i$  is the corresponding energy. Good predictions of aromaticity were obtained using the DRE. Dewar et al. used in their work the semiempirical SCF-MO orbital theory for the calculation of the  $\pi$ -energy. People were not sure whether the improvement over the HRE was because of the definition of polyenes as reference structures or because of the use of SCF-MO instead of the simpler HMO method.

### 6.2.3 Hess-Schaad Reference Structure

This doubt was dissipated by (among others) Hess and Schaad. They showed that the use of polyene-like reference structures and calculation at the HMO level gives results comparable to the DRE. That is, the crucial factor is the appropriate choice of the reference structure, and not the level at which the calculations are performed.

Hess and Schaad [7, 8] used an eight bond parameters scheme to calculate  $E_{\pi}(\text{ref})$ . The eight different bonds capture all the different single and double bonds present in hydrocarbons, according to the number of hydrocarbons attached to the carbons of the bond. The contributions of each of the bonds to  $E_{\pi}(\text{ref})$  was obtained by fitting  $E_{\pi}$  of acyclic polyenes calculated through the Hückel Molecular Orbital Theory (HMO). The  $E_{\pi}$  of the conjugated molecule was also calculated using HMO. In the HMO,  $E_{\pi}$

of conjugated molecules in the ground state is given by

$$E_{\pi} = \sum_{j=1}^{n_e} \lambda_j \quad (6.4)$$

where  $n_e$  is the number of  $\pi$ -electrons and  $\lambda_j$  are the eigenvalues of the adjacency matrix. These eigenvalues correspond to the HMO energy levels. They found good agreement between the resonance energy of cyclic polyenes obtained in this manner (in particular REPE, resonance energy per  $\pi$ -electron) and their chemical stability.

From Eq. (6.4) we see that in the HMO framework, the total  $\pi$ -electron energy of a conjugated molecule is completely defined by the topology of the molecule.

#### 6.2.4 Number of Kekulé Structures

In 1949 Carter had already realized that “*in an aromatic hydrocarbon consisting of two portions linked by a single-bond or a resonance-blocking group (for example, diphenyl) the resonance energy is approximately the sum of the resonance energies of the component rings, but the number of Kekulé structures is the product; this suggests that if the resonance energy of an aromatic hydrocarbon is a function of the number of Kekulé structures, that function must be a logarithmic one*” [1]. He then proceeded to fit the resonance energy of PAHs to the natural log of the number of Kekulé structures and to the number of double bonds. He found a good agreement between his empirical formula and molecular orbital calculations.

The relationship between the number of Kekulé structures of benzenoid PAHs and the resonance energy became clearer when Dewar and Longuet-Higgins noted the relation

$$\det(\mathbf{A}) = (-1)^{n/2} K^2 \quad (6.5)$$

which relates the adjacency matrix  $\mathbf{A}$  to the number of Kekulé structures of benzenoid PAHs [3].  $n$  is the number of carbons in these PAHs (always even), which in PAHs

is equal to the number of  $\pi$ -electrons  $n_e$ . From Eq. (6.5) follows that

$$K^2 = \prod_{j=1}^n |\lambda_j| \quad (6.6)$$

$$\ln(K) \propto \sum_{j=1}^n \ln |\lambda_j| \quad (6.7)$$

From Eq. 6.6 it follows that for two isomeric hydrocarbons, the one with smaller  $K$  will tend to have one or more energy levels closer to zero, that is, to a nonbonding orbital. The occupation of energy levels closer to nonbonding orbitals leads to instability in the molecule, and thus smaller  $K$  values can be associated with chemical instability.

Swinborne-Sheldrake and Herndon showed that  $\ln(K)$  correlates very well with the Dewar resonance energy [20]. Figure 6-1 illustrates the correlation between the  $\ln(K)$  term and Dewar Resonance Energy that these authors found.

Wilcox tried to extend the molecular orbital interpretation of the structure count to non-benzenoid alternant molecules [25] and to non-alternant molecules [26]. He concluded that although in some particular cases the number of Kekulé structures does have a relation to the resonance energy calculated from molecular orbital, no generalization can be made for non-alternant molecules.

### 6.2.5 Resonance-Structure Theory

This method was developed by Herndon [5, 6] and has been shown to be equivalent to Randić's Conjugated Circuit method.

The resonance theory is based on valence bond theory. By assuming zero overlap of the wave function and that the ground-state eigenvalue has equal contributions from the wave-functions from each Kekulé structure, the resonance energy can be calculated from

$$RE_{RT} = \frac{2}{K} \sum H_{ij} \quad (6.8)$$

Herndon showed that the  $H_{ij}$  elements are integrals that result in permutation of pairs of  $\pi$  electrons over the  $\sigma$  framework in going from one Kekulé structure to another. Three pairs of electrons in a single ring are permuted by  $\gamma_1$ , and five pairs of electrons

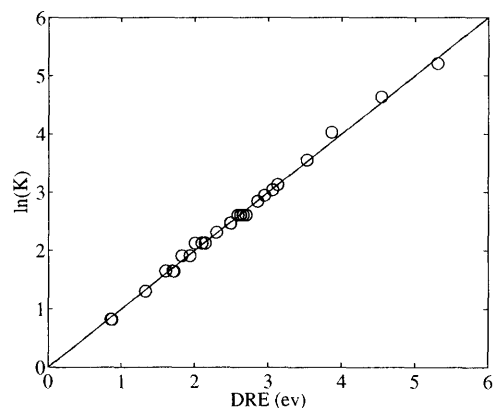


Figure 6-1:  $\ln(K)$  versus DRE plot from Herndon et al. [20].

in two neighboring rings are permuted by  $\gamma_2$ . Herndon showed that it is not necessary to take into account permutations of more than five pairs of electrons in order to obtain resonance energies in good agreement with SCF-MO [5]. Antiaromaticity arises from the permutation of an even number of pair of  $\pi$ -electrons. Thus the permutation of two and four pairs of  $\pi$ -electrons are denoted  $\omega_1$  and  $\omega_2$  respectively. Figure 6-2 gives examples of the permutations of pairs of  $\pi$ -electrons.

The values for the  $\gamma_1$  and  $\omega_1$  permutation integrals were determined by comparison with a large number of SCF-MO calculations of resonance energy. The numerical value for the ratio  $\gamma_1/\gamma_2$  is obtained from experimental measurement of the ratio of the electronic transitions for benzene ( $\gamma_1$ ) and azulene ( $\gamma_2$ ). The ratio for  $\omega_1/\omega_2$  was found to be the same as for  $\gamma_1/\gamma_2$ .

The method thus boils down to the enumeration of the Kekulé structures of a molecule and the determination of the number of each of the permutation integrals

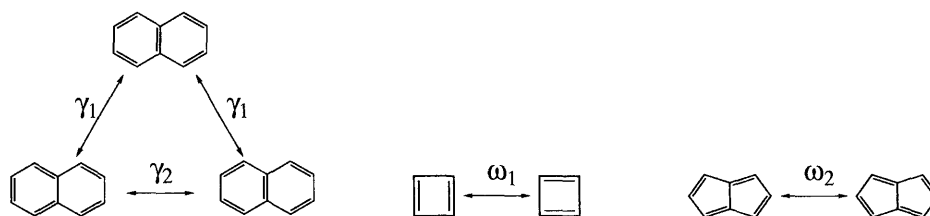


Figure 6-2: Examples of the permutations of pairs of  $\pi$ -electrons corresponding to the  $\gamma_1$ ,  $\gamma_2$ ,  $\omega_1$ , and  $\omega_2$  permutation integrals.



between them. Good agreement with the resonance energy from SCF-MO calculations was found for both alternant and non-alternant PAHs [6].

### 6.2.6 Conjugated Circuits

The conjugated circuit method for quantifying resonance energy has been introduced by Randić [14]. It can be seen as the graph theoretical equivalent of resonance structure theory [15].

Conjugated circuits in a polycyclic molecule are those in which the CC bonds are alternated between single bonds and double bonds. These circuits always have an even number of carbons, either  $(4n + 2)$  or  $4n$ . The resonance energy is calculated as a contribution of each of the circuits

$$RE_{CC} = \frac{\sum_n x_n R_n + \sum_n y_n Q_n}{K} \quad (6.9)$$

where  $R_n$  and  $Q_n$  are the contributions from the circuits with  $(4n + 2)$  and  $4n$  carbons respectively, and  $x_n$  and  $y_n$  is the number of each of these circuits in all the Kekulé structures. The numerical values for the  $R_n$  and  $Q_n$  parameters up to  $n = 4$  were derived from SCF-MO resonance energy calculations.

The conjugated circuit method has been successfully applied in the calculation of the resonance energy of a variety of PAHs [14, 17, 19, 11, 27, 16]. However, the enumeration of the conjugated circuits for large PAHs is still very challenging [15].

## 6.3 Resonance Energy in the BCGA Method

Our goal is to introduce in our estimation method an easy way to qualitatively describe the portion of  $\pi$ -electron delocalization effect on the energy of PAHs that is not captured by bond additivity. We found that the simple  $\ln(K)$  term performs this task very well.

Comparing Eqs. (6.4) and (6.7), it is clear that the  $\ln(K)$  term is related to the  $E_\pi$  of conjugated molecules. On the other hand, Hess and Schaad have shown that

the  $\pi$ -electron energy of acyclic polyenes, that is, the  $E_{\pi}(\text{ref})$ , is additive in regards to the bonds [7].

Thus we see that the bond-centered group additivity method that we propose, which includes a  $\ln(K)$  term (see Section 3.2), captures qualitatively the resonance energy of aromatic molecules. The  $\ln(K)$  term accounts for the  $E_{\pi}$  of the conjugated molecule, whereas the  $E_{\pi}$  of the reference molecules is included in the parametrization of the bond-groups.

Although the use of the  $\ln(K)$  term alone to describe the resonance energy of non-alternant molecules does not have a solid foundation in molecular orbital theory, we have found that its use, in combination with the bond-centered groups, leads to good estimations of the  $\Delta H_f^\circ$  of PAHs with both five- and six-membered rings (see Section 3.2).

## 6.4 Counting the Number of Kekulé Structures

### 6.4.1 Method for Alternant Molecules

Alternant hydrocarbons are those in which the carbon atoms can be labelled by stars and circles, so that adjacent carbons receive different labels [4]. The corresponding concept in graph theory is that of bipartite graphs. The vertices of a bipartite graph can be partitioned into two groups, such that two adjacent vertices belong to different groups. An important theorem of bipartite graphs states that

**Theorem 1** *A graph is bipartite if and only if it contains no odd-membered cycles.*

In addition, for benzenoid graphs, Eq. (6.5) is valid. Thus, for benzenoid PAHs, the calculation of the number of Kekulé structures from the adjacency matrix is trivial.

As an aside, more generally, the number of Kekulé structures for alternant molecules (for example, four-membered rings) is given by

$$\text{per}(\mathbf{A}) = K^2 \tag{6.10}$$

The determinant of a matrix  $\mathbf{A}$  is the sum of all possible products of elements  $\sum (-1)^z A_{i1}A_{j2}A_{k3} \cdots A_{xN}$  such that  $i, j, k \dots$  are all different and  $z$  is odd for half of the terms and even for the other half. The expression for the permanent is exactly the same but without the  $(-1)^z$ . As a consequence, for a  $N \times N$  matrix,  $\text{per}(\mathbf{A})$  is the sum of  $N!$  terms. Although this is also true for determinants, efficient methods for calculating the determinant exist. However, the complexity of the best known algorithms for the computation of the permanent grows as the exponent of the matrix size [21, 24].

## 6.4.2 More General Methods

The determinant and permanent of the adjacency matrix of non-alternant molecules have no relation to the number of Kekulé structure count. Other methods have been employed for the calculation of  $K$  in this case. The two most important methods were originally proposed in physics for the study of crystal lattices.

### Transfer-Matrix Method

The transfer matrix has been used in statistical mechanics for some time [15]. Klein et al. were the first to apply this method for enumeration of sub-graphs in chemical context [10].

This approach works particularly well for systems that have repeating units, such as fullerenes. It has been used to calculate the number of Kekulé structures of fullerenes up to  $C_{240}$  [19, 22]. Its implementation for more general cases is more challenging. A thorough description of the method can be found in [10, 19].

### Signed Matrix Method

A more generally applicable method is the signed matrix method. It was first proposed by Kasteleyn in the context of the statistics of non-overlapping dimers [9]. He found that the determinant of the signed matrix relates to the number of Kekulé structures

through:

$$\det(\mathbf{S}) = K^2 \quad (6.11)$$

The signed matrix is an adjacency matrix of the *directed* graph of the molecule. In a *directed* graph, each edge has an orientation. In the signed matrix, the orientation is chosen so that each smallest ring has an odd number of edges oriented in the clockwise direction. The sign of the elements in the signed matrix are chosen so that if the orientation is from vertex  $i$  to vertex  $j$ ,  $S_{ij} = -1$  and  $S_{ji} = +1$ .

The signed matrix method has proved to be a powerful method to calculate the number of Kekulé structures of planar graphs [11, 12]. This method was first introduced for chemical enumeration by Klein and co-workers [11] and they have since used it for counting of number of Kekulé structures of a variety of PAHs [11, 13, 27, 12].

## 6.5 Algorithm for Kekulé Structure Counting

Unfortunately the author was not fully aware of the implementation of the signed matrix method for the enumeration of the number of Kekulé structures. We thus devised a new algorithm for counting the number of Kekulé structures for any planar graph (both alternant and non-alternant). This algorithm is described in this section.

### 6.5.1 Idea and Implementation

The idea behind the algorithm is very simple. We want to form pairs of adjacent nodes, and each node can belong to only one pair. Each pair represents a double bond.

The algorithm to count the number of Kekulé structures ( $K$ ) is as follows:

1. While there are still unvisited nodes, pick a node  $i$  and check if it has already been visited.
  - (a) If this node has already been visited go back to 1.
  - (b) Else proceed to 2
2. Make a list  $L_i$  of all the nodes that are adjacent to  $i$ .

3. While there are still nodes in this list, pick a node  $j$  from this list and check if it has been visited
  - (a) If  $j$  has not yet been visited, mark both  $i$  and  $j$  as visited and return to 1.
  - (b) Else go back to 3
4. If the while loop in step 3 ended with no appropriate adjacent node  $j$  being found, go to step 5
5. Find a new list
  - (a) Go back up in the running of the algorithm, until a list  $L_i$  is found in which there were still unvisited nodes  $j$ .
  - (b) Set all the nodes that were marked as visited after  $L_i$  as unvisited.
  - (c) Go step to 3 for that list  $L_i$ .
  - (d) If there are no lists left that satisfy the criterion in 5a, all the possible Kekulé structures have already been found. END
6. If there are no more unvisited nodes, this means that all the nodes were successfully assigned to pairs, and a Kekulé structure has been found. Increment  $K$  by one. Go to 5

As evidenced by steps 3a and 5, this is a recursive algorithm. Also, one notes that there are two different kinds of nodes:  $i$  and  $j$ . The nodes  $i$  are picked randomly, and we chose to always select the (not-visited) node that has the lowest ID number. On the other hand, nodes  $j$  can only be chosen from the active list  $L_i$ , which consists of the nodes that are adjacent to the active node  $i$ . Among the nodes in  $L_i$ , we also always choose to select the node  $j$  that has the lowest ID first. The working of the algorithm can best be understood with an example. Let's say we want to calculate the number of Kekulé structures ( $K$ ) of acenaphthalene. The schematic of the procedure described below is found in Figure 6-3. We first assign an ID number to each of the carbon atoms.

- i. Start with all nodes set as unvisited, and  $K=0$
- ii. First pick a node  $i$ . We select the one with the lowest node ID number:  $i=1$
- iii. The list  $L_1$  with the nodes adjacent to node 1 is composed of  $L_1=\{2, 6, 10\}$ 
  - (a) Among the nodes in  $L_1$  we start by choosing  $j=2$ . This node has not been visited yet. Mark nodes 1 and 2 as visited. See scheme (1).

- (b) Go back to step 1.  $i=3$
  - (c)  $L_3=\{2, 4\}$
  - (d) Node 2 has been visited already (as marked by the double bond in scheme **(1)**), so  $j=4$ .
  - (e) Mark nodes 3 and 4 as visited. See scheme **(2)**.
  - (f) Go back to step 1.  $i=5$
  - (g)  $L_5=\{4, 6\}$ . Node 4 has been visited already,  $j=6$
  - (h) Mark nodes 5 and 6 as visited. See scheme **(3)**.
  - (i) Go back to step 1.  $i=7$
  - (j)  $L_7=\{6, 8\}$ . Node 6 has been visited already,  $j=8$
  - (k) Mark nodes 7 and 8 as visited. See scheme **(4)**.
  - (l) Go back to step 1.  $i=9$
  - (m)  $L_9=\{8,10\}$ . Node 8 has been visited already,  $j=10$
  - (n) Mark nodes 9 and 10 as visited. See scheme **(5)**.
  - (o) Go back to step 1.  $i=11$
  - (p)  $L_9=\{10, 12\}$ . Node 10 has been visited already,  $j=12$
  - (q) Mark nodes 11 and 12 as visited. See scheme **(6)**.
  - (r) There are no more unvisited nodes. We reached step 6, increment K by one,  $K=1$ .
- iv. The previous list of nodes that still had unvisited nodes was list  $L_1$ . We go back to step 3 for this list. Set all the nodes that were set to visited at step 3 and after as unvisited. That means that all the nodes are set to unvisited. We completed the cycle for  $j=2$ , so now we choose  $j=6$ .
- (a) Mark nodes 1 and 6 as visited.
  - (b) Go back to step 1.  $i=2$ .
  - (c)  $L_2=\{1, 3, 12\}$ . Node 1 has been visited already,  $j=3$
  - (d) Proceeding in the same way as in step iii., we find one more Kekule structure (see scheme **(8)**),  $K=2$ .
- v. The previous list of adjacent nodes that still had unvisited nodes was list  $L_2$ . We go back to step 3 for this list. Set all the nodes that were set to visited at step 3 and after as unvisited. Only nodes 1 and 6 remain set as visited.
- (a) From  $L_2=\{1, 3, 12\}$ , 1 has been visited, and we just finished the cycle for  $j=3$ , thus we set  $j=12$ .
  - (b) Mark nodes 2 and 12 as visited. See scheme **(9)**.
  - (c) Go back to step 1.  $i=3$ .

- (d)  $L_3=\{2, 4\}$ . Node 2 has been visited already,  $j=4$
  - (e) Mark nodes 3 and 4 as visited. See scheme (10).
  - (f) Go back to step 1.  $i=5$ .
  - (g)  $L_5=\{4, 6\}$ . However both nodes 4 and 6 have already been visited (see step 4), so we go back and find the previous list of adjacent nodes that still had unvisited nodes.
- vi. That list is  $L_1=\{2, 6, 10\}$ . All the nodes are set to unvisited. Since we already tried  $j=2$  and  $j=6$ , now we set  $j=10$ .
  - vii. Proceeding in the same way as in step iii., we reach once more step 6 and find one more Kekulé structure (see scheme (11)),  $K=3$ .
  - viii. We go to step 5, but we don't find any more lists that satisfy 5a, so the process ends, with  $K=3$ .

### 6.5.2 $\pi$ -Radicals with an Odd Number of Carbons

In  $\pi$ -radicals such as phenalene, one of the carbons will always be unpaired. In the bond-centered group additivity method for this class of PAHs (Section 5.2.5), we assign the thermochemical properties of the resonance species with the largest number of Kekulé structures to the  $\pi$ -radical. Thus we calculate, for the unpaired electron at each carbon position, the number of Kekulé structures for that resonance species.

### 6.5.3 Heterocyclic PAHs and PAHs with a Triple Bond

The Bond-Centered Group Additivity Method that we propose can also estimate the thermochemical properties of PAHs containing the furan substructure and of PAHs containing triple bonds.

For the purpose of counting the number of Kekulé structures, we consider that the pair of  $\pi$ -electrons of the oxygen in the furan structure does not form  $\pi$ -bonds with the  $\pi$ -electrons of the neighboring carbons. Thus, in the algorithm described in Section 6.5.1, the oxygen in furan substructures is not included as one of the nodes that participates in the resonance.

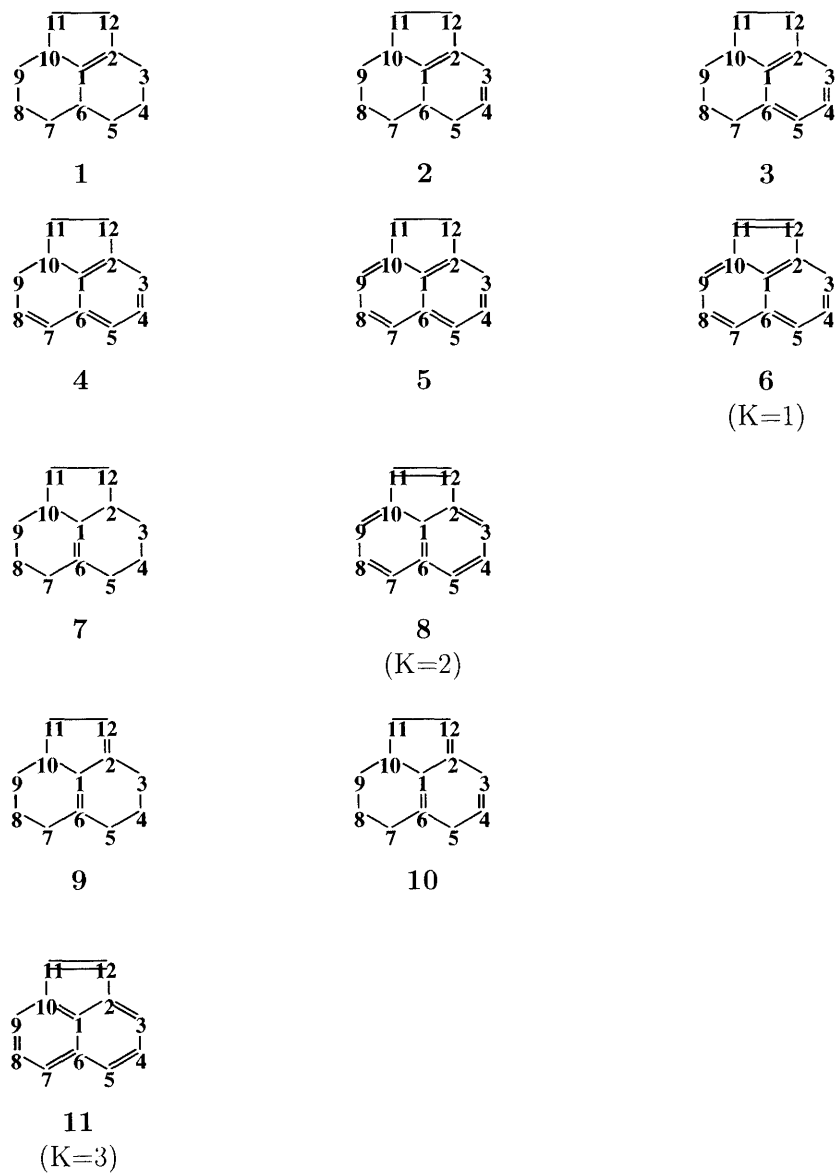


Figure 6-3: Example of the algorithm for the calculation of the number of Kekulé structures. Counting  $K$  for acenaphthalene, as described in the example given in the text.



In the case of triple bonds in aromatic molecules, each of the carbon atoms participating in the triple bond also has two  $\pi$ -electrons. However, these  $\pi$ -electrons are not in the same  $\pi$ -orbital. One of the  $\pi$ -orbitals is perpendicular to the plane of the ring, and the other is in the plane of the ring. The first  $\pi$ -orbital participates in the  $\pi$ -electrons cloud that characterizes aromatic molecules, whereas the  $\pi$ -electrons in the second  $\pi$ -orbital can be considered to be localized. They do not participate in the resonance structure. For example, the resonance structures of benzyne are shown in the scheme in Section 4.3.1. Thus in the algorithm for counting the number of Kekulé structures, the carbons participating in the triple bond are treated just like the other aromatic carbons.

#### 6.5.4 Performance of the Algorithm

The algorithm described in Section 6.5.1 is very fast for PAHs up to  $n \approx 60$  nodes. For example, it calculates the number of Kekulé structures of the  $C_{60}$  fullerene in a couple of seconds in a 1GHz laptop with 256 MB of RAM. However, in the worst case, the algorithm is expected to scale with the exponential of the number of nodes. As exposed in Section 6.5.1, there are two classes of nodes in the algorithm:  $i$ , which are picked randomly (we always choose the non-visited node with the smallest ID) and  $j$ , which are picked from the active list  $L_i$ . At each level of the tree, all the nodes  $j$  in the active list  $L_i$  have to be tested. In each list  $L_i$  there will be at most 2 nodes (3 for the root node) since each carbon in a PAH has a connectivity of 3. Also, there will be  $n/2$  levels in which nodes  $j$  will have to be chosen, where  $n$  is the number of nodes (carbon atoms). Thus the computational time scaling behavior for this algorithm is

$$\sim 2^{n/2} \tag{6.12}$$

In a few tests that we performed, we found that the scaling is not always as bad as in Eq. 6.12. In particular, the algorithm is faster for PAHs containing only six-membered rings than for PAHs that also contain five-membered rings. Nevertheless, the scaling of the algorithm is still exponential with the number of nodes. In general it is too

slow to be used for the estimation of thermochemical properties of PAHs with more than  $\approx 60$  carbons for the purpose of automatic reaction mechanism generation.

We suggest that in the future, more efficient algorithms be incorporated for large benzenoid PAHs and for PAHs with high symmetry, such as fullerenes.

## 6.6 Conclusions

We have described in this Chapter the importance of the inclusion in the estimation method for  $\Delta H_f^\circ$  of a term that captures the resonance energy in PAHs. We briefly discussed some existing methods for estimating resonance energy, based on molecular orbital theory and graph theory. We justified our choice of the use of number of Kekulé structure count (in particular  $\ln(K)$ ) for this purpose.

We presented a new algorithm for the counting of the number of Kekulé structures. This algorithm works very well for PAHs with up to  $\sim 60$  carbons, which were the PAHs emphasized in this work. If the number of Kekulé structures of larger PAHs is to be calculated on a regular basis, we suggested that the signed matrix method be used (Section 6.4.2).

# Bibliography

- [1] P. G. Carter. An empirical equation for the resonance energy of polycyclic aromatic hydrocarbons. *Transactions of the Faraday Society*, 45:597-602, 1949.
- [2] M. J. S. Dewar and C. Llano. Ground states of conjugated molecules. XI. Improved treatment of hydrocarbons. *Journal of the American Chemical Society*, 91(4):789-795, 1969.
- [3] M. J. S. Dewar and H. C. Longuet-Higgins. The correspondence between the resonance and molecular-orbital theories. *Proceedings of the Royal Society of London.*, A214:482-493, 1952.
- [4] I. Gutman and O. E. Polansky. *Mathematical Concepts in Organic Chemistry*. Springer-Verlag, Berlin, 1986.
- [5] W. C. Herndon. Resonance energies of aromatic-hydrocarbons - quantitative test of resonance theory. *Journal of the American Chemical Society*, 95(7):2404-2406, 1973.
- [6] W. C. Herndon and M. L. Ellzey. Resonance theory. V. Resonance energies of benzenoid and nonbenzenoid pi systems. *Journal of the American Chemical Society*, 96(21):6631-6642, 1974.
- [7] Jr. Hess, B. A. and L. J. Schaad. Hückel molecular orbital  $\pi$  resonance energies. A new approach. *Journal of the American Chemical Society*, 93(2):305-310, 1971.
- [8] Jr. Hess, B. A. and L. J. Schaad. Hückel molecular orbital  $\pi$  resonance energies. Nonalternant hydrocarbons. *Journal of Organic Chemistry*, 36(22):3418-3423, 1971.
- [9] P. W. Kasteleyn. Dimer statistics and phase transitions. *Journal of Mathematical Physics*, 4(2):287-293, 1963.
- [10] D. J. Klein, G. E. Hite, and T. G. Schmalz. Transfer-matrix method for subgraph enumeration: Applications to polypyrene fusenes. *Journal of Computational Chemistry*, 7(4):443-456, 1986.
- [11] D. J. Klein and X. Liu. Many-body conjugated-circuit computations. *Journal of Computational Chemistry*, 12(10):1260-1264, 1991.

- [12] D. J. Klein, H. Zhu, R. Valenti, and M. A. Garcia-Bach. Many-body valence-bond theory. *International Journal of Quantum Chemistry*, 65:421–438, 1997.
- [13] X. Liu, D. J. Klein, W. A. Seitz, and T. G. Schmalz. Sixty-atom carbon cages. *Journal of Computational Chemistry*, 12(10):1265–1269, 1991.
- [14] M. Randić. Aromaticity and conjugation. *Journal of the American Chemical Society*, 99(2):444–450, 1977.
- [15] M. Randić. Aromaticity of polycyclic conjugated hydrocarbons. *Chemical Reviews*, 103:3449–3605, 2003.
- [16] M. Randić and X. Guo. Giant benzenoid hydrocarbons. Superphenalene resonance energy. *New Journal of Chemistry*, 23(2):251–260, 1999.
- [17] M. Randić and N. Trinajstić. Conjugation and aromaticity of corannulenes. *Journal of the American Chemical Society*, 106:4428–4434, 1984.
- [18] L. J. Schaad and Jr. Hess, B. A. Dewar resonance energy. *Chemical Reviews*, 101(5):1465–1476, 2001.
- [19] T. G. Schmalz, W. A. Seitz, D. J. Klein, and G. E. Hite. Elemental carbon cages. *Journal of the American Chemical Society*, 110(4):1113–1127, 1988.
- [20] R. Swinborne-Sheldrake and W. C. Herndon. Kekulé structures and resonance energies of benzenoid hydrocarbons. *Tetrahedron Letters*, (10):755–758, 1975.
- [21] F. Torrens. Computing the Kekulé structure count for alternant hydrocarbons. *International Journal of Quantum Chemistry*, 88:392–397, 2001.
- [22] F. Torrens. Table of periodic properties of fullerenes based on structural parameters. *Journal of Chemical Information and Computer Sciences*, 44(1):60–67, 2004.
- [23] N. Trinajstić. *Chemical Graph Theory*, volume II. CRC Press, Inc., Boca Raton, Florida, 1983.
- [24] E. W. Weisstein. Mathworld, 2004.
- [25] Wilcox Jr., C. F. Stability of molecules containing  $(4n)$ -rings. *Tetrahedron Letters*, 7:795–800, 1968.
- [26] Wilcox Jr., C. F. Stability of molecules containing nonalternant rings. *Journal of the American Chemical Society*, 91(10):2732–2736, 1969.
- [27] H. Zhu, A. T. Balaban, D. J. Klein, and T. P. Zivkovic. Conjugated-circuit computations on two-dimensional carbon networks. *Journal of Chemical Physics*, 101(6):5281–5292, 1994.

## Chapter 7

# Estimation of Thermochemical Properties for Non-Aromatic Molecules and Radicals

### 7.1 Introduction

Thermochemical properties of chemical species are critical for the modelling of reacting systems. Thermodynamic consistency requires that reverse rate constants be calculated from the forward rate constants and from the equilibrium constants. The latter are obtained from the thermochemical properties of reactants and products. Consequently, low temperature model predictions depend heavily on barrier heights and enthalpy changes of the reactions, while the model predictions at high temperature rely sensitively on entropy change (as  $\Delta S$  is multiplied by  $T$ ).

The number of existing chemical species is almost infinite. It is not feasible to generate and tabulate the thermochemical properties for each of them. Although immense experimental and computational effort has been dedicated to this area, only a small fraction of species have had their thermochemical properties determined with satisfactory accuracy and precision. In many cases, the only option is to resort to estimation methods to obtain the thermochemical properties of chemical species.

Our group has developed an automatic reaction mechanism generation software (RMG) [19], and the estimation of the thermochemical properties of the species included in the reaction mechanism is one of the fundamental building blocks of the software. The desired features that guided the development of the thermochemical properties estimator for RMG (referred to as RMG thermo) are:

- i. It should automatically provide thermochemical properties for *every* species generated by RMG, while also having the capability to work independently as a thermochemical estimator;
- ii. It should have an easily maintainable and expandable database, that can grow as new group values are determined;
- iii. The machine time for the estimation should be as short as possible;
- iv. The estimated thermochemical properties should be as accurate as possible.

Since our group is currently working on various aspects of combustion of hydrocarbon fuels, the RMG thermo should handle molecules containing carbon, hydrogen and oxygen. However, the concept of automatic reaction mechanism generation is not restricted to these species, and the expansion of RMG thermo capability to other elements should be simple and straightforward.

Thermochemical properties estimation methods are based on the assumption that a molecule can be divided into substructures which have a constant contribution to the property in question. Many of these methods have been developed, each defining the substructures slightly differently (see for example [1, 24, 3, 26, 14]). Some of these methods have been summarized in [16]. The group additivity method of Benson [3] has been used to estimate the thermochemical properties in RMG due to its simplicity, extendability and to the wide availability of group values for stable molecules [20, 5] as well as for hydrogen bond increments (HBI) for the estimation of radicals [11].

It is not surprising that other thermochemical properties estimation programs, such as THERM [17], NIST's Structure & Properties Software [12] and Chetah [2] also use Benson's group additivity method. The group values in these programs are stored

as lists. It is possible to edit these lists and include new groups, but when a molecule is given that contains a group not found in the database, these programs are unable to calculate its properties. The THERM program contains the most extensive library. NIST's Structure & Properties Software is the most sophisticated and user friendly of these programs, and it includes some of the non-group interactions from Benson's method, such as gauche interactions and *cis* corrections. It also calculates symmetry for simple molecules (including cyclic compounds), assuming facile interconversion of conformers.

In this Chapter we will first briefly describe Benson's group additivity method. Next a new way to organize the database for Benson's groups, based on tree structures, will be presented. This organization allows us to meet the three first requirements for RMG thermo, as listed earlier.

## 7.2 Estimation Method

In Benson's group additivity method, each 'group' contributes a given amount to the thermochemical properties of the molecule. A 'group' is defined as a heavy atom (all the atoms with the exception of hydrogen) with all its ligands, or neighboring atoms. For aliphatic molecules, Benson's group additivity method predicts  $\Delta H_f^\circ$  0.5 kcal mol<sup>-1</sup> and  $S_{298}^\circ$  and  $C_p^\circ$  to within 0.3 cal K<sup>-1</sup> mol<sup>-1</sup> [3].

$\Delta H_f^\circ$  and  $C_p^\circ$  of stable molecules are estimated by simply adding the contributions of each of the groups present in the molecule:

$$\Delta H_f^\circ(R) = \sum_i H_{f,i} \quad (7.1)$$

$$C_p^\circ(R) = \sum_i C_{p,i} \quad (7.2)$$

Each of the groups in this method does not contain information about the symmetry or optical isomerism of the molecule, thus the entropy calculated by Benson's group additivity method has to be corrected to account for the entropy lowering due to

symmetrical rotations and entropy increase due to optical isomers:

$$S_{298}^{\circ}(R) = \sum_i S_i - R \ln(\sigma / \text{optisom}) \quad (7.3)$$

Benson's group additivity method is based on the fact that only local characteristics affect the thermochemical properties of molecules. Therefore, this method inherently cannot describe non-nearest neighbors interactions, such as those arising in alkenes with *cis* conformations, gauche interactions and the strain originated in rings. Benson [3] has derived some corrections to account for these non-nearest neighbors interactions.

**Cis corrections** Benson's group values were derived for *trans* conformation in alkenes.

When two groups are in the *cis* position, they repel each other increasing the heat of formation of the alkene. Benson provided corrections for these cases [3].

**Gauche interactions** Gauche interactions are next-nearest neighbors interactions between large groups. Gauche interaction corrections for alkanes, ethers [3], and ketenes [21] are available.

**Ring corrections** The group values of Benson's method were developed for aliphatic molecules, and require corrections for ring structures, to account for the loss of rotational movement and to the additional energy due to ring strain. Benson provides ring corrections for most of the rings up to 10 membered rings and for some bi-cycles as well.

Radicals are treated through the Hydrogen Bond Increment (HBI) method proposed by Lay et al. [11], where the thermochemical properties are calculated for the stable species and corrections are added for the radical, accounting for the bond energy and entropy and heat capacity changes due to the hydrogen loss and/or change in vibrational frequencies. The H abstraction reaction can be written





with  $\Delta H_{rxn,298}^\circ = \text{BDE}$ . The thermochemical properties of the radical are related to the thermochemical properties of the corresponding stable species through:

$$\Delta H_f^\circ(\text{R}\bullet) = \text{BDE}(\text{R-H}) + \Delta H_f^\circ(\text{RH}) - \Delta H_f^\circ(\text{H}\bullet) \quad (7.5)$$

$$S_{int,298}^\circ(\text{R}\bullet) = S_{int,298}^\circ(\text{RH}) + \Delta S_{298}^\circ(\text{HBI}) \quad (7.6)$$

$$C_p(T)(\text{R}\bullet) = C_p(T)(\text{RH}) + \Delta C_p(T)(\text{HBI}) \quad (7.7)$$

where  $\Delta H_f^\circ(\text{H}\bullet) = 52.153 \text{ kcal mol}^{-1}$  and  $S_{int}^\circ$  is the intrinsic entropy (excluding symmetry). BDE is the bond dissociation energy and corresponds to the hydrogen bond increment (HBI) for  $\Delta H_f^\circ$ .  $\Delta S_{298}^\circ(\text{HBI})$  and  $\Delta C_p(T)(\text{HBI})$  are the HBI group values for estimating the entropy and the heat capacity of the radical from its parent. Symmetry is not included in the values of  $\Delta S_{298}^\circ(\text{HBI})$ , and thus the calculation of  $S_{298}^\circ$  for radicals should take into account the difference in the symmetry of the radical and its parent stable molecule:

$$S_{298}^\circ(\text{R}\bullet) = S_{298}^\circ(\text{RH}) + \Delta S_{298}^\circ(\text{HBI}) - R \ln(\sigma_{radical}/\sigma_{parent}) \quad (7.8)$$

For molecules composed only of carbon, oxygen and hydrogen atoms, there are almost two hundred groups in Benson's method with numerical values, and almost one hundred HBI groups.

### 7.3 The Thermochemistry Database

The database for RMG thermo is made of three parts: the data structure, the dictionary, and the library. The data structure (described in Section 7.3.1) provides a framework in which the data are stored. The dictionary (described in Section 7.3.2) defines each group. And the library holds the values corresponding to the thermochemical contribution of each of the groups. Each group is assigned a unique name, and this name links the position of the group in the data structure, to its definition (in the dictionary) and its values (in the library).

In addition to the Benson's groups, the database also holds values for the HBI groups for radicals and for the corrections described in the previous sections.

### 7.3.1 Data Structure

Traditionally, programs that implement the Benson's group additivity method organize the groups database as a list. This means that each time the program looks for a group in the database, it will try to match up to two hundred entries before finding the correct group. Unordered lists are generally used to store entirely unrelated data. If a logical relationship between the data exists, it makes sense to make use of this logic to design a database with a more intelligent structure.

#### Main Groups Tree

Clearly the groups in Benson's method are not unrelated to each other. The groups for (oxygenated) hydrocarbons can promptly be divided into two classes: one in which the heavy (central) atom is a carbon and the other in which it is an oxygen. Next, the groups in each of these classes can be further differentiated according to the bonds (i.e., hybridization) of the central atom. Thus in the case of carbon as a central atom, the carbon can have four single bonds, two single bonds and a double bond, two double bonds, and so on. This classification can go on and on, if at each level groups are differentiated according to their outskirts. Figure 7-1 gives an example of this incremental specification of the groups for one of the carbons in propanoic acid.

A tree structure naturally presents itself. The topmost node of this thermochemical database tree (level L0) is simply a heavy atom. In the second level (L1) the atom is specified, currently it can be either a carbon or an oxygen. In the next level (L2), the connectivity of this central atom is specified. For example, the carbon atom is specified to have either four single bonds (Cs), one double bond and two single bonds (Cds), two double bonds (Cdd), one triple bond and one single bond (Ct) or two benzene bonds and a single bond (Cb). The atoms that are bonded to the central atom (whether H, C, or O) are specified in the next level (L3). Next (in level L4) the

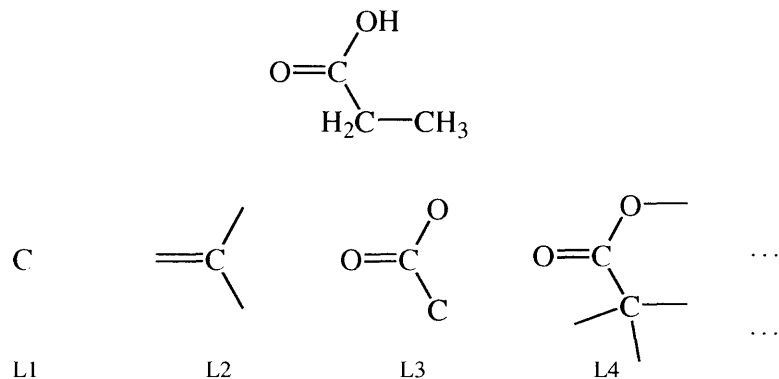


Figure 7-1: Example of the incremental specification of a group.

connectivities of these neighboring atoms are defined. In the usual Benson's group additivity method, this is as far as a group has to be defined. However, if sufficient information is available, more precise estimates can be obtained using more detailed functional group definitions. Sumathy and Green [21] developed groups for ketenes, molecules that have been included in oxidation mechanisms of hydrocarbons (see for example [7]), but whose thermochemical properties cannot be described by Benson's group additivity method. It is simple to include these new, more specific groups in a database organized as a tree. In order to describe ketene groups, two more levels (L6 and L7) were included in the tree. These levels differentiate the more distant neighbors of the central atom (see Figure 7.3.1) allowing the specification of whether a ketene group is attached to the central atom (Cds-Cdd-Od) or whether it is an allenic group (Cds-Cdd-Cd). This is an example of how easily the tree can be extended to accommodate new groups as they are developed. Figure 7.3.1 gives an example of a partial tree with its nodes and connectivities.

Developing a tree as described in the previous paragraph results in about 1000 leaves for groups with carbon as the central atom and almost 40 groups with oxygen as the central atom. Obviously, values for the thermochemical properties are not available for the majority of the groups. Benson in his book [3] derived about 80 values for groups with carbon as the central atom. Sumathi and Green have provided values for about 30 more carbon centered groups [21, 22, 23]. Values are available for fewer than 20 groups with oxygen as the central atom [3]. Generation of values

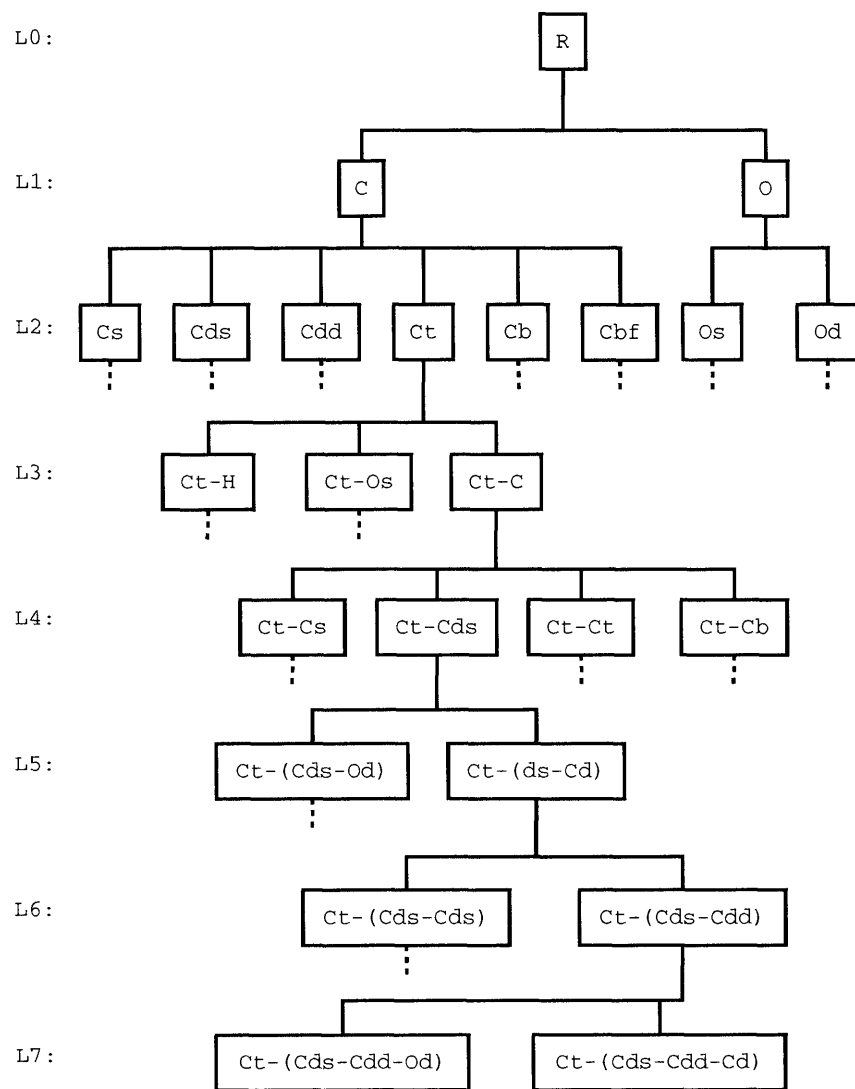


Figure 7-2: Partial representation of the thermochemical database tree.

for all the possible groups (through quantum chemical calculations, for example) is a colossal task. We therefore assigned estimated values for the groups with missing thermochemical values. These groups are assigned the values of a similar group. The implicit assumption is that groups that have similar structures will make similar contributions to the thermochemistry of a molecule. The tree structure naturally gathers together groups that are similar. Thus one could assign the value of a sibling or a cousin to a missing group. Clearly, the assignment based on the tree structure is not unique, since a group often has more than one sibling or cousin. For a unique assignment we have to rely on chemical knowledge. The unique assignment rules that we propose for missing groups are summarized in Table 7.3.1, in order of priority.

The assignment rules described in Table 7.3.1 are mostly straightforward. Cs (and not Cds) is chosen to substitute (Cds-Od) because from an analysis of the available Benson's group values [3], groups in which Cs substitutes (Cds-Od) have values closer to the original group than groups in which Cds is the substitute.

As an example of how assignments were made, take the group Cs-(Cds-Cdd-Cd)(Cds-Od)(Cb)H, which does not have a value. From Table 7.3.1, (Cds-Cdd-Cd) should be first changed to (Cds-Cds), and thus the group is assigned the same value of Cs-(Cds-Cds)(Cds-Od)(Cb)H, which in turn also has no value, and is assigned according to the rules in Table 7.3.1 the value of Cs-(Cds-Cds)(Cds-Od)(Cds-Cds)H. Finally, this group is assigned the value of Cs-(Cs)(Cds-Od)(Cs)H, which is known.

Table 7.1: Rules for value assignment for "missing" thermochemical groups.

	If an unknown group contains	It is assigned the value of the same group with
1.	(Cds-Cdd-Cd)	(Cds-Cds)
2.	(Cdd-Cd)	Cds
3.	Cb	(Cds-Cds)
4.	Ct	(Cds-Cds)
5.	(Cds-Cds)	Cs
6.	(Cds-Od)	Cs
7.	(Cds-Cdd-Od)	(Cds-Od)
8.	Os	Cs

This sequential value assignment makes it unnecessary to manually update the tree after a value is added to a previously unknown node. All the nodes that are assigned the value of this node will automatically reference the new value.

### **HBI Groups Tree**

Just as group values for thermochemical properties of stable molecules depend on the environment around the central atom, HBI values also depend on the environment around the radical site. Thus a database for HBI values benefits from a tree structure. The HBI tree is basically organized the same way as the main groups tree.

The HBI groups tree was organized around the available data. Thus, regions in which a lot of knowledge is available are more dense and developed than regions where knowledge is scarce. Moreover, the children of a given tree node do not always span the whole set represented by the father node. All the nodes were assigned a value, and thus if a group in a molecule matches a node, but does not match any of its children, it receives the value of the node. Node CsJ and its children are shown as an example in Figure 7.3.1. Since no data are available for radicals at a Cs that are bonded to more than one oxygen atom, these children have not been included in the tree. If a molecule has such a group, it will only match up to node CsJ. This node has been assigned the value of node C2CsJO. Consequently, every radical at a Cs that is bonded to more than one oxygen atom will receive the HBI group corresponding to the C2CsJO radical.

### **Corrections Tree**

The non-nearest neighbor corrections were also organized as a tree structure. Since these corrections arise from the interaction of the neighbors from two adjacent groups, the nodes in this tree are centered on two atoms, instead of one, as in the previous trees. Thus two atoms connected by a single bond might give rise to a *gauche* interaction [3]. (Corrections arising from the repulsion of H atoms on 1,5-C atoms have not been included yet). Two carbons connected by a double might give rise to a *cis*-correction [3] or a ketene correction [21]. Finally two carbon atoms connected through

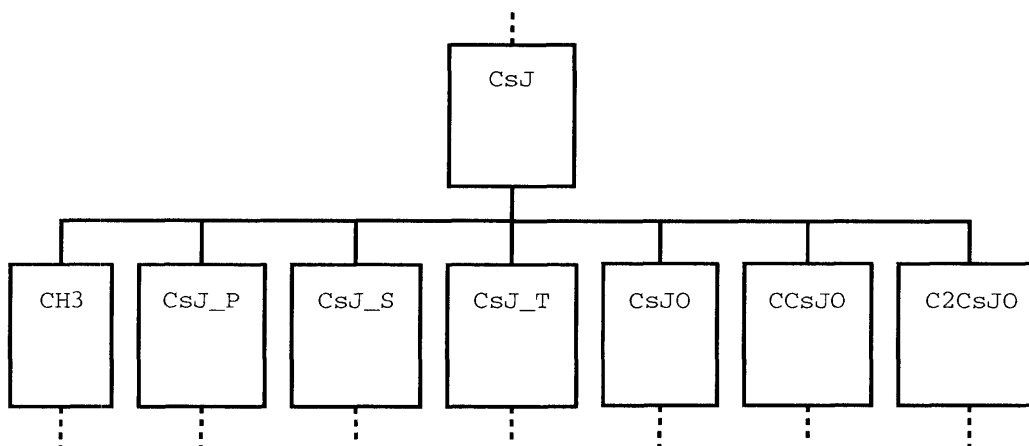


Figure 7-3: Partial representation of the HBI database tree. Only children for which data are available have been included in the tree. For example, data are not available for radicals at a Cs that are bonded to more than one oxygen atom. Such groups will only match up to the CsJ group, and thus will receive the value assigned to this node. This node has been assigned the value of the C2CsJO node.

a benzene bond might lead to an *ortho* correction [3]. *Meta* and *para* corrections have also been introduced (see Section 4.4).

### Ring Corrections Tree

In multi ring structures, we chose to apply corrections only to the smallest ring, which is a good approximation also for the bi-cycles corrections provided by Benson. For example, instead of applying the correction for spiropentane ( $\Delta H_{f,298K}^o = 63.5 \text{ kcal/mol}$  and  $S_{int,298K}^o = 67.6 \text{ cal/molK}$ ), the correction for cyclopropane ( $\Delta H_{f,298K}^o = 27.6 \text{ kcal/mol}$  and  $S_{int,298K}^o = 32.1 \text{ cal/molK}$ ) is applied two times. This choice makes dealing with polycyclic structures feasible, since otherwise the identification of bicyclic corrections would not be unique

A tree structure was made by Paul Yelvington. The tree has only two levels. In the first level, the rings are differentiated according to number of atoms in the ring. The size of the ring is the main factor influencing the enthalpy and entropy correction to rings. The second level is basically a list with all the ring corrections available for rings of a particular size, up to ten atoms. Since corrections are not available for

all the possible rings, the first level of the tree (where the ring size is determined) receives a “typical” correction for that ring size.

### 7.3.2 Dictionary

Each of the group entries in the various trees are associated to an entry in the corresponding dictionary. In the dictionary, the chemical connectivity of the group is represented through an adjacency list. For example, the carbon atom in methanol is represented through the following adjacency lists:

<table style="border-collapse: collapse; width: 100%;"> <tr> <td style="padding: 2px 10px;">1</td> <td style="padding: 2px 10px;">*</td> <td style="padding: 2px 10px;">C</td> <td style="padding: 2px 10px;">0</td> <td style="padding: 2px 10px;">{2,S}</td> <td style="padding: 2px 10px;">{3,S}</td> <td style="padding: 2px 10px;">{4,S}</td> <td style="padding: 2px 10px;">{5,S}</td> </tr> <tr> <td style="padding: 2px 10px;">2</td> <td style="padding: 2px 10px;"></td> <td style="padding: 2px 10px;">O</td> <td style="padding: 2px 10px;">0</td> <td style="padding: 2px 10px;">{1,S}</td> <td colspan="3"></td> </tr> <tr> <td style="padding: 2px 10px;">3</td> <td style="padding: 2px 10px;"></td> <td style="padding: 2px 10px;">H</td> <td style="padding: 2px 10px;">0</td> <td style="padding: 2px 10px;">{1,S}</td> <td colspan="3"></td> </tr> <tr> <td style="padding: 2px 10px;">4</td> <td style="padding: 2px 10px;"></td> <td style="padding: 2px 10px;">H</td> <td style="padding: 2px 10px;">0</td> <td style="padding: 2px 10px;">{1,S}</td> <td colspan="3"></td> </tr> <tr> <td style="padding: 2px 10px;">5</td> <td style="padding: 2px 10px;"></td> <td style="padding: 2px 10px;">H</td> <td style="padding: 2px 10px;">0</td> <td style="padding: 2px 10px;">{1,S}</td> <td colspan="3"></td> </tr> </table>	1	*	C	0	{2,S}	{3,S}	{4,S}	{5,S}	2		O	0	{1,S}				3		H	0	{1,S}				4		H	0	{1,S}				5		H	0	{1,S}				OR	<table style="border-collapse: collapse; width: 100%;"> <tr> <td style="padding: 2px 10px;">1</td> <td style="padding: 2px 10px;">*</td> <td style="padding: 2px 10px;">Cs</td> <td style="padding: 2px 10px;">0</td> <td style="padding: 2px 10px;">{2,S}</td> </tr> <tr> <td style="padding: 2px 10px;">2</td> <td style="padding: 2px 10px;"></td> <td style="padding: 2px 10px;">O</td> <td style="padding: 2px 10px;">0</td> <td style="padding: 2px 10px;">{1,S}</td> </tr> </table>	1	*	Cs	0	{2,S}	2		O	0	{1,S}
1	*	C	0	{2,S}	{3,S}	{4,S}	{5,S}																																													
2		O	0	{1,S}																																																
3		H	0	{1,S}																																																
4		H	0	{1,S}																																																
5		H	0	{1,S}																																																
1	*	Cs	0	{2,S}																																																
2		O	0	{1,S}																																																

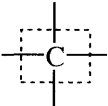
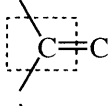
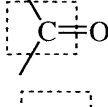

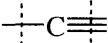
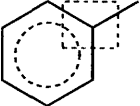
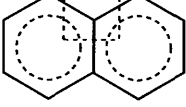
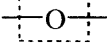
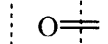
The first number in a line corresponds to the ID of the atom, the \* marks the center of the functional group, the next entry in the line indicates the atom, followed by the number of free electrons at that atom (0 for no radical, 1 for monoradicals, 2 for biradicals and so on). Finally, the information in the curly braces indicate to what other atom in the adjacency list the current atom is bonded to and through what kind of bond.

Currently RMG allows carbon, oxygen and hydrogen atoms. Additionally, functional group elements are also supported. In a functional group element, in addition to the type of element, the bonds that this element has are also specified. The Cs used in the second adjacency list for methanol is a functional group element. A list of the functional group elements implemented in RMG is shown in Table 7.2. In the adjacency list representation it is not necessary to saturate the functional group with hydrogens.

RMG recognizes single, double, triple, and benzene bonds, represented respectively by ‘S’, ‘D’, ‘T’, and ‘B’. When a new molecule is generated in RMG it is always assumed to be in the most stable conformation. However, RMG allows the user to specify whether a double bond is in a *cis*- or *trans*- conformation by entering Dcis or Dtrans in the adjacency list representation of the molecule. In the case of a *cis*



Table 7.2: Functional Group Elements (FGE) defined in RMG.

FGE	Chemical Structure	Description
Cs		Carbon with four single bonds
Cds		Carbon with two single bonds and a double bond to a carbon
CO		Carbon with two single bonds and a double bond to an oxygen
Cdd		Carbon with two double bonds
Ct		Carbon with one single bond and one triple bond
Cb		Carbon with one single bond and two benzene bonds
Cbf		Carbon with three benzene bonds
Os		Oxygen with two single bonds
Od		Oxygen with a double bond
Oa	$\uparrow\text{O}\uparrow$	Triplet oxygen
R	C/O/H	Any atom
R!H	C/O	Any non-hydrogen atom

molecule, its thermochemical properties will be calculated using the values derived for the *trans* conformation and corrected for the *cis* conformation by adding *cis* corrections. Analogously, when a biradical is formed and no criterion is given to determine whether it is a singlet or a triplet, it is assumed to be in the triplet state. However, the user can specify the multiplicity of a biradical by entering ‘2s’ or ‘2t’ for singlet and triplet states, respectively, in the adjacency list of the biradical.

As mentioned in Section 7.3.1, since the corrections are centered on two atoms, both are marked with a \* in the adjacency list, as being centers of the functional group for the correction.

In the adjacency list for the ring corrections only one of the atoms in the ring needs to be designated as the center of the ring correction functional group.

### 7.3.3 Library

For each tree, a corresponding library file was created. In the library, each functional group, identified by its unique name, is associated to thermochemical properties in Benson’s format ( $\Delta H_f^\circ$ ,  $S_{298}^\circ$  and  $C_p^\circ$  at 300, 400, 500, 600, 800, 1000, and 1500K). Every datum has been labelled with a reference, allowing the user to check the source of every value.

#### Main Groups Library

The core of the group values used in the RMG database stem from Benson [3] and Stein and Fahr [20]. Values for some additional groups were taken from the THERM database [17]. The group values for peroxides in the RMG database are those revised by Lay and Bozzelli [10]. Additionally some group values were estimated by Bozzelli, with  $S$  and  $C_p$ ’s mostly calculated through MOPAC. The RMG thermo database has also been further enriched with group values derived or updated by our research group. An example is the development of groups for ketenes, a very important class of molecules produced during the oxidation of hydrocarbon fuels, derived by Sumathi and Green using the CBS-Q method [21]. These groups consider the ketene fragment

(-C=C=O) as one entity, as is done for (-CO) in Benson's group additivity. Sumathi and Green also derived some missing groups for unsaturated hydrocarbons by using the G2 method to perform ab initio molecular orbital calculations on a series of large unsaturated hydrocarbons [22]. Finally, a consistent set of groups for oxygenated molecules was derived using the CBS-Q method [23]. These new group values were included in the RMG database, and allow the calculation of consistent thermochemical properties for alcohols, ethers, esters, hydroperoxides and alkylperoxides.

### HBI Groups Library

Lay et al. [11] calculated HBI values for the main hydrocarbon groups, while Sumathi and Green [23], Wijaya et. al [25], and Chen and Bozzelli [4] developed HBI values for oxygenated hydrocarbons. Sumathi and Green [23] provide a more comprehensive set of HBI values for radicals centered at a carbon atom, and thus their values were used. HBI values for  $\gamma$ - and  $\beta$ -hydroperoxyalkyl radicals were taken from [25]. Chen and Bozzelli's values for radicals centered at the oxygen were used [4].

HBI values for biradicals were derived from thermochemical properties published in several sources [6, 15, 18, 13, 8, 9, 12]. When data was available, differentiation between triplet and singlet states was made.

### Corrections Library

Values for the *gauche* and *cis*- correction are from Benson [3] and Wijaya et al. [25]. Ketene correction values from Sumathi and Green [21] were also included in the library. Ring corrections values were obtained from Benson [3].

## 7.4 Symmetry and Optical Isomers

The entropy of a molecule calculated by the group additivity method has to be corrected by  $-R\ln(\sigma)$ , where  $\sigma$  is the symmetry of the molecule. An algorithm for the determination of the symmetry in molecules was developed and is described in Appendix A.

The entropy calculated for chiral molecules has to be corrected by  $R\ln(2)$  to account for the two optical isomers. In RMG, molecules that have a Cs group bonded to four different branches are assumed to have two optical isomers. Although this rule is generally valid, it is not always true for rings. Asymmetric peroxides ( $R_1OOR_2$ ) also exhibit optical isomerism, and RMG recognizes.

## 7.5 Conclusions

The database of thermochemical properties for the Benson's group additivity method was organized as a tree structure. A tree structure takes advantage of the chemical logic behind the group values, being much more efficient than a list. In a tree structure, groups that are similar to each other are naturally grouped together. It is easy to add new group values and to extend the database. Moreover, nodes for which no data are available were assigned the value of a similar node, and thus RMG can estimate the thermochemical properties of any molecule.

Bibliography

# Bibliography

- [1] T. L. Allen. Bond energies and the interactions between next-nearest neighbors. I. Saturated hydrocarbons, diamond, sulfanes,  $S_8$ , and organic sulfur compounds. *The Journal of Chemical Physics*, 31(4):1039–1049, 1959.
- [2] B. Balaraju, B. K. Harrison, K. R. Mudalier, and A. Viswaanathan. Chetah The ASTM computer program for chemical thermodynamic and energy release evaluation, 2001.
- [3] S. W. Benson. *Thermochemical Kinetics*. John Wiley & Sons, New York, 2<sup>nd</sup> edition, 1976.
- [4] C.-J. Chen and J. W. Bozzelli. Analysis of tertiary butyl radical +  $O_2$ , isobutene +  $HO_2$ , isobutene + OH, and isobutene-OH adducts +  $O_2$ : A detailed tertiary butyl oxidation mechanism. *Journal of Physical Chemistry A*, 103(48):9731–9769, 1999.
- [5] N. Cohen and S. W. Benson. Estimation of heats of formation of organic-compounds by additivity methods. *Chemical Reviews*, 93(7):2419–2438, 1993.
- [6] K. M. Ervin, S. Gronert, S. E. Barlow, M. K. Gilles, A. G. Harrison, V. M. Bierbaum, C. H. DePuy, W. C. Lineberger, and G. B. Ellison. Bond strengths of ethylene and acetylene. *Journal of the American Chemical Society*, 112:5750–5759, 1990.
- [7] Y. Hidaka, T. Nishimori, K. Sato, Y. Henmi, R. Okuda, and K. Inami. Shock-tube and modeling study of ethylene pyrolysis and oxidation. *Combustion and Flame*, 117(4):755–776, 1999.
- [8] R. Janoschek and M. J. Rossi. Thermochemical properties of free radicals from G3MP2B3 calculations. *International Journal of Chemical Kinetics*, 34(9):550–560, 2002.
- [9] G.-S. Kim, T. L. Nguyen, A. M. Mebel, S. H. Lin, and M. T. Nguyen. Ab initio/RRKM study of the potential energy surface of triplet ethylene and product branching ratios of the  $C(^3P) + CH_4$  reaction. *Journal of Physical Chemistry A*, 107(11):1788–1796, 2003.

- [10] T. H. Lay and J. W. Bozzelli. Enthalpies of formation and group additivity of alkyl peroxides and trioxides. *Journal of Physical Chemistry A*, 101(49):9505–9510, 1997.
- [11] T. H. Lay, J. W. Bozzelli, A. M. Dean, and E. R. Ritter. Hydrogen atom bond increments for calculation of thermodynamic properties of hydrocarbon radical species. *Journal of Physical Chemistry*, 99(39):14514–14527, 1995.
- [12] P. J. Linstrom and W. G. Mallard, editors. *NIST Chemistry WebBook*, volume Number 69 of *NIST Standard Reference Database*. National Institute of Standards and Technology, Gaithersburg MD, 20899 (<http://webbook.nist.gov>), March 2003.
- [13] T. L. Nguyen, G.-S. Kim, A. M. Mebel, and M. T. Nguyen. A theoretical re-evaluation of the heat of formation of phenylcarbene. *Chemical Physics Letters*, 349(5,6):571–577, 2001.
- [14] J. B. Pedley, R. D. Naylor, and S. P. Kirby. *Thermochemical Data of Organic Compounds*. Chapman and Hall, London, 2<sup>nd</sup> edition, 1986.
- [15] J. C. Poutsma, J. J. Nash, J. A. Paulino, and R. R. Squires. Absolute heats of formation of phenylcarbene and vinylcarbene. *Journal of the American Chemical Society*, 119(20):4686–4697, 1997.
- [16] R. C. Reid, J. M. Prausnitz, and B. E. Poling. *The Properties of Gases and Liquids*. McGraw-Hill, New York, 4<sup>th</sup> edition, 1987.
- [17] E. R. Ritter and J. W. Bozzelli. Thermodynamic property estimation for radicals and molecules, 1987.
- [18] C. A. Schalley, S. Blanksby, J. N. Harvey, D. Schroeder, W. Zummack, J. H. Bowie, and H. Schwarz. A combined neutralization-reionization mass spectrometric and theoretical study of oxyallyl and other elusive[C<sub>3</sub>H<sub>4</sub>, $\emptyset$ ] neutrals. *European Journal of Organic Chemistry*, (6):987–1009, 1998.
- [19] J. Song. *Building Robust Chemical Reaction Mechanisms: Next Generation of Automatic Model Construction Software*. Phd thesis, Massachusetts Institute of Technology, 2004.
- [20] S. E. Stein and A. Fahr. High-temperature stabilities of hydrocarbons. *Journal of Physical Chemistry*, 89:3714–3725, 1985.
- [21] R. Sumathi and W. H. Green. Thermodynamic properties of ketenes: Group additivity values from quantum chemical calculations. *Journal of Physical Chemistry A*, 106:7937–7949, 2002.
- [22] R. Sumathi and W. H. Green Jr. Missing thermochemical groups for large unsaturated hydrocarbons: Contrasting predictions of G2 and CBS-Q. *Journal of Physical Chemistry A*, 106(46):11141–11149, 2002.

- [23] R. Sumathi and W. H. Green Jr. Oxygenate, oxyalkyl and alkoxy carbonyl thermochemistry and rates for hydrogen abstraction from oxygenates. *Physical Chemistry Chemical Physics*, 5(16):3402–3417, 2003.
- [24] T.-P. Thinh, J.-L. Duran, and R. S. Ramalho. Estimation of ideal gas heat capacities of hydrocarbons from group contribution techniques. New and accurate approach. *Industrial & engineering chemistry process design and development*, 10(4):576–582, 1971.
- [25] C. D. Wijaya, R. Sumathi, and W. H. Green Jr. Thermodynamics properties and kinetic parameters for cyclic ether formation from hydroperoxyalkyl radicals. *Journal of Physical Chemistry A*, 107:4908–4920, 2003.
- [26] Y. Yoneda. An estimation of the thermodynamic properties of organic compounds in the ideal gas state. i. acyclic compounds and cyclic compounds with a ring of cyclopentane, cyclohexane, benzene, or naphthalene. *Bulletin of the Chemical Society of Japan*, 52(5):1297–1314, 1979.





# Chapter 8

## BCGA in RMG

### 8.1 Introduction

The bond-centered group additivity method presented in this work has been implemented into a software. This implementation allows the estimation of the thermochemical properties of PAH molecules by simply giving their chemical structure. The software is integrated to RMG, the chemical reaction mechanism generator software developed by in our group by Dr. Jing Song [2]. Users of RMG will be able to generate kinetic mechanisms that include PAH molecules with thermochemical properties calculated through the bend-centered group additivity method presented in this work.

In implementing the bond-centered group additivity method into RMG, care has been taken to maintain the object oriented structure of the software.

### 8.2 RMG- Chemical Reaction Mechanism Generator Software

RMG has been developed to automatically generate large-scale chemical reaction mechanism for complex reaction systems [2]. It was thoughtfully designed using object oriented technology, making reusability and extendability of the software very easy.

RMG is composed of seven packages, each providing one functionality to the program. For example, the **rxn** package handles the generation of all possible reactions from a given set of species, following the reaction rules defined in the reaction families. Here we will describe briefly the **chemUtil** and the **chem** packages, since they are used to estimate thermochemical properties. For a more detailed description of these and the other packages and of the design of RMG, please refer to the thesis by Dr. Jing Song [2].

### 8.2.1 RMG Packages Relevant to this Work

The **chemUtil** package provides objects for organizing the data as a *tree* and to represent chemical structures as *graphs*. A graph is composed of nodes and arcs. In the **chemUtil** package, arcs, nodes and graphs are each modelled as a class. The *Graph* class has as attributes a collection of arcs and a collection of nodes. Both the *Arc* and the *Node* classes inherit from the *GraphComponent* class, which models the similarities between arcs and nodes. For example, both arcs and nodes have a collection of neighbors, and both have an element that define the type of arc or node stored in the object. The *Graph* class provides methods for testing graph equivalence and for matching of sub-graphs. This last method is the nucleus of the implementation of any additivity estimation scheme, since it allows the identification of each of the groups that compose the molecule.

The *Tree* class allows the organization of the data in the form of a tree. A tree has a root node that has no parent. Every other node in the tree has a parent node, and the root node is an ancestor of all the other nodes in the tree. Each child node is more specific than its father node and sibling nodes are disjoint from each other. For example, the atom-centered groups for the estimation of the thermo of the aliphatic molecules is organized as a tree. The root node is 'R!H', that is, any atom, except for hydrogen. The children of the root node are the 'C' and the 'O' nodes and so on (see Chapter 7).

The second package involved in the estimation of thermochemical properties is the **chem** package. While the **chemUtil** package deals with the handling of data

structures, and thus is based solely on graph theory, the **chem** package couples the graph theoretical representation of molecules with their chemical properties. The *ChemGraph* class gives chemical meaning to a graph. It is composed of atoms and bonds (as opposed to nodes and arcs). Additionally, since *ChemGraph* represents molecules, it has thermochemical properties. Another chemical structure present in the **chem** package is the *FunctionalGroup* class. A *FunctionalGroup* represents a structural pattern that has a well determined chemical behavior. For example, in reacting systems multiple bonds (double or triple) behave similarly when attacked by radicals. From the thermochemistry standpoint, *FunctionalGroup* corresponds to the atom- or bond-centered groups. Once a *ChemGraph* is read or generated in RMG, each of its atoms is categorized into a functional group element, (*FGElement*). The *FGElement* class defines not only the atom type, but also the types of bonds through which it is connected. RMG currently specifies 12 types of functional group elements (see Table 7.2). For example, the ‘Cb’ functional group is defined as a carbon atom with two benzene bonds and one single bond, whereas the ‘Cbf’ group is defined as a carbon atom with three benzene bonds. The functional group elements should be disjoint from each other and their union should cover all the possible types of carbon in the C/O/H system. Consequently, it should be possible to assign one unique functional group element to every carbon or oxygen atom in a molecule. The introduction of the *FGElement* class simplifies and speeds up the definition of *FunctionalGroup*. Both *ChemGraphs* and *FunctionalGroups* are represented through an adjacency list (see Chapter 7).

Every time a new *ChemGraph* object is created, it calls the *GeneralGAPP* interface to generate its thermochemical properties. These properties are stored in the *ThermoData* class. Moreover, the *ThermoData* class can calculate the thermochemical properties of its corresponding *ChemGraph* at any temperature.

The interface *GeneralGAPP* specifies only one method: the method to generate the thermo data. Currently, the class that implements this method is the *GATP* class. In the following sections we will present the highlights of the *GATP* class and then discuss in more detail the new thermo estimator class that implements the

bond-centered group additivity method presented in this work.

### 8.3 GATP

Currently the method to generate thermo data (`generateThermoData(ChemGraph)`) is implemented in the *GATP* class. Atom-centered group additivity is used for all molecules. The library for the thermo estimator constitutes another class, the *ThermoGAGroupLibrary* class. This class is a composition of the *GATP* class. This means that when a *GATP* object is created for the calculation of the thermo properties of a *ChemGraph*, the *ThermoGAGroupLibrary* is initialized. When the *GATP* is no longer needed, the *ThermoGAGroupLibrary* is also destroyed. Moreover, the *ThermoGAGroupLibrary* class is a singleton, meaning that at each time, there is only one instance of this class. Even though the *GATP* class might be called several times to estimate the thermochemical properties of different *ChemGraphs*, they all use the same thermo library.

As outlined in Dr. Jing Song's PhD Thesis [2], the `generateThermoData(ChemGraph)` function is composed of the following main steps:

- i. If *ChemGraph* is a free radical, add hydrogen(s) to obtain the corresponding stable molecule;
- ii. Make a list of the heavy atoms in the stable molecule;
- iii. Search the *ThermoGAGroupLibrary* for the group values of each heavy atom;
- iv. Sum the group contributions found in step 3 into a *ThermoData* object;
- v. If *ChemGraph* is a free radical, find proper HBI radical group in *ThermoGAGroupLibrary* and add HBI correction to *ThermoData*;
- vi. Make the symmetry correction to the entropy;
- vii. Add ring correction to *ThermoData*, if any;
- viii. Add other correction to *ThermoData*, if any;
- ix. Return *ThermoData*.

## 8.4 The bondGroups Package

The Bond-Centered Group Additivity method is implemented in RMG as a new package, called **bondGroups**. The **bondGroups** package is composed of two classes, *BGATP* and *BGThermoLibrary*. The *BGATP* class implements the `generateThermoData(ChemGraph)` method from the *GeneralGAPP* interface.

*BGATP* calculates the thermochemical properties of PAHs using the Bond-Centered Group Additivity method and calls *GATP* to calculate the thermo of non-aromatic molecules. If a molecule is composed of both aromatic and non-aromatic parts, *BGATP* first separates the molecule into a non-aromatic part and an aromatic part. The thermochemistry of the non-aromatic part of the molecule is calculated by *GATP*. *BGATP* calculates the thermo of the aromatic part and sums the thermochemistry of both parts to obtain the thermochemistry of the entire molecule. The UML (unified modelling language) design diagram for the thermo property estimator in RMG is shown in Figure 8-1. The steps included in the *BGATP* implementation of the `generateThermoData(ChemGraph)` method are as follows:

- i. Determine whether the molecule has an aromatic part or not.
- ii. If the molecule has both aromatic and non aromatic parts, separate the molecule into parts that are composed of only aromatic rings and parts that are composed of only non-aromatic parts. Call `BGATP.generateThermoData(ChemGraph)` for each of the separated parts.
- iii. Else if the molecule is purely aromatic, compute its thermochemistry and add it to *ThermoData*. No symmetry correction to the entropy is made yet.
- iv. Else (the molecule is not aromatic) call *GATP* to calculate its thermochemical properties and add it to *ThermoData*. *GATP* returns the entropy with symmetry correction for the non-aromatic part only. Add  $R \ln(\sigma_{NOTarom})$  to this symmetry to obtain  $S_{int}^{\circ}$ , where  $\sigma_{NOTarom}$  is the symmetry number of the non-aromatic molecule.
- v. Make the symmetry correction to the entropy,  $S_{298}^{\circ} = S_{int}^{\circ} R \ln(\sigma)$ , where  $\sigma$  is the symmetry number of the entire molecule
- vi. Return *ThermoData*.

The symmetry number for aromatic molecules is calculated through an algorithm developed by Sally Petway, and is described in Appendix A.

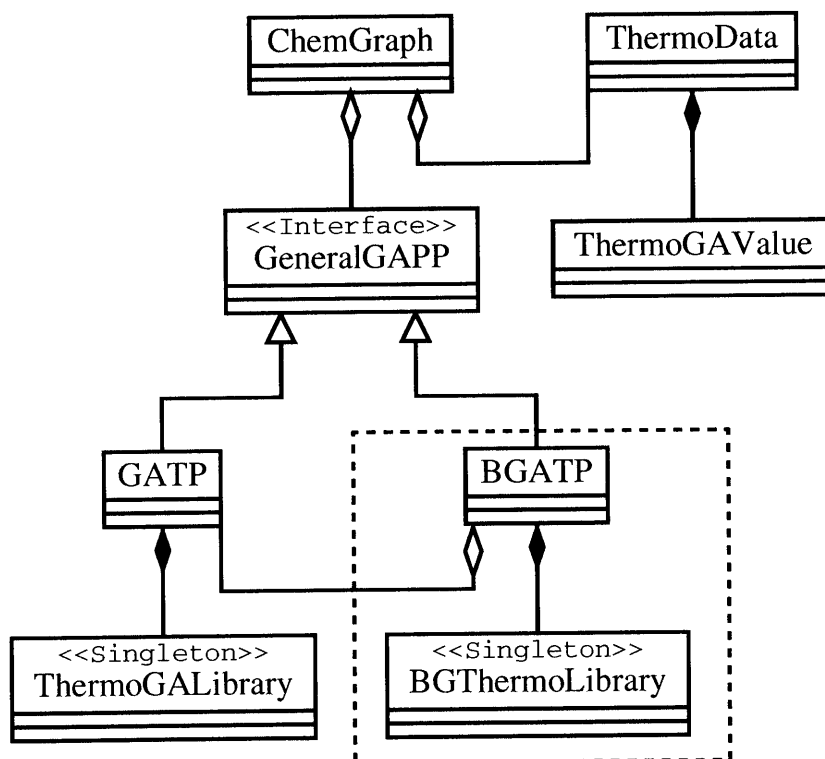


Figure 8-1: UML design diagram for the thermo estimator in RMG. This diagram shows the relation between the classes involved in the estimation of the thermochemical properties. The classes included in the hashed boundary were developed in this work. For an explanation of UML symbols, refer to [1].

If a  $\sigma$ -radical site is at the aromatic part of the molecule, the calculation of the appropriate correction is included in step 3 in a similar way as described in Section 8.3.  **$\pi$ -radicals are treated as molecules with both an aromatic part and a non-aromatic part.**

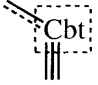
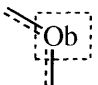
In order to use the Bond-Centered Group Additivity method for PAHs, the *BGATP* has to be selected as the default thermo estimator. This choice is made in the `ChemGraph.generateThermoData()` method.

### 8.4.1 New Functional Group Elements

RMG originally defined 12 functional group elements, as shown in Table 7.2. In each functional group element, the bonds of the central atom are completely defined. Every atom belonging to a molecule should be categorized into one of these functional group elements.

In order to describe PAHs containing furan and or benzyne structures, it was necessary to introduce two new functional groups: ‘Ob’ and ‘Cbt’, as shown in Table 8.1. The ‘Ob’ functional group element represents an oxygen atom that is bonded through two benzene bonds. The ‘Cbt’ functional group element represents a carbon atom that is bonded through a benzene bond and through a triple bond.

Table 8.1: New Functional Group Elements defined in RMG. These new FGE allow the description of aromatic molecules containing furan rings and triple bonds.

FGE	Chemical Structure	Description
Cbt		Carbon one triple bond and one benzene bond
Ob		Oxygen with two benzene bonds

## 8.4.2 Organization of the Database

As in the atom-centered groups thermochemical database (see Section 7.3.1), the database for the bond-centered group additivity method is composed of three files: the tree, the dictionary and the library.

The dictionary file defines each group through a unique string name and an adjacency list. The tree file specifies the tree structure in which the bond-centered groups are organized. The root node of this tree is a bond in an aromatic ring. In the first level the atom types to which this bond is connected are specified (C-C or C-O) and so on. Finally, the library associates each group to its thermochemical values.

The representation of each bond-centered group as an adjacency list is not straightforward. In the following discussion we will use the notation for aromatic atom-centered groups introduced in Section 3.2.1. While there is a one to one correspondence between the ‘A’ atom-centered group and the ‘Cb’ functional group element, the atom-centered groups ‘B’, ‘C’, and ‘D’ all correspond to the ‘Cbf’ functional group element. The ‘B’ atom-centered group can be easily characterized because it is always bonded to two ‘Cb’ and one ‘Cbf’ functional group element. However, the ‘C’ atom-centered group can be bonded to either one ‘Cb’ and two ‘Cbf’ or to three ‘Cbf’ functional group elements. What differentiates the ‘C’ and the ‘D’ atom-centered groups is the number of rings to which they belong. The first belongs to two rings only, whereas the latter belongs to three. For example, the only difference in the bonds shown in bold Figure 8-2 is that the ‘CC6’ bond belongs to one ring only and the ‘DD6666’ bond belongs to two rings. The adjacency list for these two bonds encompassed by the hashed rectangle is exactly the same. There is no easy way to identify the difference between these two bond-groups in RMG.

To overcome this difficulty, the children of a node in the tree were organized as a LinkedList, and not as a HashSet, as was originally the case in RMG. This choice means that the order in which the nodes are organized in the database does matter. The nodes that come first are read (and matched) first. In the case of bonds ‘CC6’ and ‘DD6666’, the adjacency lists for these bonds represent the structures shown



in Figure 8-3. Note that the adjacency list representation for bond ‘CC6’ would also match the bond-group ‘DD6666’, but the reverse is not true. Thus the bond ‘DD6666’ comes first in the database. The bond-centered groups database has been carefully designed so that the correct bond-group is matched. In general, the bonds that contain the ‘D’ atom centered group come first. Unlike in the atom-centered groups database, here the order in which the nodes of the tree appear in the database matters.

All the possible representations of each bond-centered group were explicitly included in the database. For example, four different adjacency lists represent the ‘CC66’ bond-group, as shown in Figure 8-4. Values were assigned only to the first entry in the library. The values of the subsequent bond-centered groups that actually represent the same group refer to the value of the first entry.

## 8.5 Identification of Aromaticity

When a kinetic mechanism is generated automatically, aromatic molecules are formed from the reaction of non-aromatic molecules. Thus, in order to automatically generate PAH formation and growth mechanisms it is crucial for RMG to have the capability to identify as aromatic, rings that are actually aromatic, but are represented by single and double (or triple) bonds.

This capability has been implemented in the `ChemGraph.makeAromatic()` method. This method is called every time a cyclic `ChemGraph` is formed, before its thermochemical properties are calculated. It identifies ring structures that have more than one possible Kekulé structure as being aromatic. Moreover, some structures, such as the furan ring, that only have one Kekulé structure but are considered to be aromatic in the BCGA method are also identified as aromatic. The library “aromaticStructure” stores these structures. The pseudo-code for the `ChemGraph.makeAromatic()` method is as follows:

- i. For each ring structure *rStruc* in the molecule, test if any of the structures stored in the “aromaticStructure” library is a subgraph of *rStruc*. If it is a

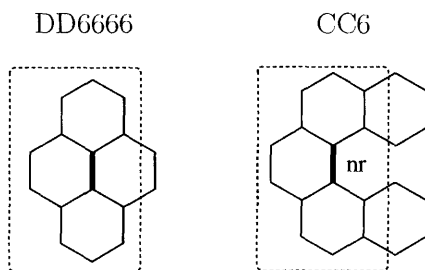


Figure 8-2: In this case, the only difference between the CC6 and the DD6666 group lies on whether the bond in question belongs to two rings or to one ring only.

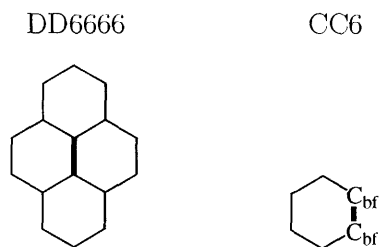


Figure 8-3: Adjacency list representation for the CC6 and DD6666 groups

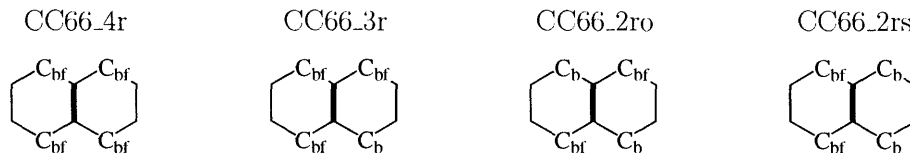


Figure 8-4: Adjacency list representation of all the 'CC66' bond-groups. Each of these bond groups is explicitly included in the database

- subgraph, transform all the single and double bonds in that subgraph to benzene bonds;
- ii. Make a list *aromNodes* of all the nodes in the *rStruc* that could actually be in an aromatic ring;
  - iii. Check if the part of the *rStruc* that is formed by the nodes in *aromNodes* has more than one Kekulé structure (*K*);
  - iv. If  $K > 1$ , then the nodes in *aromNodes* are indeed part of an aromatic ring. All the bonds connecting these nodes are set to benzene bonds.

The nodes that could actually be aromatic are those that have the following Functional Group Elements: 'Cd', 'Ct', 'Cb', 'Cbf', and 'Cbt'. The method described here correctly identifies the aromaticity of the ChemGraphs shown in Figure 8-5.

## 8.6 Conclusions

The bond-centered group additivity method has been successfully implemented into RMG. RMG now has the capability of using this method to calculate the thermochemical properties of PAHs with five- and six-membered rings, containing furan and benzyne structures, as well as of molecules containing both aromatic and non-aromatic parts. The estimation method for unsubstituted  $\pi$ -radicals has not been implemented into RMG yet.

RMG is now also able to correctly identify ring structures that are represented through alternating single and double (or triple) bonds as aromatic. This capability allows the generation of kinetic mechanisms containing reactions in which aromatic molecules are formed from non-aromatic molecules.

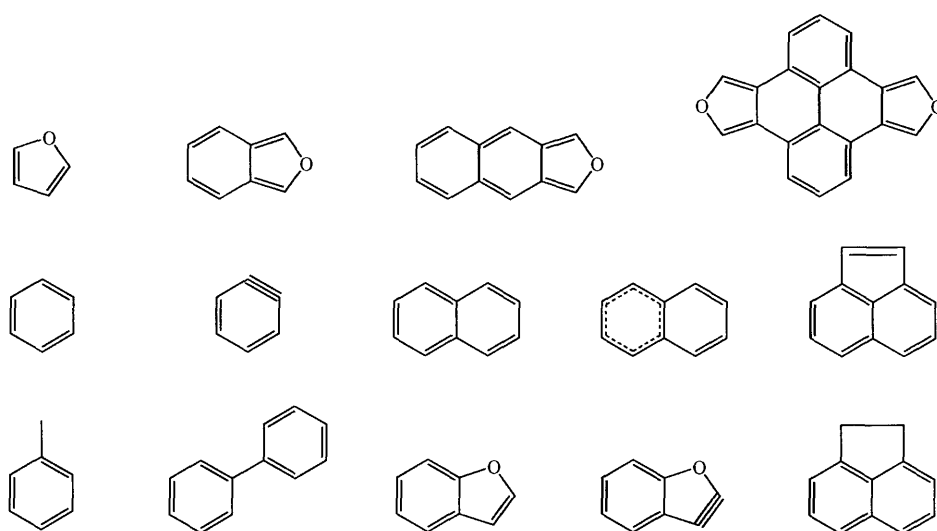


Figure 8-5: These ChemGraphs are correctly identified by the ChemGraph.makeAromatic() method as being aromatic. The dotted lines indicate benzene bonds.

# Bibliography

- [1] M. Fowler. *UML Distilled - A Brief Guide to the Standard Object Modeling Language*. Addison-Wesley, Boston, 3<sup>rd</sup> edition, 2004.
- [2] J. Song. *Building Robust Chemical Reaction Mechanisms: Next Generation of Automatic Model Construction Software*. Phd thesis, Massachusetts Institute of Technology, 2004.



# Chapter 9

## Equilibrium Calculations

### 9.1 Introduction

In order to describe the chemistry of a combustion system, both kinetic rate parameters for the important reactions and self-consistent thermochemical properties of the species involved are essential. Yet, it is possible to draw interesting conclusions from thermochemical properties alone.

At infinite time, any reacting system will reach thermodynamic equilibrium, where the Gibbs free energy of the system is minimized. However, most systems are kinetically constrained, i.e., reaction pathways that lead to very stable products might have very high activation barriers, and thus be very slow. By studying the concentrations of a system at global thermodynamic equilibrium, it is possible to identify which aspects of the experimental observations are due to the thermochemistry of the species and which are not (and thus are determined by kinetics).

### 9.2 Global Equilibrium Calculations

Equilibrium calculations were performed in collaboration with Dr. Henning Richter using the Equil application from Chemkin [8]. The Gibbs free energy is minimized for a given temperature, pressure, initial concentration of the reactants (which fixes the C/O/H ratios) and products allowed in the final condition. Almost 300 species

were included in the calculations, roughly half of which were polycyclic aromatic hydrocarbons. Up to ovalene, the  $\Delta H_f^\circ$  of the PAHs included in this study correspond to the  $\Delta H_{f,\text{homo}}^\circ$  described in Chapters 3 to 5. The  $S_{298}^\circ$  and  $C_p^\circ$  used are the ones calculated from B3LYP/6-31G(d). The thermochemical properties of the three PAHs larger than ovalene included in this study (see Figure 9-1) were calculated through the BCGA method presented in Chapter 3.  $C_{60}$ ,  $C_{70}$ ,  $C_{76}$ ,  $C_{78}$ ,  $C_{80}$ ,  $C_{82}$ , and  $C_{84}$  fullerenes were also included in this study. The  $\Delta H_f^\circ$  calculated by Cioslowski using B3LYP/6-31G(d) and homodesmotic reactions with  $C_{60}$  as a reference molecule were adopted [3]. The  $S_{298}^\circ$  and  $C_p^\circ$  were calculated using the BCGA method. The thermochemical properties for the smaller species were adopted as described in [11]. A complete list of the species included in this study and the thermochemical properties used can be found in Appendix E.1.

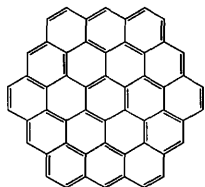
Each equilibrium calculation was done for one fuel, at fixed temperature and pressure. Benzene was used as the fuel for most of the calculations. The fuel to air ratio ( $\phi$ ) was varied from 1.6 to 10 the temperature ranged from 300 to 4000 K, and the pressure was set to either 20 Torr or 1 atm.

## 9.3 Results and Discussion

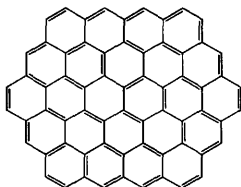
### 9.3.1 Sensitivity to the Thermochemical Properties

The equilibrium concentrations of individual species are very dependent on the assumed thermo. A few kcal mol<sup>-1</sup> difference in  $\Delta G$  corresponds to order of magnitude

Circumcoronene ( $C_{54}H_{18}$ )



$C_{60}H_{20}$



$C_{80}H_{22}$

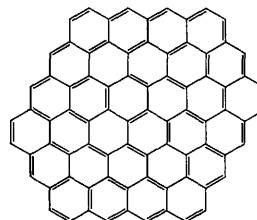


Figure 9-1: PAHs larger than ovalene included in the equilibrium study.



changes in the concentration. However, the overall semi-quantitative conclusions that can be drawn from equilibrium calculations are very robust. This robustness is shown here by comparing the effect of using two different  $\Delta H_f^\circ$  values for  $C_{60}$  in the equilibrium calculations.

Cioslowski adopted a  $\Delta H_{f,\text{exp}}^\circ$  of  $C_{60}$  of 618 kcal mol<sup>-1</sup> [3]. More recently Diky and Kabo recommended a value of 604 kcal mol<sup>-1</sup> based on the analysis of many published data [4]. The equilibrium concentrations of the fullerenes when each of the  $\Delta H_f^\circ$  for  $C_{60}$  is used is shown in Figure 9-2. The concentration of the other fullerenes are practically not affected by the different  $\Delta H_f^\circ$  of  $C_{60}$ . However, the concentration of the latter increases by almost two orders of magnitude when a 14 kcal mol<sup>-1</sup> lower  $\Delta H_f^\circ$  is used. Thus, accurate quantitative calculations of equilibrium concentrations of individual species require that the relative thermochemistry of the species involved be well known. However, we expect that overall trends do not depend that heavily on accurate thermochemistry. For example, the overall concentration of fullerenes is not affected by the different  $\Delta H_f^\circ$  at all. For all the other calculations described here a 618 kcal mol<sup>-1</sup>  $\Delta H_f^\circ$  value for  $C_{60}$  was used.

### 9.3.2 Sooting Limits

Experimentally one observes soot formation for a middle temperature range and only above a critical  $\phi$  value. The higher temperature sooting limit boundary is attributed to thermodynamic constraints, whereas the lower temperature boundary is attributed to kinetic limitations. This soot formation region is thought to be pretty much independent of fuel type [2]. Kamimoto and Bae determined the soot formation region for toluene at 5 atm in a combustion bomb for C/O ratios up to 2.0 [7]. They found the high-temperature boundary for the soot formation region at these conditions to be around 2600K. The same was observed by Akihama et al. in modelling studies of combustion in a diesel engine cylinder [2].

Table 9.1 provides the equivalence between  $\phi$  and C/O ratio for benzene.  $\phi = 1$  is defined as the stoichiometric ratio between the fuel and  $O_2$  necessary for the complete combustion to  $CO_2$  and  $H_2O$ .

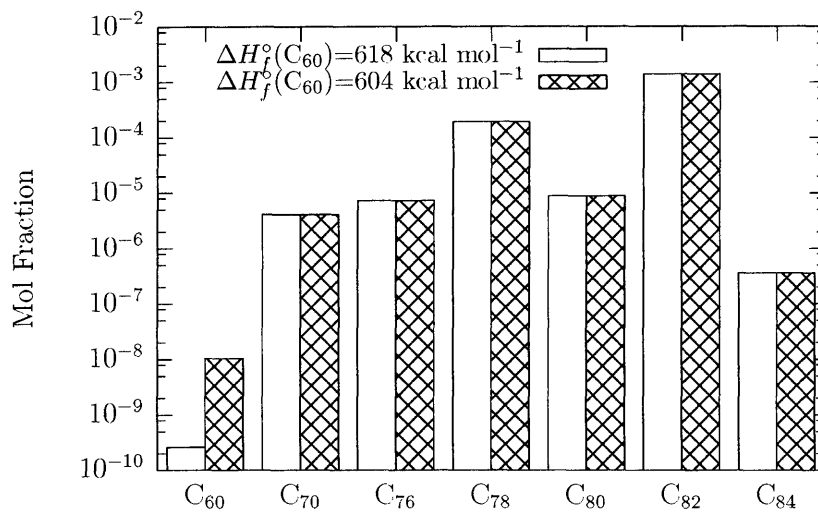


Figure 9-2: Effect of different values of  $\Delta H_f^\circ$  of  $\text{C}_{60}$  on the equilibrium concentrations of fullerenes. Fuel: benzene,  $\phi = 3.5$ , 30% Ar, 2200 K, 20 Torr.

Table 9.1: Relation between  $\phi$  and C/O for benzene.  $\phi = 1$  is defined as the stoichiometric ratio between the fuel and  $\text{O}_2$  necessary for the complete combustion to  $\text{CO}_2$  and  $\text{H}_2\text{O}$ .

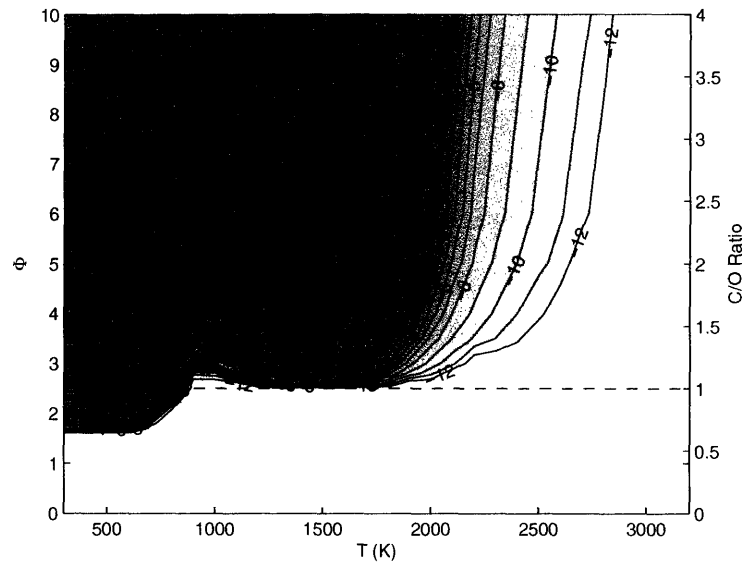
$\phi$	C/O ratio
1.0	0.40
1.6	0.64
1.7	0.68
1.8	0.72
2.0	0.80
2.5	1.00
2.8	1.12
3.0	1.20
3.5	1.40
4.0	1.60
5.0	2.00
6.0	2.40
10.0	4.00

The distinction between large PAHs and soot is not very clear. In this exploratory study of sooting limits, we consider significant concentrations of PAHs at equilibrium to be an indication of “soot”, where PAHs are all the aromatic species with more than two rings. We are assuming that soot has a similar  $\Delta G$  per carbon and C/H ratio as large PAHs (very young soot particles are known to have a C/H ratio of 3 [6]). Thus if the equilibria strongly disfavor PAHs, it will probably also disfavor soot. Fullerenes were not included in these equilibrium calculations.

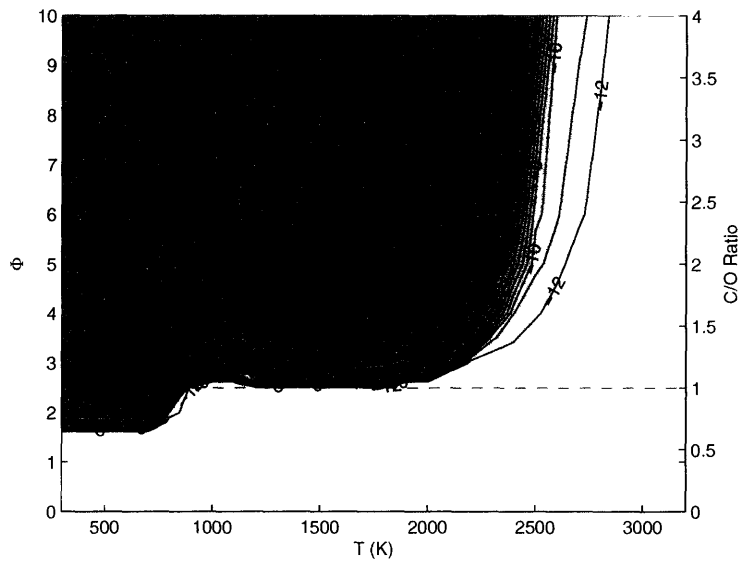
Figures 9-3(a) and 9-3(b) show the equilibrium concentrations of PAHs as a function of temperature and  $\phi$  for benzene as fuel and 1atm. The corresponding C/O ratios are given in the secondary y-axis. Calculations were performed including PAHs up to ovalene only (Figure 9-3(a)) and including the three large PAHs of Figure 9-1 (Figure 9-3(b)). The high temperature boundary for soot formation is present, but equilibrium calculations predict that PAHs are also stable at lower temperatures. Thus the high-temperature boundary of the sooting region is indeed due to thermodynamic stability, while the low temperature boundary must be a kinetic limitation.

The sooting limit region does not change considerably depending on whether the three large PAHs are included or not in the equilibrium calculations. One observes that the high-temperature sooting limit becomes sharper when the larger PAHs are included, because the larger PAHs are more stable at higher temperatures. In both cases the high-temperature boundary of the sooting limit is around 2700K, in good agreement with the experimental and modelling results discussed previously. This is a very encouraging finding, indicating that equilibrium calculations using sensible thermodynamics have the potential to predict the high-temperature sooting limit boundary.

It has frequently been stated that at equilibrium the critical C/O ratio should be 1 [15, 5]. The logic behind this belief is that as long as there is enough oxygen to form CO, no soot would be formed at equilibrium. Thus Wright and others concluded that flames are not at equilibrium, because experimentally, soot is observed at C/O ratios smaller than 1 [14, 15]. In the equilibrium studies performed here, we indeed observe a clear “sooting limit” at C/O = 1.0 for flame temperatures. Equilibrium



(a) Including PAHs up to ovalene only



(b) Including the three PAHs of Figure 9-1

Figure 9-3: Sooting limit predictions. The plots show equilibrium concentrations of PAHs as a function of temperature and  $\phi$  (C/O ratio on the secondary y-axis). The concentrations are in log scale. Benzene is used as fuel, calculations were done for 1atm.

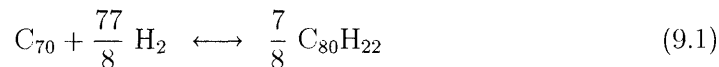
calculations using methane and ethylene as fuels also resulted in critical C/O ratio of 1. However, it is still too precipitate to conclude that flames are not at equilibrium. The local C/O ratio of a flame should be taken account, and not the C/O ratio at the inlet of the burner, even in premixed flames. Diffusion effects have been shown to increase the local C/O ratio of premixed flames up to 25% [9]. Moreover, very close to the burner, when the fuel oxidation begins, oxygen gets trapped as CO and CO<sub>2</sub>, so that further down in the flame, when PAH formation and growth occur, the actual local C/O ratio is probably higher than at the burner. Thus, it is possible that when soot formation is observed, the actual C/O ratio is higher than 1.

### 9.3.3 Fullerenes versus PAHs

In Figure 9-4 the equilibrium concentrations of PAHs and fullerenes are shown as a function of  $\phi$  and temperature. One notes that at 1atm fullerenes are thermodynamically stable only for  $\phi \geq 2.5$  (C/O $\geq$ 1). Thus as there is a clear “sooting limit” for the formation of PAHs, the same limit is also valid for fullerenes.

At equilibrium, fullerenes and PAHs are present at markedly different temperatures. While PAHs are present at lower temperatures, at higher temperatures fullerenes are more stable. This behavior has been observed experimentally for benzene flames [10].

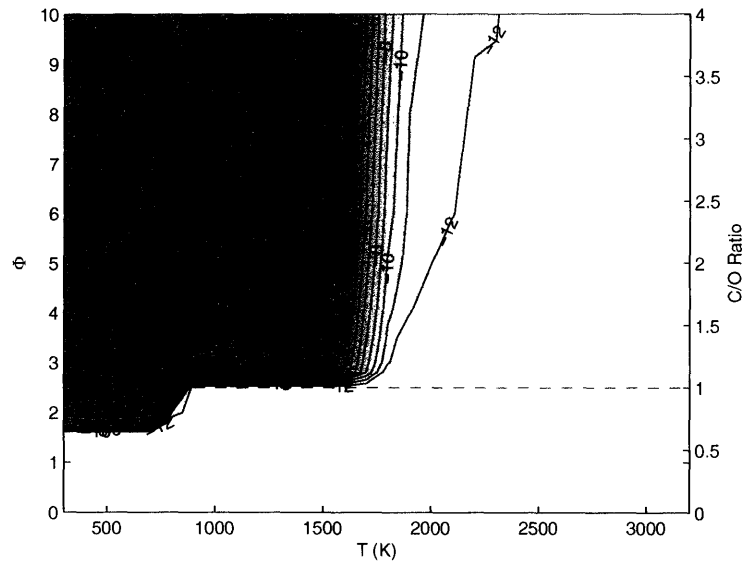
The equilibrium between fullerenes, large PAHs and H<sub>2</sub> seems to explain this sudden shift in the stability of fullerenes and PAHs. Figure 9-5 shows a plot of the equilibrium constant ( $K_{eq}$ ) for hypothetical reactions involving a prototype fullerene (C<sub>70</sub>), H<sub>2</sub>, and the largest PAH included in this study, C<sub>80</sub>H<sub>22</sub>:



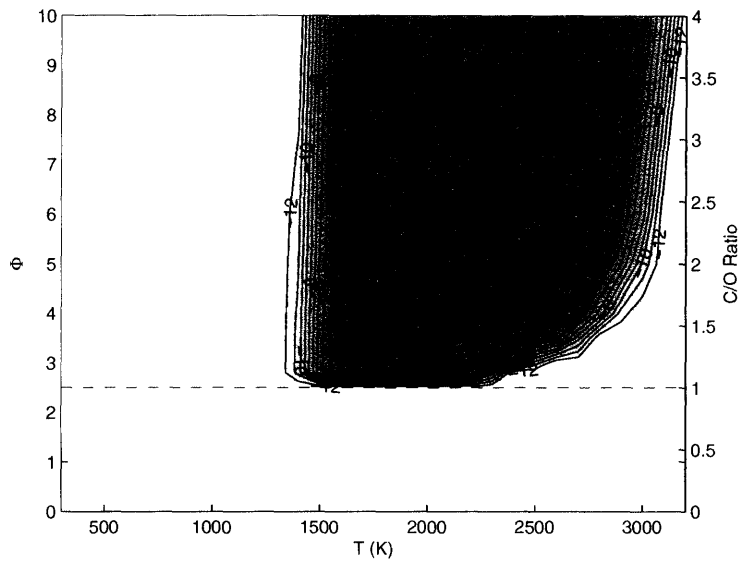
where ( $K_{eq}$ ) is given by:

$$K_{eq} = \exp\left(-\frac{\Delta G^\circ}{RT}\right) \quad (9.2)$$

The temperature at which the  $K_{eq}$  for the largest PAH included in this study is equal



(a) PAH



(b) Fullerenes

Figure 9-4: Equilibrium concentrations of PAHs and fullerenes as a function of temperature and  $\phi$ . The concentrations are in log scale. Benzene is used as fuel, calculations were done for 1atm. PAHs are not formed at  $\phi < 1.7$  and fullerenes are not formed for  $\phi < 2.5$ .

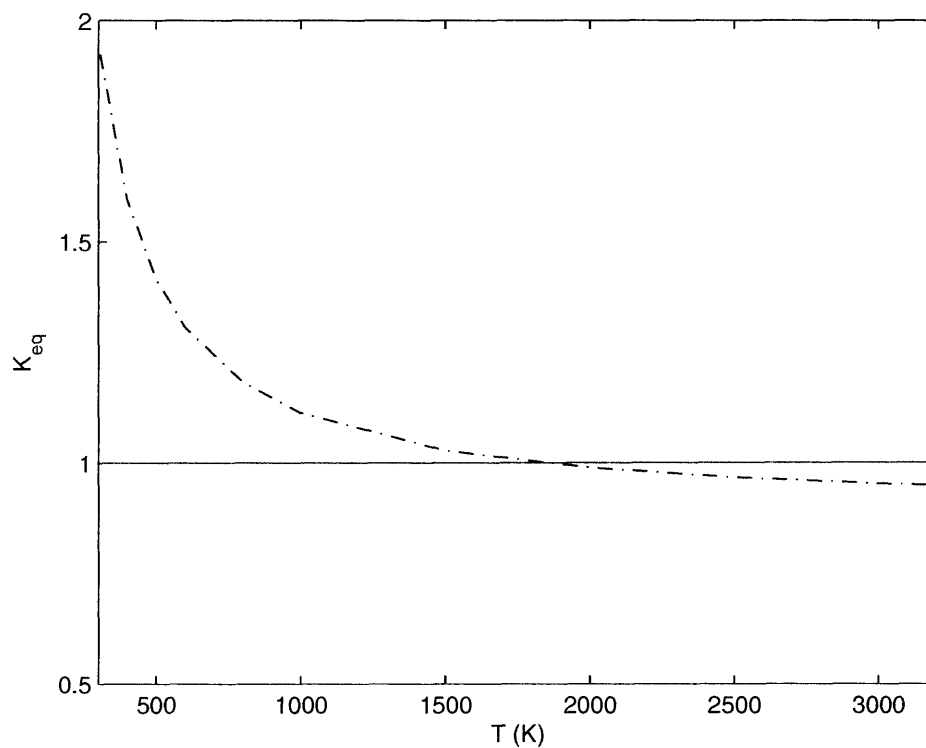


Figure 9-5: Equilibrium constant for  $C_{70} + \frac{77}{8} H_2 \rightleftharpoons \frac{7}{8} C_{80}H_{22}$ . The  $K_{eq}$  for two PAHs are shown. For  $K_{eq} > 1$  the PAHs are favored at equilibrium, and for  $K_{eq} < 1$  the fullerenes are favored.

to one (around 1800K) is roughly the temperature at which the shift between PAHs and fullerenes occur, as seen in Figure 9-4.

### 9.3.4 Concentrations of the Different Fullerenes

The equilibrium concentrations of PAHs and each of the fullerenes included in this study are shown in Figure 9-6 for  $\phi = 3.0$  at 1atm. Results including and not including the three large PAHs are shown. Although the temperature range at which the fullerenes are present differ in the two cases, the relative stability of the fullerenes remain mostly the same.

$C_{82}$  is predicted to be very thermodynamically stable, but experimentally it is not a major fullerene in flames, where much higher concentrations of  $C_{60}$ ,  $C_{70}$ ,  $C_{76}$ ,  $C_{78}$ , and  $C_{84}$  are found [13, 12]. Aihara used weighted HOMO-LUMO energy band gap to predict kinetic stability of fullerenes, and concluded that while  $C_{60}$  and  $C_{70}$  are very stable kinetically,  $C_{82}$  is not [1].

Another indication that the formation of fullerenes is very much kinetically limited is the much higher equilibrium concentration of  $C_{70}$  than  $C_{60}$ . Experimentally the ratio of  $C_{70}$  to  $C_{60}$  is around 2. Thermodynamics alone cannot predict which species will occur, but it can give a guideline of what is possible and what is not.

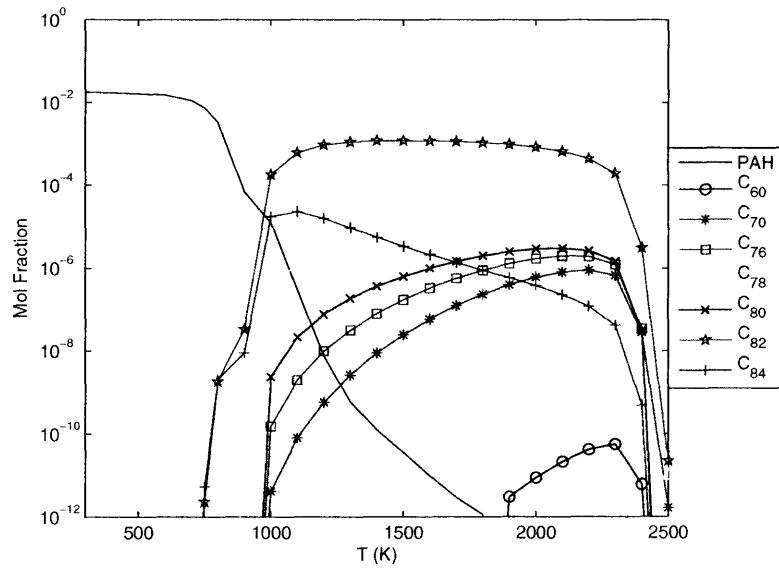
## 9.4 Conclusions

This simple preliminary equilibrium study offered plenty of interesting insights into the thermodynamic driven behavior combustion systems.

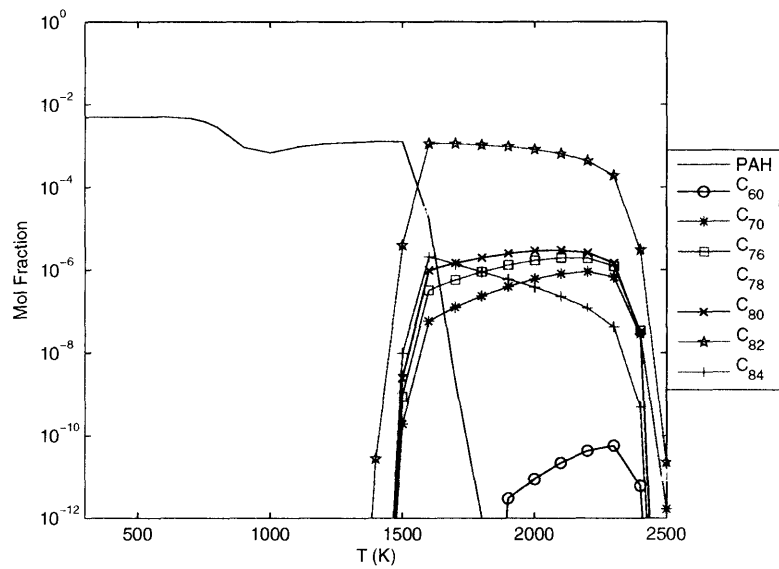
Equilibrium concentrations are strongly affected by relative thermochemical properties of the species included in the study. Thus, for a quantitative prediction of relative concentrations of individual species, accurate thermochemical properties for each of the species is mandatory.

A limited set of PAHs appears to be sufficient for sooting limit predictions. The high-temperature boundary of the experimentally observed sooting region can be predicted from equilibrium calculations in which PAHs are considered to be an indication





(a) Only with PAHs up to ovalene



(b) Including the three large PAHs from Figure 9-1

Figure 9-6: Equilibrium concentrations of overall PAHs and individual fullerenes for  $\phi = 3.0$  at 1 atm.

of soot. Equilibrium calculations predict a sooting region only for C/O ratios greater than 1, although experimentally soot is observed at C/O ratios smaller than 1. However, it is still precipitate to conclude that flames are not at equilibrium, because the local C/O ratio in flames can be larger than 1, due to diffusion effects and by trapping of the oxygen as CO and CO<sub>2</sub> early on the flame.

PAHs and fullerenes are thermodynamically stable at markedly different temperatures. Higher temperatures favor the formation of fullerenes over PAHs. Thermodynamic stability alone cannot account for the detection of some PAHs and not of others. Fullerenes such as C<sub>82</sub> are calculated to have high equilibrium concentrations, but are either not observed experimentally or are observed only at extremely low concentrations, presumably due to their high reactivity.

Equilibrium calculations are a very rich area that has not been thoroughly explored yet. With the implementation of the BCGA method into a computer program, it is now very easy to generate consistent thermochemical data for a wide variety of polycyclic aromatic molecules and radicals, including very large species. With this consistent set of thermochemical data, many studies can be performed that will provide great insight into the thermodynamic stability of complex combustion systems.

# Bibliography

- [1] J. Aihara. Weighted homo-lumo energy separation as an index of kinetic stability for fullerenes. *Theoretical Chemistry Accounts*, 102(1-6):134-138, 1999.
- [2] K. Akihama, Y. Takatori, I. Kazuhisa, S. Sasaki, and A. M. Dean. Mechanism of the smokeless rich diesel combustion by reducing temperature. *SAE Technical Paper Series*, 2001-01-0655, 2001.
- [3] J. Cioslowski, N. Rao, and D. Moncrieff. Standard enthalpies of formation of fullerenes and their dependence on structural motifs. *Journal of the American Chemical Society*, 122:8265-8270, 2000.
- [4] V. V. Diky and G. J. Kabo. Thermodynamic properties of C<sub>60</sub> and C<sub>70</sub> fullerenes. *Russian Chemical Reviews*, 69(2):95-104, 2000.
- [5] B. S. Haynes and H. G. Wagner. Soot formation. *Progress in Energy and Combustion Science*, 7:229-273, 1981.
- [6] K. H. Homann. Fullerenes and soot formation- new pathways to large particles in flames. *Angewandte Chemie- International Edition*, 37:2434-2451, 1998.
- [7] T. Kanimoto and M.-H. Bae. High combustion temperature for the reduction of particulate in diesel engines. *SAE Technical Paper Series*, 880423, 1988.
- [8] R. J. Kee, F. M. Rupley, J. A. Miller, M. E. Coltrin, J. F. Grear, E. Meeks, H. K. Moffat, A. E. Lutz, G. Dixon-Lewis, M. D. Smooke, J. Warnatz, G. H. Evans, R. S. Larson, R. E. Mitchell, L. R. Petzhold, W. C. Reynolds, M. Caracotsios, W. E. Stewart, P. Glarborg, C. Wang, O. Adigun, W. G. Houf, C. P. Chou, and S. F. Miller. Chemkin collection, 2002.
- [9] C. J. Pope, R. A. Shandross, and J. B. Howard. Variation of equivalence ratio and element ratios with distance from burner in premixed one-dimensional flames. *Combustion and Flame*, 116:605-614, 1999.
- [10] H. Richter. Personal communication, 2004.
- [11] H. Richter and J. B. Howard. Formation and consumption of single-ring aromatic hydrocarbons and their precursors in premixed acetylene, ethylene and benzene flames. *Physical Chemistry Chemical Physics*, 4:2038-2055, 2002.

- [12] H. Richter, A. J. Labrocca, W. J. Grieco, K. Taghizadeh, A. L. Lafleur, and J. B. Howard. Generation of higher fullerenes in flames. *Journal of Physical Chemistry B*, 101(9):1556–1560, 1997.
- [13] H. Richter, K. Taghizadeh, W. J. Grieco, A. L. Lafleur, and J. B. Howard. Preparative-scale liquid chromatography and characterization of large fullerenes generated in low-pressure benzene flames. *Journal of Physical Chemistry*, 100(50):19603–19610, 1996.
- [14] J. C. Street and A. Thomas. Carbon formation in pre-mixed flames. *Fuel*, 34:4–36, 1955.
- [15] F. J. Wright. The formation of carbon under well-stirred conditions. *The Combustion Institute*, 12:867–875, 1969.

# Chapter 10

## Conclusions and Recommendations

### 10.1 Conclusions

In this work we have proposed an accurate and consistent estimation method of the thermochemical properties for polycyclic aromatic molecules and radicals based on Bond-Centered Group Additivity. A term based on the number of Kekulé structures was included to account for the resonance energy characteristic of this class of species.

#### 10.1.1 Assessment of the Available Experimental Data

The estimation method was derived from sound thermochemical properties for this class of molecules. An extensive assessment of the available experimental data was performed. Heats of formation in the gas phase are calculated from the heats of formation of the crystal ( $\Delta H_{f,(cr)}^\circ$ ) measured through combustion experiments and from heats of sublimation ( $\Delta H_{subl}^\circ$ ) calculated from vapor pressure measurements. For many of the PAHs only one experimental value for  $\Delta H_{f,(cr)}^\circ$  and/or  $\Delta H_{subl}^\circ$  is available. When more than one  $\Delta H_{f,(cr)}^\circ$  or  $\Delta H_{subl}^\circ$  are available, it is not uncommon for them to differ from each other by a couple of kcal mol<sup>-1</sup>. Gas phase  $S_{298}^\circ$  were calculated for the first time for many PAHs from the entropy of the crystal and the entropy of sublimation calculated from vapor pressure data available in the literature. As in the case of the enthalpies, for most of the PAHs only one entropy of the crystal value is

available. Entropy of sublimation calculated from vapor pressure data published by different authors can differ from each other by a couple of  $\text{cal K}^{-1} \text{mol}^{-1}$ .

Experimental thermochemical data for polycyclic aromatic molecules are extremely scant. Moreover, the uncertainties in each value are often much larger than the reported experimental uncertainties. However, since often only one value is available for a given molecule, it is not possible to have a solid assessment of the uncertainty. Users of experimental thermochemical data for PAHs should always be critical of every value and conscious of the large uncertainty associated with the values. For example, the  $\Delta H_{\text{subl}}^{\circ}$  of naphthalene derived in 1951 by Magnus et al. [4] was recently confirmed to be too low by  $\sim 10 \text{ kcal mol}^{-1}$  [5] after many theoretical studies had indicated so [1, 2, 6].

### 10.1.2 Computational Methods

The B3LYP/6-31G(d) method was adopted for all the calculations. The entropies calculated in this way are shown to be as adequate as the available experimental  $S_{298}^{\circ}$ , despite the many low frequency vibrations present in PAHs. Uncertainties in the quantum chemical entropy calculated by assuming that all the frequencies were off by  $\pm 20 \text{ cal K}^{-1} \text{mol}^{-1}$  were in many cases smaller than the discrepancy between different experimental values.

Many reaction schemes were tested for the calculation of the  $\Delta H_f^{\circ}$  of PAHs with five- and six-membered rings from absolute energies given by the B3LYP/6-31G(d) calculations. A homodesmotic reaction scheme that provides the maximum cancellation of the electron correlation energy is proposed. The assessment of the quality of the reaction scheme was made by comparing the values calculated from the proposed homodesmotic reaction scheme ( $\Delta H_{f,\text{homo}}^{\circ}$ ) with the  $\Delta H_{f,\text{exp}}^{\circ}$ . The MAD and RMS between the  $\Delta H_{f,\text{homo}}^{\circ}$  and the available  $\Delta H_{f,\text{exp}}^{\circ}$  are 1.4 and 2.2  $\text{kcal mol}^{-1}$  respectively. From the  $\Delta H_f^{\circ}$  calculated through the various reaction schemes tested, there are indications that some of the available  $\Delta H_{f,\text{exp}}^{\circ}$  might not be correct. Both corannulene and benzo[k]fluoranthene only have one experimental heat of formation each, and most of the reaction schemes tested give  $\Delta H_f^{\circ}$ 's that are higher than the  $\Delta H_{f,\text{exp}}^{\circ}$  of

these molecules by  $\sim 10$  kcal mol<sup>-1</sup>.

### 10.1.3 Bond-Centered Group Additivity Method

A bond-centered group additivity method (BCGA) is proposed for polycyclic aromatic molecules. Bond-centered groups describe a larger structure than atom-centered groups, allowing a better capture of structural features that influence the thermochemistry of polycyclic aromatic molecules. Resonance energy is described through the natural logarithm of the number of Kekulé structures. An algorithm has been developed to count the number of Kekulé structures of molecules with rings of any size. The method is shown to have good predictive capabilities through the “leave one out” procedure. The BCGA method estimates the thermochemical properties of PAHs up to the C<sub>60</sub> and C<sub>70</sub> fullerenes very accurately. For PAHs with five- and six-membered rings the method estimates the  $\Delta H_{f,\text{homo}}^\circ$  with MAD and RMS of 2.8 and 4.3 kcal mol<sup>-1</sup> respectively. The method is also shown to provide a reasonable extrapolation to a hypothetical infinite gaseous graphene sheet.

Bond-group values were derived also for polycyclic aromatic molecules with the furan ring and with triple bonds. A linking between the BCGA method and Benson’s method based on atom-centered groups has also been developed, allowing estimation of the thermochemical properties of substituted polycyclic aromatic molecules. HBI values for  $\sigma$ -radicals were refined to capture the influence that the structural environment around the radical site has on the thermochemical properties of the radical. An estimation method for radicals in which not all the  $\pi$ -electrons can be paired is presented.

Error bars were calculated for all the values derived in this work, allowing the estimation of uncertainties of the thermochemical properties in addition to the properties themselves.

The method presented in this work is certainly the most comprehensive estimation method proposed for polycyclic aromatic molecules and radicals. The possibility of calculating consistent thermochemical properties for such a variety of aromatic molecules will aid in the quest of obtaining a better understanding of combustion

processes. This method also provides a firm ground upon new bond-centered group values can be derived to describe other polycyclic aromatic molecules.

#### **10.1.4 Organization of Thermochemical Database**

Benson's atom-centered group additivity method was organized as a tree structure for use in the automatic reaction mechanism software (RMG) developed in our group [7]. A tree structure captures the relationship between the groups. The groups are organized hierarchically, with a general group on the top of the tree. As one goes down the tree, the groups become more and more specific. This organization naturally puts similar groups close to each other in the tree, making it easier for a human to grasp rapidly the information contained in the groups. Groups for which no values are available were assigned the values of other similar groups. The assignment is unique and has been clearly documented. Extension of the thermochemical database is also made very easy with the tree structure, since it allows the addition of more specific group values as they are derived. All sources for the group values included in this database have been clearly documented.

The bond-centered groups database was also organized as a tree structure. Unlike the atom-centered tree structure, for the bond-centered groups the children of a particular father are organized in a particular order. An ordered list of siblings is necessary due to the definition of the bond-centered groups. Again, the organization of the bond-centered groups as a tree structure makes it very easy to extend it in the future, if more specific bond-groups are desired. That would be the case if the BCGA method is extended to estimate the thermochemical properties of higher fullerenes, for example.

#### **10.1.5 Implementation of the BCGA Method into RMG**

The Bond-Centered Group Additivity method developed in this work was implemented into the automatic reaction mechanism generation software (RMG) developed by Dr. Jing Song [7]. The program was developed using object oriented technology



to ensure easy extendability.

This implementation allows users, both experts and beginners, to easily estimate consistent thermochemical properties of polycyclic aromatic molecules and radicals. The thermochemical estimator of RMG can work independently from the main automatic reaction mechanism generation program.

RMG is now also able to correctly identify ring structures that are represented through alternating single and double (or triple) bonds as aromatic. This capability is crucial for the generation of kinetic mechanisms containing reactions in which aromatic molecules are formed from non-aromatic molecules.

### 10.1.6 Equilibrium Calculations

The simple preliminary equilibrium study performed offered plenty of interesting insights into the thermodynamic driven behavior of combustion systems.

Equilibrium concentrations are strongly affected by relative thermochemical properties of the species included in the study. Thus, for a quantitative prediction of relative concentrations of individual species, accurate thermochemical properties for each of the species is mandatory. However, the overall semi-quantitative conclusions that can be drawn from equilibrium calculations are very robust.

The high-temperature boundary for the sooting region can be predicted from equilibrium calculations including a limited set of PAHs. The inclusion of larger PAHs makes the sooting limit sharper, without changing considerably the sooting region otherwise. Equilibrium calculations predict soot formation only for C/O ratios larger than 1.

PAHs and fullerenes are thermodynamically stable at markedly different temperatures. Higher temperatures favor the formation of fullerenes over PAHs. However, thermodynamic stability alone cannot account for the detection of some PAHs and not of others. Fullerenes such as C<sub>82</sub> appear at high concentrations in equilibrium calculations, but are either not observed experimentally or are observed only at extremely low concentrations, presumably due to their high reactivity

## 10.2 Recommendations for Future Work

This work has identified some areas in which more work needs to be done. It has also opened new avenues that could be followed by future researchers in the area.

### 10.2.1 Determination of More Experimental Data

The importance of accurate experimental data cannot be overemphasized. Experimentalists are highly encouraged to measure  $\Delta H_f^\circ$  vapor pressure and low temperature heat capacity of more PAHs. These values are essential for the validation of any estimation procedure.

This work has identified some experimental values that might not be very accurate. The  $\Delta H_f^\circ$  of corannulene and benzo[k]fluoranthene are believed to be too low by a couple of kcal mol<sup>-1</sup> (Section 2.3). The “experimental” entropy of naphthacene, calculated from the third law method based on experimental heat capacity and vapor pressure data, is believed to be too low by  $\sim 10$  cal K<sup>-1</sup> mol<sup>-1</sup>. The experimental entropy of phenylacetylene is based on an arguable vibrational frequency assignment (Section 4.4.3). We recommend that these experimental values for these PAHs be measured again.

### 10.2.2 Expansion of the Method

There are many more types of polycyclic aromatic molecules than the ones studied in this work. We developed a method for the most important aromatic molecules, but much more work can be done to extend the method. The solid foundation provided here can easily be built upon.

The method proposed here predicts the thermochemical properties of C<sub>60</sub> and C<sub>70</sub> fullerenes accurately, but more specific groups are necessary to describe higher fullerenes (specially their  $\Delta H_f^\circ$ ). Once these more specialized bond-centered group values are derived, it will be very easy to incorporate them into the tree structure of the present database.

There are a myriad of molecules in nature. The development of an estimation method for them must be made step by step. Each step should be guided by the necessity of accurate thermochemical properties for a particular class of molecules. More specific HBI values for radicals could be derived, as well as more specific groups for substituted aromatic molecules. Furthermore, new bond-centered groups for PAHs with different sized rings could be derived. Four- and seven-membered rings, for instance, are significant intermediates of combustion. The bond-centered group additivity method could also be extended for other molecules. An example are conjugated rings with exocyclic double bonds, such as quinones and fulvenes. Bond-centered groups could also be derived for other heteroaromatic structures, such as pyridines and thiophenes.

### 10.2.3 Kekulé Structure Count

The algorithm that has been currently implemented for the counting of the number of Kekulé structures is very slow for molecules with more than 70 carbon atoms. It should either be optimized, or the signed matrix method proposed by Klein and Lu [3] should be implemented.

### 10.2.4 Equilibrium Calculations

With the implementation of the BCGA method into RMG, it is now very easy to obtain consistent thermochemical data for a wide variety of polycyclic aromatic molecules. Equilibrium calculations are very easy and can provide good insight on how thermodynamic stability between a large number of molecules affect their concentration at equilibrium. Comparison between equilibrium concentrations and concentrations measured experimentally can help determine which behavior of the reacting system is due to thermodynamic constraints and which is due to kinetic constraints.

Although in this study we performed equilibrium calculations both with and without three large PAHs ( $C_{54}H_{18}$ ,  $C_{60}H_{20}$ , and  $C_{80}H_{22}$ ), further studies could be done to assess the effect of the inclusion of even larger PAHs, and of isomers of the PAHs.

It would be interesting to perform equilibrium calculations with a wide variety of fuels. For example, experimentally it is observed that the regions in which fullerenes and PAHs are formed are much more overlapped for methane as a fuel than for benzene. Equilibrium calculations using methane as fuel could determine whether this observation is due to thermodynamics or not. Different pressures should also be tested. It is known, for example, that the formation of fullerenes is favored at low pressures.

### **10.2.5 Generation of Reaction Mechanisms for Soot Formation**

The ultimate goal is to gain an in-depth understanding of combustion systems, so that more efficient, less polluting engines can be designed, or the optimal conditions for fullerene formation in a flame can be found.

This in depth understanding can be achieved through the generation of reaction mechanisms that can describe the chemistry of combustion. With the BCGA method proposed in this work we took an important step towards reaching this goal. However, before complete mechanisms for soot formation are generated, a better understanding of the reactions involving large PAHs and soot is necessary. The reaction pathways for PAH growth have not been completely clarified yet. Current PAH growth mechanisms assume that reactions involving small PAHs can be directly transferred to large PAHs. That might not necessarily be the case.

Methods for model reduction will also play a crucial role in automatically generated reaction mechanisms for PAH formation and growth. These reaction mechanisms, which might involve hundreds or even thousands of PAH isomers, can easily become too large to be manageable, and so probably need to be reduced if they are to be used for predictions and/or coupled with fluid dynamic models.

# Bibliography

- [1] M. J. S. Dewar, A. J. Harget, and N. Trinajstić. Ground states of conjugated molecules. XV. Bond localization and resonance energies in compounds containing nitrogen or oxygen. *Journal of the American Chemical Society*, 91(23):6321-6325, 1969.
- [2] W. C. Herndon, P. U. Biedermann, and I. Agranat. Molecular structure parameters and predictions of enthalpies of formation for catacondensed and pericondensed polycyclic aromatic hydrocarbons. *Journal of Organic Chemistry*, 63:7445-7448, 1998.
- [3] D. J. Klein and X. Liu. Many-body conjugated-circuit computations. *Journal of Computational Chemistry*, 12(10):1260-1264, 1991.
- [4] A. Magnus, H. Hartmann, and F. Becker. Verbrennungswärmen und Resonanzenergien von mehrkernigen aromatischen Kohlenwasserstoffen. *Zeitschrift für Physikalische Chemie*, 197:75-91, 1951.
- [5] Y. Nagano. Standard enthalpies of formation of phenanthrene and naphthacene. *Journal of Chemical Thermodynamics*, 34:377-383, 2002.
- [6] J. M. Schulman and R. L. Disch. Bowl-shaped hydrocarbons related to c60. *Journal of Computational Chemistry*, 19(2):189-194, 1998.
- [7] J. Song. *Building Robust Chemical Reaction Mechanisms: Next Generation of Automatic Model Construction Software*. Phd thesis, Massachusetts Institute of Technology, 2004.



# Appendix A

## Symmetry Numbers

### A.1 Aliphatic Molecules

The symmetry of a molecule ( $\sigma$ ) is defined as the “total number of independent permutations of identical atoms (or groups) in a molecule that can be arrived at by simple rigid rotations of the entire molecule” [1]. The total symmetry ( $\sigma$ ) of a molecule arises from two different contributions: the internal symmetry ( $\sigma_{int}$ ) and the external symmetry ( $\sigma_{ext}$ ).

$$\sigma = \sigma_{int} \times \sigma_{ext} \tag{A.1}$$

The internal symmetry correspond to the number of permutations of identical atoms arrived at through internal rotations, whereas the external symmetry takes into account the rotation of the whole molecule. For example, methanol has an external symmetry of 1, and an internal symmetry of 3, due to rotation around the O-C bond. The total symmetry of methanol is 3.

Dr. Jing Song and the author developed an algorithm to calculate the total symmetry of aliphatic molecules using a different approach. Instead of dividing the total symmetry of the molecule into an internal and an external contribution, it is divided into the contribution of the symmetry around each component of the molecule: atom, bond, and axis. The symmetry of each of these elements are multiplied to provide

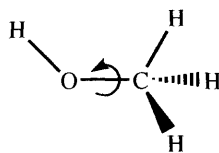


Figure A-1: Methanol has an external symmetry of 1 and an internal symmetry of 3 due to rotation around the O-C bond

the total symmetry of the molecule.

$$\sigma_{acyclic} = \prod_i \sigma_{atom,i} \times \prod_j \times \sigma_{bond,j} \prod_k \sigma_{axis,k} \quad (\text{A.2})$$

The atoms that can display symmetry are the carbon atom with four single bonds (Cs), the oxygen atom with two single bonds (Os), the allenic carbon atom (Cdd), the carbon atom radical with three single bonds (Cs\*) and the carbon biradical with two single bonds (Cs\*\*). The symmetry rules for atoms are shown in Table A.1. For example, for Cs, if all its substituents are equal (as in CH<sub>4</sub>), then the molecule will exhibit a symmetry of 12. This total symmetry of 12 already accounts for the internal and the external symmetry. Each of the C-H bond in methane has an internal symmetry of 3 (as is clear from Figure A-2). There are four of these C-H bonds, that is, the external symmetry of the molecule is 4. Thus its total symmetry is 12. If three of the substituents are equal and one is different the total symmetry number is 3, as in methanol. The Cs\* radical is assumed to be dynamically flat. This assumption is based on the fact that it has a low “umbrella” frequency. In methyl radical this frequency is about 450cm<sup>-1</sup>. The “umbrella” frequency corresponds to an internal inversion that allows all six permutations of the three identical H atoms in CH<sub>3</sub>.

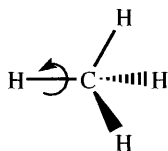


Figure A-2: Methane has internal symmetry of 3 and external symmetry of 4. Thus its total symmetry is 12. Another way of viewing the symmetry of methane is analyzing the symmetry of the Cs atom



Table A.1: Symmetry rules for atoms

$i^{th}$ atom	Neighbor				$\sigma_{atom,i}$
	1	2	3	4	
$  \begin{array}{c}  1 \\    \\  4 - \text{Cs} - 2 \\    \\  3  \end{array}  $	A	A	A	A	12
	A	A	A	B	3
	A	A	B	B	2
	A	A	B	C	1
$  \begin{array}{c}  1 \\     \\  \text{C} \\     \\  2  \end{array}  $	A	A	-	-	2
	A	B	-	-	1
$  \begin{array}{c}  1 - \text{Os} - 2 \\    \\  3  \end{array}  $	A	A	-	-	2
	A	B	-	-	1
$  \begin{array}{c}  1 \quad 2 \\  \diagdown \quad / \\  \text{Cs} \\    \\  3  \end{array}  $	A	A	A	-	6
	A	A	B	-	2
	A	B	C	-	1
$  \begin{array}{c}  1 - \overset{\cdot\cdot}{\text{C}} - 2 \\    \\  \text{Cs}  \end{array}  $	A	A	-	-	2
	A	B	-	-	1

The Cb atom (carbon atom in a benzene ring) is not included in Table A.1 because the rules presented in this section apply only to non-cyclic structures. Rules for symmetry number determination are described in Section A.2. The symmetry provided by the Cds group (a carbon atom with a double bond and two single bond) is due to the rotation along the axis of the double bond, and thus it is included in the symmetry rules for a symmetry axis in Table A.3, and not in Table A.1.

A bond can also be a center of symmetry, as is the case in ethane. Table A.2 shows the symmetry rules for bonds. In ethane, each of the carbon atoms are a center of symmetry 3, according to Table A.1. The single bond between the two carbon atoms is also a center of symmetry, contributing 2 to the overall symmetry of the molecule (see Table A.2). Thus, according to Eq. (A.2) the total symmetry for ethane is 18. Benzene bonds are not included since they only appear in cyclic structures. The next section deals with molecules that contain cycles.

Finally we define also axis of symmetry. In addition to the symmetry described in Table A.2, double bonds can also be an axis of symmetry. That is, the molecule is symmetric with respect to rotation along the axis formed by the double bond(s).

Table A.2: Symmetry rules for single, double and triple bonds

$j^{\text{th}}$ bond	Neighbor		$\sigma_{\text{bond},j}$
	1	2	
1—2	A	A	2
	A	B	1
1=2	A	A	2
	A	B	1
1≡2	A	A	2
	A	B	1

The symmetry rules for these axis are shown in Table A.3.

Thus the total symmetry of a molecule is separated into the contributions of the symmetry of each of the components of the molecule: atoms, bonds, and axis of symmetry. This method has been implemented into RMG, allowing it to calculate symmetry of non-cyclic structures.

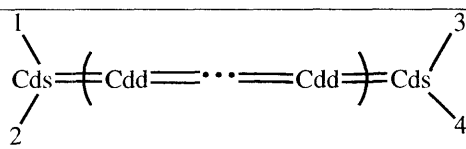
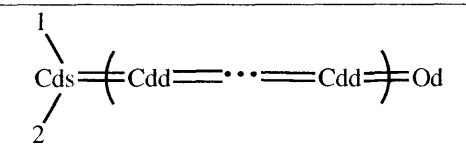
## A.2 Cyclic Molecules

The symmetry rules presented in the last Section do not apply to atoms and bonds that belong to ring structures. Sally Petway developed and implemented an algorithm in RMG that determines the symmetry number of ring structures. This algorithm compares each of the graph components that belong to a ring to each other. Graph components are nodes (representing atoms) and arcs (representing bonds). The symmetry number of the cyclic structure is equal to the largest number of equivalent graph components.

If all nodes in the ring are equivalent, all arcs in the ring are equivalent, and if all the substituents at the nodes are equal, then the symmetry number is multiplied by two. This provision corrects for the additional symmetry of one ring molecules. Although molecules such as cyclopentane, cyclohexane, and cycloheptane are not planar, they are treated as dynamically flat. The reason is because the ring puckering frequency in these cyclic structures is extremely low, which indicates an extremely fast ring puckering motion.

Some structures introduce non-planarities to the molecule, decreasing its sym-

Table A.3: Symmetry rules for symmetry axis. The symmetry given in this table refer to rotation along the axis. All the other combinations that are not presented in this table do not contribute to the symmetry

$i^{th}$ atom	Neighbor				$\sigma_{axis,k}$
	1	2	3	4	
	A	A	A	A	2
	A	A	B	B	2
	A	B	A	B	1
	A	B	B	A	1
	A	A	-	-	2
	A	B	-	-	1

metry number. Among these are the corannulene core and a six-membered ring surrounded by alternating five- and six-membered rings (see Figure A-3). Thus if the calculated symmetry number of a molecule is even, and it contains either of the subgraphs (structures) that introduce non-planarity to the molecule, its symmetry number should be divided by two. For example, all the Cb's of corannulene (there are 10 of them) are equivalent, leading to a symmetry number of 10. However, since corannulene contains the “five-membered ring completely surrounded by six-membered rings” subgraph, its symmetry number is divided by two, leading to the correct final symmetry number of 5.

For molecules that have both a cyclic and a non-cyclic part, the total symmetry number is calculated by multiplying the symmetry of the acyclic and the symmetry



Figure A-3: Subgraphs included in the symmetry correction library. Currently the symmetry correction library contains only substructures that introduce non-planarity to a molecule

of the cyclic parts.

$$\sigma = \sigma_{acyclic} \times \sigma_{cyclic} \tag{A.3}$$

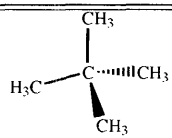
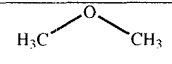
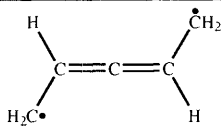
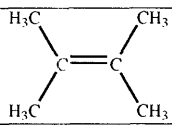
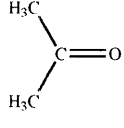
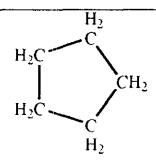
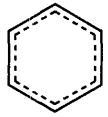
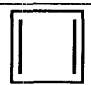
### A.3 Algorithm for Symmetry Calculation

The complete algorithm to calculate the symmetry number of a molecule is:

- i. Start with  $\sigma = 1$ ;
- ii. For each atom  $i$  that does not belong to a ring, identify its symmetry according to the rules outlined in Table A.1 and multiply  $\sigma = \sigma \times \sigma_{atom,i}$ ;
- iii. For each bond  $j$  that does not belong to a ring, identify its symmetry according to the rules outlined in Table A.2 and multiply  $\sigma = \sigma \times \sigma_{bond,j}$ ;
- iv. Identify if there are symmetry axis,  $\sigma = \sigma \times \sigma_{axis,k}$ ;
- v. If there are rings in the molecule
  - (a) For each ring system, find all the equivalent nodes (atoms). Save the number of nodes in the largest set of equivalent nodes,  $\sigma_{nodes}$ ;
  - (b) For each ring system, find all the equivalent arcs (bonds). Save the number of arcs in the largest set of equivalent arcs,  $\sigma_{arcs}$ ;
  - (c) If  $\sigma_{nodes} > \sigma_{arcs}$ ,  $\sigma = \sigma \times \sigma_{nodes}$ ;
  - (d) Else if  $\sigma_{nodes} < \sigma_{arcs}$ ,  $\sigma = \sigma \times \sigma_{arcs}$ ;
  - (e) Else ( $\sigma_{nodes} == \sigma_{arcs}$ )
    - i. If all the substituents of the ring are equal AND  $\sigma_{nodes}$  is equal to the number of nodes in the ring system and  $\sigma_{arcs}$  is equal to the number of arcs in the ring system, AND all the substituents of the ring are equal, then  $\sigma = 2 \times \sigma \times \sigma_{nodes}$ ;
    - ii. Else  $\sigma = \sigma \times \sigma_{nodes}$ ;
  - (f) Search the “symmetry corrections” library. If  $\sigma$  is even and if any of the subgraphs (substructures) present in the library is present in the molecule,  $\sigma = \sigma \div 2$ ;
- vi. Return  $\sigma$ .

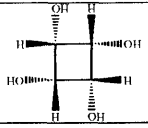
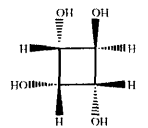
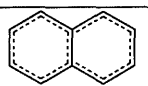
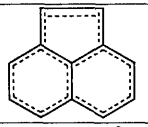
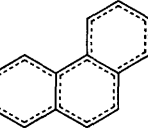
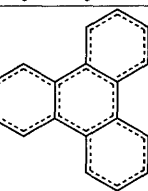
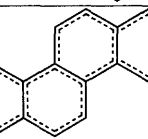
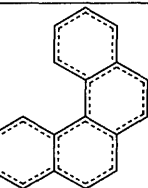
### A.4 Examples

Table A.4: Symmetry number calculated from the algorithm described in this section. Some of the symmetry numbers calculated by this algorithm are not correct, and are shown in *italics*

Molecule	Symmetry	Comments
	972	$\sigma_{atom} = 12$ for the central carbon $\sigma_{atom} = 3$ for each of the four $-CH_3$
	18	$\sigma_{atom} = 2$ for the central oxygen $\sigma_{atom} = 3$ for each of the two $-CH_3$
	8	$\sigma_{atom} = 2$ for the central Cdd $\sigma_{atom} = 2$ for each of the two $-CH_2$
HO-OH	2	$\sigma_{bond} = 2$ for the single bond between the two oxygens
	324	$\sigma_{bond} = 2$ for the central double bond $\sigma_{atom} = 3$ for each of the four $-CH_3$ $\sigma_{axis} = 2$ for the axis along the double bond
	18	$\sigma_{atom} = 3$ for each of the two $-CH_3$ $\sigma_{axis} = 2$ for the axis along the double bond
	10	$\sigma_{nodes} = \sigma_{arcs} = 5$ $\sigma = 2 \times \sigma_{nodes}$
	12	$\sigma_{nodes} = \sigma_{arcs} = 6$ and criteria 5(e)i is satisfied, thus $\sigma = 2 \times \sigma_{nodes}$
	4	$\sigma_{nodes} = 4$ all four carbons are equivalent

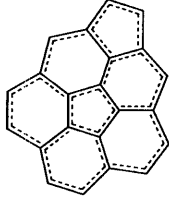


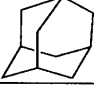
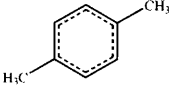

*continued*

Table A.4: *continued*

Molecule	Symmetry	Comments
	4	$\sigma_{nodes} = \sigma_{arcs} = 4$ , however, the substituents at the ring are not all equal, thus $\sigma = \sigma \times \sigma_{nodes}$
	4	Currently the adjacency list representation of the molecular structure does not contain stereochemical information. The adjacency list for this molecule and the previous are the same, and thus the symmetry calculated for this molecule is 4, even though its real symmetry number is 1.
	4	
	2	
	2	
	6	
	2	
	2	

*continued*

Table A.4: *continued*

Molecule	Symmetry	Comments
	1	Although $\sigma_{nodes} = 2$ , this molecule has a corannulene substructure, and thus it is non-planar. Its final symmetry number has to be divided by two.
	30	$\sigma_{nodes} = 60$ , but $C_{60}$ contains the corannulene substructure, thus its symmetry number is divided by 2. However, the correct symmetry number for $C_{60}$ is 180.
	10	$\sigma_{nodes} = 20$ , but $C_{70}$ contains the corannulene substructure, thus its symmetry number is divided by 2.
	12	$\sigma_{arcs} = 12$
	36	$\sigma_{nodes} = 4$ since the four unsubstituted CB's are equivalent $\sigma_{atom} = 3$ for each of the two $CH_3$
	8	$\sigma_{nodes} = 2$ for each of the two benzene rings $\sigma_{bond} = 2$ for the single bond connecting the benzene rings

## A.5 Discussion

Currently the adjacency list representation of the molecular structure does not differentiate between stereoisomer. Thus the algorithm described in this section will always return the highest possible symmetry number in these cases.

The symmetry number for all other molecules, except for  $C_{60}$ , is calculated correctly using the algorithm presented here. It is not clear exactly why the symmetry of  $C_{60}$  is calculated to be 6 times smaller than the real value. We believe it is because of the unusual perfect sphere structure of this fullerene. Since only  $C_{60}$  has this perfect sphere structure, this problem is not expected to arise for other molecules.

## A.6 Conclusions

A algorithm for the determination of the symmetry number of aliphatic and cyclic molecules was developed by Dr. Jing Song, Sally Petway and the author. It has been implemented in RMG, allowing the application of the symmetry correction in the calculation of the entropy from group additivity methods.



# Bibliography

- [1] S. W. Benson. *Thermochemical Kinetics*. John Wiley & Sons, New York, 2<sup>nd</sup> edition, 1976.


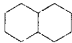
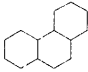
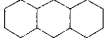
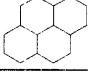
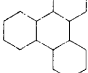
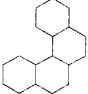
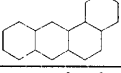
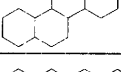
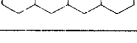


# Appendix B

## Polycyclic Aromatic Molecules

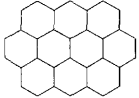
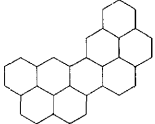
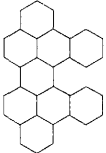
### Included in this Study

**Table B.1:** Benzenoid PAHs included in the development of the estimation method. Only the sigma bonds are shown in the structure of the PAHs. The  $\Delta H_{f, \text{homo}}^{\circ}$  listed here were calculated using the Homodesmic4 reaction scheme (see main text). The enthalpies of formation estimated through the bond-centered group additivity method proposed in this work are given in the last column.

Structure	Name Formula	Kekulé Count	$\Delta H_{f, \text{homo}}^{\circ}$ (kcal mol <sup>-1</sup> )	weight	$\Delta H_{f, \text{est}}^{\circ}$ (kcal mol <sup>-1</sup> )
	Benzene C6H6	2	19.8	2.00	19.7
	Naphthalene C10H8	3	36.0	2.00	36.2
	Phenanthrene C14H10	5	48.2	0.50	48.0
	Anthracene C14H10	4	56.1	0.67	55.1
	Pyrene C16H10	6	56.1	0.38	57.6
	Triphenylene C18H12	9	65.7	0.33	65.3
	Benzo[ <i>c</i> ]phenanthrene C18H12	8	68.0	0.22	66.9
	Benzo[ <i>a</i> ]anthracene C18H12	7	66.7	0.33	65.9
	Chrysene C18H12	8	61.9	0.22	63.8
	Naphthacene C18H12	5	77.6	0.40	75.2

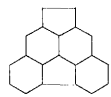
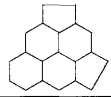
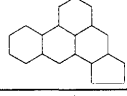
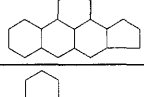
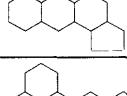
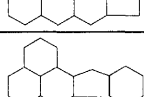
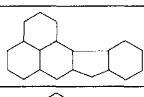
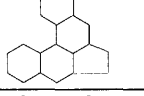

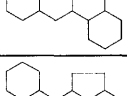
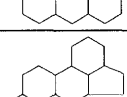
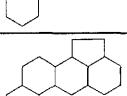
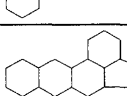
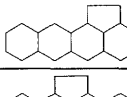
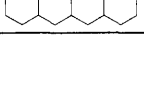


Structure	Name Formula	Kekulé Count	$\Delta H_{f, \text{homo}}^{\circ}$ (kcal mol <sup>-1</sup> )	weight	$\Delta H_{f, \text{est}}^{\circ}$ (kcal mol <sup>-1</sup> )
	Benzo[ <i>e</i> ]pyrene C <sub>20</sub> H <sub>12</sub>	11	69.7	0.24	69.7
	Perylene C <sub>20</sub> H <sub>12</sub>	9	76.5	0.24	73.3
	Benzo[ <i>a</i> ]pyrene C <sub>20</sub> H <sub>12</sub>	9	71.6	0.24	72.3
	Benzo[ <i>ghi</i> ]perylene C <sub>22</sub> H <sub>12</sub>	14	72.8	0.19	73.8
	Dibenzo[ <i>def,mno</i> ]chrysene (Anthanthrene) C <sub>22</sub> H <sub>12</sub>	10	81.5	0.21	81.5
	Dibenzo[ <i>c,g</i> ]phenanthrene C <sub>22</sub> H <sub>14</sub>	13	87.1	0.14	85.5
	Benzo[ <i>b</i> ]triphenylene C <sub>22</sub> H <sub>14</sub>	13	83.6	0.25	82.6
	Benzo[ <i>g</i> ]chrysene C <sub>22</sub> H <sub>14</sub>	14	85.9	0.22	84.8
	Dibenzo[ <i>b,g</i> ]phenanthrene C <sub>22</sub> H <sub>14</sub>	11	86.9	0.22	85.2
	Benzo[ <i>c</i> ]crysene C <sub>22</sub> H <sub>14</sub>	13	81.5	0.14	82.4
	Dibenz[ <i>a,j</i> ]anthracene C <sub>22</sub> H <sub>14</sub>	12	78.1	0.22	77.1
	Pentaphene C <sub>22</sub> H <sub>14</sub>	10	84.5	0.25	83.4
	Benzo[ <i>a</i> ]naphthacene C <sub>22</sub> H <sub>14</sub>	9	87.5	0.25	85.4
	Dibenz[ <i>a,h</i> ]anthracene C <sub>22</sub> H <sub>14</sub>	12	77.8	0.22	77.1
	Benzo[ <i>b</i> ]chrysene C <sub>22</sub> H <sub>14</sub>	11	81.0	0.22	82.1

Structure	Name Formula	Kekulé Count	$\Delta H_{f, \text{homo}}^{\circ}$ (kcal mol <sup>-1</sup> )	weight	$\Delta H_{f, \text{est}}^{\circ}$ (kcal mol <sup>-1</sup> )
	Picene C22H14	13	75.3	0.14	79.3
	Pentacene C22H14	6	99.9	0.29	96.1
	Coronene C24H12	20	75.2	0.17	76.0
	Dibenzo[ <i>def,p</i> ]chrysene C24H14	16	92.2	0.18	90.6
	Dibenzo[ <i>fg,op</i> ]naphthacene C24H14	20	84.2	0.18	82.0
	Dibenzo[ <i>a,h</i> ]pyrene C24H14	13	88.2	0.18	87.7
	Naphtho[2,1- <i>a</i> ]pyrene C24H14	15	84.1	0.18	87.3
	Naphtho[2,3- <i>a</i> ]pyrene C24H14	12	91.2	0.19	91.2
	Benzo[ <i>a</i> ]perylene C24H14	12	100.2	0.18	95.8
	Naphtho[1,2,3,4- <i>def</i> ]chrysene C24H14	17	84.8	0.18	83.8
	Phenanthro[3,4- <i>c</i> ]phenanthrene C26H16	21	105.1	0.11	104.3
	Dibenzo[ <i>g,p</i> ]chrysene C26H16	24	107.1	0.18	106.2
	Hexacene C26H16	7	122.4	0.22	117.6
	Benzo[ <i>a</i> ]coronene C28H14	34	90.4	0.13	89.6
	Dibenzo[ <i>bc,kl</i> ]coronene C30H14	20	112.3	0.12	109.8

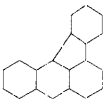
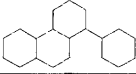
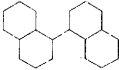
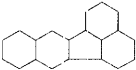
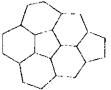
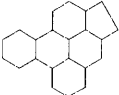
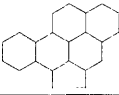
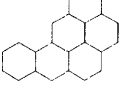
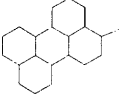
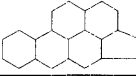
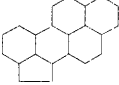
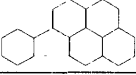
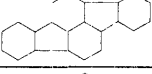
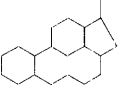
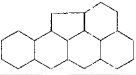
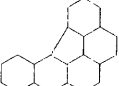
Structure	Name Formula	Kekulé Count	$\Delta H_{f, \text{homo}}^{\circ}$ (kcal mol <sup>-1</sup> )	weight	$\Delta H_{f, \text{est}}^{\circ}$ (kcal mol <sup>-1</sup> )
	Ovalene C32H14	50	102.2	0.11	100.0
	Dinaphtho[1,2,8,7- <i>defg</i> :2',1',8',7'- <i>ijkl</i> ]-pentaphene C32H16	36	116.0	0.12	113.7
	Tetrabenzo[ <i>a,cd,lm,o</i> ]perylene C34H18	61	131.9	0.11	128.6

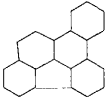
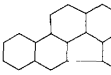


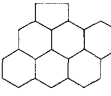
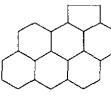
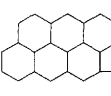
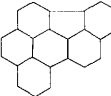
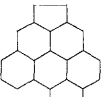
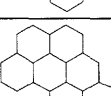
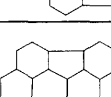
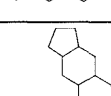
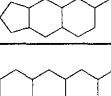
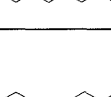
**Table B.2:** PAHs with five- and six-membered rings included in the development of the estimation method. Only the sigma bonds are shown in the structure of the PAHs. The  $\Delta H_{f,\text{homo}}^\circ$  listed here were calculated using the Homodesmic4 reaction scheme (see main text). The enthalpies of formation estimated through the bond-centered group additivity method proposed in this work are given in the last column. The  $\Delta H_{f,\text{est}}^\circ$  of PAHs that contain the bond-groups BD6665o and/or BD6655oo are given in parenthesis.

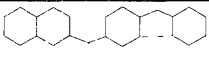
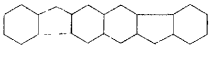
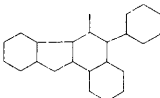
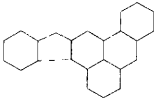
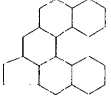
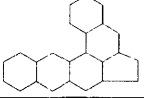
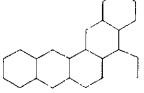
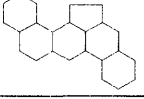
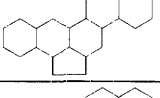
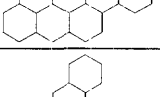
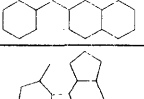
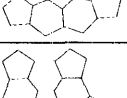
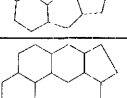
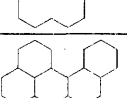
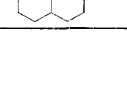
Structure	Name Formula	Kekulé Count	$\Delta H_{f,\text{homo}}^\circ$ (kcal mol <sup>-1</sup> )	weight	$\Delta H_{f,\text{est}}^\circ$ (kcal mol <sup>-1</sup> )
	<i>as</i> -Indacene C <sub>12</sub> H <sub>8</sub>	2	99.7	0.07	86.2
	<i>s</i> -Indacene C <sub>12</sub> H <sub>8</sub>	2	93.5	0.09	91.5
	Acenaphthylene C <sub>12</sub> H <sub>8</sub>	3	62.1	0.20	60.9
	Pyracylene C <sub>14</sub> H <sub>8</sub>	4	102.3	0.10	96.4
	Fluoranthene C <sub>16</sub> H <sub>10</sub>	6	67.3	0.17	64.6
	Acephenanthrene C <sub>16</sub> H <sub>10</sub>	5	72.1	0.13	73.5
	Aceanthrylene C <sub>16</sub> H <sub>10</sub>	4	78.8	0.13	76.6
	Cyclopenta[ <i>cd</i> ]pyrene C <sub>18</sub> H <sub>10</sub>	6	83.1	0.14	85.6
	Benzo[ <i>mno</i> ]aceanthrylene C <sub>18</sub> H <sub>10</sub>	4	101.3	0.14	99.2
	Benzo[ <i>ghi</i> ]fluoranthene C <sub>18</sub> H <sub>10</sub>	8	87.4	0.14	86.1
	Cyclopent[ <i>cd</i> ]fluoranthene C <sub>18</sub> H <sub>10</sub>	7	104.7	0.10	102.8
	Cyclopent[ <i>hi</i> ]acephenanthrene C <sub>18</sub> H <sub>10</sub>	5	95.1	0.08	95.4
	Dibenzo[ <i>ghi,mno</i> ]fluoranthene (Corannulene) C <sub>20</sub> H <sub>10</sub>	11	117.4	0.34	117.9
	Dicyclopenta[ <i>cd,fg</i> ]pyrene C <sub>20</sub> H <sub>10</sub>	7	109.3	0.08	107.0
	Dicyclopenta[ <i>cd,jk</i> ]pyrene C <sub>20</sub> H <sub>10</sub>	7	113.7	0.09	110.5
	Cyclopenta[ <i>cd</i> ]benzo[ <i>ghi</i> ]fluoranthene C <sub>20</sub> H <sub>10</sub>	9	129.9	0.09	125.0




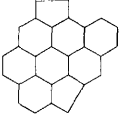
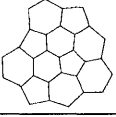


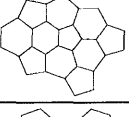
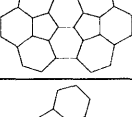
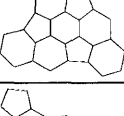
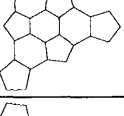
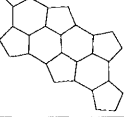
Structure	Name Formula	Kekulé Count	$\Delta H_{f, \text{homo}}^{\circ}$ (kcal mol <sup>-1</sup> )	weight	$\Delta H_{f, \text{est}}^{\circ}$ (kcal mol <sup>-1</sup> )
	Cyclopenta[ <i>fg</i> ]benzo[ <i>ghi</i> ]fluoranthene C <sub>20</sub> H <sub>10</sub>	8	130.0	0.09	127.3
	Dicyclopenta[ <i>cd,mn</i> ]pyrene C <sub>20</sub> H <sub>10</sub>	6	115.6	0.09	113.5
	Benzo[ <i>de</i> ]cyclopent[ <i>a</i> ]anthracene C <sub>20</sub> H <sub>12</sub>	5	95.7	0.10	99.7
	Benzo[ <i>de</i> ]cyclopent[ <i>b</i> ]anthracene C <sub>20</sub> H <sub>12</sub>	5	95.0	0.10	99.7
	Benzo[ <i>fg</i> ]cyclopent[ <i>a</i> ]anthracene C <sub>20</sub> H <sub>12</sub>	3	107.9	0.10	112.1
	Benzo[ <i>fg</i> ]cyclopent[ <i>b</i> ]anthracene C <sub>20</sub> H <sub>12</sub>	3	107.7	0.13	112.8
	Indeno[2,1- <i>a</i> ]phenalene C <sub>20</sub> H <sub>12</sub>	6	88.8	0.13	91.5
	Indeno[1,2- <i>a</i> ]phenalene C <sub>20</sub> H <sub>12</sub>	3	106.5	0.13	109.5
	Benz[ <i>a</i> ]acephenanthrylene C <sub>20</sub> H <sub>12</sub>	8	89.4	0.10	92.4
	Benz[ <i>l</i> ]acephenanthrylene C <sub>20</sub> H <sub>12</sub>	8	91.4	0.10	92.4
	Benz[ <i>e</i> ]aceanthrylene C <sub>20</sub> H <sub>12</sub>	7	87.6	0.10	88.2
	Benz[ <i>l</i> ]aceanthrylene C <sub>20</sub> H <sub>12</sub>	7	92.6	0.10	93.8
	Cyclopenta[ <i>hi</i> ]chrysene C <sub>20</sub> H <sub>12</sub>	8	86.5	0.10	89.3
	Benz[ <i>j</i> ]aceanthrylene C <sub>20</sub> H <sub>12</sub>	7	90.2	0.10	90.7
	Benz[ <i>k</i> ]acephenanthrylene C <sub>20</sub> H <sub>12</sub>	7	90.0	0.13	91.4
	Cyclopenta[ <i>de</i> ]naphthacene C <sub>20</sub> H <sub>12</sub>	5	100.0	0.13	96.7
	Benz[ <i>d</i> ]aceanthrylene C <sub>20</sub> H <sub>12</sub>	5	96.7	0.10	93.6



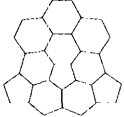

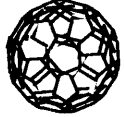
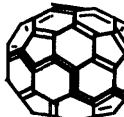


Structure	Name Formula	Kekulé Count	$\Delta H_{f,\text{homo}}^{\circ}$ (kcal mol <sup>-1</sup> )	weight	$\Delta H_{f,\text{est}}^{\circ}$ (kcal mol <sup>-1</sup> )
	Benz[ <i>a</i> ]aceanthrylene C <sub>20</sub> H <sub>12</sub>	8	85.4	0.13	87.1
	Benz[ <i>e</i> ]acephenanthrylene C <sub>20</sub> H <sub>12</sub>	10	77.8	0.13	77.2
	Benzo[ <i>j</i> ]fluoranthene C <sub>20</sub> H <sub>12</sub>	9	82.6	0.13	84.8
	Benzo[ <i>k</i> ]fluoranthene C <sub>20</sub> H <sub>12</sub>	9	82.6	0.14	81.2
	Cyclopenta[ <i>bc</i> ]corannulene C <sub>22</sub> H <sub>10</sub>	12	156.8	0.13	153.4
	Benzo[ <i>l</i> ]cyclopenta[ <i>cd</i> ]pyrene C <sub>22</sub> H <sub>12</sub>	11	94.9	0.12	97.7
	Indeno[5,6,7,1- <i>defg</i> ]chrysene C <sub>22</sub> H <sub>12</sub>	9	97.6	0.12	100.4
	Benzo[ <i>def</i> ]cyclopenta[ <i>qr</i> ]chrysene C <sub>22</sub> H <sub>12</sub>	9	98.3	0.12	100.2
	Cyclopenta[ <i>cd</i> ]perylene C <sub>22</sub> H <sub>12</sub>	9	100.6	0.12	101.2
	Indeno[1,7,6,5- <i>cdef</i> ]chrysene C <sub>22</sub> H <sub>12</sub>	9	97.7	0.12	100.2
	Indeno[1,7- <i>ab</i> ]pyrene C <sub>22</sub> H <sub>12</sub>	9	95.2	0.12	95.5
	Indeno[1,2,3- <i>cd</i> ]pyrene C <sub>22</sub> H <sub>12</sub>	12	88.2	0.12	89.3
	Indeno[1,2,3- <i>cd</i> ]fluoranthene C <sub>22</sub> H <sub>12</sub>	13	108.1	0.09	108.0
	Phenanthro[10,1,2,3- <i>cdef</i> ]fluorene C <sub>22</sub> H <sub>12</sub>	7	111.0	0.12	110.8
	Indeno[6,7,1,2- <i>defg</i> ]naphthacene C <sub>22</sub> H <sub>12</sub>	5	118.2	0.12	116.2
	Naphtho[4,5,6- <i>abc</i> ]aceanthrylene C <sub>22</sub> H <sub>12</sub>	11	103.7	0.12	108.0

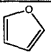
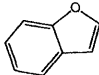
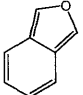
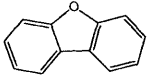
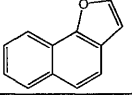
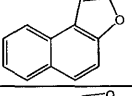
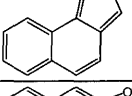
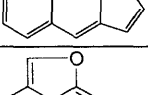
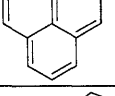
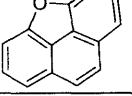
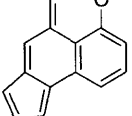
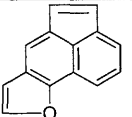
Structure	Name Formula	Kekulé Count	$\Delta H_{f, \text{homo}}^{\circ}$ (kcal mol <sup>-1</sup> )	weight	$\Delta H_{f, \text{est}}^{\circ}$ (kcal mol <sup>-1</sup> )
	Indeno[3,2,1,7- <i>defg</i> ]chrysene C22H12	14	96.5	0.12	99.1
	Indeno[4,3,2,1- <i>cdef</i> ]chrysene C22H12	13	97.6	0.12	99.2
	Dicyclopenta[ <i>bc,ef</i> ]corannulene C24H10	13	188.4	0.07	185.4
	Dicyclopenta[ <i>bc,hi</i> ]corannulene C24H10	13	194.3	0.08	189.0
	Benz[ <i>mno</i> ]indeno[5,6,7,1- <i>defg</i> ]chrysene C24H12	10	105.4	0.10	107.1
	Dibenzo[ <i>def,mno</i> ]cyclopenta[ <i>hi</i> ] chrysene C24H12	10	104.4	0.10	107.1
	Benz[ <i>mno</i> ]indeno[1,7,6,5- <i>cdef</i> ]chrysene C24H12	10	108.2	0.11	109.4
	Acenaphtho[1,2,3- <i>cde</i> ]pyrene C24H12	17	105.3	0.10	108.6
	Cyclopenta[ <i>fg</i> ]benzo[ <i>ghi</i> ]perylene C24H12	14	99.1	0.10	101.8
	Cyclopenta[ <i>cd</i> ]benzo[ <i>ghi</i> ]perylene C24H12	14	98.4	0.10	101.8
	Benzo[ <i>mno</i> ]naphtho[2,1,8- <i>bcd</i> ]aceanthrylene C24H12	5	139.9	0.11	138.1
	Cyclopent[ <i>b</i> ]indeno[4,5- <i>g</i> ]phenanthrene C24H14	2	157.1	0.06	165.9
	Dicyclopenta[ <i>a,c</i> ]naphthacene C24H14	5	138.6	0.05	143.7
	Fluoreno[3,4- <i>b</i> ]fluorene C24H14	5	130.8	0.08	131.2

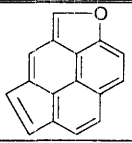
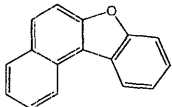
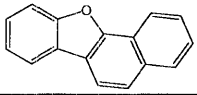
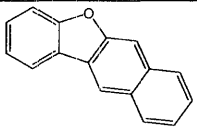
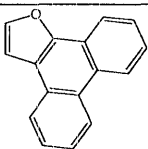
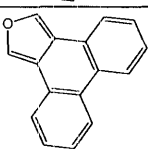
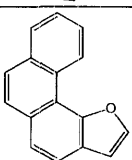
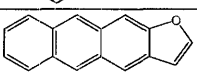
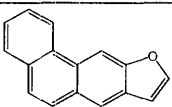
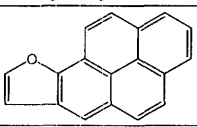
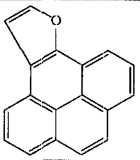
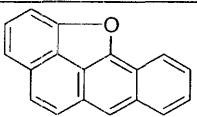
Structure	Name Formula	Kekulé Count	$\Delta H_{f,\text{homo}}^{\circ}$ (kcal mol <sup>-1</sup> )	weight	$\Delta H_{f,\text{est}}^{\circ}$ (kcal mol <sup>-1</sup> )
	Benz[b]indeno[2,1- <i>h</i> ]fluorene C <sub>24</sub> H <sub>14</sub>	7	122.4	0.09	121.0
	Fluoreno[3,2- <i>b</i> ]fluorene C <sub>24</sub> H <sub>14</sub>	5	129.4	0.09	127.6
	Benz[a]indeno[1,2- <i>c</i> ]fluorene C <sub>24</sub> H <sub>14</sub>	6	138.8	0.08	135.9
	Fluoreno[4,3,2- <i>de</i> ]anthracene C <sub>24</sub> H <sub>14</sub>	4	123.9	0.10	126.4
	Naphth[1,2- <i>a</i> ]acephenanthrylene C <sub>24</sub> H <sub>14</sub>	13	109.1	0.08	111.0
	Dibenz[ <i>a,k</i> ]acephenanthrylene C <sub>24</sub> H <sub>14</sub>	11	107.7	0.10	110.7
	Cyclopenta[ <i>fg</i> ]pentaphene C <sub>24</sub> H <sub>14</sub>	10	105.0	0.10	105.7
	Dibenz[ <i>e,l</i> ]aceanthrylene C <sub>24</sub> H <sub>14</sub>	12	101.8	0.08	105.8
	Benzo[ <i>b</i> ]cyclopenta[ <i>qr</i> ]chrysene C <sub>24</sub> H <sub>14</sub>	11	102.4	0.08	104.4
	Indeno[7,1- <i>bc</i> ]chrysene C <sub>24</sub> H <sub>14</sub>	11	106.8	0.08	110.0
	Dibenz[ <i>a,e</i> ]acephenanthrylene C <sub>24</sub> H <sub>14</sub>	16	95.7	0.10	96.1
	Tricyclopenta[ <i>bc,ef,kl</i> ]corannulene C <sub>26</sub> H <sub>10</sub>	14	224.6	0.05	221.1
	Tricyclopenta[ <i>bc,ef,hi</i> ]corannulene C <sub>26</sub> H <sub>10</sub>	15	218.5	0.04	216.2
	Cyclopenta[ <i>bc</i> ]coronene C <sub>26</sub> H <sub>12</sub>	20	102.6	0.10	104.0
	C <sub>26</sub> H <sub>12</sub>	20	122.7	0.10	119.1

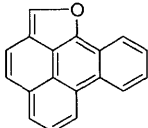
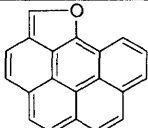
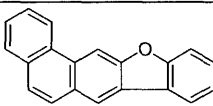
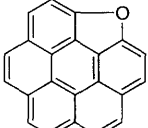
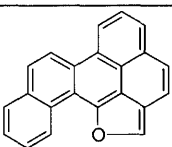
Structure	Name Formula	Kekulé Count	$\Delta H_{f, \text{homo}}^{\circ}$ (kcal mol <sup>-1</sup> )	weight	$\Delta H_{f, \text{est}}^{\circ}$ (kcal mol <sup>-1</sup> )
	Indeno[123,bc]corannulene C26H12	23	161.0	0.12	157.9
	Tetracyclopenta[bc,ef,hi,kl]corannulene C28H10	17	253.4	0.04	247.3
	Acenaphtho[123,abc]corannulene C28H12	31	177.2	0.10	178.1
	C28H12	10	159.2	0.06	153.4
	C30H10	24	274.5	0.05	287.8
	C30H10	22	275.6	0.04	283.1
	“HB” (Half-Buckminsterfullerene) C30H10	22	269.5	0.02	272.3
	C30H10	20	279.3	0.04	284.9
	“Double-corannulene” C30H12	44	194.3	0.16	(191.6)
	C30H12	35	217.7	0.05	220.5
	C30H12	4	279.6	0.02	288.6
	C30H12	9	268.1	0.02	261.8

Structure	Name Formula	Kekulé Count	$\Delta H_{f, \text{homo}}^{\circ}$ (kcal mol <sup>-1</sup> )	weight	$\Delta H_{f, \text{est}}^{\circ}$ (kcal mol <sup>-1</sup> )
	C30H12	28	212.3	0.06	(205.1)
	C32H10	29	298.5	0.03	307.7
	C32H12	38	225.3	0.06	(206.7)
	C32H12	50	214.2	0.14	(199.8)
	Buckminsterfullerene C60	12500	604.6	0.10	(602.4)
	C70	52168	655.8	0.06	(659.1)

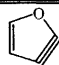
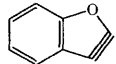
**Table B.3:** PAHs with the furan substructure included in the development of the estimation method. The  $\Delta H_{f, \text{homo}}^{\circ}$  listed here were calculated using the homodesmotic reaction scheme (see main text). The enthalpies of formation estimated through the bond-centered group additivity method proposed in this work are given in the last column.

Structure	Name Formula	Kekulé Count	$\Delta H_{f, \text{homo}}^{\circ}$ (kcal mol <sup>-1</sup> )	weight	$\Delta H_{f, \text{est}}^{\circ}$ (kcal mol <sup>-1</sup> )
	Furan C <sub>4</sub> H <sub>4</sub> O	1	-8.3	0.50	-8.3
	Benzo-b-furan C <sub>8</sub> H <sub>6</sub> O	2	4.1	0.33	4.1
	Benzo-c-furan C <sub>8</sub> H <sub>6</sub> O	1	18.4	0.33	18.3
	Dibenzofuran C <sub>12</sub> H <sub>8</sub> O	4	13.1	0.25	10.4
	Naphtho[1,2-b]furan C <sub>12</sub> H <sub>8</sub> O	3	16.4	0.22	15.6
	Naphtho[2,1-b]furan C <sub>12</sub> H <sub>8</sub> O	3	16.5	0.22	19.5
	Naphtho[2,1-c]furan C <sub>12</sub> H <sub>8</sub> O	2	26.1	0.22	25.4
	Naphtho[2,3-b]furan C <sub>12</sub> H <sub>8</sub> O	3	21.9	0.25	20.7
	Phenylene-Furan C <sub>14</sub> H <sub>8</sub> O	3	39.0	0.19	38.8
	Phenanthrene-Furan C <sub>14</sub> H <sub>8</sub> O	5	36.8	0.19	37.3
	C <sub>14</sub> H <sub>8</sub> O_3	2	56.5	0.10	58.1
	C <sub>14</sub> H <sub>8</sub> O_4	3	40.9	0.10	41.1

Structure	Name Formula	Kekulé Count	$\Delta H_{f, \text{homo}}^{\circ}$ (kcal mol <sup>-1</sup> )	weight	$\Delta H_{f, \text{est}}^{\circ}$ (kcal mol <sup>-1</sup> )
	Cyclopenta-Phenalene-Furan C16H8O	3	71.0	0.10	66.8
	Benzo[4,5]naphtha[a- 2,3]furan C16H10O	6	21.6	0.18	30.6
	Benzene-naphthalene-furan C16H10O	6	25.8	0.18	25.3
	Naphthalene-benzene-furan2 C16H10O	6	30.2	0.20	26.9
	Phenanthren-furan2 C16H10O	5	31.4	0.18	31.5
	Phenanthrene[9,10-c]furan C16H10O	4	39.2	0.18	39.7
	C16H10O_5	5	31.7	0.14	33.8
	C16H10O_6	4	42.4	0.20	45.2
	C16H10O_7	5	33.7	0.18	32.4
	C18H10O_1	6	38.0	0.15	37.9
	C18H10O_2	6	35.9	0.15	36.3
	C18H10O_3	7	51.5	0.15	54.1

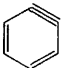
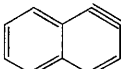
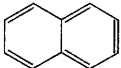
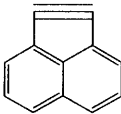
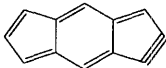
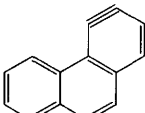
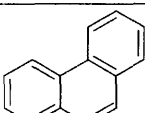
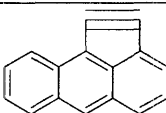
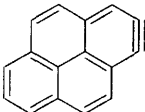
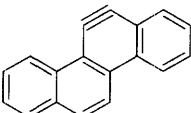
Structure	Name Formula	Kekulé Count	$\Delta H_{f,\text{homo}}^{\circ}$ (kcal mol <sup>-1</sup> )	weight	$\Delta H_{f,\text{est}}^{\circ}$ (kcal mol <sup>-1</sup> )
	C18H10O_4	5	49.5	0.15	46.9
	C20H10O_1	6	54.8	0.13	52.1
	C20H12O_1	10	41.3	0.15	38.6
	C22H10O	14	70.3	0.12	68.1
	C22H12O_1	8	62.8	0.12	65.9

**Table B.4:** PAHs with the furan substructure and with triple bonds included in the development of the estimation method. The  $\Delta H_{f,\text{homo}}^{\circ}$  listed here were calculated using the homodesmotic reaction scheme (see main text). The enthalpies of formation estimated through the bond-centered group additivity method proposed in this work are given in the last column

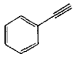
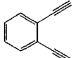
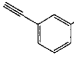
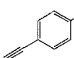
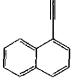
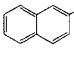
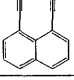
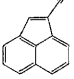
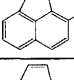
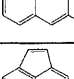
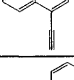
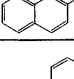
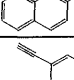
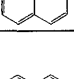
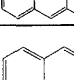

Structure	Name Formula	Kekulé Count	$\Delta H_{f,\text{homo}}^{\circ}$ (kcal mol <sup>-1</sup> )	weight	$\Delta H_{f,\text{est}}^{\circ}$ (kcal mol <sup>-1</sup> )
	C4H2O	1	130.1	0.22	129.6
	C8H4O	2	136.8	0.18	137.3

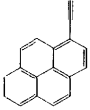
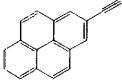
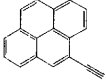
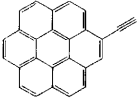


**Table B.5:** PAHs with triple bonds included in the development of the estimation method. The  $\Delta H_{f, \text{homo}}^{\circ}$  listed here were calculated using the homodesmotic reaction scheme (see main text). The enthalpies of formation estimated through the bond-centered group additivity method proposed in this work are given in the last column

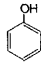
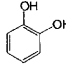
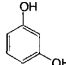
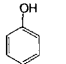
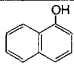
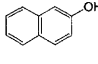
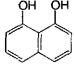
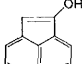
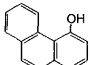
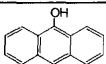
Structure	Name Formula	Kekulé Count	$\Delta H_{f, \text{homo}}^{\circ}$ (kcal mol <sup>-1</sup> )	weight	$\Delta H_{f, \text{est}}^{\circ}$ (kcal mol <sup>-1</sup> )
	Benzene C <sub>6</sub> H <sub>4</sub>	2	106.6	0.50	106.9
	Benzo[1,2]benzynes C <sub>10</sub> H <sub>6</sub>	3	121.6	0.33	121.6
	Benzo[2,3]benzynes C <sub>10</sub> H <sub>6</sub>	3	124.1	0.33	123.5
	Acenaphthynes C <sub>12</sub> H <sub>6</sub>	3	173.1	0.13	173.1
	AI5 C <sub>12</sub> H <sub>6</sub>	2	208.4	0.08	208.4
	Phenanthr-3,4-yne C <sub>14</sub> H <sub>8</sub>	5	131.8	0.22	131.1
	Phenanthr-9,10-yne C <sub>14</sub> H <sub>8</sub>	5	132.0	0.22	131.5
	CI5 C <sub>16</sub> H <sub>8</sub>	4	192.6	0.12	186.9
	Pyren-1,2-yne C <sub>16</sub> H <sub>8</sub>	6	142.7	0.19	143.1
	Chrys-12-yne C <sub>18</sub> H <sub>10</sub>	8	143.3	0.14	145.1

**Table B.6:** Acetylene substituted PAHs included in the development of the estimation method. The  $\Delta H_{f,\text{homo}}^{\circ}$  listed here were calculated using the homodesmotic reaction scheme (see main text). The enthalpies of formation estimated through the bond-centered group additivity method proposed in this work are given in the last column

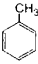
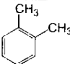
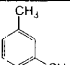
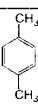
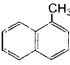
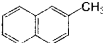
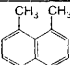
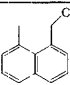
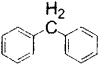
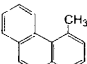
Structure	Name Formula	$\Delta H_{f,\text{homo}}^{\circ}$ (kcal mol <sup>-1</sup> )	weight	$\Delta H_{f,\text{est}}^{\circ}$ (kcal mol <sup>-1</sup> )
	Phenylacetylene C <sub>8</sub> H <sub>6</sub>	73.3	2.00	73.3
	1,2-Diacetylphenyl C <sub>10</sub> H <sub>6</sub>	128.0	0.67	128.0
	1,3-Diacetylphenyl C <sub>10</sub> H <sub>6</sub>	127.3	0.67	126.8
	1,4-Diacetylphenyl C <sub>10</sub> H <sub>6</sub>	126.7	0.67	126.8
	1-Acetylnaphthalene C <sub>12</sub> H <sub>8</sub>	89.5	0.17	89.4
	2-Acetylnaphthalene C <sub>12</sub> H <sub>8</sub>	89.4	0.17	89.5
	1,8-Diacetylnaphthalene C <sub>14</sub> H <sub>8</sub>	149.6	0.17	149.6
	1-Acetylacenaphthalene C <sub>14</sub> H <sub>8</sub>	113.2	0.17	113.2
	3-Acetylacenaphthalene C <sub>14</sub> H <sub>8</sub>	115.1	0.33	115.5
	4-Acetylacenaphthalene C <sub>14</sub> H <sub>8</sub>	115.8	0.33	115.6
	5-Acetylacenaphthalene C <sub>14</sub> H <sub>8</sub>	114.9	0.40	115.5
	1-Acetylphenanthrene C <sub>16</sub> H <sub>10</sub>	102.0	0.40	101.6
	2-Acetylphenanthrene C <sub>16</sub> H <sub>10</sub>	101.6	0.24	101.7
	4-Acetylphenanthrene C <sub>16</sub> H <sub>10</sub>	106.5	0.24	106.5
	1-Acetylanthracene C <sub>16</sub> H <sub>10</sub>	109.4	0.24	109.4
	2-Acetylanthracene C <sub>16</sub> H <sub>10</sub>	109.3	2.00	109.5

Structure	Name Formula	$\Delta H_{f, \text{homo}}^{\circ}$ (kcal mol <sup>-1</sup> )	weight	$\Delta H_{f, \text{est}}^{\circ}$ (kcal mol <sup>-1</sup> )
	1-Acetylnaphthalene C18H10	106.3	0.67	107.3
	2-Acetylnaphthalene C18H10	106.9	0.67	107.4
	4-Acetylnaphthalene C18H10	106.8	0.67	107.3
	Acetyl-coronene C26H12	128.6	0.13	128.5

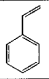
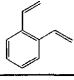
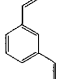
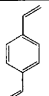
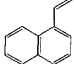
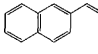
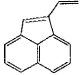
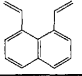
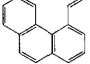
**Table B.7:** Hydroxyl substituted PAHs included in the development of the estimation method. The  $\Delta H_{f, \text{homo}}^{\circ}$  listed here were calculated using the homodesmotic reaction scheme (see main text). The enthalpies of formation estimated through the bond-centered group additivity method proposed in this work are given in the last column

Structure	Name Formula	$\Delta H_{f, \text{homo}}^{\circ}$ (kcal mol <sup>-1</sup> )	weight	$\Delta H_{f, \text{est}}^{\circ}$ (kcal mol <sup>-1</sup> )
	Phenol C <sub>6</sub> H <sub>6</sub> O	-23.0	2.00	-23.1
	1,2-Benzenediol C <sub>6</sub> H <sub>6</sub> O <sub>2</sub>	-66.8	0.67	-66.5
	1,3-Benzenediol (Resorcinol) C <sub>6</sub> H <sub>6</sub> O <sub>2</sub>	-66.5	0.67	-66.8
	1,4-Benzenediol (Hydroquinone) C <sub>6</sub> H <sub>6</sub> O <sub>2</sub>	-64.2	0.67	-63.2
	Naphthol-1 C <sub>10</sub> H <sub>8</sub> O	-7.0	0.67	-6.6
	Naphthol-2 C <sub>10</sub> H <sub>8</sub> O	-7.2	0.67	-6.9
	1,8-Naphthalediol C <sub>10</sub> H <sub>8</sub> O <sub>2</sub>	-52.3	0.40	-52.3
	Acenaphthalen-1-ol C <sub>12</sub> H <sub>8</sub> O	18.9	0.17	18.9
	Phenanthrol-4 C <sub>14</sub> H <sub>10</sub> O	7.6	0.33	7.6
	Anthracenol-9 C <sub>14</sub> H <sub>10</sub> O	14.4	0.40	13.4

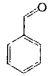
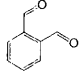
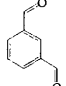
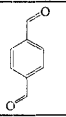
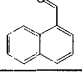
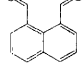
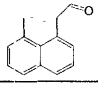
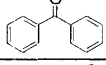
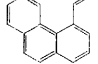
**Table B.8:** Methyl substituted PAHs included in the development of the estimation method. The  $\Delta H_{f, \text{homo}}^{\circ}$  listed here were calculated using the homodesmotic reaction scheme (see main text). The enthalpies of formation estimated through the bond-centered group additivity method proposed in this work are given in the last column

Structure	Name Formula	$\Delta H_{f, \text{homo}}^{\circ}$ (kcal mol <sup>-1</sup> )	weight	$\Delta H_{f, \text{est}}^{\circ}$ (kcal mol <sup>-1</sup> )
	Toluene C7H8	12.0	2.00	11.5
	C8H10	5.2	0.67	6.3
	C8H10	4.1	0.67	3.2
	C8H10	4.1	0.67	3.2
	1-Methyl-Naphthalene C11H10	29.3	0.67	30.3
	2-Methyl-Naphthalene C11H10	27.9	0.67	27.7
	1,8-Dimethyl-Naphthalene C12H12	29.1	0.40	17.5
	1-Methyl-Acenaphthalene C13H10	53.1	0.17	52.7
	Diphenylmethane C13H12	41.3	0.93	40.5
	4-Methyl-Phenanthrene C15H12	47.7	0.33	48.0

**Table B.9:** Ethylene substituted PAHs included in the development of the estimation method. The  $\Delta H_{f,\text{homo}}^{\circ}$  listed here were calculated using the homodesmotic reaction scheme (see main text). The enthalpies of formation estimated through the bond-centered group additivity method proposed in this work are given in the last column

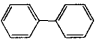
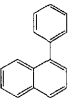
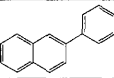
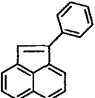
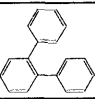
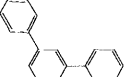
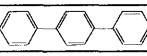
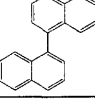
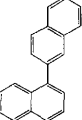
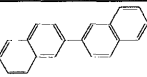
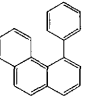
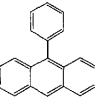
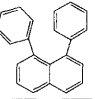
Structure	Name Formula	$\Delta H_{f,\text{homo}}^{\circ}$ (kcal mol <sup>-1</sup> )	weight	$\Delta H_{f,\text{est}}^{\circ}$ (kcal mol <sup>-1</sup> )
	Styrene C <sub>8</sub> H <sub>8</sub>	35.1	2.00	34.7
	1,2-diethyl-Benzene C <sub>10</sub> H <sub>10</sub>	53.6	0.67	53.6
	1,3-diethyl-Benzene C <sub>10</sub> H <sub>10</sub>	50.6	0.67	49.7
	1,4-diethyl-Benzene C <sub>10</sub> H <sub>10</sub>	50.1	0.67	49.7
	1-ethyl-Naphthalene C <sub>12</sub> H <sub>10</sub>	53.9	0.67	53.6
	2-ethyl-Naphthalene C <sub>12</sub> H <sub>10</sub>	51.0	0.67	50.9
	1-ethyl-Acenaphthalene C <sub>14</sub> H <sub>10</sub>	75.8	0.17	75.9
	1,8-diethyl-Naphthalene C <sub>14</sub> H <sub>12</sub>	75.3	0.40	74.4
	4-ethyl-Phenanthrene C <sub>16</sub> H <sub>12</sub>	70.3	0.33	71.2

**Table B.10:** Aldehyde substituted PAHs included in the development of the estimation method. The  $\Delta H_{f, \text{homo}}^{\circ}$  listed here were calculated using the homodesmic reaction scheme (see main text). The enthalpies of formation estimated through the bond-centered group additivity method proposed in this work are given in the last column

Structure	Name Formula	$\Delta H_{f, \text{homo}}^{\circ}$ (kcal mol <sup>-1</sup> )	weight	$\Delta H_{f, \text{est}}^{\circ}$ (kcal mol <sup>-1</sup> )
	Benzaldehyde C7H6O	-8.8	1.00	-9.2
	C8H6O2	-34.0	0.40	-34.0
	C8H6O2	-37.2	0.40	-37.2
	C8H6O2	-36.9	0.40	-36.9
	1-Naphthalenecarboxaldehyde C11H8O	7.6	0.50	9.6
	1,8-Naphthalenedicarboxaldehyde C12H8O2	-12.5	0.40	
	Aldehyde_1_acenaphthalene C13H8O	32.1	0.15	32.0
	Benzophenone C13H10O	11.9 <sup>a</sup>	0.50	22.3
	4-Aldehyde-Phenanthrene C15H10O	28.7	0.29	27.3

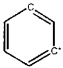
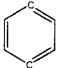
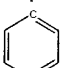
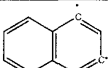
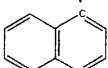
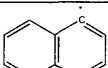
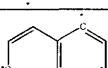
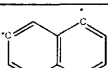
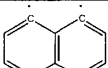
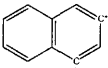
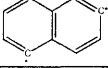
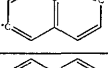
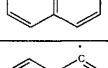
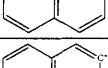
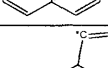
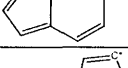
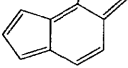
<sup>a</sup> Experimental value as reported in the NIST webbook: <http://webbook.nist.gov/chemistry/>

**Table B.11:** Biarenes included in the development of the estimation method. The  $\Delta H_{f, \text{homo}}^{\circ}$  listed here were calculated using the homodesmotic reaction scheme (see main text). The enthalpies of formation estimated through the bond-centered group additivity method proposed in this work are given in the last column

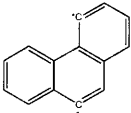
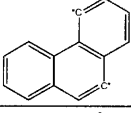
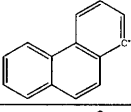
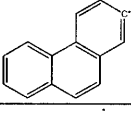
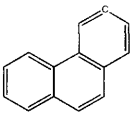
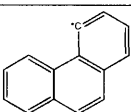
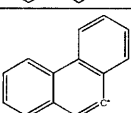
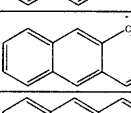
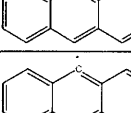
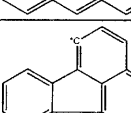
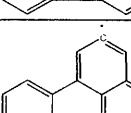
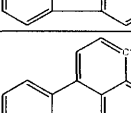
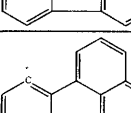
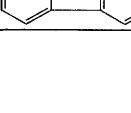
Structure	Name Formula	$\Delta H_{f, \text{homo}}^{\circ}$ (kcal mol <sup>-1</sup> )	weight	$\Delta H_{f, \text{est}}^{\circ}$ (kcal mol <sup>-1</sup> )
	Biphenyl C <sub>12</sub> H <sub>8</sub>	43.5	2.00	43.4
	Benzyl-1-naphthalene C <sub>16</sub> H <sub>12</sub>	62.2	0.67	62.2
	Benzyl-2-naphthalene C <sub>16</sub> H <sub>12</sub>	59.6	0.67	59.6
	Phenyl-1-acenaphthalene C <sub>18</sub> H <sub>12</sub>	84.1	0.17	84.6
	C <sub>18</sub> H <sub>14</sub>	70.8	0.67	68.6
	C <sub>18</sub> H <sub>14</sub>	67.2	0.67	67.0
	C <sub>18</sub> H <sub>14</sub>	67.0	0.67	67.0
	1,1'-binaphthalene C <sub>20</sub> H <sub>14</sub>	79.7	0.40	81.1
	1,2'-binaphthalene C <sub>20</sub> H <sub>14</sub>	78.1	0.40	78.4
	2,2'-binaphthalene C <sub>20</sub> H <sub>14</sub>	75.9	0.40	75.8
	Benzyl-4-Phenanthrene C <sub>20</sub> H <sub>14</sub>	79.9	0.33	79.9
	Benzyl-5-anthracene C <sub>20</sub> H <sub>14</sub>	81.0	0.33	82.3
	1,8-Biphenylnaphthalene C <sub>22</sub> H <sub>16</sub>	95.3	0.40	95.3

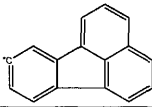
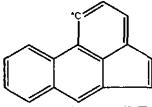
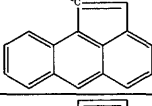
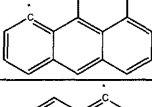
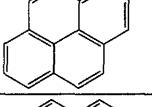
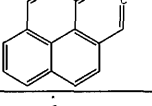
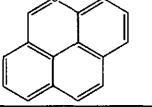
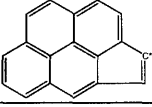
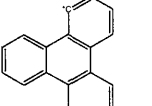
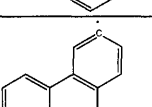
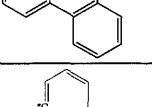
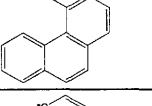


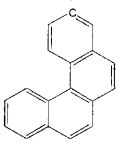
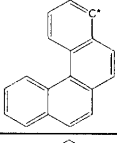
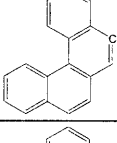
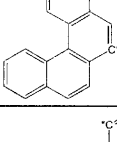
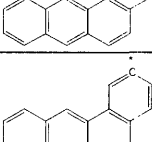
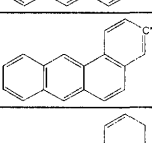
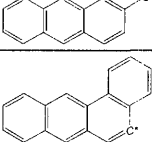
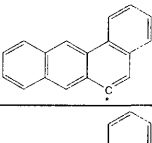
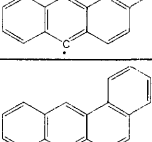
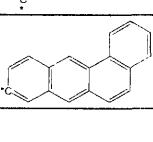


**Table B.12:**  $\sigma$ -radicals included in the development of the BDE values

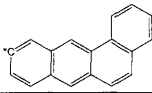
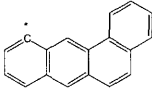
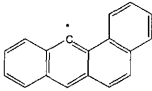
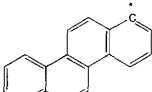
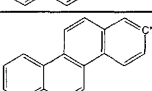
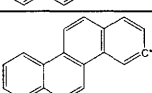
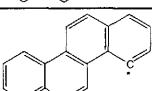
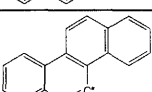
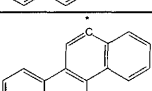
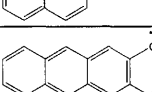
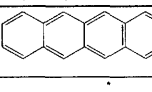
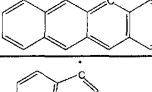
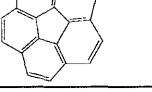
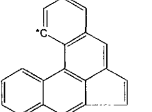
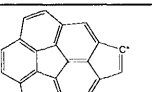
Structure	Name Formula	BDE <sub>homo</sub> (kcal mol <sup>-1</sup> )	weight
	m-Benzyne C <sub>6</sub> H <sub>4</sub>	228.6	0.29
	p-Benzyne C <sub>6</sub> H <sub>4</sub>	227.3	0.29
	Phenyl C <sub>6</sub> H <sub>5</sub>	112.9	0.50
	1,3-Dihydronaphthalene C <sub>8</sub> H <sub>6</sub>	228.9	0.29
	1,4-Dihydronaphthalene C <sub>8</sub> H <sub>6</sub>	227.8	0.29
	1,5-Dihydronaphthalene C <sub>8</sub> H <sub>6</sub>	227.8	0.29
	1,6-Dihydronaphthalene C <sub>8</sub> H <sub>6</sub>	226.1	0.29
	1,7-Dihydronaphthalene C <sub>8</sub> H <sub>6</sub>	226.5	0.29
	1,8-Dihydronaphthalene C <sub>8</sub> H <sub>6</sub>	226.9	0.29
	2,4-Dihydronaphthalene C <sub>8</sub> H <sub>6</sub>	228.9	0.29
	2,5-Dihydronaphthalene C <sub>8</sub> H <sub>6</sub>	226.1	0.29
	2,6-Dihydronaphthalene C <sub>8</sub> H <sub>6</sub>	226.3	0.29
	2,7-Dihydronaphthalene C <sub>8</sub> H <sub>6</sub>	226.4	0.29
	1-Naphthalenyl C <sub>8</sub> H <sub>7</sub>	113.1	0.50
	2-Naphthalenyl C <sub>8</sub> H <sub>7</sub>	113.0	0.50
	1-As-Indacenyl C <sub>12</sub> H <sub>7</sub>	113.3	0.06
	2-As-Indacenyl C <sub>12</sub> H <sub>7</sub>	113.9	0.06

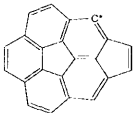
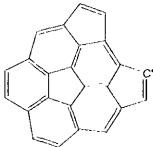
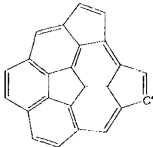
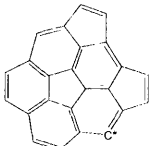
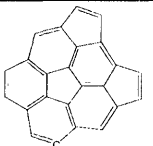
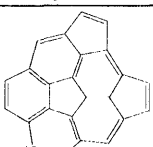
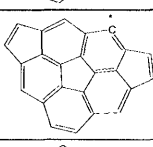
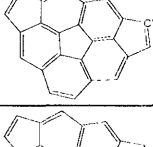
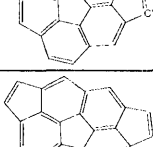
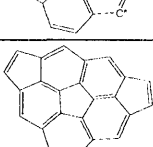
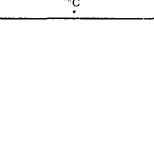
Structure	Name Formula	BDE <sub>homo</sub> (kcal mol <sup>-1</sup> )	weight
	3-As-Indacenyl C <sub>12</sub> H <sub>7</sub>	113.2	0.06
	4-As-Indacenyl C <sub>12</sub> H <sub>7</sub>	110.0	0.06
	1-S-Indacenyl C <sub>12</sub> H <sub>7</sub>	117.0	0.08
	2-S-Indacenyl C <sub>12</sub> H <sub>7</sub>	119.4	0.08
	4-S-Indacenyl C <sub>12</sub> H <sub>7</sub>	113.2	0.08
	1-Acenaphthalenyl C <sub>12</sub> H <sub>7</sub>	117.2	0.15
	3-Acenaphthalenyl C <sub>12</sub> H <sub>7</sub>	112.8	0.15
	4-Acenaphthalenyl C <sub>12</sub> H <sub>7</sub>	112.8	0.15
	5-Acenaphthalenyl C <sub>12</sub> H <sub>7</sub>	113.4	0.15
	1,4-Dihydrophenanthrene C <sub>14</sub> H <sub>8</sub>	225.7	0.20
	1,5-Dihydrophenanthrene C <sub>14</sub> H <sub>8</sub>	224.4	0.20
	2,4-Dihydrophenanthrene C <sub>14</sub> H <sub>8</sub>	226.9	0.20
	2,5-Dihydrophenanthrene C <sub>14</sub> H <sub>8</sub>	224.4	0.20
	3,5-Dihydrophenanthrene C <sub>14</sub> H <sub>8</sub>	224.4	0.20
	4,5-Dihydrophenanthrene C <sub>14</sub> H <sub>8</sub>	225.0	0.20

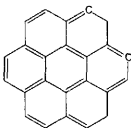
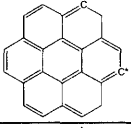
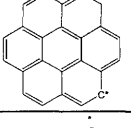
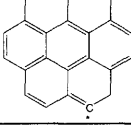
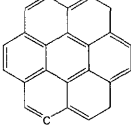
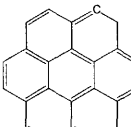
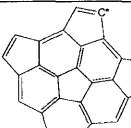
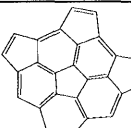

Structure	Name Formula	BDE <sub>homo</sub> (kcal mol <sup>-1</sup> )	weight
	4,9-Dihydrophenanthrene C <sub>14</sub> H <sub>8</sub>	224.2	0.20
	4,10-Dihydrophenanthrene C <sub>14</sub> H <sub>8</sub>	225.8	0.20
	1-Phenanthrenyl C <sub>14</sub> H <sub>9</sub>	113.1	0.29
	2-Phenanthrenyl C <sub>14</sub> H <sub>9</sub>	113.2	0.29
	3-Phenanthrenyl C <sub>14</sub> H <sub>9</sub>	113.0	0.29
	4-Phenanthrenyl C <sub>14</sub> H <sub>9</sub>	111.1	0.29
	9-Phenanthrenyl C <sub>14</sub> H <sub>9</sub>	113.0	0.29
	1-Anthracenyl C <sub>14</sub> H <sub>9</sub>	113.0	0.33
	2-Anthracenyl C <sub>14</sub> H <sub>9</sub>	112.9	0.33
	5-Anthracenyl C <sub>14</sub> H <sub>9</sub>	113.4	0.33
	1-Fluoranthenyl C <sub>16</sub> H <sub>9</sub>	113.0	0.13
	2-Fluoranthenyl C <sub>16</sub> H <sub>9</sub>	112.7	0.13
	3-Fluoranthenyl C <sub>16</sub> H <sub>9</sub>	113.5	0.13
	7-Fluoranthenyl C <sub>16</sub> H <sub>9</sub>	112.9	0.13

Structure	Name Formula	BDE <sub>homo</sub> (kcal mol <sup>-1</sup> )	weight
	8-Fluoranthrenyl C <sub>16</sub> H <sub>9</sub>	113.1	0.13
	1-Acephenanthrenyl C <sub>16</sub> H <sub>9</sub>	112.4	0.11
	1-Aceanthrylenyl C <sub>16</sub> H <sub>9</sub>	116.6	0.11
	10-Aceanthrylenyl C <sub>16</sub> H <sub>9</sub>	112.8	0.11
	1-Pyrenyl C <sub>16</sub> H <sub>9</sub>	113.5	0.24
	2-Pyrenyl C <sub>16</sub> H <sub>9</sub>	112.9	0.24
	4-Pyrenyl C <sub>16</sub> H <sub>9</sub>	113.0	0.24
	3-Cyclopenta[cd]pyrenyl C <sub>18</sub> H <sub>9</sub>	116.8	0.12
	1-Triphenylenyl C <sub>18</sub> H <sub>11</sub>	110.3	0.22
	2-Triphenylenyl C <sub>18</sub> H <sub>11</sub>	113.1	0.22
	1-Benzo[c]phenanthrenyl C <sub>18</sub> H <sub>11</sub>	106.0	0.17
	2-Benzo[c]phenanthrenyl C <sub>18</sub> H <sub>11</sub>	112.7	0.17

Structure	Name Formula	BDE <sub>homo</sub> (kcal mol <sup>-1</sup> )	weight
	3-Benzo[c]phenanthrenyl C <sub>18</sub> H <sub>11</sub>	113.2	0.17
	4-Benzo[c]phenanthrenyl C <sub>18</sub> H <sub>11</sub>	113.0	0.17
	5-Benzo[c]phenanthrenyl C <sub>18</sub> H <sub>11</sub>	113.2	0.17
	6-Benzo[c]phenanthrenyl C <sub>18</sub> H <sub>11</sub>	113.0	0.17
	1-Benz[a]anthracenyl C <sub>18</sub> H <sub>11</sub>	111.1	0.22
	2-Benz[a]anthracenyl C <sub>18</sub> H <sub>11</sub>	112.9	0.22
	3-Benz[a]anthracenyl C <sub>18</sub> H <sub>11</sub>	113.2	0.22
	4-Benz[a]anthracenyl C <sub>18</sub> H <sub>11</sub>	113.1	0.22
	5-Benz[a]anthracenyl C <sub>18</sub> H <sub>11</sub>	112.9	0.22
	6-Benz[a]anthracenyl C <sub>18</sub> H <sub>11</sub>	112.9	0.22
	7-Benz[a]anthracenyl C <sub>18</sub> H <sub>11</sub>	113.4	0.22
	8-Benz[a]anthracenyl C <sub>18</sub> H <sub>11</sub>	113.1	0.22
	9-Benz[a]anthracenyl C <sub>18</sub> H <sub>11</sub>	112.9	0.22

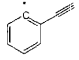
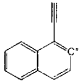
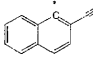
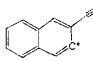
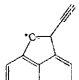
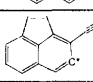
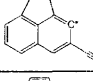
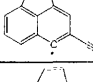
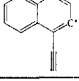
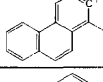
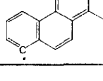
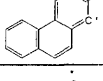
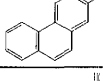
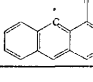
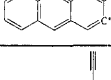
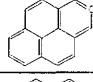
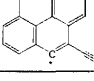
Structure	Name Formula	BDE <sub>homo</sub> (kcal mol <sup>-1</sup> )	weight
	10-Benz[a]anthracenyl C <sub>18</sub> H <sub>11</sub>	112.9	0.22
	11-Benz[a]anthracenyl C <sub>18</sub> H <sub>11</sub>	113.0	0.22
	12-Benz[a]anthracenyl C <sub>18</sub> H <sub>11</sub>	111.4	0.22
	1-Chrysenyl C <sub>18</sub> H <sub>11</sub>	113.2	0.17
	2-Chrysenyl C <sub>18</sub> H <sub>11</sub>	113.3	0.17
	3-Chrysenyl C <sub>18</sub> H <sub>11</sub>	113.0	0.17
	4-Chrysenyl C <sub>18</sub> H <sub>11</sub>	110.8	0.17
	5-Chrysenyl C <sub>18</sub> H <sub>11</sub>	110.8	0.17
	12-Chrysenyl C <sub>18</sub> H <sub>11</sub>	113.1	0.17
	1-Naphthacenyl C <sub>18</sub> H <sub>11</sub>	112.9	0.25
	2-Naphthacenyl C <sub>18</sub> H <sub>11</sub>	112.8	0.25
	5-Naphthacenyl C <sub>18</sub> H <sub>11</sub>	113.3	0.25
	1-Corannulenyl C <sub>20</sub> H <sub>9</sub>	112.4	0.15
	1-Benz[a]acephenanthrylenyl C <sub>20</sub> H <sub>11</sub>	106.3	0.09
	1-Cyclopenta[bc]corannulen-1-yl C <sub>22</sub> H <sub>9</sub>	116.6	0.08

Structure	Name Formula	BDE <sub>homo</sub> (kcal mol <sup>-1</sup> )	weight
	2-Cyclopenta[bc]corannulen-3-yl C <sub>22</sub> H <sub>9</sub>	112.6	0.08
	Dicyclopenta[bc,ef]corannulen-2-yl C <sub>24</sub> H <sub>9</sub>	116.6	0.05
	Dicyclopenta[bc,ef]corannulen-1-yl C <sub>24</sub> H <sub>9</sub>	116.5	0.05
	Dicyclopenta[bc,ef]corannulen-5-yl C <sub>24</sub> H <sub>9</sub>	112.5	0.05
	Dicyclopenta[bc,ef]corannulen-6-yl C <sub>24</sub> H <sub>9</sub>	112.2	0.05
	Dicyclopenta[bc,ef]corannulen-7-yl C <sub>24</sub> H <sub>9</sub>	112.3	0.05
	Dicyclopenta[bc,hi]corannulen-3-yl C <sub>24</sub> H <sub>9</sub>	112.5	0.06
	Dicyclopenta[bc,hi]corannulen-2-yl C <sub>24</sub> H <sub>9</sub>	116.6	0.06
	Dicyclopenta[bc,hi]corannulen-1-yl C <sub>24</sub> H <sub>9</sub>	116.7	0.06
	Dicyclopenta[bc,hi]corannulen-7-yl C <sub>24</sub> H <sub>9</sub>	112.6	0.06
	Dicyclopenta[bc,hi]corannulen-8-yl C <sub>24</sub> H <sub>9</sub>	112.1	0.06


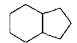
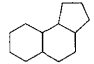
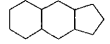
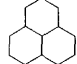
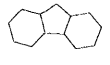
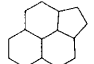
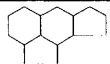
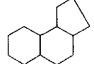

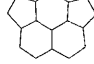
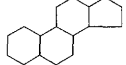
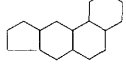
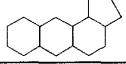
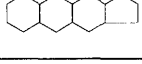
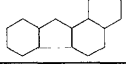
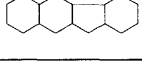
Structure	Name Formula	BDE <sub>homo</sub> (kcal mol <sup>-1</sup> )	weight
	1,3-dihydrocoronene C <sub>24</sub> H <sub>10</sub>	226.8	0.11
	1,4-dihydrocoronene C <sub>24</sub> H <sub>10</sub>	226.8	0.11
	1,5-dihydrocoronene C <sub>24</sub> H <sub>10</sub>	226.5	0.11
	16-dihydrocoronene C <sub>24</sub> H <sub>10</sub>	226.6	0.11
	17-dihydrocoronene C <sub>24</sub> H <sub>10</sub>	226.6	0.11
	1-Coroneryl C <sub>24</sub> H <sub>11</sub>	113.2	0.13
	Tricyclopenta[bc,ef,hi]corannulen-4-yl C <sub>26</sub> H <sub>9</sub>	116.5	0.03
	Tricyclopenta[bc,ef,hi]corannulen-1-yl C <sub>26</sub> H <sub>9</sub>	116.6	0.03
	Tricyclopenta[bc,ef,hi]corannulen-8-yl C <sub>26</sub> H <sub>9</sub>	112.1	0.03

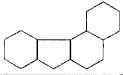
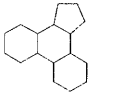
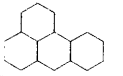
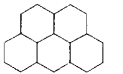
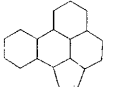
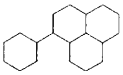
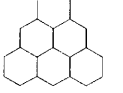
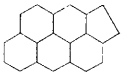
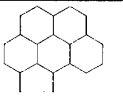


**Table B.13:** Acetylene substituted  $\sigma$ -radicals included in this study

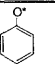
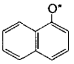
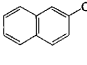
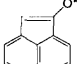
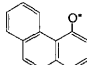
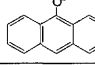
Structure	Name Formula	BDE <sub>homo</sub> (kcal mol <sup>-1</sup> )	weight
	Phenylacetylen-2-yl C <sub>8</sub> H <sub>5</sub>	114.2	0.50
	1-Acetylnaphthalen-2-yl C <sub>12</sub> H <sub>7</sub>	114.0	0.33
	2-Acetylnaphthalen-1-yl C <sub>12</sub> H <sub>7</sub>	114.3	0.33
	2-Acetylnaphthalen-3-yl C <sub>12</sub> H <sub>7</sub>	114.2	0.33
	1-Acetylnaphthalen-2-yl C <sub>14</sub> H <sub>7</sub>	118.2	0.13
	2-Acetylnaphthalen-3-yl C <sub>14</sub> H <sub>7</sub>	114.7	0.13
	3-Acetylnaphthalen-2-yl C <sub>14</sub> H <sub>7</sub>	114.6	0.13
	3-Acetylnaphthalen-4-yl C <sub>14</sub> H <sub>7</sub>	114.6	0.13
	4-Acetylnaphthalen-3-yl C <sub>14</sub> H <sub>7</sub>	113.9	0.13
	Acetyl-1-phenanthren-2-yl C <sub>16</sub> H <sub>9</sub>	114.3	0.22
	Acetyl-1-phenanthren-8-yl C <sub>16</sub> H <sub>9</sub>	113.3	0.22
	Acetyl-2-phenanthren-1-yl C <sub>16</sub> H <sub>9</sub>	114.4	0.22
	Acetyl-2-phenanthren-3-yl C <sub>16</sub> H <sub>9</sub>	114.2	0.22
	Acetyl-1-anthracen-9-yl C <sub>16</sub> H <sub>9</sub>	113.9	0.25
	Acetyl-2-anthracen-3-yl C <sub>16</sub> H <sub>9</sub>	114.2	0.25
	Acetyl-1-pyren-2-yl C <sub>18</sub> H <sub>9</sub>	114.0	0.18
	Acetyl-4-pyren-5-yl C <sub>18</sub> H <sub>9</sub>	114.1	0.18

**Table B.14:** Unsubstituted  $\pi$ -radicals included in this study. Only the sigma bonds are shown in the molecular structure. These radicals have a free electron that moves freely over the  $\pi$ -cloud over the  $\sigma$ -bonds framework.

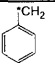
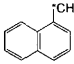
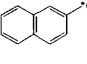
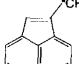
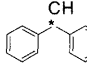
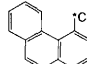
Structure	Name Formula	Kekulé Count	BDE (kcal/mol)	weight
	Cyclopentadiene_pi C5H5	5	63.2	0.20
	Indenyl C9H7	11	65.7	0.17
	Cyclopenta[a]naphthalene C13H9	21	80.0	0.13
	Cyclopenta[b]naphthalene C13H9	19	78.9	0.14
	Phenalene_pi C13H9	20	62.3	0.07
	Fluorene C13H9	22	73.8	0.14
	C15H9	33	87.6	0.12
	Cyclopenta[d]acenaphthalene C15H9	25	100.8	0.08
	Cyclopenta[e]acenaphthalene C15H9	27	104.4	0.08
	Cyclopenta[def]phenanthrene C15H9	29	90.2	0.12
	C17H9	46	119.9	0.08
	Cyclopenta[a]phenanthrene C17H11	37	92.0	0.10
	Cyclopenta[b]phenanthrene C17H11	35	94.1	0.12
	Cyclopenta[a]anthracene C17H11	33	99.6	0.12
	Cyclopenta[b]anthracene C17H11	29	97.0	0.13
	Benzo[a]fluorene C17H11	41	83.2	0.10
	Benzo[b]fluorene C17H11	36	85.4	0.12

Structure	Name Formula	Kekulé Count	BDE (kcal/mol)	weight
	Benzo[c]fluorene C17H11	40	86.0	0.10
	Cyclopenta[1]phenanthrene C17H11	40	91.1	0.08
	Benzanthrene_pi C17H11	36	75.9	0.07
	C19H11	52	80.5	0.06
	Benzo[f,g]aceanthrylene C19H11	62	97.3	0.10
	Benzo[cd]fluoranthrene C19H11	65	86.6	0.10
	Naphtho[lmno]acephenanthr ene C21H11	52	107.9	0.10
	Cyclopenta[cd]benzo[jk]pyre ne C21H11	76	105.8	0.10
	Naphtho[fghi]aceanthrylene C21H11	86	105.8	0.04

**Table B.15:** Oxyl substituted  $\pi$ -radicals

Structure	Name Formula	$\Delta H_{f, \text{homo}}^{\circ}$ (kcal mol <sup>-1</sup> )	BDE (kcal mol <sup>-1</sup> )	weight
	Phenoxy C <sub>6</sub> H <sub>5</sub> O	12.9	88.1	0.33
	1-Naphthoxy C <sub>10</sub> H <sub>7</sub> O	22.5	81.6	0.25
	2-Naphthoxy C <sub>10</sub> H <sub>7</sub> O	26.8	86.1	0.25
	1-Acenaphthoxy C <sub>12</sub> H <sub>7</sub> O	40.4	73.6	0.12
	Phenanthroxy-4 C <sub>14</sub> H <sub>9</sub> O	37.7	82.2	0.18
	Anthracenoxi-5 C <sub>14</sub> H <sub>9</sub> O	32.9	70.7	0.20

**Table B.16:** Methylene substituted  $\pi$ -radicals

Structure	Name Formula	$\Delta H_{f, \text{homo}}^{\circ}$ (kcal mol <sup>-1</sup> )	BDE (kcal mol <sup>-1</sup> )	weight
	Benzyl radical C <sub>7</sub> H <sub>7</sub>	49.5	89.7	0.33
	1-Methyl-Naphthalene C <sub>11</sub> H <sub>9</sub>	65.3	88.1	0.25
	2-Methyl-Naphthalene C <sub>11</sub> H <sub>9</sub>	64.7	88.9	0.25
	1-Methyl-Acenaphthalene C <sub>13</sub> H <sub>9</sub>	81.8	90.5	0.12
	Diphenylmethane C <sub>13</sub> H <sub>11</sub>	101.8	112.7	0.39
	4-Methyl-Phenanthrene C <sub>15</sub> H <sub>11</sub>	84.0	88.4	0.18

## Appendix C

# Examples of Thermochemical Properties Estimation Using BCGA

### C.1 PAHs with Five-and Six-Membered Rings

Table C.1: Estimation of the thermochemical properties using BCGA for the PAHs in Figure 2-1. In the first rows of this table the number of Kekulé structures and the symmetry number of each of the PAHs are shown. Next the number of each of the bonds contained in the PAHs are given. The  $\Delta H_{f,\text{est}}^\circ$  is the sum of the contributions of each of the bonds and of the term accounting for the resonance energy ( $-16.59\ln(K)$ ).  $\Delta H_{f,\text{est}}^\circ$  in kcal mol<sup>-1</sup>,  $S_{298}^\circ$  and  $C_p^\circ$  in cal K<sup>-1</sup> mol<sup>-1</sup>.

	(1)	(2)	(3)	(4)	(5)	(7)	(8)	(9)	(10)
# K	11	10	13	34	50	2	8	7	8
Symmetry	1	2	1	2	4	2	2	2	2
AA5	-	-	-	-	-	4	-	1	1
AA6	8	6	9	8	6	1	6	5	4
AB5	-	-	-	-	-	2	-	2	2
AB6	4	12	6	8	16	2	6	2	6
AC5	-	-	-	-	-	2	-	-	-
AC6	4	-	4	4	-	-	2	4	2
CC5	-	-	-	-	-	-	1	2	1
CC6	2	-	3	2	-	1	-	-	-
BB65	-	-	-	-	-	-	-	-	-
BB66	-	-	-	-	-	-	-	-	-
BC65	-	-	-	-	-	2	-	-	-
BC66	-	-	3	-	-	-	-	-	-
CC65	-	-	-	-	-	-	-	1	-
CC66	1	-	1	1	-	-	-	-	-
DD65	-	-	-	-	-	-	2	-	2
DD6666	1	3	-	6	11	-	-	-	-
DD6665	-	-	-	-	-	-	-	-	-
DD6665o	-	-	-	-	-	-	-	-	-
DD6655	-	-	-	-	-	-	-	1	1
DD6655o	-	-	-	-	-	-	-	-	-
DD6655oo	-	-	-	-	-	-	-	-	-
BD65	-	-	-	-	-	-	-	2	2
BD66	2	6	-	4	8	-	3	-	2
CD65	-	-	-	-	-	-	2	2	2
CD66	2	-	-	2	-	-	-	-	-
$\Delta H_{f,\text{est}}^\circ$	69.7	81.5	82.4	89.6	100	86.2	86.1	102.8	127.3
$S_{298}^\circ$	113.6	113.8	122.7	130.6	133.2	88.7	101.1	104	105.7
$C_{p,300}^\circ$	61.7	65.7	69.6	82.8	91.3	38.2	53.9	54.5	58.6

*continued*

Table C.1: *continued*

	(11)	(12)	(13)	(14)	(15)	(16)	(17)	(18)	(19)	(20)
# K	8	8	12	9	13	14	23	22	44	35
Symmetry	2	1	1	2	1	1	1	5	2	3
AA5	1	-	1	1	2	1	-	5	-	-
AA6	6	8	3	6	1	5	6	-	6	6
AB5	2	-	2	2	4	2	-	-	-	-
AB6	6	4	10	4	10	8	8	-	8	6
AC5	-	-	-	-	-	-	-	10	-	-
AC6	2	4	-	4	-	2	4	-	4	6
CC5	-	2	-	-	-	-	2	-	-	3
CC6	2	1	-	2	-	1	-	5	2	-
BB65	-	-	-	-	-	-	-	-	-	-
BB66	-	-	-	-	-	-	-	-	-	-
BC65	-	-	-	-	-	-	-	-	-	-
BC66	2	1	-	-	-	-	-	-	-	-
CC65	-	1	-	-	-	-	1	-	-	-
CC66	-	-	-	-	-	-	-	-	-	-
DD65	-	-	5	-	5	-	5	5	10	6
DD6666	-	-	-	-	-	3	-	-	-	-
DD6665	-	-	-	1	-	1	-	-	-	-
DD6665o	-	-	-	-	-	-	-	-	-	-
DD6655	-	-	-	-	-	-	-	-	-	3
DD6655o	-	-	1	-	2	-	1	5	-	-
DD6655oo	-	-	-	-	-	-	-	-	1	-
BD65	2	-	2	2	4	2	-	-	-	-
BD66	-	1	4	1	3	3	4	-	4	3
CD65	-	2	-	-	-	-	2	10	-	6
CD66	1	-	-	4	-	2	-	-	4	-
$\Delta H_{f,est}^{\circ}$	92.4	87.1	153.4	101.2	189	101.8	157.9	272.3	191.6	220.5
$S_{298}^{\circ}$	111.4	113.1	109.1	116.6	112.7	119.9	123.1	120.8	126.6	128.3
$C_{p,300}^{\circ}$	62	62	62.6	66.4	67.2	70.7	75	82	83.7	84

## C.2 Furans

Furan  
Chemical Formula: C4H4O  
Symmetry: 2  
# Kekule Structures: 1  
Groups  
A05\_A  
AA5  
AA5  
AA5  
A05\_A  
Hf(298K)= -8.32 kcal/mol  
S(298K)= 63.95 cal/(mol K)  
Cp(300K)= 17.02 cal/(mol K)

Benzo[b]furan  
Chemical Formula: C8H6O  
Symmetry: 1  
# Kekule Structures: 2  
Groups  
B05\_B  
BB6500  
AB5  
AA5  
A05\_A  
AB6  
AA6  
AA6  
AA6  
AB6  
Hf(298K)= 4.15 kcal/mol  
S(298K)= 78.76 cal/(mol K)  
Cp(300K)= 29.43 cal/(mol K)

Benzo[c]furan  
Chemical Formula: C8H6O  
Symmetry: 2  
# Kekule Structures: 1  
Groups  
A05\_B  
AB5  
BB6500  
AB5  
A05\_B

AB6  
AA6  
AA6  
AA6  
AB6  
Hf(298K)= 18.32 kcal/mol  
S(298K)= 77.78 cal/(mol K)  
Cp(300K)= 29.83 cal/(mol K)

Dibenzofuran  
Chemical Formula: C12H8O  
Symmetry: 2  
# Kekule Structures: 4  
Groups  
B05\_C3  
BC6500\_1r5  
B05\_C3  
CC5  
BC6500\_1r5  
AB6  
AA6  
AA6  
AA6  
AC6  
AC6  
AA6  
AA6  
AA6  
AB6  
Hf(298K)= 10.36 kcal/mol  
S(298K)= 90.94 cal/(mol K)  
Cp(300K)= 42.02 cal/(mol K)

Naphtho[1,2-b]furan  
Chemical Formula: C12H8O  
Symmetry: 1  
# Kekule Structures: 3  
Groups  
AC6  
BC6600\_1r  
AB6  
AA6  
AA6  
AA6  
AB6



AA6  
 AB6  
 BC6500\_1r6  
 CC6  
 AB5  
 AA5  
 A05\_A  
 Cb0  
 Hf(298K)= 13.56 kcal/mol  
 S(298K)= 99.76 cal/(mol K)  
 Cp(300K)= 42.93 cal/(mol K)

Naphtho[2,1-b]furan  
 Chemical Formula: C12H8O  
 Symmetry: 1

# Kekule Structures: 3

Groups

AC6  
 BC6600\_1r  
 AB6  
 AA6  
 AA6  
 AA6  
 AB6  
 AA6  
 AB6  
 BC6500\_1r6  
 CC6  
 B05\_C2  
 A05\_A  
 AA5  
 AC5  
 Hf(298K)= 14.80 kcal/mol  
 S(298K)= 92.67 cal/(mol K)  
 Cp(300K)= 42.68 cal/(mol K)

Naphtho[2,1-c]furan  
 Chemical Formula: C12H8O  
 Symmetry: 1

# Kekule Structures: 2

Groups

AC6  
 BC6600\_1r  
 AB6  
 AA6

AA6  
 AA6  
 AB6  
 AA6  
 AB6  
 BC6500\_1r6  
 CC6  
 AB5  
 A05\_B  
 A05\_C  
 AX5

Hf(298K)= 25.43 kcal/mol  
 S(298K)= 92.42 cal/(mol K)  
 Cp(300K)= 42.67 cal/(mol K)

Naphtho[2,3-b]furan  
 Chemical Formula: C12H8O  
 Symmetry: 1

# Kekule Structures: 3

Groups

AB6  
 BB6600  
 AB6  
 AA6  
 AA6  
 AA6  
 AB6  
 AB6  
 AB6  
 BB6500  
 AB6  
 AB6  
 B05\_B  
 A05\_A  
 AA5  
 AB5

Hf(298K)= 20.70 kcal/mol  
 S(298K)= 92.20 cal/(mol K)  
 Cp(300K)= 42.50 cal/(mol K)

Phenalene-Furan  
 Chemical Formula: C14H8O  
 Symmetry: 1

# Kekule Structures: 3

Groups

BD6660

DD6665-  
 BD6560  
 AB6  
 AA6  
 AB6  
 BD6560  
 AB6  
 AA6  
 AB6  
 BD6660  
 AB6  
 AA6  
 AA6  
 AB6  
 AB5  
 A05\_B  
 B05\_D  
 Hf(298K)= 38.80 kcal/mol  
 S(298K)= 95.36 cal/(mol K)  
 Cp(300K)= 47.03 cal/(mol K)

Phenanthrene-Furan

Chemical Formula: C14H8O

Symmetry: 2

# Kekule Structures: 5

Groups

BD6560

BD6650

AB6

AA6

AA6

AB6

AB6

AA6

AB6

BD6650

DD6566

AB6

AA6

AA6

AB6

BD6560

B05\_D

B05\_D

Hf(298K)= 37.35

S(298K)= 94.05

Cp(300K)= 46.75

C14H8O\_3

Chemical Formula: C14H8O

Symmetry: 1

# Kekule Structures: 2

Groups

BD6560

CD6650\_1r

AC6

AA6

AA6

AB6

CC6

BC6500\_1r6

AB6

AB6

BD6560

AB5

B05\_D

A05\_B

AB5

AA5

AA5

AC5

Hf(298K)= 58.09 kcal/mol

S(298K)= 97.22 cal/(mol K)

Cp(300K)= 47.95 cal/(mol K)

C14H8O\_4

Chemical Formula: C14H8O

Symmetry: 1

# Kekule Structures: 3

Groups

BD6560

CD6650\_1r

AC6

AA6

AA6

AB6

CC6

BC6500\_1r6

AB6

AB6

BD6560  
 AB5  
 AB5  
 AA5  
 AB5  
 AA5  
 A05\_A  
 Cb0  
 Hf(298K)= 39.04 kcal/mol  
 S(298K)= 103.80 cal/(mol K)  
 Cp(300K)= 48.22 cal/(mol K)

Cyclopenta-Phenalene-Furan  
 Chemical Formula: C16H80  
 Symmetry: 1  
 # Kekule Structures: 3

Groups  
 BD6560  
 DD6665-  
 BD6660  
 AB6  
 AA6  
 AB6  
 DD6665-  
 BD6560

AB6  
 AB6  
 BD6560  
 AB5  
 B05\_D  
 A05\_B  
 AB5  
 AA5  
 AB5  
 BD6560  
 AB6  
 AA6  
 AB6

Hf(298K)= 66.74 kcal/mol  
 S(298K)= 99.59 cal/(mol K)  
 Cp(300K)= 52.36 cal/(mol K)

Benzo[4,5]naphtha[a-2,3]furan  
 Chemical Formula: C16H100  
 Symmetry: 1

# Kekule Structures: 6

Groups

AB6  
 CC6  
 CC6  
 BC6600\_1r  
 AB6  
 AA6  
 AC6  
 AA6  
 AA6  
 AA6

AB6  
 CC5  
 BC6500\_1r5  
 B05\_C3  
 B05\_C1

AB6  
 AA6  
 AA6  
 AA6  
 AC6  
 Hf(298K)= 36.45 kcal/mol  
 S(298K)= 100.66 cal/(mol K)  
 Cp(300K)= 60.06 cal/(mol K)

Benzene-naphthalene-furan  
 Chemical Formula: C16H100

Symmetry: 1

# Kekule Structures: 6

Groups

CC6  
 CC6  
 AC6  
 AA6  
 AB6  
 BC6600\_1r  
 CC5  
 BC6500\_1r5  
 B05\_C3  
 C05\_C3

AB6  
 AA6  
 AA6  
 AA6

AC6  
AC6  
AA6  
AA6  
AA6  
AB6  
Hf(298K)= 28.78 kcal/mol  
S(298K)= 100.74 cal/(mol K)  
Cp(300K)= 59.81 cal/(mol K)

Naphthalene-benzene-furan2

Chemical Formula: C16H100

Symmetry: 1

# Kekule Structures: 6

Groups

AB6

BC6500\_1r5

AC6

CC5

BC6500\_1r5

B05\_C3

B05\_C3

AB6

AB6

BB6600

AB6

AC6

AA6

AA6

AA6

AB6

AA6

AA6

AA6

AB6

Hf(298K)= 26.91 kcal/mol

S(298K)= 105.76 cal/(mol K)

Cp(300K)= 55.09 cal/(mol K)

Phenanthren-furan2

Chemical Formula: C16H100

Symmetry: 1

# Kekule Structures: 5

Groups

AA5

AX5  
CC6500\_2r66  
C05\_C2  
A05\_A  
CC6  
CC6600\_2rs  
CC6  
CC6600\_2rs  
CC6  
AC6  
AA6  
AA6  
AA6  
AC6  
AC6  
AA6  
AA6  
AA6  
AC6  
Hf(298K)= 31.55 kcal/mol  
S(298K)= 106.03 cal/(mol K)  
Cp(300K)= 55.26 cal/(mol K)

Phenanthrene[9,10-c]furan

Chemical Formula: C16H100

Symmetry: 2

# Kekule Structures: 4

Groups

A05\_C

AC5

CC6500\_2r66

AX5

A05\_C

CC6

CC6600\_2rs

CC6

CC6600\_2rs

CC6

AC6

AA6

AA6

AA6

AC6

AC6

AA6

AA6  
AA6  
AC6  
Hf(298K)= 39.67 kcal/mol  
S(298K)= 105.24 cal/(mol K)  
Cp(300K)= 55.41 cal/(mol K)

C16H100\_5  
Chemical Formula: C16H100  
Symmetry: 1  
# Kekule Structures: 5

Groups

AA6  
AA6  
AC6  
BC6600\_1r  
AB6  
AA6  
CC6  
BC6600

AB6  
AA6  
AB6  
CC6  
BC6500\_1r6

AB6  
AA6  
AB6  
AB5  
AA5  
A05\_A  
Cb0

Hf(298K)= 31.70 kcal/mol  
S(298K)= 112.17 cal/(mol K)  
Cp(300K)= 55.88 cal/(mol K)

C16H100\_6  
Chemical Formula: C16H100  
Symmetry: 1  
# Kekule Structures: 4

Groups

AB6  
BB6600  
AB6  
AA6

AA6  
AA6  
AB6  
AB6  
BB6600  
AB6  
AB6  
AB6  
AB6  
BB6500

AB6  
AB6  
AB5

AA5  
A05\_A  
B05\_B

Hf(298K)= 39.56 kcal/mol  
S(298K)= 105.64 cal/(mol K)  
Cp(300K)= 55.57 cal/(mol K)

C16H100\_7  
Chemical Formula: C16H100  
Symmetry: 1  
# Kekule Structures: 5

Groups

AB6  
AA6  
AB6  
BC6600\_1r  
CC6  
BC6600\_1r  
AB6

AB6  
BB6500  
AB6

AC6  
AB5  
AA5  
A05\_A  
B05\_B

AC6  
AA6  
AA6  
AA6  
AB6

Hf(298K)=	32.44	kcal/mol	AA6		
S(298K)=	105.86	cal/(mol K)	AB6		
Cp(300K)=	55.53	cal/(mol K)	BD6660		
			BD6660		
C18H100_1			AB6		
Chemical Formula:	C18H100		AA6		
Symmetry:	1		AA6		
# Kekule Structures:	6		AC6		
Groups			AB6		
AB6			AA6		
AA6			AB6		
AB6			CC6500_2r66		
BD6660			CC6		
DD6666			AC6		
BD6660			AA6		
AB6			AC5		
AB6			AA5		
BC6500_1r6			A05_A		
CC6			C05_C2		
CD6660_1r			Hf(298K)=	36.34	kcal/mol
AB5			S(298K)=	108.46	cal/(mol K)
AA5			Cp(300K)=	59.86	cal/(mol K)
A05_A					
Cb0			C18H100_3		
BD6660			Chemical Formula:	C18H100	
AB6			Symmetry:	1	
AA6			# Kekule Structures:	7	
AA6			Groups		
AB6			DD6566		
AC6			BD6650		
AA6			AB6		
AB6			AA6		
Hf(298K)=	35.82	kcal/mol	AB6		
S(298K)=	116.26	cal/(mol K)	BD6650		
Cp(300K)=	60.50	cal/(mol K)	AB6		
			AB6		
C18H100_2			BC6600_1r		
Chemical Formula:	C18H100		CC6		
Symmetry:	1		CD6560_1r6		
# Kekule Structures:	6		AB6		
Groups			AA6		
CC6			AA6		
CD6660_1r			AA6		
DD6666			AC6		
CD6660_1r			BD6560		

AB6			# Kekule Structures: 6	
AA6			Groups	
AA6			BD6560	
AB6			DD6665-	
B05_D			BD6660	
C05_D			AB6	
Hf(298K)=	47.49	kcal/mol	AA6	
S(298K)=	108.59	cal/(mol K)	AB6	
Cp(300K)=	59.59	cal/(mol K)	DD6666	
			DD6666	
C18H100_4			CD6660_1r	
Chemical Formula:	C18H100		CC6	
Symmetry:	1		CD6560_1r6	
# Kekule Structures:	5		BD6660	
Groups			AB6	
BD6560			AA6	
DD6665-			AA6	
BD6660			AC6	
AB6			BD6660	
AA6			AB6	
AB6			AA6	
CD6660_1r			AB6	
CC6			AB6	
CC600_2rs			AA6	
CC6			AB6	
CD6560_1r6			AB5	
AB5			A05_B	
A05_B			C05_D	
C05_D			Hf(298K)=	
AC6	52.11	kcal/mol	S(298K)=	
AA6	111.21	cal/(mol K)	Cp(300K)=	
AA6	64.50	cal/(mol K)		
AB6				
AC6			C20H120_1	
AA6			Chemical Formula:	
AA6			C20H120	
AA6			Symmetry:	1
AC6			# Kekule Structures:	10
Hf(298K)=	46.90	kcal/mol	Groups	
S(298K)=	109.05	cal/(mol K)	AA6	
Cp(300K)=	59.83	cal/(mol K)	AC6	
			BC6600_1r	
			AB6	
			AA6	
			AA6	
			CC6	
			BC6600_1r	

AB6  
 AA6  
 AB6  
 AB6  
 AC6  
 BC6500\_1r5  
 AB6  
 AC6  
 CC5  
 BC6500\_1r5  
 B05\_C3  
 B05\_C3  
 AB6  
 AA6  
 AA6  
 AA6  
 AC6  
 Hf(298K)= 38.66 kcal/mol  
 S(298K)= 119.42 cal/(mol K)  
 Cp(300K)= 68.12 cal/(mol K)  
  
 C22H100  
 Chemical Formula: C22H100  
 Symmetry: 2  
 # Kekule Structures: 14  
 Groups  
 AB6  
 BD6560  
 DD6665-  
 BD6660  
 AB6  
 AA6  
 DD6566  
 DD6665-  
 DD6666  
 DD6666  
 DD6666  
 BD6660  
 AB6  
 AA6  
 AB6  
 BD6560  
 BD6660  
 AB6  
 AA6

AB6  
 BD6660  
 AB6  
 AA6  
 AB6  
 AB6  
 AA6  
 AB6  
 B05\_D  
 B05\_D  
 Hf(298K)= 68.11 kcal/mol  
 S(298K)= 113.62 cal/(mol K)  
 Cp(300K)= 69.03 cal/(mol K)  
  
 C22H120\_1  
 Chemical Formula: C22H120  
 Symmetry: 1  
 # Kekule Structures: 8  
 Groups  
 AC6  
 CC6600\_3r  
 CC6  
 BC6600\_1r  
 AB6  
 AA6  
 CC6  
 CD6560\_1r6  
 DD6665-  
 CD6660\_1r  
 CC6  
 BD6560  
 AB6  
 AA6  
 AB6  
 BD6660  
 AB6  
 AA6  
 AA6  
 AC6  
 AC6  
 AA6  
 AA6  
 AA6  
 AB6  
 CO5\_D



A05\_B  
 AB5  
 Hf(298K)= 65.84 kcal/mol  
 S(298K)= 121.46 cal/(mol K)  
 Cp(300K)= 72.78 cal/(mol K)

Cp(300K)= 33.29 cal/(mol K)

### C.3 Arynes

Benzyne  
 Chemical Formula: C6H4  
 Symmetry: 2  
 # Kekule Structures: 2  
 Groups  
 Father Cb0 Child I05  
 II6  
 AI6  
 AA6  
 AA6  
 AA6  
 AI6  
 Hf(298K)= 106.93 kcal/mol  
 S(298K)= 68.12 cal/(mol K)  
 Cp(300K)= 20.36 cal/(mol K)

Benzo[2,3]Benzyne  
 Chemical Formula: C10H6  
 Symmetry: 2  
 # Kekule Structures: 3

Groups

AA6  
 AB6  
 AB6  
 AI6  
 II6  
 AI6  
 BB6600

AB6  
 AB6  
 AA6  
 AA6  
 Hf(298K)= 123.48 kcal/mol  
 S(298K)= 81.56 cal/(mol K)  
 Cp(300K)= 33.43 cal/(mol K)

Benzo[1,2]benzyne  
 Chemical Formula: C10H6  
 Symmetry: 1  
 # Kekule Structures: 3  
 Groups  
 AA6  
 AB6  
 AB6  
 AA6  
 AI6  
 II6  
 BB6600  
 BI6  
 AB6  
 AA6  
 AA6  
 Hf(298K)= 121.64 kcal/mol  
 S(298K)= 83.02 cal/(mol K)

Acenaphthyne  
 Chemical Formula: C12H6  
 Symmetry: 2  
 # Kekule Structures: 3

Groups

BD6560  
 BD6650  
 AB6  
 AA6  
 AB6  
 AA6  
 AB6  
 AA6  
 AA6  
 AB6  
 BD6560

BI5  
 II5  
 BI5  
 Hf(298K)= 173.08 kcal/mol  
 S(298K)= 87.34 cal/(mol K)  
 Cp(300K)= 38.46 cal/(mol K)

AI5  
 Chemical Formula: C12H6  
 Symmetry: 1  
 # Kekule Structures: 2  
 Groups  
 AB6  
 BB6500  
 AB6  
 AB6  
 BB6500  
 AB6  
 AB5  
 AI5  
 BI5  
 II5  
 AB5  
 AA5  
 AA5  
 AB5  
 Hf(298K)= 208.41 kcal/mol  
 S(298K)= 93.05 cal/(mol K)  
 Cp(300K)= 40.26 cal/(mol K)

Phenanthry-3,4-yne  
 Chemical Formula: C14H8  
 Symmetry: 1  
 # Kekule Structures: 5  
 Groups  
 AC6  
 BC6600\_1r  
 AB6  
 AA6  
 AA6  
 AA6  
 AB6  
 AA6  
 AB6  
 BC6600\_1r  
 CC6  
 AB6  
 AA6  
 AI6  
 CI6  
 II6  
 Hf(298K)= 131.07 kcal/mol

S(298K)= 96.43 cal/(mol K)  
 Cp(300K)= 46.07 cal/(mol K)

Phenanthr-9,10-yne  
 Chemical Formula: C14H8  
 Symmetry: 2  
 # Kekule Structures: 5  
 Groups  
 AC6  
 BC6600\_1r  
 AB6  
 AA6  
 AA6  
 AA6  
 BI6  
 II6  
 BI6  
 BC6600\_1r  
 CC6  
 AB6  
 AA6  
 AA6  
 AA6  
 AC6  
 Hf(298K)= 131.55 kcal/mol  
 S(298K)= 95.38 cal/(mol K)  
 Cp(300K)= 46.18 cal/(mol K)

CI5  
 Chemical Formula: C16H8  
 Symmetry: 1  
 # Kekule Structures: 4  
 Groups  
 AC6  
 BC6600\_1r  
 AB6  
 AA6  
 AA6  
 AA6  
 AB6  
 AB6  
 BD6650  
 CD6560\_1r6  
 CC6  
 AB6

AA6  
AA6  
AB6  
BD6560  
XI5  
BI5  
II5  
Hf(298K)= 186.91 kcal/mol  
S(298K)= 102.59 cal/(mol K)  
Cp(300K)= 51.52 cal/(mol K)

Pyren-1,2-yne

Chemical Formula: C<sub>16</sub>H<sub>8</sub>

Symmetry: 1

# Kekule Structures: 6

Groups

BD6660

BD6660

AB6

AA6

AA6

AB6

AB6

AA6

AB6

BD6660

DD6666

BI6

II6

AI6

BD6660

AB6

AB6

AA6

AB6

Hf(298K)= 143.07 kcal/mol

S(298K)= 99.45 cal/(mol K)

Cp(300K)= 50.84 cal/(mol K)

Chrys-1,2-yne

Chemical Formula: C<sub>18</sub>H<sub>10</sub>

Symmetry: 1

# Kekule Structures: 8

Groups

AC6

BC6600\_1r

AB6

AA6

AA6

AA6

AB6

AA6

AC6

CC6600\_2ro

CC6

CC6

BC6600\_1r

BI6

CI6

II6

AC6

AA6

AA6

AA6

AB6

Hf(298K)= 145.07 kcal/mol

S(298K)= 110.41 cal/(mol K)

Cp(300K)= 58.94 cal/(mol K)



# Appendix D

## Statistical Analysis

### D.1 Ring Corrections Method

Table D.1: Regression coefficients for  $\Delta H_f^\circ$  of the 139 PAHs. The method shown in this table does not differentiate the bond-groups according to the size of the ring(s) they belong to. Two ring correction parameters are included in this method: R5 accounts for the five-membered rings that are not completely surrounded by six-membered rings, whereas R5o accounts for the five-membered rings that are completely surrounded by six-membered rings. The heat of formation and standard error are given in kcal mol<sup>-1</sup>.

	$\Delta H_f^\circ$ (kcal mol <sup>-1</sup> )	std. error	t-Values	VIF
$\ln(K)$	-13.2	2.9	-4.6	119.5
AAx	4.8	0.3	13.8	74.0
ABx	6.5	0.4	16.7	37.4
ACx	4.2	1.0	4.2	9.7
CCx	11.5	1.8	6.5	12.7
BB6x	-3.7	0.9	-4.2	11.1
BC6x	-5.5	0.8	-6.6	3.5
CC6x	-3.8	1.5	-2.5	3.7
DD6x	2.6	0.5	4.7	23.2
R5	19.7	1.3	14.7	4.0
R5o	25.0	3.7	6.7	16.6
MAD	9.1			
RMS	14.4			

## D.2 Collinearity Diagnosis for BCGA for PAHs with Five-and Six-Membered Rings

**Table D.2:** Regression coefficient for the heat of formation calculated from ordinary least square (OLS) regression of the 133 PAHs that do not contain the DD6665o nor the DD6655oo bonds. Heat of formation and standard error values are given in kcal mol<sup>-1</sup>. The t-values indicate that all the coefficients are significant. However, variance inflation factors (VIF) >10 are an indication of collinearity problems.

	$\Delta H_f^\circ$	std. error	t-Values	VIF
ln(K)	-19.59	1.1	-17.0	146.7
AA5	10.39	0.7	15.2	3.6
AA6	5.54	0.1	40.7	92.5
AB5	10.72	0.4	26.0	2.8
AB6	7.10	0.2	36.3	51.7
AC5	6.70	0.6	10.4	2.7
AC6	4.32	0.3	12.5	11.1
CC5	15.87	0.8	19.0	4.4
CC6	13.15	0.7	19.0	13.4
BB6x	-3.90	0.5	-7.2	21.4
BC6x	-4.74	0.3	-14.2	4.3
CC6x	-2.29	0.5	-4.1	3.9
DD65	13.24	0.4	37.1	3.4
DD6666	2.71	0.3	7.8	3.4
DD6665-	7.20	0.7	10.2	1.4
DD6655-	20.43	1.2	15.9	1.4
DD6655o	16.40	1.0	15.5	2.6
MAD	2.54			
RMS	3.64			

**Table D.3:** Regression coefficient for the intrinsic entropy and heat capacities calculated from ordinary least square (OLS) regression of the 133 PAHs that do not contain the DD6650 nor the DD6650o bonds. The coefficients and standard error values are given in  $\text{cal K}^{-1} \text{mol}^{-1}$ .

	$S_{\text{int},298}$				$C_{p,300}$				$C_{p,400}$				$C_{p,500}$			
	Coeff.	std. error	t-Values	VIF	Coeff.	std. error	t-Values	VIF	Coeff.	std. error	t-Values	VIF	Coeff.	std. error	t-Values	VIF
AA5	13.0	0.2	66.1	3.1	3.4	<0.1	68.0	3.1	4.6	<0.1	106.7	3.1	5.6	<0.1	150.9	3.1
AA6	11.6	<0.1	1968.7	1.7	3.4	<0.1	2304.7	1.7	4.6	<0.1	3563.3	1.7	5.6	<0.1	5029.6	1.7
AB5	6.5	0.1	50.2	2.8	3.4	<0.1	107.0	2.8	4.6	<0.1	162.2	2.8	5.5	<0.1	224.8	2.8
AB6	3.6	<0.1	94.7	20.5	3.4	<0.1	359.7	20.5	4.6	<0.1	546.9	20.5	5.5	<0.1	760.8	20.5
AC5	7.0	0.2	35.1	2.7	3.5	<0.1	71.6	2.7	4.6	<0.1	107.1	2.7	5.5	<0.1	147.4	2.7
AC6	4.3	0.1	46.1	8.5	3.5	<0.1	150.8	8.5	4.6	<0.1	225.9	8.5	5.5	<0.1	312.4	8.5
CC5	-1.9	0.2	-8.5	4.0	3.3	0.1	52.2	4.0	4.4	0.1	80.7	4.0	5.2	<0.1	112.5	4.0
CC6	-5.3	0.2	-27.7	11.4	3.4	<0.1	69.4	11.4	4.5	<0.1	105.5	11.4	5.4	<0.1	146.3	11.4
BB6x	-1.1	0.1	-7.3	19.1	-1.3	<0.1	-35.6	19.1	-1.9	<0.1	-57.6	19.1	-2.3	<0.1	-82.3	19.1
BC6x	-1.2	0.1	-12.1	3.8	-1.4	<0.1	-56.6	3.8	-1.9	<0.1	-89.7	3.8	-2.3	<0.1	-127.2	3.8
CC6x	-1.0	0.2	-6.1	3.9	-1.4	<0.1	-34.7	3.9	-1.9	<0.1	-54.4	3.9	-2.4	<0.1	-76.7	3.9
DD65	2.3	0.1	22.1	2.8	1.4	<0.1	53.6	2.8	1.9	<0.1	85.0	2.8	2.4	<0.1	119.9	2.8
DD6666	0.8	0.1	8.3	2.5	1.5	<0.1	66.8	2.5	2.0	<0.1	102.6	2.5	2.4	<0.1	143.5	2.5
DD6665-	1.4	0.2	6.2	1.4	1.4	0.1	25.8	1.4	1.9	<0.1	40.7	1.4	2.3	<0.1	57.3	1.4
DD6655-	1.8	0.4	4.6	1.3	1.3	0.1	13.3	1.3	1.9	0.1	22.3	1.3	2.3	0.1	32.1	1.3
DD6655o	0.8	0.3	2.6	2.3	1.2	0.1	14.8	2.3	1.8	0.1	25.9	2.3	2.2	0.1	38.1	2.3

Table D3: (continued)

	$C_{p,600}$				$C_{p,800}$				$C_{p,1000}$				$C_{p,1500}$			
	Coeff.	std. error	t-Values	VIF	Coeff.	std. error	t-Values	VIF	Coeff.	std. error	t-Values	VIF	Coeff.	std. error	t-Values	VIF
AA5	6.4	<0.1	196.4	3.1	7.5	<0.1	241.5	3.1	8.3	<0.1	198.4	3.1	9.3	0.1	116.6	3.1
AA6	6.4	<0.1	6556.3	1.7	7.6	<0.1	8102.0	1.7	8.3	<0.1	6682.8	1.7	9.5	<0.1	3950.8	1.7
AB5	6.2	<0.1	288.9	2.8	7.2	<0.1	349.9	2.8	7.8	<0.1	284.6	2.8	8.6	0.1	164.6	2.8
AB6	6.2	<0.1	981.9	20.5	7.3	<0.1	1196.8	20.5	7.9	<0.1	976.9	20.5	8.8	<0.1	567.2	20.5
AC5	6.2	<0.1	188.8	2.7	7.1	<0.1	228.0	2.7	7.7	<0.1	185.0	2.7	8.6	0.1	106.6	2.7
AC6	6.2	<0.1	402.0	8.5	7.2	<0.1	489.0	8.5	7.9	<0.1	398.8	8.5	8.8	<0.1	231.2	8.5
CC5	5.9	<0.1	144.7	4.0	6.8	<0.1	174.2	4.0	7.3	0.1	140.5	4.0	7.9	0.1	79.7	4.0
CC6	6.1	<0.1	188.1	11.4	7.0	<0.1	227.3	11.4	7.6	<0.1	184.4	11.4	8.4	0.1	106.1	11.4
BB6x	-2.6	<0.1	-107.4	19.1	-3.1	<0.1	-131.7	19.1	-3.3	<0.1	-106.9	19.1	-3.6	0.1	-60.5	19.1
BC6x	-2.7	<0.1	-165.4	3.8	-3.1	<0.1	-202.1	3.8	-3.4	<0.1	-164.1	3.8	-3.7	<0.1	-93.8	3.8
CC6x	-2.7	<0.1	-99.5	3.9	-3.1	<0.1	-121.5	3.9	-3.4	<0.1	-98.6	3.9	-3.7	0.1	-56.3	3.9
DD65	2.7	<0.1	155.4	2.8	3.1	<0.1	189.1	2.8	3.4	<0.1	153.6	2.8	3.7	<0.1	88.2	2.8
DD6666	2.7	<0.1	185.7	2.5	3.2	<0.1	225.9	2.5	3.4	<0.1	183.3	2.5	3.8	<0.1	104.9	2.5
DD6665-	2.7	<0.1	74.4	1.4	3.1	<0.1	90.1	1.4	3.3	<0.1	72.5	1.4	3.6	0.1	40.7	1.4
DD6655-	2.7	0.1	41.9	1.3	3.1	0.1	51.3	1.3	3.4	0.1	41.7	1.3	3.7	0.2	23.9	1.3
DD6655o	2.6	0.1	50.4	2.3	3.1	<0.1	61.8	2.3	3.3	0.1	49.9	2.3	3.6	0.1	28.0	2.3



**Table D.4:** Correlation matrix for the standardized and centered matrix of the independent variables corresponding to the 133 PAHs that do not contain the DD6650 nor DD6655 bond-groups. This matrix shows only the pair wise correlation between the independent variables.

$\ln(K)$	AA5	AA6	AB5	AB6	AC5	AC6	CC5	CC6	BB6x	BC6x	CC6x	DD65	DD6666	DD6665	DD6666	DD65	CC6x	BC6x	BB6x	CC6	CC5	AC6	AC5	AB6	AB5	AA6	AA5	ln(K)	
1	-0.31	0.95	-0.28	0.75	-0.26	0.13	-0.09	0.09	0.71	0.12	0.05	-0.07	0.03	-0.11	-0.13	-0.13	0.05	-0.07	0.12	0.09	0.09	0.13	-0.26	0.75	-0.28	0.95	-0.31	1	
-0.31	1	-0.24	0.61	-0.22	0.45	-0.45	-0.32	-0.22	-0.10	-0.20	-0.23	-0.04	-0.16	0.10	0.08	0.18	-0.23	-0.04	-0.20	-0.22	-0.32	-0.45	-0.26	-0.22	0.61	-0.24	0.95	-0.31	
0.95	-0.24	1	-0.21	0.60	-0.18	0.06	-0.06	0.04	0.61	0.09	0.03	-0.12	-0.06	-0.11	-0.10	-0.14	0.03	-0.12	0.09	0.04	0.04	0.06	-0.18	0.60	-0.21	1	-0.24	0.61	
-0.28	0.61	-0.21	1	-0.17	-0.02	-0.39	-0.10	-0.36	-0.12	-0.11	-0.28	-0.01	-0.14	0.27	0.09	0.13	-0.28	-0.01	-0.11	-0.12	-0.36	-0.39	-0.02	-0.17	1	-0.21	1	-0.28	
0.75	-0.22	0.60	-0.17	1	-0.24	-0.15	-0.17	-0.15	0.91	0.11	-0.21	-0.05	0.09	-0.04	-0.16	-0.14	-0.21	-0.05	0.11	-0.15	-0.17	-0.15	-0.24	1	-0.17	0.60	-0.17	0.60	
-0.26	0.45	-0.18	-0.02	-0.24	1	-0.34	-0.19	-0.03	-0.10	-0.16	-0.07	0.08	-0.16	-0.05	-0.14	-0.14	-0.07	-0.05	-0.16	-0.10	-0.03	-0.34	1	-0.24	-0.02	-0.18	-0.02	-0.24	-0.18
0.13	-0.45	0.06	-0.39	-0.15	-0.34	1	0.24	0.77	-0.15	-0.16	-0.07	0.08	-0.16	-0.05	-0.14	-0.14	-0.07	-0.05	-0.16	0.77	0.24	-0.34	1	-0.24	-0.15	0.06	-0.39	-0.15	-0.45
-0.09	-0.32	-0.06	-0.10	-0.17	-0.19	0.24	1	-0.28	-0.09	-0.05	0.69	-0.23	-0.15	-0.22	-0.11	-0.29	0.69	-0.23	0.39	-0.28	1	0.24	-0.19	0.24	-0.10	-0.06	-0.32	-0.06	-0.32
0.09	-0.22	0.04	-0.36	-0.15	-0.03	0.77	-0.28	1	-0.09	-0.05	0.13	0.08	-0.18	-0.07	0.23	-0.07	0.13	0.08	-0.05	-0.28	1	0.24	-0.19	0.24	-0.10	-0.06	-0.32	-0.06	-0.32
0.71	-0.10	0.61	-0.12	0.91	-0.10	-0.15	-0.09	-0.15	1	0.47	0.62	-0.30	-0.16	-0.25	-0.22	-0.19	0.62	-0.30	0.47	-0.15	-0.09	-0.15	-0.10	-0.10	0.91	-0.12	0.61	-0.12	0.61
0.12	-0.20	0.09	-0.11	0.11	-0.16	0.39	-0.05	0.47	-0.05	1	-0.10	-0.25	-0.10	-0.10	-0.07	-0.07	-0.10	-0.10	-0.05	0.47	-0.05	-0.16	0.39	-0.05	0.11	-0.16	0.09	-0.11	-0.20
0.05	-0.23	0.03	-0.28	-0.21	-0.07	0.69	0.13	0.62	-0.07	1	1	-0.16	-0.24	-0.24	-0.18	-0.20	1	-0.25	1	-0.07	-0.05	-0.07	0.69	0.13	-0.21	-0.28	0.03	-0.23	0.05
-0.07	-0.04	-0.12	-0.01	-0.05	0.08	-0.23	0.08	-0.30	-0.10	-0.25	-0.16	-0.09	-0.09	-0.15	-0.04	-0.13	-0.16	-0.16	-0.10	-0.07	-0.05	-0.23	0.08	-0.30	-0.01	-0.12	-0.04	-0.12	-0.07
0.03	-0.16	-0.06	-0.14	0.09	-0.16	-0.15	-0.18	-0.16	-0.10	-0.24	-0.09	-0.16	1	-0.04	0.23	0.61	-0.09	-0.16	-0.24	-0.10	-0.04	-0.23	0.08	-0.30	-0.14	-0.06	-0.14	-0.06	-0.16
-0.11	0.10	-0.11	0.27	-0.04	-0.05	-0.22	-0.07	-0.25	-0.10	-0.24	-0.09	-0.16	1	0.19	-0.13	-0.14	-0.09	-0.16	-0.24	-0.25	-0.07	-0.22	-0.07	-0.25	-0.10	-0.11	-0.11	0.27	-0.04
-0.13	0.08	-0.10	0.09	-0.16	0.14	-0.11	0.23	-0.22	-0.07	-0.18	-0.04	-0.13	-0.13	1	-0.13	-0.14	-0.04	-0.16	-0.24	-0.22	-0.22	-0.11	0.23	-0.22	-0.10	-0.10	-0.10	0.09	-0.16
-0.13	0.18	-0.14	0.13	-0.14	0.39	-0.29	-0.07	-0.19	-0.07	-0.20	-0.13	-0.14	-0.14	-0.14	0.14	1	-0.13	-0.14	-0.20	-0.07	-0.19	-0.29	0.39	-0.29	-0.14	-0.14	-0.14	0.13	-0.14

**Table D.5:** Eigenvalues and condition indices for the standardized and centered matrix of independent variables corresponding to the 133 PAHs that do not contain the DD6650 nor the DD6650o bonds. Condition numbers >10 indicate weak collinearities that might be starting to affect the regression estimates, condition indices between 30 to 100 indicate moderate to strong dependencies, and indices larger than 100 indicate serious collinearity problems. The variance decomposition proportions show how much each principal component contributes to the variance of the regression coefficient. When a principal component contributes heavily (more than 50%) to the variance of two or more coefficients, it is an indication of collinearity problems.

Principal Component	Eigenvalue	Condition Number	Variance Decomposition Proportion															
			ln	AA5	AA6	AB5	AB6	AC5	AC6	BB6x	BC6x	CC6x	DD65	DD655o				
1	3.9265	1.00	0.0002	0.0001	0.0102	0.0010	0.0041	0.0011	0.0040	0.0002	0.0003	0.0002	0.0010	0.0029	0.0011	0.0000	0.0000	0.0000
2	3.1327	1.12	0.0001	0.0000	0.0077	0.0007	0.0043	0.0030	0.0101	0.0174	0.0108	0.0174	0.0002	0.0001	0.0001	0.0000	0.0000	0.0000
3	1.8744	1.45	0.0001	0.0002	0.0154	0.0033	0.0009	0.0016	0.0211	0.0107	0.0253	0.0107	0.0001	0.0007	0.0008	0.0004	0.0000	0.0000
4	1.6906	1.52	0.0000	0.0001	0.0131	0.0067	0.0471	0.0008	0.0079	0.0139	0.0007	0.0139	0.0034	0.0007	0.0002	0.0015	0.0009	0.0000
5	1.3021	1.74	0.0004	0.0003	0.0379	0.0011	0.0054	0.0070	0.0246	0.0025	0.0010	0.0025	0.0094	0.0056	0.0013	0.0010	0.0009	0.0000
6	1.1274	1.87	0.0005	0.0039	0.0027	0.0001	0.0095	0.0318	0.0077	0.0008	0.0027	0.0008	0.0054	0.0160	0.0367	0.0056	0.0001	0.0000
7	0.9397	2.04	0.0008	0.0011	0.0016	0.0079	0.0435	0.0017	0.0077	0.0001	0.0063	0.0001	0.0353	0.0057	0.0249	0.0026	0.0014	0.0000
8	0.7424	2.30	0.0020	0.0075	0.0018	0.0016	0.0015	0.0061	0.0004	0.0025	0.0046	0.0025	0.0213	0.0006	0.0007	0.0060	0.0268	0.0001
9	0.6579	2.44	0.0017	0.0085	0.0003	0.0206	0.0082	0.0000	0.0034	0.0061	0.0038	0.0061	0.0014	0.0003	0.0170	0.3544	0.0002	0.0001
10	0.5539	2.66	0.0000	0.0008	0.0291	0.0482	0.0732	0.0038	0.0028	0.0608	0.0085	0.0608	0.0523	0.0000	0.0005	0.1112	0.0004	0.0000
11	0.4048	3.11	0.0038	0.0161	0.0027	0.0001	0.0033	0.0020	0.0125	0.0026	0.0002	0.0026	0.0299	0.0306	0.0782	0.3175	0.0009	0.0001
12	0.263	3.86	0.0037	0.0001	0.0207	0.0725	0.0655	0.0137	0.0886	0.1821	0.0212	0.1821	0.0493	0.0491	0.0579	0.0349	0.0000	0.0000
13	0.1877	4.57	0.0097	0.0313	0.0002	0.0007	0.0002	0.0044	0.0003	0.0000	0.0037	0.0000	0.0909	0.0030	0.0012	0.0068	0.0000	0.0046
14	0.1166	5.80	0.0123	0.0055	0.0900	0.0108	0.4389	0.0240	0.1973	0.1905	0.0260	0.1905	0.2605	0.0040	0.1752	0.1805	0.0002	0.0000
15	0.0503	8.84	0.0473	0.0543	0.0339	0.0167	0.0066	0.0737	0.0229	0.0008	0.0804	0.1623	0.2247	0.0089	0.0038	0.0142	0.0000	0.0418
16	0.0264	12.20	0.0677	0.0192	0.2179	0.6922	0.2182	0.3966	0.0000	0.0578	0.0950	0.0950	0.1207	0.7012	0.6960	0.3419	0.1142	0.0004
17	0.0035	33.49	0.8497	0.8509	0.5148	0.1160	0.0695	0.3869	0.5949	0.4514	0.7095	0.7933	0.0012	0.2387	0.0098	0.2426	0.0436	0.9527

### D.3. Principal Component Regression

The coefficient  $\beta$  of the ordinary least square regression are obtained by solving the linear model:

$$Y = X \beta$$

The linear model can also be written in terms of the principal component  $W$ :

$$Y = W \gamma$$

Principal components are calculated by:

$$W = X V$$

Where  $V$  is obtained from the Singular Value Decomposition of the matrix of independent variables  $X$ :

$$X = U S V'$$

The regression coefficients for the principal components are obtained through:

$$\hat{\gamma} = (W'W)^{-1}W'Y$$

Since the columns of  $W$  are orthogonal,  $W'W$  is a diagonal matrix, and each of the  $\gamma_i$  can be computed individually. The estimate of  $\beta$  is obtained from  $\hat{\gamma}$  through:

$$\hat{\beta} = V\hat{\gamma}$$

Since the principal component regression coefficients can be computed independently, the vector  $\hat{\gamma}_{(g)}$  of the  $g$  coefficients retained in the regression is obtained from  $\hat{\gamma}$  by simply eliminating the elements corresponding to the unwanted components. Analogously  $V_{(g)}$  is obtained from  $V$  by eliminating the columns corresponding to the unwanted principal components. The coefficients from the principal component regression are then given by:

$$\hat{\beta}_{(g)} = V_{(g)}\hat{\gamma}_{(g)}$$

We have worked with standardized and centered  $X$  and  $Y$ .

**Table D.6:** Statistics for the principal component regression. The amount of dispersion accounted by each principal component is given by the ration between its eigenvalue and the sum of all the eigenvalues. The last four principal components each account for less than 1% of the dispersion of the X-space. Of the four last principal components, principal components 15 and 16 have particularly low t-Values.

Prin. Comp.	Eigenvalues	Dispersion Accounted for	$\hat{\gamma}$	Std error	t-Value
1	3.9265	0.2310	-0.324	0.02	-18.02
2	3.1327	0.1843	0.366	0.02	18.24
3	1.8744	0.1103	-0.162	0.03	-6.22
4	1.6906	0.0994	0.102	0.03	3.74
5	1.3021	0.0766	0.050	0.03	1.60
6	1.1274	0.0663	0.120	0.03	3.57
7	0.9397	0.0553	-0.168	0.04	-4.58
8	0.7424	0.0437	0.054	0.04	1.31
9	0.6579	0.0387	0.120	0.04	2.73
10	0.5539	0.0326	-0.212	0.05	-4.43
11	0.4048	0.0238	-0.028	0.06	-0.49
12	0.263	0.0155	-0.147	0.07	-2.12
13	0.1877	0.0110	-0.109	0.08	-1.32
14	0.1166	0.0069	-0.112	0.10	-1.07
15	0.0503	0.0030	-0.092	0.16	-0.58
16	0.0264	0.0016	0.135	0.22	0.62
17	0.0035	0.0002	1.503	0.60	2.51

**Table D.7:** Comparison of principal component regressions eliminating the least important principal components. Although principal component 17 contributes the least to the dispersion of the X-space, it is significant, as indicated by its relatively large absolute t-value (see Table S10). Elimination of principal components 15 and 16 does not increase the MAD and RMS considerably, while decreasing the VIF considerably. The VIF of AB6 is very much determined by principal component 17, and does not decrease considerably unless this component is eliminated. The principal component regression eliminating PC 15 and 16 is adopted in this work. Heat of formation and standard errors are given in kcal mol<sup>-1</sup>.

	Principal Component Regression																			
	Ordinary Least Squares Regression				eliminating PC 17				eliminating PC 16 and 15				eliminating PC 16, 15, and 14							
	$\Delta H_f^\circ$	std. error	t-values	VIF	$\Delta H_f^\circ$	std. error	t-values	VIF	$\Delta H_f^\circ$	std. error	t-values	VIF	$\Delta H_f^\circ$	std. error	t-values	VIF				
<i>ln</i> (K)	-19.59	1.1	-17.0	146.7	7.33	0.2	82.4	2.9	-21.44	1.1	-18.1	144.3	-22.13	1.1	-18.1	144.2	-23.90	1.1	-18.3	144.2
AA5	10.39	0.7	15.2	3.6	6.56	0.6	4.9	3.1	10.60	0.6	14.7	3.5	10.19	0.6	13.7	3.4	14.13	0.6	19.7	2.9
AA6	5.54	0.1	40.7	92.5	2.33	0.0	76.6	2.4	5.77	0.1	42.0	91.0	5.85	0.1	42.0	91.0	6.08	0.1	42.2	91.0
AB5	10.72	0.4	26.0	2.8	12.13	0.4	25.5	2.8	11.11	0.4	26.3	2.8	11.38	0.4	26.4	2.8	8.82	0.3	23.9	1.7
AB6	7.10	0.2	36.3	51.7	3.71	0.1	22.5	14.3	6.64	0.2	38.1	38.1	6.85	0.2	38.4	38.0	7.23	0.2	38.2	38.0
AC5	6.70	0.6	10.4	2.7	9.21	0.6	11.3	2.7	6.78	0.6	9.9	2.7	8.64	0.6	13.6	2.3	5.13	0.5	7.8	1.5
AC6	4.32	0.3	12.5	11.1	0.57	0.3	-1.3	8.6	4.86	0.3	13.9	10.8	6.55	0.2	27.0	5.2	5.22	0.2	24.2	3.5
CC5	15.87	0.8	19.0	4.4	14.42	0.7	10.8	4.0	15.77	0.8	18.0	4.2	12.42	0.5	21.2	1.5	13.65	0.5	20.0	1.5
CC6	13.15	0.7	19.0	13.4	9.34	0.6	7.7	11.1	13.49	0.7	18.4	13.3	10.24	0.3	26.0	3.1	9.87	0.3	22.9	2.5
BB6x	-3.90	0.5	-7.2	21.4	-0.06	0.4	6.4	17.1	-1.35	0.2	-2.1	5.2	-1.99	0.2	-3.5	5.0	-2.99	0.2	-4.4	4.9
BC6x	-4.74	0.3	-14.2	4.3	-2.20	0.3	-2.7	3.6	-3.83	0.3	-12.3	3.2	-3.66	0.3	-11.3	3.1	-1.94	0.2	-4.5	1.9
CC6x	-2.29	0.5	-4.1	3.9	-1.37	0.5	0.0	3.9	-3.00	0.5	-5.1	3.9	-2.26	0.5	-3.5	3.6	2.02	0.3	9.7	1.4
DD65	13.24	0.4	37.1	3.4	10.98	0.3	29.1	3.0	14.78	0.3	48.1	2.4	14.63	0.3	47.7	2.4	14.32	0.3	46.2	2.3
DD6666	2.71	0.3	7.8	3.4	-0.06	0.3	-5.8	2.7	4.31	0.3	14.9	2.2	4.11	0.3	13.7	2.1	4.25	0.2	12.6	2.1
DD6665	7.20	0.7	10.2	1.4	5.72	0.7	6.0	1.4	8.27	0.7	11.6	1.4	7.76	0.7	10.6	1.4	10.21	0.6	14.0	1.3
DD6655	20.43	1.2	15.9	1.4	12.53	1.2	7.1	1.2	20.08	1.2	15.2	1.4	20.04	1.2	14.8	1.4	23.12	1.2	16.5	1.3
DD6655o	16.40	1.0	15.5	2.6	7.09	1.0	5.1	2.3	15.28	1.0	14.4	2.5	15.51	1.0	14.4	2.5	19.81	1.0	18.8	2.3
MAD	2.54				5.04				2.91				3.17				3.46			
RMS	3.64				7.62				4.31				4.60				5.42			

**Table D.8:** Matrix V. The columns are the eigenvectors corresponding to each principal component. Each principal component is a linear function of all independent variables. PC 17 is mainly determined by ln(K), AA6 and AB6, which are the variables with the largest VIF in the ordinary least square regression.

	PC1	PC2	PC3	PC4	PC5	PC6	PC7	PC8	PC9	PC10	PC11	PC12	PC13	PC14	PC15	PC16	PC17
ln	-0.397	0.282	-0.092	0.060	-0.029	0.101	-0.102	0.086	0.143	-0.331	0.003	-0.123	0.018	-0.072	-0.018	0.254	-0.712
AA5	0.307	0.116	0.164	0.401	0.140	0.280	0.002	0.084	-0.143	-0.092	0.087	-0.577	0.408	0.235	-0.081	0.023	0.041
AA6	-0.354	0.269	-0.090	0.086	0.034	0.166	-0.076	0.014	0.181	-0.566	0.164	0.090	-0.042	0.066	0.000	-0.200	0.564
AB5	0.274	0.130	0.222	0.105	0.418	0.144	-0.338	0.320	-0.157	-0.127	-0.269	0.092	-0.430	-0.359	0.006	-0.010	0.002
AB6	-0.309	0.394	0.013	0.034	0.011	-0.078	0.016	0.006	-0.076	0.397	-0.202	-0.192	-0.072	-0.038	0.053	0.600	0.363
AC5	0.227	0.024	-0.160	0.410	-0.243	0.164	0.340	-0.470	0.213	-0.089	-0.176	-0.133	-0.342	-0.305	0.142	0.017	-0.003
AC6	-0.286	-0.416	-0.072	-0.021	0.068	0.079	-0.159	0.069	0.026	0.008	-0.170	-0.254	0.335	-0.440	0.532	-0.090	0.094
CC5	-0.009	-0.111	-0.275	-0.485	0.372	0.126	0.088	-0.394	-0.196	-0.211	-0.263	-0.255	0.014	-0.042	-0.368	0.067	0.038
CC6	-0.242	-0.385	0.032	0.345	-0.135	0.007	-0.105	0.136	0.142	0.098	-0.047	0.008	0.041	-0.261	-0.716	0.050	0.090
BB6x	-0.281	0.385	-0.079	0.102	0.063	0.184	0.037	-0.092	-0.166	0.426	-0.194	0.013	0.064	-0.056	-0.099	-0.656	-0.124
BC6x	-0.196	-0.166	0.083	0.256	0.374	-0.552	0.088	-0.019	0.220	-0.060	-0.281	-0.225	-0.220	0.378	0.074	-0.167	-0.050
CC6x	-0.179	-0.341	-0.120	0.023	-0.191	0.517	-0.207	0.065	-0.156	0.103	-0.121	-0.063	-0.404	0.503	0.118	0.044	-0.017
DD65	0.169	0.109	-0.481	-0.111	-0.156	-0.261	-0.399	0.121	0.104	0.126	0.316	-0.468	-0.256	-0.101	-0.055	-0.157	0.037
DD6666	-0.007	0.070	0.322	-0.316	-0.522	-0.101	0.258	0.329	-0.098	-0.218	-0.347	-0.323	-0.101	-0.049	-0.075	-0.179	0.049
DD6665-	0.120	0.097	0.368	-0.232	-0.076	0.148	-0.443	-0.305	0.621	0.125	-0.205	-0.047	0.111	0.097	-0.042	-0.033	0.011
DD6655-	0.143	0.019	-0.337	-0.135	0.215	0.264	0.397	0.502	0.523	0.156	-0.126	0.037	0.056	0.050	-0.017	0.021	0.022
DD6655o	0.219	0.100	-0.433	0.182	-0.234	-0.179	-0.281	0.053	-0.106	-0.162	-0.559	0.266	0.320	0.160	-0.001	0.052	0.036

# Appendix E

## Equilibrium Calculation

### E.1 Thermochemical Properties of Species Included

UNITS:KCAL

SPECIES	HE(298)	S(298)	CP300	CP400	CP500	CP600	CP800	CP1000	CP1500	DATE	REF	ELEMENTS
*H	52.10	27.39	4.97	4.97	4.97	4.97	4.97	4.97	4.97	120186	H 1	0 0 0 0
H2	.00	31.21	6.90	6.96	7.00	7.02	7.07	7.21	7.73	121286	H 2	0 0 0 0
HE	.00	30.12	4.97	4.97	4.97	4.97	4.97	4.97	4.97	120186	HE 1	0 0 0 0
C	171.31	37.76	4.98	4.98	4.97	4.97	4.97	4.97	4.97	121086	C 1	0 0 0 0
CH	142.01	43.72	6.95	7.00	7.05	7.11	7.37	7.78	8.75	121286	C 1 H 1	0 0 0 0
CH2	102.68	45.12	7.94	8.30	8.66	9.02	9.72	10.39	11.85	S CBS-Q07/01	C 1 H 2	0 0 0 0
HCH	94.59	46.12	8.20	8.54	8.88	9.21	9.85	10.44	11.73	T CBS-Q07/01	C 1 H 2	0 0 0 0
CH3	35.41	46.40	9.30	10.06	10.82	11.55	12.93	14.15	16.33	CBS-Q 07/01	C 1 H 3	0 0 0 0
CH4	-17.90	44.47	8.43	9.84	11.14	12.41	15.00	17.25	20.63	121286	C 1 H 4	0 0 0 0
O	59.56	38.47	5.23	5.14	5.08	5.05	5.02	5.00	4.98	120186	O 1	0 0 0 0
OH	9.32	43.88	7.15	7.10	7.07	7.06	7.13	7.33	7.87	121286	O 1 H 1	0 0 0 0
H2O	-57.80	45.10	8.00	8.23	8.44	8.67	9.22	9.87	11.26	20387	H 2 O 1	0 0 0 0
C2	200.24	47.64	10.27	9.49	8.94	8.60	8.45	8.62	8.93	121286	C 2	0 0 0 0
C2H	136.03	50.17	9.21	9.79	10.31	10.78	11.56	12.14	12.96	CBS-Q 07/01	C 2 H 1	0 0 0 0
C2H2	54.19	48.66	11.32	12.47	13.39	14.15	15.32	16.21	17.94	HR11/99BLYP00	C 2 H 2	0 0 0 0
C2H3	71.60	55.90	10.47	12.37	13.99	15.37	17.57	19.20	21.86	CBS-Q 07/01	C 2 H 3	0 0 0 0
C2H4	12.54	52.38	10.23	12.79	14.94	16.83	20.05	22.51	26.22	121286	C 2 H 4	0 0 0 0
CO	-26.42	47.21	6.95	7.03	7.14	7.27	7.61	7.95	8.41	121286	C 1 O 1	0 0 0 0
N2	.00	45.77	6.95	7.01	7.08	7.19	7.50	7.83	8.32	121286	N 2	0 0 0 0
C2H5	29.30	59.38	12.36	14.88	17.19	19.29	22.88	25.72	30.21	CBS-Q 07/01	C 2 H 5	0 0 0 1
HCO	10.40	53.66	8.24	8.78	9.28	9.77	10.74	11.52	12.56	121286	H 1 C 1	0 0 0 0
C2H6	-20.04	54.73	12.58	15.69	18.62	21.30	25.82	29.30	34.61	121686	C 2 H 6	0 0 0 0
CH2O	-27.70	52.25	8.40	9.50	10.50	11.47	13.36	14.88	16.97	121286	C 1 H 2 O 1	0 0 0 0
CH3O	3.90	54.61	9.08	10.79	12.43	13.98	16.63	18.60	21.51	121686	C 1 H 3 O 1	0 0 0 0
CH2OH	-4.10	58.88	11.32	12.94	14.38	15.62	17.54	18.79	20.95	120186	H 3 C 1	0 0 0 0
CH3OH	-48.06	57.28	10.51	12.40	14.25	16.01	19.07	21.40	25.02	121686	C 1 H 4 O 1	0 0 0 0
O2	.00	49.01	7.01	7.22	7.44	7.65	8.07	8.35	8.72	121386	O 2	0 0 0 0
HO2	2.50	54.73	8.34	8.95	9.49	9.97	10.78	11.39	12.45	20387	H 1 O 2	0 0 0 0
H2O2	-32.53	55.66	10.41	11.44	12.34	13.11	14.29	15.21	16.85	120186	H 2 O 2	0 0 0 0
C3H2	129.59	62.99	15.94	17.36	18.47	19.34	20.58	21.45	23.16	CBS-Q 07/01	C 3 H 2	0 0 0 0
H2CCCH	82.12	61.61	15.62	17.74	19.49	20.94	23.16	24.79	27.57	CBS-Q 07/01	C 3 H 3	0 0 0 0
C3H4CY	68.72	57.87	12.22	15.71	18.65	21.12	24.94	27.67	31.82	CBS-Q 07/01	C 3 H 4	0 0 0 0
C3H4	43.89	57.86	13.79	16.81	19.40	21.61	25.12	27.72	31.81	CBS-Q 07/01	C 3 H 4	0 0 0 0
C3H4P	43.65	58.85	14.18	16.95	19.37	21.48	24.90	27.51	31.68	CBS-Q 07/01	C 3 H 4	0 0 0 0
*AR	.00	36.98	4.97	4.97	4.97	4.97	4.97	4.97	4.97	120186	AR 1	0 0 0 0
C2O	68.51	55.68	10.31	11.09	11.72	12.24	13.06	13.66	14.64	121286	C 2 O 1	0 0 0 0
C3H5	40.85	62.04	15.61	19.35	22.49	25.13	29.23	32.20	36.76	CBS-Q 07/01	C 3 H 5	0 0 0 1
HCCO	42.45	60.74	12.65	13.47	14.23	14.92	16.07	16.83	17.98	32387	H 1 C 2	0 0 0 0
C3H6	5.43	63.59	15.24	19.05	22.44	25.46	30.46	34.30	40.23	CBS-Q 07/01	C 3 H 6	0 0 0 1
CH2CO	-12.40	57.79	12.43	14.17	15.67	16.91	18.79	20.24	22.44	121686	C 2 H 2 O 1	0 0 0 0
HCCOH	20.43	58.71	13.22	14.78	16.16	17.35	19.15	20.30	22.29	32387	H 2 C 2	0 0 0 0
NC3H7	24.64	69.35	17.40	21.61	25.32	28.58	33.93	38.02	44.44	CBS-Q 07/01	C 3 H 7	0 0 0 2
IC3H7	21.83	68.75	16.35	20.35	24.02	27.34	32.99	37.40	44.12	CBS-Q 07/01	C 3 H 7	0 0 0 2
CH2CHO	6.00	64.01	13.18	15.15	16.96	18.60	21.30	23.34	26.35	120186	O 1 H 3	0 0 0 2



CH3CO	-5.40	63.75	12.42	14.44	16.33	18.06	20.94	23.07	26.19	120186	C	2 H	3 O	1	0 G 0
C3H8	-24.82	64.57	17.67	22.49	26.86	30.74	37.01	41.73	48.83	120186	C	3 H	8	0	0 G 0
CH3CHO	-39.51	63.05	13.25	15.87	18.31	20.52	24.17	26.88	30.87	120186	C	2 O	1 H	4	0 G 0
CO2	-94.06	51.08	8.91	9.86	10.65	11.31	12.32	12.99	13.93	121286	C	1 O	2	0	0 G 0
CH3OCH2	5.60	67.75	14.97	17.93	20.64	23.08	27.22	30.44	35.21	3/ 7/ 1 THERM	C	2 H	5 O	1	0 G 2
CH3OCH3	-43.72	64.36	15.21	18.82	22.12	25.13	30.28	34.35	40.46	103190	C	2 H	6 O	1	0 G 0
C4H	155.09	60.90	14.10	15.37	16.56	17.66	19.59	21.15	23.44	121686	C	4 H	1	0	0 G 0
C4H2	111.71	59.79	17.74	20.03	21.85	23.24	25.10	26.61	28.96	121686	C	4 H	2	0	0 G 0
HCCHCH	129.89	69.07	18.02	20.82	23.29	25.41	28.56	30.46	33.46	82489	C	4 H	3	0	0 G 0
H2CCCCH	111.33	72.96	20.24	22.43	24.44	26.23	29.10	30.93	33.68	82489	C	4 H	3	0	0 G 0
C4H4	69.15	67.35	17.32	20.61	23.62	26.30	30.53	33.20	37.25	82489	C	4 H	4	0	0 G 0
CH2CHCHCH	86.10	73.08	19.38	23.47	27.21	30.54	35.76	38.89	43.16	82489	C	4 H	5	0	0 G 0
CH2CHCCH2	74.15	75.33	19.49	23.12	26.47	29.48	34.32	37.37	41.84	82489	C	4 H	5	0	0 G 0
HCCCO	62.66	66.35	14.82	16.87	18.49	19.76	21.42	22.52	23.86	4/23/ 1 THERM	C	3 H	1 O	1	0 G 1
C4H6-1	39.78	69.48	19.52	23.77	27.49	30.74	36.07	40.15	46.53	4/30/ 1 THERM	C	4 H	6	0	0 G 1
C4H612	39.34	69.72	19.30	23.66	27.46	30.75	36.04	39.99	45.59	Burcat A 8/83	C	4 H	6	0	0 G 0
C4H613	26.05	66.51	19.11	24.32	28.50	31.86	36.85	40.52	46.33	Burcat A 8/83	C	4 H	6	0	0 G 0
HCCCHO	24.55	64.54	15.33	18.10	20.38	22.24	24.94	26.65	28.67	4/23/ 1 THERM	C	3 H	2 O	1	0 G 1
I-C4H7	30.24	70.74	20.02	25.37	29.91	33.77	39.84	44.27	51.11	Burcat2008/83	C	4 H	7	0	0 G 0
CH2CHCO	17.30	64.42	15.00	17.89	20.49	22.73	26.10	28.63	32.35	Burcat T05/99	C	3 H	3 O	1	0 G 0
CHCCHO	40.10	65.57	15.89	19.06	21.73	23.97	27.39	29.73	32.87	Therm/Burcat	C	3 H	3 O	1	0 G 1
C4H8	-1.13	73.57	20.50	25.92	30.78	35.05	41.82	46.85	55.09	120386	C	4 H	8	0	0 G 0
CH2CHCHO	-17.80	64.50	16.08	19.62	22.89	25.71	29.91	33.00	37.43	Burcat T05/99	C	3 H	4 O	1	0 G 0
C2H5CO	-8.61	73.62	18.27	21.52	24.95	28.28	33.92	37.66	45.67	Burcat T 9/92	C	3 H	5 O	1	0 G 0
C2H5CHO	-45.90	72.78	19.36	23.04	26.94	30.70	37.11	42.15	50.42	Burcat T 9/92	C	3 H	6 O	1	0 G 0
CH3COCH3	-51.90	70.66	17.81	21.78	25.69	29.21	34.63	38.76	44.84	Burcat T 5/92	C	3 H	6 O	1	0 G 0
C5H2(L)	165.25	63.70	19.90	23.26	25.97	28.07	30.84	32.81	35.39	20587	C	5 H	2	0	0 G 0
C5H3	166.77	67.33	17.04	21.74	25.59	28.60	32.48	35.15	38.73	CYCLIC Burc00	C	5 H	3	0	0 G 0
C5H3(L)	144.02	70.55	20.98	24.38	27.03	29.16	32.47	34.90	38.52	HCCCCCH2Burc00	C	5 H	3	0	0 G 0
C5H4	131.81	66.83	17.60	22.64	27.00	30.53	35.25	38.60	43.20	CYCLICBurcat00	C	5 H	4	0	0 G 0
C5H4(L)	106.10	72.03	20.82	25.08	28.52	31.30	35.41	38.48	43.02	CH2CCHCCHBur00	H	4 C	5	0	0 G 0
C5H5	62.57	64.84	19.51	25.22	29.82	33.51	38.86	42.44	47.91	HR 6/01BLYP00	C	5 H	5	0	0 G 0
C5H4H	97.32	67.59	18.28	24.06	28.79	32.65	38.35	42.20	47.84	HR 10/00 BLYP	C	5 H	5	0	0 G 0
C5H5(L)	97.11	73.41	21.91	27.14	31.38	34.80	39.81	43.15	48.14	BURCAT	C	5 H	5	0	0 G 0
C5H6	33.20	65.87	18.74	25.19	30.49	34.85	41.36	45.82	52.40	HR11/99BLYP00	C	5 H	6	0	0 G 0
H2C4O	54.60	66.44	17.27	19.62	21.79	23.73	26.81	28.73	31.51	120189	H	2 C	4 O	1	0 G 0
C6H	213.17	74.12	22.14	25.22	27.67	29.53	31.81	33.27	35.88	121686	C	6 H	1	0	0 G 0
C6H2	169.68	70.94	24.63	27.76	30.26	32.18	34.76	36.81	39.90	121686	C	6 H	2	0	0 G 0
C6H3	158.46	76.31	24.27	28.01	31.14	33.69	37.35	40.04	43.91	20387	C	6 H	3	0	0 G 0
BENZENE	103.39	68.03	19.59	25.38	30.09	33.90	39.47	43.17	48.51	HR12/99BLYP00	C	6 H	4	0	0 G 0
C6H4	123.00	76.80	24.67	30.02	34.40	37.84	42.32	45.06	49.30	BURCAT	C	6 H	4	0	0 G 0
C6H5	81.01	69.27	19.77	26.43	31.83	36.19	42.48	46.56	52.27	YUB3LYP04/04	C	6 H	5	0	0 G 0
C6H5(L)	140.60	84.28	26.90	31.87	36.27	40.04	45.65	48.93	53.93	82489	C	6 H	5	0	0 G 0
C6H6	19.80	64.53	20.19	27.48	33.45	38.30	45.41	50.12	56.81	YUB3LYP04/04	C	6 H	6	0	0 G 0
C6H6F	53.60	70.39	22.08	29.11	34.85	39.51	46.38	51.01	57.97	YUB3LYP04/04	C	6 H	6	0	0 G 0
C6H7	49.35	72.56	22.90	30.54	36.82	41.98	49.68	54.96	62.82	HR 6/99 BLYP	C	6 H	7	0	0 G 0
C6H813	25.41	72.50	22.74	30.88	37.73	43.48	52.30	58.48	67.44	121494THERM	C	6 H	8	0	0 G 0

C6H814	26.05	70.82	22.70	30.71	37.48	43.19	52.03	58.28	67.36	121494THERM	C	6	H	8	0	0	G	0	
C5H5CH3	24.38	74.16	28.07	35.72	41.88	46.85	54.29	59.98	67.74	Burcat10/94	C	6	H	8	0	0	G	0	
C5H40	13.20	69.76	20.38	26.15	30.80	34.53	39.91	43.45	48.62	10/00BURCBLYP	C	5	H	4	0	1	0	G	0
C5H50	42.94	72.74	27.19	32.57	36.97	43.45	43.45	47.76	53.72	ZHONG/BOZ1998	C	5	H	5	0	1	0	G	0
C5H40H	15.90	74.09	23.05	29.40	34.44	38.41	43.98	47.53	52.85	ALZUETA 2000	C	5	H	5	0	1	0	G	0
C6H5CH	110.58	75.80	24.56	32.53	38.94	44.07	51.45	56.25	63.16	T CBSRAD7/01	C	7	H	6	0	0	G	1	
C7H7	49.50	75.64	26.16	34.44	41.20	46.69	54.78	60.24	68.37	YUB3LYP04/04	C	7	H	7	0	0	G	0	
C7H8	12.90	76.91	25.37	33.94	41.09	47.01	55.94	62.06	70.86	YUB3LYP04/04	C	7	H	8	0	0	G	1	
C6H50	12.90	74.41	23.49	30.66	36.48	41.18	48.01	52.50	58.97	YUB3LYP04/04	C	6	H	5	0	1	0	G	0
C6H40H	32.90	70.91	22.37	28.97	34.45	38.98	45.80	50.49	57.38	MOPAC	C	6	H	5	0	1	0	G	0
C6H50H	-23.00	75.49	25.21	32.80	38.93	43.85	50.93	55.51	62.04	YUB3LYP04/04	C	6	H	6	0	1	0	G	1
C6H60H	10.29	81.34	26.03	34.37	41.21	46.75	54.83	60.37	68.54	MOPACRS	C	6	H	7	0	1	0	G	0
A1C2HJ2	135.76	81.76	28.19	35.57	41.52	46.30	53.20	57.75	64.47	YUB3LYP04/04	C	8	H	5	0	0	G	0	
C8H6	73.31	79.07	28.66	36.68	43.20	48.47	56.17	61.32	69.02	YUB3LYP04/04	C	8	H	6	0	0	G	0	
C6H5CHCH	95.41	82.57	29.58	38.39	45.53	51.27	59.58	64.99	72.62	YUB3LYP04/04	C	8	H	7	0	0	G	1	
C8H7J2	95.93	83.09	29.37	38.01	45.06	50.79	59.16	64.67	72.42	YUB3LYP04/04	C	8	H	7	0	0	G	1	
C8H8	35.10	82.09	29.23	38.66	46.40	52.74	62.14	68.50	77.83	YUB3LYP04/04	C	8	H	8	0	0	G	1	
C6H5CO	26.10	84.90	25.73	32.70	38.60	43.57	51.16	56.38	63.44	therm/Marinov	C	7	H	5	0	1	0	G	1
C8H9	41.55	82.73	31.50	41.13	49.24	56.04	66.45	73.65	83.58	C8H10BD THERM	C	8	H	9	0	0	G	1	
C8H10	7.00	82.33	31.09	41.05	50.08	57.74	68.73	76.68	87.81	Burcat T 9/96	C	8	H	10	0	0	G	0	
C6H5CHO	-8.79	80.31	26.85	35.03	41.86	47.44	55.52	60.94	68.53	Burcat 3/86	C	7	H	6	0	1	0	G	0
C6H302	27.53	78.61	25.85	31.70	36.48	40.37	46.04	49.77	54.92	HR BLYP-THERM	C	6	H	3	0	2	0	G	0
C6H5CH20H	-24.00	79.01	27.78	36.80	44.90	51.69	61.11	67.83	77.15	Burcat 7/87	C	7	H	8	0	1	0	G	0
C7H80	-23.90	87.41	28.13	37.00	44.55	50.94	60.84	67.76	77.42	EBG92	C	7	H	8	0	1	0	G	0
C6H50CH3	-17.10	84.01	29.71	38.94	46.54	52.77	62.06	68.38	77.45	6/16/ 1 THERM	C	7	H	8	0	1	0	G	2
OC6H402	-22.02	79.03	26.34	33.05	38.53	42.96	49.44	53.72	59.76	YUB3LYP04/04	C	6	H	4	0	2	0	G	0
PC6H402	-29.00	77.25	26.08	33.34	38.71	42.80	49.31	56.77	97.24	YUB3LYP04/04	C	6	H	4	0	2	0	G	0
INDENEJ	66.17	79.62	29.80	39.95	48.14	54.73	64.24	70.45	79.45	YUB3LYP04/04	C	9	H	7	0	0	G	0	
C6H5C3H2	112.93	94.28	30.93	39.56	46.90	53.11	62.76	69.56	79.03	1/17/ 0 THERM	C	9	H	7	0	0	G	1	
INDENE	35.47	80.32	30.17	40.77	49.45	56.53	66.97	73.95	84.02	YUB3LYP04/04	C	9	H	8	0	0	G	0	
C6H303	-41.61	88.06	27.48	33.76	38.96	43.25	49.65	53.99	60.04	HR AM1 7/99	C	6	H	3	0	3	0	G	0
A2T1	120.08	83.07	31.94	41.74	49.66	56.02	65.16	71.05	79.19	YUB3LYP04/04	C	10	H	6	0	0	G	0	
A2T2	122.52	81.65	31.99	41.75	49.68	56.09	65.41	71.53	80.18	YUB3LYP04/04	C	10	H	6	0	0	G	0	
C10H7J1	97.43	84.14	32.00	42.70	51.39	58.41	68.63	75.34	84.88	YUB3LYP04/04	C	10	H	7	0	0	G	0	
C10H7J2	97.30	84.10	32.07	42.76	51.44	58.46	68.66	75.37	84.91	YUB3LYP04/04	C	10	H	7	0	0	G	0	
C10H8	36.00	80.13	32.49	43.83	53.06	60.52	71.38	78.49	88.48	YUB3LYP04/04	C	10	H	8	0	0	G	0	
A2CH2-1	65.38	90.60	38.34	50.70	60.75	68.87	80.73	88.58	100.01	YUB3LYP04/04	C	11	H	9	0	0	G	1	
A2CH2-2	64.73	90.42	38.39	50.72	60.75	68.87	80.72	88.59	100.02	YUB3LYP04/04	C	11	H	9	0	0	G	1	
A2CH3-1	29.42	90.44	38.84	51.22	61.43	69.81	82.27	90.65	102.62	YUB3LYP04/04	C	11	H	10	0	0	G	1	
A2CH3-2	27.96	91.63	37.69	50.30	60.70	69.23	81.91	90.43	102.53	YUB3LYP04/04	C	11	H	10	0	0	G	1	
C10H70-1	22.49	89.11	35.56	46.78	55.87	63.21	73.83	80.77	90.57	YUB3LYP04/04	C	10	H	7	0	1	0	G	0
C10H70-2	26.80	89.32	35.72	46.92	56.00	63.31	73.91	80.82	90.60	YUB3LYP04/04	C	10	H	7	0	1	0	G	0
C10H70H-1	-6.92	88.68	38.33	49.96	59.28	66.69	77.23	84.00	93.71	YUB3LYP04/04	C	10	H	8	0	1	0	G	1
C10H70H-2	-7.12	90.09	37.75	49.37	58.74	66.26	77.04	83.99	93.76	YUB3LYP04/04	C	10	H	8	0	1	0	G	1
A2R5T	171.53	87.27	36.99	48.16	57.21	64.49	75.00	81.81	91.29	YUB3LYP04/04	C	12	H	6	0	0	G	0	
A2C2H-1J2	151.92	94.92	40.42	51.84	61.05	68.45	79.11	86.08	96.10	YUB3LYP04/04	C	12	H	7	0	0	G	0	
A2C2H-2J1	152.09	95.29	40.44	51.85	61.05	68.44	79.10	86.06	96.09	YUB3LYP04/04	C	12	H	7	0	0	G	0	

A2C2H-2J3	151.98	95.21	40.52	51.92	61.12	68.51	79.15	86.11	96.12	YUB3LYP04/04	C	12 H	7	0	0 G 0
A2R5J1	127.62	88.42	36.66	48.91	58.82	66.78	78.23	85.64	95.99	YUB3LYP04/04	C	12 H	7	0	0 G 0
A2R5J3	123.20	88.37	36.68	48.97	58.89	66.85	78.30	85.68	96.01	YUB3LYP04/04	C	12 H	7	0	0 G 0
A2R5J4	123.20	88.45	36.80	49.08	59.00	66.95	78.37	85.73	96.04	YUB3LYP04/04	C	12 H	7	0	0 G 0
A2R5J5	123.83	88.38	36.69	48.98	58.91	66.87	78.30	85.69	96.01	YUB3LYP04/04	C	12 H	7	0	0 G 0
A2C2H-1	89.58	93.51	40.88	52.95	62.74	70.63	82.10	89.67	100.65	YUB3LYP04/04	C	12 H	8	0	0 G 0
A2C2H-2	89.45	93.87	40.97	53.03	62.80	70.68	82.13	89.69	100.67	YUB3LYP04/04	C	12 H	8	0	0 G 0
A2R5	62.11	85.78	37.21	50.15	60.61	69.01	81.09	88.87	99.63	YUB3LYP04/04	C	12 H	8	0	0 G 0
BIPHEN	100.51	87.07	37.89	50.67	61.04	69.40	81.52	89.43	100.66	YUB3LYP04/04	C	12 H	8	0	0 G 0
A2VINP	110.47	96.11	41.95	54.87	65.27	73.62	85.71	93.77	105.68	HR 7/99 BLYP	C	12 H	9	0	0 G 1
C12H9	103.78	97.72	39.56	52.76	63.44	72.03	84.42	92.46	103.74	YUB3LYP04/04	C	12 H	9	0	0 G 1
HAZR5	68.09	89.31	39.38	52.72	63.56	72.32	85.08	93.50	105.47	HR 4/99 BLYP	C	12 H	9	0	0 G 0
BIPHENH	121.31	92.03	39.74	53.10	63.94	72.68	85.35	93.68	105.52	HR 4/99 BLYP00	C	12 H	9	0	0 G 0
A2C2H3-2	50.98	95.67	42.46	55.64	66.41	75.18	88.03	96.54	108.58	YUB3LYP04/04	C	12 H	10	0	0 G 1
C12H10	43.50	93.25	40.99	54.46	65.46	74.37	87.39	95.98	108.22	YUB3LYP04/04	C	12 H	10	0	0 G 1
A2R5H2	37.40	89.32	39.12	53.01	64.44	73.78	87.60	96.85	110.01	YUB3LYP04/04	C	12 H	10	0	0 G 0
FLUORENE	41.80	92.38	42.07	56.71	68.69	78.42	92.70	102.17	115.62	YUB3LYP04/04	C	13 H	10	0	0 G 0
BENZYL	41.39	106.34	43.32	58.85	71.60	81.99	97.32	107.54	122.09	YUB3LYP04/04	C	13 H	12	0	0 G 2
BENZYLBJ	102.35	110.56	42.90	57.79	69.96	79.86	94.36	103.96	117.54	YUB3LYP04/04	C	13 H	11	0	0 G 2
C6H5OC6H5	15.40	104.34	42.14	56.55	68.24	77.67	91.31	100.22	112.82	YUB3LYP04/04	C	12 H	10	0	0 G 2
A2R5YN1J2	179.71	99.48	44.93	57.90	68.33	76.67	88.61	96.31	107.19	YUB3LYP04/04	C	14 H	7	0	0 G 0
A2R5YN3J4	178.19	99.58	45.24	58.24	68.68	77.00	88.85	96.46	107.26	YUB3LYP04/04	C	14 H	7	0	0 G 0
A2R5YN4J3	178.80	99.46	45.16	58.16	68.60	76.93	88.80	96.43	107.23	YUB3LYP04/04	C	14 H	7	0	0 G 0
A2R5YN4J5	178.80	99.53	45.17	58.16	68.59	76.92	88.79	96.42	107.23	YUB3LYP04/04	C	14 H	7	0	0 G 0
A2R5YN5J4	177.16	99.41	45.16	58.17	68.61	76.94	88.82	96.45	107.25	YUB3LYP04/04	C	14 H	7	0	0 G 0
A2R5YNE1	113.22	98.10	45.58	59.21	70.21	79.03	91.73	100.00	111.79	YUB3LYP04/04	C	14 H	8	0	0 G 0
A2R5YNE3	115.18	98.15	45.71	59.36	70.36	79.17	91.83	100.05	111.81	YUB3LYP04/04	C	14 H	8	0	0 G 0
A2R5YNE4	115.85	98.13	45.74	59.38	70.38	79.19	91.84	100.06	111.81	YUB3LYP04/04	C	14 H	8	0	0 G 0
A2R5YNE5	114.95	97.94	45.64	59.30	70.31	79.13	91.81	100.05	111.80	YUB3LYP04/04	C	14 H	8	0	0 G 0
A2R5R5	102.31	89.65	42.27	56.73	68.39	77.73	91.10	99.71	111.75	YUB3LYP04/04	C	14 H	8	0	0 G 0
A3J1	109.65	97.79	44.29	59.00	70.94	80.57	94.54	103.66	116.50	YUB3LYP04/04	C	14 H	9	0	0 G 0
A3J2	109.72	97.79	44.37	59.07	71.00	80.62	94.57	103.69	116.52	YUB3LYP04/04	C	14 H	9	0	0 G 0
A3J3	109.47	97.72	44.35	59.05	70.98	80.61	94.57	103.69	116.53	YUB3LYP04/04	C	14 H	9	0	0 G 0
A3J4	107.62	97.49	44.23	58.96	70.92	80.57	94.55	103.68	116.53	YUB3LYP04/04	C	14 H	9	0	0 G 0
A3J9	109.55	97.85	44.33	59.03	70.96	80.59	94.54	103.66	116.51	YUB3LYP04/04	C	14 H	9	0	0 G 0
A3LJ1	117.41	97.65	44.47	59.17	71.10	80.71	94.64	103.74	116.56	YUB3LYP04/04	C	14 H	9	0	0 G 0
A3LJ2	117.29	97.63	44.54	59.22	71.14	80.75	94.67	103.77	116.58	YUB3LYP04/04	C	14 H	9	0	0 G 0
A3LJ9	117.78	96.36	44.34	59.04	70.98	80.61	94.57	103.69	116.53	YUB3LYP04/04	C	14 H	9	0	0 G 0
A3	48.20	95.16	44.80	60.16	72.64	82.71	97.31	106.83	120.12	YUB3LYP04/04	C	14 H	10	0	0 G 0
A3L	56.06	93.63	44.94	60.29	72.76	82.82	97.40	106.89	120.17	YUB3LYP04/04	C	14 H	10	0	0 G 0
A3CH2	84.04	102.99	50.36	66.83	80.19	90.97	106.61	116.89	131.63	YUB3LYP04/04	C	15 H	11	0	0 G 0
A3CH2R	56.77	95.01	46.40	62.63	75.84	86.54	102.13	112.35	126.68	YUB3LYP04/04	C	15 H	10	0	0 G 0
A3CH3	47.79	99.95	50.47	67.45	81.29	92.50	108.85	119.58	134.64	YUB3LYP04/04	C	15 H	12	0	0 G 1
A3C2H-1J2	164.60	108.66	52.76	68.18	80.64	90.64	105.04	114.41	127.73	YUB3LYP04/04	C	16 H	9	0	0 G 0
A3C2H-2J1	164.30	108.99	52.74	68.16	80.62	90.62	105.02	114.39	127.72	YUB3LYP04/04	C	16 H	9	0	0 G 0
A3LC2H-1J2	171.98	108.09	52.84	68.27	80.75	90.77	105.27	114.76	128.41	YUB3LYP04/04	C	16 H	9	0	0 G 0
A3LC2H-2J1	171.87	108.46	52.95	68.36	80.81	90.83	105.30	114.78	128.42	YUB3LYP04/04	C	16 H	9	0	0 G 0

A31C2H-2J3	171.87	108.46	52.95	68.36	80.81	90.83	105.30	114.78	128.42	YUB3LYP04/04	C	16 H	9	0	0 G 0
A3C2H-1	102.04	107.22	53.22	69.30	82.33	92.83	108.03	118.00	132.28	YUB3LYP04/04	C	16 H	10	0	0 G 0
A3C2H-2	101.63	107.51	53.28	69.34	82.36	92.84	108.04	118.01	132.29	YUB3LYP04/04	C	16 H	10	0	0 G 0
A31C2H-1	109.47	106.99	53.30	69.39	82.41	92.91	108.10	118.07	132.33	YUB3LYP04/04	C	16 H	10	0	0 G 0
A31C2H-2	109.36	107.35	53.41	69.47	82.48	92.96	108.13	118.09	132.34	YUB3LYP04/04	C	16 H	10	0	0 G 0
A21C6H4	106.96	104.90	50.71	67.29	80.76	91.63	107.42	117.75	132.19	HR04/00 BLYP	C	16 H	10	0	0 G 0
A22C6H4	109.25	102.40	50.26	66.97	80.53	91.48	107.34	117.71	132.17	HR12/99 BLYP	C	16 H	10	0	0 G 0
FLTHNJ1	128.61	101.58	48.67	64.97	78.16	88.76	104.04	113.91	127.62	YUB3LYP04/04	C	16 H	9	0	0 G 0
FLTHNJ3	129.09	101.64	48.72	65.02	78.20	88.80	104.07	113.93	127.62	YUB3LYP04/04	C	16 H	9	0	0 G 0
FLTHNJ7	128.52	101.61	48.68	64.99	78.18	88.79	104.06	113.92	127.62	YUB3LYP04/04	C	16 H	9	0	0 G 0
A3R5J7	133.60	101.68	49.07	65.36	78.52	89.06	104.19	113.91	127.34	YUB3LYP04/04	C	16 H	9	0	0 G 0
A3R5J10	132.05	101.30	48.97	65.29	78.46	89.02	104.15	113.86	127.28	YUB3LYP04/04	C	16 H	9	0	0 G 0
A3LR5J7	140.33	101.80	49.25	65.52	78.66	89.18	104.27	113.96	127.38	YUB3LYP04/04	C	16 H	9	0	0 G 0
A3LR5J10	139.90	101.97	49.24	65.51	78.66	89.20	104.35	114.11	127.70	YUB3LYP04/04	C	16 H	9	0	0 G 0
PYRENEJ1	117.92	100.02	48.51	64.81	78.00	88.62	103.93	113.84	127.58	YUB3LYP04/04	C	16 H	9	0	0 G 0
PYRENEJ2	117.36	98.70	48.62	64.91	78.10	88.70	103.99	113.88	127.61	YUB3LYP04/04	C	16 H	9	0	0 G 0
PYRENEJ4	117.49	100.10	48.56	64.85	78.05	88.66	103.96	113.85	127.59	YUB3LYP04/04	C	16 H	9	0	0 G 0
A2C6H5-2	62.25	108.22	53.52	71.01	85.27	96.82	113.73	124.94	141.35	YUB3LYP04/04	C	16 H	12	0	0 G 1
FLTHN	67.32	99.07	49.26	66.20	79.93	90.97	106.86	117.11	131.24	YUB3LYP04/04	C	16 H	10	0	0 G 0
A3R5	72.10	100.58	49.53	66.48	80.18	91.19	107.02	117.21	131.28	YUB3LYP04/04	C	16 H	10	0	0 G 0
A3LR5	78.83	100.70	49.72	66.64	80.32	91.31	107.10	117.27	131.31	YUB3LYP04/04	C	16 H	10	0	0 G 0
PYRENE	56.16	96.03	49.04	65.99	79.72	90.78	106.72	117.02	131.19	YUB3LYP04/04	C	16 H	10	0	0 G 0
C17H12	57.86	107.18	54.39	73.05	88.26	100.61	118.64	130.52	147.27	YUB3LYP04/04	C	17 H	12	0	0 G 0
BENZNAPJP	116.24	123.37	57.08	74.24	88.69	100.81	119.32	132.08	149.77	5/ 7/97 THERM	C	17 H	13	0	0 G 2
BENZNAP	54.69	122.25	57.87	75.83	90.92	103.54	122.73	135.92	154.27	5/ 7/97 THERM	C	17 H	14	0	0 G 2
CPDPRJ1	144.57	104.25	53.36	71.24	85.65	97.17	113.62	124.11	138.43	YUB3LYP04/04	C	18 H	9	0	0 G 0
CPDPRJ5	144.57	104.25	53.36	71.24	85.65	97.17	113.62	124.11	138.43	YUB3LYP04/04	C	18 H	9	0	0 G 0
CPDPRJ6	144.57	104.25	53.36	71.24	85.65	97.17	113.62	124.11	138.43	YUB3LYP04/04	C	18 H	9	0	0 G 0
CPDPRJ8	144.57	104.25	53.36	71.24	85.65	97.17	113.62	124.11	138.43	YUB3LYP04/04	C	18 H	9	0	0 G 0
CPDPRJ9	144.57	104.25	53.36	71.24	85.65	97.17	113.62	124.11	138.43	YUB3LYP04/04	C	18 H	9	0	0 G 0
CPDPRJ10	144.57	104.25	53.36	71.24	85.65	97.17	113.62	124.11	138.43	YUB3LYP04/04	C	18 H	9	0	0 G 0
PYC2H-1J2	168.68	110.91	56.99	74.01	87.72	98.71	114.45	124.59	138.80	YUB3LYP04/04	C	18 H	9	0	0 G 0
PYC2H-2J1	169.49	110.84	57.07	74.08	87.80	98.80	114.63	124.90	139.44	YUB3LYP04/04	C	18 H	9	0	0 G 0
PYC2H-4J5	169.29	110.98	56.89	73.92	87.65	98.64	114.39	124.55	138.77	YUB3LYP04/04	C	18 H	9	0	0 G 0
CPDFTJ1	165.95	106.24	53.67	71.54	85.93	97.42	113.79	124.20	138.42	YUB3LYP04/04	C	18 H	9	0	0 G 0
CPDFTJ10	165.95	106.24	53.67	71.54	85.93	97.42	113.79	124.20	138.42	YUB3LYP04/04	C	18 H	9	0	0 G 0
BGHIF2	148.94	104.80	52.81	70.69	85.12	96.69	113.24	123.80	138.18	YUB3LYP04/04	C	18 H	9	0	0 G 0
BGHIFJ3	148.94	104.80	52.81	70.69	85.12	96.69	113.24	123.80	138.18	YUB3LYP04/04	C	18 H	9	0	0 G 0
BGHIFJ5	148.94	104.80	52.81	70.69	85.12	96.69	113.24	123.80	138.18	YUB3LYP04/04	C	18 H	9	0	0 G 0
CPDPRJ	83.07	103.14	53.83	72.36	87.32	99.30	116.45	127.41	142.36	YUB3LYP04/04	C	18 H	9	0	0 G 0
PYC2H-1	106.39	109.49	57.47	75.13	89.41	100.89	117.43	128.19	143.37	YUB3LYP04/04	C	18 H	10	0	0 G 0
PYC2H-2	106.98	108.36	57.54	75.19	89.46	100.93	117.46	128.20	143.37	YUB3LYP04/04	C	18 H	10	0	0 G 0
PYC2H-4	106.92	109.44	57.44	75.11	89.40	100.88	117.43	128.18	143.36	YUB3LYP04/04	C	18 H	10	0	0 G 0
CPDFTLH	104.70	104.14	54.24	72.74	87.65	99.59	116.65	127.54	142.41	YUB3LYP04/04	C	18 H	10	0	0 G 0
BGHIF	87.44	102.12	53.53	72.07	87.05	99.07	116.28	127.30	142.31	YUB3LYP04/04	C	18 H	10	0	0 G 0
A4J1	126.10	111.01	56.62	75.36	90.56	102.81	120.53	132.06	148.20	YUB3LYP04/04	C	18 H	11	0	0 G 0
A4J4	128.13	111.33	56.67	75.39	90.58	102.82	120.52	132.04	148.17	YUB3LYP04/04	C	18 H	11	0	0 G 0
A4J12	126.40	111.12	56.52	75.26	90.47	102.73	120.47	132.01	148.17	YUB3LYP04/04	C	18 H	11	0	0 G 0

A4LJ1	138.89	111.19	56.97	75.67	90.84	103.05	120.69	132.17	148.26	YUB3LYP04/04	C	18	H	11	0	G	0
CHRYSENJ1	123.47	111.73	56.69	75.40	90.58	102.80	120.49	131.99	148.13	YUB3LYP04/04	C	18	H	11	0	G	0
CHRYSENJ4	121.01	111.17	56.61	75.34	90.54	102.78	120.49	132.02	148.16	YUB3LYP04/04	C	18	H	11	0	G	0
CHRYSENJ5	120.97	111.28	56.65	75.37	90.56	102.80	120.50	132.03	148.16	YUB3LYP04/04	C	18	H	11	0	G	0
A4	66.73	110.17	57.18	76.55	92.27	104.95	123.30	135.21	151.79	YUB3LYP04/04	C	18	H	12	0	G	0
A4L	77.65	107.05	57.36	76.73	92.44	105.10	123.41	135.30	151.85	YUB3LYP04/04	C	18	H	12	0	G	0
CHRYSEN	61.92	109.13	57.20	76.54	92.26	104.98	123.47	135.59	152.70	YUB3LYP04/04	C	18	H	12	0	G	0
BGHIJFRJ5	191.57	109.60	58.16	77.58	93.21	105.70	123.52	134.89	150.53	YUB3LYP04/04	C	20	H	9	0	G	0
BGHIJFRJ6	191.57	109.60	58.16	77.58	93.21	105.70	123.52	134.89	150.53	YUB3LYP04/04	C	20	H	9	0	G	0
CORJ1	170.82	106.54	57.39	76.94	92.67	105.23	123.11	134.46	149.84	YUB3LYP04/04	C	20	H	9	0	G	0
BGHIJFR	129.89	110.06	58.66	78.74	94.89	107.78	126.14	137.77	153.50	YUB3LYP04/04	C	20	H	10	0	G	0
COR	117.43	102.12	57.90	78.07	94.36	107.41	126.10	138.06	154.42	YUB3LYP04/04	C	20	H	10	0	G	0
DCPCDFG	109.35	106.39	58.74	78.82	94.97	107.86	126.19	137.80	153.51	YUB3LYP04/04	C	20	H	10	0	G	0
DCPCDJK	113.70	107.87	58.74	78.83	94.99	107.88	126.21	137.82	153.52	YUB3LYP04/04	C	20	H	10	0	G	0
DCPCDMN	115.65	106.72	58.71	78.76	94.93	107.88	126.38	138.21	154.45	YUB3LYP04/04	C	20	H	10	0	G	0
BAPYRJ7	131.58	113.28	60.93	81.24	97.67	110.86	129.83	142.05	158.86	YUB3LYP04/04	C	20	H	11	0	G	0
BAPYRJ10	131.58	113.28	60.93	81.24	97.67	110.86	129.83	142.05	158.86	YUB3LYP04/04	C	20	H	11	0	G	0
BEPYRENJ1	129.66	113.34	60.75	81.03	97.44	110.64	129.63	141.86	158.68	YUB3LYP04/04	C	20	H	11	0	G	0
BEPYRENJ9	129.66	113.34	60.75	81.03	97.44	110.64	129.63	141.86	158.68	YUB3LYP04/04	C	20	H	11	0	G	0
BEPYRENJ1	138.00	115.84	61.09	81.36	97.76	110.93	129.88	142.07	158.90	YUB3LYP04/04	C	20	H	11	0	G	0
BBFLUORJ1	137.77	115.20	60.86	81.15	97.57	110.77	129.75	141.97	158.75	YUB3LYP04/04	C	20	H	11	0	G	0
BBFLUORJ12	137.77	115.20	60.86	81.15	97.57	110.77	129.75	141.97	158.75	YUB3LYP04/04	C	20	H	11	0	G	0
BAPYR	71.62	112.55	61.50	82.43	99.39	113.04	132.70	145.39	162.85	YUB3LYP04/04	C	20	H	12	0	G	0
BEPYREN	69.70	112.03	60.76	81.21	98.58	113.17	135.18	149.45	163.80	YUB3LYP04/04	C	20	H	12	0	G	0
BEPYREN	76.50	113.36	61.56	82.48	99.43	113.06	132.71	145.38	162.83	YUB3LYP04/04	C	20	H	12	0	G	0
BBFLUOR	77.81	113.90	61.59	82.54	99.50	113.15	132.79	145.45	162.88	YUB3LYP04/04	C	20	H	12	0	G	0
BKFLUOR	82.58	112.41	61.61	82.57	99.54	113.18	132.82	145.48	162.90	YUB3LYP04/04	C	20	H	12	0	G	0
CORIJ1	210.45	110.45	62.09	83.27	100.25	113.75	132.85	144.85	161.00	YUB3LYP04/04	C	22	H	9	0	G	0
CORIJ6	210.45	110.45	62.09	83.27	100.25	113.75	132.85	144.85	161.00	YUB3LYP04/04	C	22	H	9	0	G	0
CORIJ7	210.45	110.45	62.09	83.27	100.25	113.75	132.85	144.85	161.00	YUB3LYP04/04	C	22	H	9	0	G	0
CORIJ10	210.45	110.45	62.09	83.27	100.25	113.75	132.85	144.85	161.00	YUB3LYP04/04	C	22	H	9	0	G	0
COR1	156.86	109.26	62.73	84.53	102.06	116.04	135.92	148.51	165.60	YUB3LYP04/04	C	22	H	10	0	G	0
ANTHANJ10	143.01	116.03	65.35	87.21	104.86	119.02	139.31	152.29	170.00	YUB3LYP04/04	C	22	H	11	0	G	0
BGHIPEJ1	134.35	116.49	65.24	87.12	104.78	118.95	139.26	152.25	169.97	YUB3LYP04/04	C	22	H	11	0	G	0
BGHIPEJ7	134.35	116.49	65.24	87.12	104.78	118.95	139.26	152.25	169.97	YUB3LYP04/04	C	22	H	11	0	G	0
BGHIPEJ10	134.35	116.49	65.24	87.12	104.78	118.95	139.26	152.25	169.97	YUB3LYP04/04	C	22	H	11	0	G	0
BGHIPEJ11	134.35	116.49	65.24	87.12	104.78	118.95	139.26	152.25	169.97	YUB3LYP04/04	C	22	H	11	0	G	0
BGHIPEJ12	134.35	116.49	65.24	87.12	104.78	118.95	139.26	152.25	169.97	YUB3LYP04/04	C	22	H	11	0	G	0
ANTHAN	81.50	114.93	65.81	88.32	106.53	121.15	142.14	155.59	173.94	YUB3LYP04/04	C	22	H	12	0	G	0
BGHIJPER	72.85	114.01	65.71	88.23	106.45	121.08	142.09	155.55	173.90	YUB3LYP04/04	C	22	H	12	0	G	0
INPYR	88.23	116.41	65.89	88.41	106.63	121.24	142.22	155.65	173.96	YUB3LYP04/04	C	22	H	12	0	G	0
COR2BCEJF6	242.02	114.48	66.95	89.69	107.88	122.31	142.61	155.27	172.18	YUB3LYP04/04	C	24	H	9	0	G	0
COR2BCEJF7	242.02	114.48	66.95	89.69	107.88	122.31	142.61	155.27	172.18	YUB3LYP04/04	C	24	H	9	0	G	0
COR2BCEJF8	242.02	114.48	66.95	89.69	107.88	122.31	142.61	155.27	172.18	YUB3LYP04/04	C	24	H	9	0	G	0
COR2BCHIJ4	247.83	114.51	66.89	89.69	107.91	122.35	142.64	155.28	172.18	YUB3LYP04/04	C	24	H	9	0	G	0
COR2BCEJF	188.43	113.24	67.50	90.92	109.68	124.60	145.68	158.93	176.77	YUB3LYP04/04	C	24	H	10	0	G	0
COR2BCHI	194.36	113.27	67.50	90.93	109.70	124.62	145.70	158.94	176.78	YUB3LYP04/04	C	24	H	10	0	G	0

CORONEN	75.19	112.57	69.90	94.01	113.49	129.11	151.46	165.72	184.97	YUB3LYP04/04	C	24	H	12	0	0	G	0
CPDBPER	98.40	119.46	70.49	94.58	114.02	129.58	151.80	165.94	185.07	YUB3LYP04/04	C	24	H	12	0	0	G	0
CPFBPER	99.07	119.49	70.52	94.60	114.03	129.58	151.79	165.93	185.06	YUB3LYP04/04	C	24	H	12	0	0	G	0
COR3BCEFI	271.60	118.56	71.80	96.18	115.62	130.98	152.46	165.74	183.37	J1 YUB3LYP	C	26	H	9	0	0	G	0
COR3BCEFI	271.60	118.56	71.80	96.18	115.62	130.98	152.46	165.74	183.37	J10 YUB3LYP	C	26	H	9	0	0	G	0
COR3BCEFKL	271.60	118.56	71.80	96.18	115.62	130.98	152.46	165.74	183.37	J6 as ij	C	26	H	9	0	0	G	0
COR3BCEFKL	271.60	118.56	71.80	96.18	115.62	130.98	152.46	165.74	183.37	J7 as ij	C	26	H	9	0	0	G	0
COR3BCEFI	218.52	117.27	72.26	97.28	117.28	133.14	155.43	169.33	187.93	YUB3LYP04/04	C	26	H	10	0	0	G	0
COR3BCEFKL	224.58	117.29	72.26	97.28	117.30	133.16	155.45	169.34	187.94	YUB3LYP04/04	C	26	H	10	0	0	G	0
COR4J1	309.05	122.43	76.53	102.52	123.21	139.54	162.34	176.42	195.16	YUB3LYP04/04	C	28	H	9	0	0	G	0
COR4J10	309.05	122.43	76.53	102.52	123.21	139.54	162.34	176.42	195.16	YUB3LYP04/04	C	28	H	9	0	0	G	0
COR4	247.54	121.33	77.00	103.63	124.87	141.67	165.17	179.73	199.09	YUB3LYP04/04	C	28	H	10	0	0	G	0
HB	269.53	122.26	81.75	109.97	132.44	150.17	174.90	190.12	210.24	YUB3LYP04/04	C	30	H	10	0	0	G	0
OVALENE	115.81	133.91	91.10	122.25	147.42	167.60	196.48	214.89	239.75	YUGROUP07/04	C	32	H	14	0	0	G	0
CIRCUM	150.03	174.40	146.34	196.50	237.24	269.52	314.46	343.62	382.20	YUGROUP07/04	C	54	H	18	0	0	G	0
C66	180.13	199.40	176.26	236.63	285.60	324.43	378.33	413.18	459.10	2/13/ 2 THERM	C	66	H	20	0	0	G	0
C80	211.39	224.46	210.62	282.73	341.16	387.53	451.71	493.06	547.34	2/13/ 2 THERM	C	80	H	22	0	0	G	0
CIRCUMI	150.03	183.55	146.34	196.50	237.24	269.52	314.46	343.62	382.20	2/13/ 2 THERM	C	54	H	18	0	0	G	0
C66Is	180.13	209.92	176.26	236.63	285.60	324.43	378.33	413.18	459.10	2/13/ 2 THERM	C	66	H	20	0	0	G	1
C80Is	211.39	235.79	210.62	282.73	341.16	387.53	451.71	493.06	547.34	2/13/ 2 THERM	C	80	H	22	0	0	G	0
C60	618.15	128.01	121.57	170.32	208.69	238.49	278.68	301.69	328.47	YUGROUP07/04	C	60		0	0	0	G	0
C60MOD	602.05	128.01	121.57	170.32	208.69	238.49	278.68	301.69	328.47	YUHnew	C	60		0	0	0	G	0
C70	657.76	147.82	142.61	199.17	243.75	278.43	325.32	352.25	383.51	YUGROUP07/04	C	70		0	0	0	G	0
C76	699.16	156.92	155.72	216.86	265.12	302.70	353.63	382.97	417.18	YUGROUP07/04	C	76		0	0	0	G	0
C78	702.66	161.92	159.55	222.31	271.84	310.42	362.69	392.79	427.66	YUGROUP07/04	C	78		0	0	0	G	0
C80	724.66	161.42	164.65	228.84	279.53	319.05	372.68	403.67	439.85	YUGROUP07/04	C	80		0	0	0	G	0
C82	720.16	166.22	168.55	234.36	286.34	326.86	381.84	413.59	450.54	YUGROUP07/04	C	82		0	0	0	G	0
C84	716.46	144.92	172.55	239.93	293.15	334.64	390.92	423.40	461.23	YUGROUP07/04	C	84		0	0	0	G	0

## Appendix F

Ph.D.CEP Capstone Paper – An  
Analysis of the Carbon Nanotubes  
Industry and Strategy for Nano-C





Ph.D.CEP Capstone Paper –  
An Analysis of the Carbon Nanotubes Industry  
and Strategy for Nano-C

Joanna Yu

August 21, 2005

## **Executive Summary**

This capstone paper is an integral part of the Ph.D. in Chemical Engineering Practice thesis, and it should “bring the business and management perspective of the MIT Sloan School of Management experience into conjunction with the research topic of the thesis project”. I chose to analyze the dynamics of the incipient carbon nanotubes industry and to suggest possible strategic alternatives for Nano-C, a start-up company with know-how and intellectual property on the synthesis of single-walled carbon nanotubes (SWNT) in flames. The next five years or so will be crucial for the carbon nanotubes industry, and many of the uncertainties surrounding it are expected to be resolved. In order to best position itself for the future, Nano-C should focus on ensuring that its flame-synthesis technology can be an enabling technology for the consistent production of large scale quantities of carbon nanotubes with high-purity and controlled characteristics.

Usually the market for carbon nanotubes is divided into two segments: MWNTs and SWNTs. We think that this division is not enough to capture all nuances of

the carbon nanotubes market. Thus we defined four different segments, ranging from the bulk material with no requirements on characteristics (type I CNT) to individual nanotubes with tailored properties (type IV CNT). This study was focused on the type II CNT: bulk material with some requirements on characteristics. We chose this segment because we consider it to be on the frontier of technology.

Currently technologists are trying to develop processes that can produce large quantities of nanotubes with controlled and consistent diameter, length, and minimal purity. Application developers are struggling to incorporate these nanotubes into commercially feasible devices, while scientists are investigating the properties of these nanotubes. Knowledge in all these fronts has to advance in tandem, since they are interdependent.

Depending on the outcomes of the many uncertainties surrounding the carbon nanotube industry, different scenarios might unfold. Independent of which scenario becomes reality, the best way for Nano-C to prepare itself for the future is to ensure that its promising technology for the production of carbon nanotubes in flames can be an enabling technology for the production of large scale quantities of high-quality carbon nanotubes. To achieve this goal, Nano-C has to gain a better understanding of its combustion process and demonstrate its scalability. A partnership with an application developer would be extremely valuable, because in addition to providing feedback on the performance of Nano-C's material, such a partner would increase Nano-C's awareness in the media.

# Contents

<b>1</b>	<b>Introduction</b>	<b>326</b>
<b>2</b>	<b>Background</b>	<b>327</b>
2.1	Carbon Nanotubes Timeline . . . . .	327
2.2	Carbon Nanotubes Properties . . . . .	328
2.3	CNT Characterization . . . . .	329
2.4	SWNT Production Methods . . . . .	329
<b>3</b>	<b>SWNT Industry Analysis</b>	<b>331</b>
3.1	Scientific and Technological Environment . . . . .	332
3.2	Value Creation . . . . .	337
3.3	Value Capture . . . . .	338
3.3.1	Suppliers . . . . .	338
3.3.2	Potential Entrants . . . . .	340
3.3.3	Substitutes . . . . .	340
3.3.4	Competitors . . . . .	341
3.3.5	Buyers . . . . .	347
3.3.6	Value Chain Overseers . . . . .	350
<b>4</b>	<b>Exercise in Predicting the Future</b>	<b>352</b>
4.1	Scenario Planning . . . . .	352
4.2	Future Market Sizes . . . . .	358
<b>5</b>	<b>Strategy for Nano-C</b>	<b>359</b>
5.1	Current Situation of Nano-C's type II CNT Business . . . . .	360
5.1.1	Nano-C's Competitive Advantage . . . . .	361
5.1.2	Nano-C's Weaknesses . . . . .	362
5.2	Generation of Strategies . . . . .	363

5.3	Near Term (2005 – 2010) Strategy . . . . .	364
5.4	Longer Term (after 2010) Strategy . . . . .	370
5.4.1	Nano-C Has Enabling Technology . . . . .	370
5.4.2	Nano-C Does Not Have Enabling Technology . . . . .	371
<b>6</b>	<b>Conclusions and Final Remarks</b>	<b>372</b>
<b>7</b>	<b>Additional Information</b>	<b>373</b>
7.1	Interviewees . . . . .	373
7.2	Survey Questionnaires and Respondents . . . . .	374
7.2.1	Researchers Working in Industry, Academia, and Governmental Laboratories . . . . .	375
7.2.2	Carbon Nanotube Producers . . . . .	376
7.2.3	nanotube@mit.edu Mailing List . . . . .	377
7.3	Other Contacts . . . . .	379
7.4	Acknowledgements . . . . .	379
	<b>References</b>	<b>380</b>

## List of Figures

1	Interdependencies in science, technology, and applications . . . . .	333
2	Porter's "Five Forces" . . . . .	339

## List of Tables

1	Summary of major carbon nanotubes production method . . . . .	330
2	Carbon nanotube market segmentation . . . . .	336
3	Percentage of first authors of publications from each continent . . . . .	337
4	Percentage of patents filed in each language . . . . .	337
5	Overview of important competitors in the type II CNT market . . . . .	342
6	Key uncertainties in the type II CNT industry and outcomes considered	355
7	Outcomes for each of the key uncertainties . . . . .	356
8	Future market sizes for CNT and for CNT-based applications . . . . .	359
9	Nano-C's strategy generation table - R&D decision area . . . . .	363
10	Nano-C's strategy generation table - Marketing and Growth decision areas . . . . .	364
11	Nano-C's current strategy and suggested strategy for the near future	369

# 1 Introduction

The ultimate goal of this thesis work is a better understanding of the combustion process. In the main body of this document we have presented a method developed for the estimation of the thermochemical properties of polycyclic aromatic hydrocarbons, important precursors in the formation of soot and fullerenes in fuel-rich flames. Such an estimation method is a vital constituent of the development of combustion models that include soot formation. Models for combustion would be useful for companies like Nano-C<sup>1</sup>, which was originally founded with to commercialize flame-synthesized fullerenes. Today Nano-C is also trying to enter the carbon nanotubes market, using a flame environment to synthesize this material. This capstone paper aims at applying the knowledge that I gained in one year at the MIT Sloan School of Management to grasp the dynamics of the nascent carbon nanotubes market, and to analyze possible strategic alternatives for Nano-C.

Carbon nanotubes were first observed and described as such in 1991 by Iijima [1]. The words “carbon nanotubes” are used to denote tubes of graphitic sheets. It is not appropriate to call them molecules, because presently technologists are not dealing with molecules of determined characteristics<sup>2</sup>, but rather with a mix of many different species.

Carbon nanotubes can broadly be classified into single-walled carbon nanotubes (SWNT) and multi-walled carbon nanotubes (MWNT). MWNT are already being incorporated into commercial products, such as lithium-ion batteries and conductive polymers. Small percentages of MWNT can improve the performance of these products considerably. No tight control of the characteristics of the nanotubes (number of concentric nanotubes, chirality, defects, purity) is required for these applications.

---

<sup>1</sup>Nano-C was founded by Prof. Jack Howard, a member of my thesis committee.

<sup>2</sup>This situation will probably change, research groups working on the forefront of CNT research, such as the Dresselhaus Group at MIT, are performing “single molecule experiments” to learn more about the properties of individual CNTs [2].

Since the nanotubes only play a role as an additive, the major consideration is the price of this raw material. On the other hand, researchers are developing applications that are based on the special properties of SWNT, requiring a more controlled quality. The nanotubes used in these applications will probably be able to command a higher price.

In this work we will restrict ourselves only to the incipient SWNT industry, taking the perspective of a SWNT supplier. The data presented in this work was collected through interviews with various experts in the nanotubes field, survey for identification of lead times<sup>3</sup>, and from secondary data. This report is divided into three parts. The first part provides some background on carbon nanotubes as well as references for a more in depth understanding. In the second part, an analysis of the industry of single walled carbon nanotubes (SWNT) is performed. We segment the market of carbon nanotubes into four different types of nanotubes, and focus our attention on one of these types. Finally, the third part is an analysis of the business strategy of Nano-C, a particular producer of SWNTs.

## 2 Background

In this section we are going to give a very brief overview about carbon nanotubes. Where pertinent, references will be given where more detailed information can be obtained.

### 2.1 Carbon Nanotubes Timeline

Since the late XIX century scientists were already dealing with “carbon filaments”. However it was not until 1991, when Iijima observed multi-walled carbon nanotubes using high-resolution transmission electron microscopy, and systematically described

---

<sup>3</sup>See Section 7.2.

these “helical microtubules of graphitic carbon” [1], that the carbon nanotube field was launched. Here we provide a brief (and inevitably incomplete) timeline of carbon nanotubes, based on the timelines from [3, 4].

**1889:** T. Hughes and C. Chambers patent (US 405,480) production of carbon filaments for glow-lamps.

**1960:** R. Bacon of the National Carbide Co. makes graphite nanoscrolls.

**1973:** R. Baker studies growth of cup-stacked carbon filaments using in-situ microscopy.

**1976:** A. Oberlin and M. Endo report growth of carbon filaments having single-layer cylindrical graphite cores.

**1979:** P. Wiles and J. Abrahamson find carbon filaments having several layers of crystalline carbon wrapped together in deposits from arc discharge.

**1985:** H. W. Kroto, R. E. Smalley, and colleagues synthesize  $C_{60}$ .

**1991:** S. Iijima observes multi-walled CNTs in arc discharge deposits.

**1993:** S. Iijima and D. Bethune synthesize single-walled CNTs.

**1995:** A.G. Rinzler and others use carbon nanotubes as field emitters.

**1997:** A. C. Dillon and others suggest hydrogen storage in carbon nanotubes.

**1998:** Z. F. Ren and colleagues synthesize aligned nanotube films using chemical vapor deposition.

**2001:** P.C. Collins, M.S. Arnold, and P. Avouris report the integration of carbon nanotubes into logic circuits

## 2.2 Carbon Nanotubes Properties

Carbon nanotubes are graphene sheets rolled seamlessly into a cylinder. The graphene sheet can be wrapped in many different ways, represented by the chiral vector  $(n, m)$ . One third of these ways lead to metallic nanotubes, while the others lead to semiconducting nanotubes.

Carbon nanotubes have been exalted for many special properties, including their astounding mechanical strength (about 50 times the tensile strength of steel), very



special electrical properties (for example, it is estimated that they have a current carrying capacity of 1 billion amps/cm<sup>2</sup>, whereas copper wires burn out at 1 million amps/cm<sup>2</sup>), efficient conductivity of heat (carbon nanotubes are predicted to conduct heat two times more efficiently than nearly pure diamond) and near unidimensionality [5, 6].

### **2.3 CNT Characterization**

Nowadays most CNT producers (including Nano-C) supply SEM and TEM images, TGA and Raman spectra of the samples. It is agreed however that these characterization techniques are not ideal for the determination of purity, diameter and chirality distribution. A full Raman spectra analysis can provide very detailed information about the samples, however it requires a large set of spectra using different wavelengths, and is thus very costly and time consuming. Electron microscopy images can only observe small fractions of the sample at a time, and thus a rigorous characterization requires taking many images, and building a statistical histogram, which is of course also very time consuming.

It is expected that other methods, such as spectrofluorimetry [7, 8] and Rayleigh scattering [9] might provide a faster (although not as information rich) method than Raman spectroscopy [2].

Customers and suppliers of carbon nanotubes have yet to find good systems to work with each other [10], and concerted efforts for the definition of standard procedures for the determination of the quality of samples of carbon nanotubes are underway, for example by NIST [11], and by the European NanoBusiness Association [12].

### **2.4 SWNT Production Methods**

There are four main production methods, and a summary of each of the methods is found in Table 1, adapted from [5, 13, 14, 15].

Method	Arc Discharge Method	Chemical Vapor Deposition	Laser Ablation	Flame Synthesis
How	Connect two graphite rods to a power supply. place them a few millimeters apart, and turn on the switch. Carbon vaporises and forms a hot plasma.	Place substrate in oven, heat to about 600 °C, and slowly add a carbon containing gas such as methane. As the gas decomposes, it frees up carbon atoms, which recombine in the form of nanotubes.	Blast graphite with intense laser pulses, generating carbon gas form which the nanotubes form.	Burn hydrocarbon fuels in a premixed flame with a catalyst precursor such as iron pentacarbonyl ( $\text{Fe}(\text{CO})_5$ ).
SWNT	Short tubes with diameters ranging from 0.6 to 1.4 nm	Long tubes with diameters ranging from 0.6 to 4 nm	Long bundles of tubes with individual tube diameters from 1 to 2 nm	Short tubes with diameters around 1.5 nm
Pros	Can easily produce SWNTs. MWNTs. SWNTs have few structural defects; MWNTs without catalysts, not too expensive, open air synthesis possible	Easy to scale-up; long length, simple process. SWNT diameter is controllable, quite pure.	Primarily SWNTs, with good diameter control and few defects. The reaction product is quite pure.	Easy to scale-up. Production is expected to be very inexpensive. Primarily SWNTs.
Cons	Tubes tend to be short with random sizes and directions; discontinuous process; often needs a lot of purification	NTs are usually MWNTs and often riddled with defects.	Lasers are an expensive source of energy; some scale-up issues.	Low conversion of carbon; tubes tend to be short.

Table 1: Summary of major carbon nanotubes production method. Adapted from [5, 13, 14, 15]

The HiPco (High pressure CO disproportionation) [16] and the CoMoCAT [17] processes are variations of the chemical vapor deposition method.

### 3 SWNT Industry Analysis

The SWNT industry is very incipient. It is still in the fluid phase, as defined by Utterback [18] with “a dynamic relationship among product innovation, the marketplace, and the firms that emerge and compete on the basis of particular innovations”. The potential of nanotubes is known. However, the performance of this material in devices is not well understood, and CNT producers are struggling to improve the controllability and reproducibility of the process. It is still unclear which production technology will ultimately succeed in delivering large quantities of material with consistent quality, or which applications will successfully enter the market.

In the next couple of sections we will discuss the situation of the SWNT industry as it is now (2005), beginning by making sense of the current scientific and technological environment (Section 3.1) and then performing an industry analysis on the form of Porter’s Five Forces [19] (Sections 3.2 and 3.3). In Section 4 we will use scenario planning to do a little exercise in predicting the future. Of course, “predicting the future is easy, getting it right is the hard part”<sup>4</sup>. However, much of the interest in carbon nanotubes lies on its *potential*, that is, on the possibility that in the *future*, it might be used in applications ranging from super strong nylon to curing cancer [20]. Thus the identification of possible scenarios for the evolution of the SWNT industry is useful for the players in this industry to position themselves for a higher probability of success.

---

<sup>4</sup>Quote attributed to Howard Frank, director of the Information Technology Office at the Defense Advanced Research Projects Agency (DARPA) in Arlington, Virginia, U.S.A. Source: Computerworld June 3, 1996 page 70

### 3.1 Scientific and Technological Environment

In Section 2 we described briefly some of the currently available knowledge on carbon nanotubes. A sample list of unknowns and uncertainties is also very illustrative of the fluid state of the industry today:

- To date, no commercial product has been released that makes use of controlled properties of SWNT.
- Samsung has been promising a CNT-based field emission display “in the next couple of months” since 1999. Their current estimate is that they will have a commercial product by 2006.
- In most applications, it is not clear what the relationship between the properties of the nanotubes and the performance of the device is.
- Improvements in CNT-synthesis methods still rely on well-educated guesses and serendipity. CNT growth mechanism is still not well understood.
- Separation and purification of SWNT is difficult, different separations yield different material and it is thought that SWNT’s are damaged during the separation process.
- There are still no standardized test methods for determining the quality of carbon nanotubes [11, 12].
- CNT-based application developers complain about lack of consistency of CNT samples from suppliers.
- Scalability of the CNT production processes has not been proven<sup>5</sup>.

As illustrated by this list, for CNTs to make a major impact, the knowledge in this field has to advance in many areas (see Figure 1). The development of applications that can harness the full potential of CNTs require a better understanding of the properties (science) of this material (Dependency 1 in Figure 1), as well as the advancement of technology for producing, handling, and characterizing large quantities of CNTs (Dependency 2). On the other hand, the advancement of technology also relies on basic science (Dependency 3). For example, the design of processes for the

---

<sup>5</sup>Thomas Swan is the first supplier of SWNT to build a large scale facility, which came online in April 2004 [21]. Its current capacity is 6kg/month [22]. They are most likely currently running below capacity.

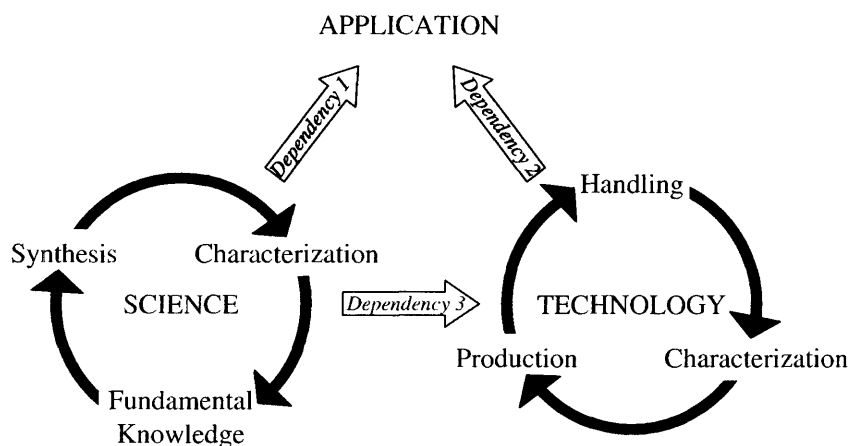


Figure 1: Interdependencies in science, technology, and applications

production of carbon nanotubes would benefit immensely from a better understanding of the CNT growth mechanisms.

Basic science is taking big strides, scientists working in the field agree that we know much more about CNT today than two years ago<sup>6</sup>. The synthesis of individual nanotubes, characterization techniques, and the acquisition of fundamental knowledge on the properties of CNT have been developing in tandem, since one is dependent on the other. For example, research on characterization techniques require the capability to control the synthesis of individual carbon nanotubes to yield molecules with the desired properties. The ability to characterize the carbon nanotubes is essential in the study of their properties for the development of fundamental knowledge, which in turn can improve the control of the synthesis. Similar interdependencies are found in the development of the technology for the production of carbon nanotubes. These interdependencies are also depicted in Figure 1.

The term carbon nanotubes is applied to a material consisting of rolled sheets of graphite. It has been used broadly to describe materials of very different compositions, as discussed in Section 2.3. In this work we have been focusing on SWNTs, but we

<sup>6</sup>For example, in the 2005 review article on Raman spectroscopy of carbon nanotubes by Dresselhaus et al. [23], 35 out of the 90 references were published on or after 2003.

think that when analyzing the CNT industry, it is useful to segment the market further. We broadly divide the market for carbon nanotubes into four segments according to the requirement imposed on the characteristics of the nanotubes:

**I. Bulk material with no requirements on characteristics.** This material is usually MWNTs, with considerable amount of impurities, such as amorphous carbon and catalysts. The market for this material is pretty much established, with estimated sales of several tens of mega-tons/year [24, 25, 26]. This segment is dominated by large players such as Hyperion Catalysis, Arkema, and Showa Denko Carbon, who use the chemical vapor deposition method to grow carbon nanotubes. This segment of the market is price sensitive, since carbon nanotubes are substituting other materials (such as carbon black) that are currently being used<sup>7</sup>. For example, Lithium-ion batteries currently contain about 5% carbon nanotube bulk material with no real control on diameters as intercalation media, to increase the cyclability of the batteries. The bulk material used contains about 20% CNT, leading to circa 1% of carbon nanotubes in the batteries [28].

**II. Bulk material with some requirements on characteristics.** Some applications require nanotubes with controlled characteristics, such as narrow diameter distribution, smaller diameters (preferably SWNTs or DWNTs), certain chiralities (metallic versus semiconducting), certain length, minimal purity, few defects. Currently technologists are working on this frontier, trying to develop processes that can produce large quantities of nanotubes (kg/month) with consistent characteristics. An example of an application using this type of material is field emission displays, where a paste of carbon nanotubes are applied to

---

<sup>7</sup>In economics, goods are said to be substitutes when “an increase in the price of one leads to an increase in the quantity demanded of the other” [27]. According to this definition, carbon black and carbon nanotubes are substitutes (if the price of carbon black would hypothetically increase to the same level as the price of carbon nanotubes, the demand for the latter would increase significantly), although there are significant differences between the two in terms of price and performance.

the surface of a glass substrate. This segment of the market is not very price sensitive, since carbon nanotubes should improve the performance of the applications considerably, and will probably make up only a fraction of the cost of the final product.

### **III. A small number of nanotubes with some requirements on characteristics.**

Usually the requirements on the characteristics of nanotubes in this segment are higher than in segment II. This segment of the market does not face as big a pressure as in segment II for mass-production of nanotubes, rather, the challenge in segment III lies in the ability to efficiently manipulate individual or few strands of nanotubes. This segment is also not very price sensitive, for the same reasons as in segment II.

**IV. Individual nanotubes with tailored properties.** This segment of the market is still in the hands of scientists, who are trying to gain a better understanding of carbon nanotubes. The hope is that one day we will build devices with specially tailored single molecules of carbon nanotube that will heap the full potential of this material. For example, carbon nanotubes are being considered for drug release, because of their nanometer dimensions, they can evade the body's clearance mechanisms and enter cells. Additionally, since they have unique conductivity properties, "the release of their contents can be triggered by remote electronic signals" [29]. This is the least price sensitive market segment. since these carbon nanotubes will be used for applications that would not exist if it were not for this material.

Table 2 provides an overview of each of these market segments, with examples of current and potential applications for each of them. Whether or not the nanotube is grown directly on the device (as has been proposed for field emission displays) is also an important factor for the carbon nanotube producer. Applications in which

Table 2: Carbon nanotube market segmentation according to different requirements on material. Examples of current and potential applications for each segment of material is given, also taking into account whether the CNT is grown on the device or separately

Material	Applications	
	CNT grown on device	CNT grown separately
I. Bulk material with no requirements on characteristics	–	Li-ion batteries, polymer composites
II. Bulk material with some requirements on characteristics	FED <sup>a</sup>	FED , memory, transparent conductive films, supercapacitors, sensors
III. A small number of nanotubes with some requirements on characteristics	AFM <sup>b</sup> tips	AFM tips, sensors
IV. Individual nanotubes with tailored properties	transistors	transistors, drug delivery, other biomedical applications

<sup>a</sup>Field-emission displays

<sup>b</sup>Atomic force microscopy

the CNT is grown directly on the device will not contribute to the market of carbon nanotubes. In this work we will focus on the market segment of type II CNT, since it is currently on the frontier of technology. The challenge in the business of type III CNT lies not in the production of the material, but in its manipulation. There is still a long way for science to go before commercial applications of type IV material reaches the market.

The CNT industry is global. Most of the basic science is conducted in the US and in Asia. Asia lies far ahead of North America and Europe in number of publications in scientific journals and in number of patents filed, as seen in Tables 3 and 4. The values in these tables were obtained from a search for the keywords “carbon nanotube” on SciFinder Scholar conducted on July 15, 2005. According to Thomas Pitstick, Director of Business Development of CNI, “The majority of material [from CNI]



Table 3: Percentage of the first authors of publications containing the keyword “carbon nanotube” from each continent

Continent	Percentage
Asia	46.5 %
North America	28.3 %
Europe	23.1 %
Latin America	1.0 %
Oceania	1.0 %
Africa	0.1 %

Table 4: Percentage of patents containing the keyword “carbon nanotube” filed in each language. Patents filed in English include US, European, and International patents

Language	Percentage
Japanese	49 %
English	33 %
Chinese	8 %
Korean	6 %
Others	4 %

is shipped to Asia and US entities. Europe seems to be somewhat behind” [30]. Nevertheless, producers of type II CNT are found in North America, Europe and in Asia (see Table 5).

### 3.2 Value Creation

An essential component of any industry analysis is a discussion on the size of the market. However, a direct assessment of the market size is difficult. All the companies producing type II CNT are privately owned, and thus not required to disclose any financial information from which some insight into the size of the nanotube market could be obtained. Moreover, many companies announce that they have very large production capacities with the intention of deterring potential entrants from getting access to the market. Press releases have to be taken with a grain of salt, since they often paint a rosy picture of the situation.

Nevertheless, it is possible to establish some benchmark values for the SWNT market size. The market consultancy firm Frost & Sullivan reports that in 2001 the size of this market was US\$30,000 [31]. Taking into account that current prices of SWNT range from US\$100/g to US\$2,000/g [32], we can estimate that between 15g to 300g of SWNT were sold in 2001.

The estimated worldwide capacity for the production of SWNT can provide an

upper-bound for the type II CNT market size. From [22, 33] we estimate this capacity to be around 1 kg/day. Assuming an average price of US\$500/g for SWNT, we get a market size of the US\$100 million order of magnitude for 2005. The actual market size is certainly significantly smaller than this figure. Most of the SWNT producers operate well under capacity, and a considerable portion of the nanotubes that they produce is given away as samples to university research labs or companies developing applications using SWNTs. It is also very likely that that most of the nanotubes that are actually sold are of the “as produced” grade, commanding a lower price.

From the information we gathered, we can infer that the present SWNT market is restricted to selling very small quantities for research and development purposes, since there are still no commercial products. The industry demand for SWNT is currently driven by the hype around SWNT, which has led many technology companies to start experimenting with SWNT.

### **3.3 Value Capture**

In addition to the market size (value creation), when analyzing an industry one needs to consider how the value created is distributed among the various players. Once the focus of the study is defined (producers of type II CNT), one can identify the players as suppliers, potential entrants, substitutes, competitors, and buyers. These players are Porter’s “Five Forces” (see Figure 2) [19]. In this work we will focus on the producers of type II CNT as defined in Section 3.1.

#### **3.3.1 Suppliers**

There are four main suppliers to the producers of type II CNT s:

1. Suppliers of carbon source
2. Suppliers of catalysts
3. Analytical equipment manufacturers

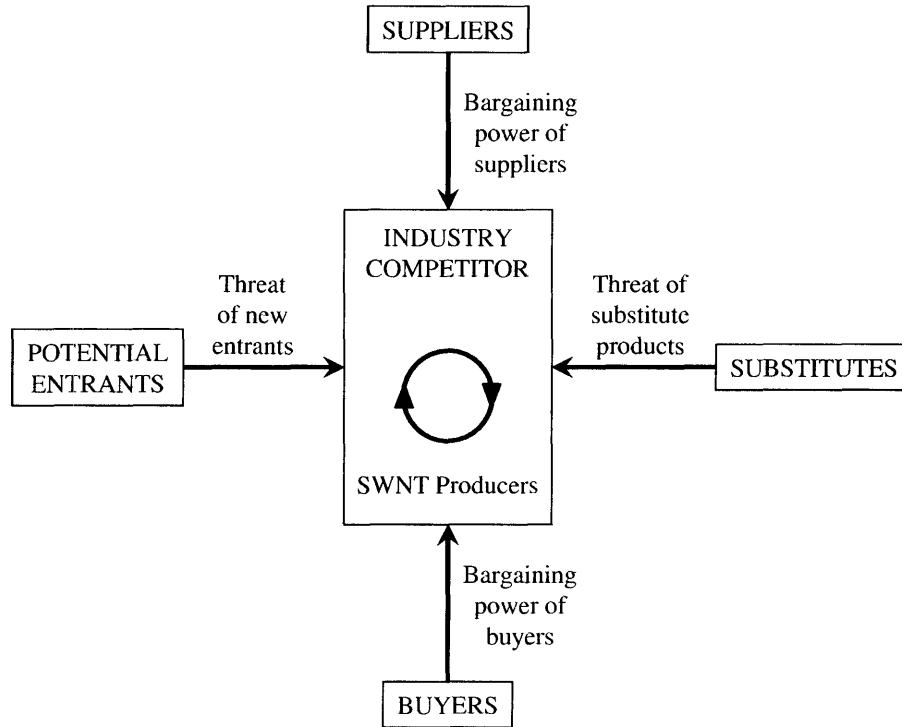


Figure 2: Porter's "Five Forces" [19]

#### 4. Suppliers of knowledge

The product from the first two suppliers are commodities, so these suppliers do not have much bargaining power. Companies that produce type II CNT are mostly very small and associated to a university or other research institutes, and thus in most cases they do not buy their own analytical equipment (scanning electron microscope, transmission electron microscope, Raman spectrometer, ...). However, currently we lack clear and defined methods for the characterization of samples. Thus, equipment manufacturers will be willing to work in close collaboration with the first few big type II CNT producers so that they can influence the definition of the standard analytical techniques in such a way that it benefits their equipment [34].

Currently the incumbents in the type II CNT market are closely associated with universities where the know-how for the production of SWNT was developed (see Section 3.3.4), and thus one could say that the suppliers of knowledge and the in-

cumbents are vertically integrated. But this does not have to continue to be the case, and one can envision a future where the incumbents will license their processes from the knowledge generators.

### 3.3.2 Potential Entrants

Since this is an incipient field (fluid phase, as Utterback [18] puts it), many companies are entering the market. Large capacities have yet to be built, and most companies have not yet developed a fixed network of clients. There are no proper distribution channels, because sales of type II CNT are made on a one by one basis.

Most importantly, a truly enabling technology has not been developed yet [18]. If somebody invents a new method for producing nanotubes which can provide commercial quantities of type II CNT with very well controlled properties at a competitive price<sup>8</sup>, it can rapidly gain significant market share.

Thus, the barriers to entry are low, the most important requirement is to know how to make type II CNT in commercial quantities.

### 3.3.3 Substitutes

Many of the applications for which type II CNT are being considered today already exist, but use some other technology. For example, Nantero envisions its non-volatile random access memory (NRAM), based on CNTs, to “replace all existing forms of memory, such as DRAM, SRAM and flash memory”[36]. However, if the performance improvement of the NRAM is not compatible with its price premium, Nantero’s memory will not be able to gain market share.

This relationship between performance improvement and price is a balance that has to be struck in all the applications of type II CNT , such as SWNT-based field emission displays versus LCD or plasma displays, SWNT-based versus silicon-based

---

<sup>8</sup>The company Thomas Swan thinks that a competitive price for type II material is of the order of US\$10’s/kg [35]

transistors, and CNT-based cancer treatment [20] and chemotherapy. In analyzing which markets SWNT-based products might conquer a significant share of the market, four aspects have to be taken into account:

1. Cost of the type II CNT-based product (type II CNT may or may not play a significant role in this cost)
2. Performance of the type II CNT-based product
3. Cost of the competing product (substitute)
4. Performance of the competing product

SWNT-based products that aim at substituting existing products will face a tough competition, since the existing products have already had an earlier start and have had time to mature<sup>9</sup> More importantly, an array of complements have developed around the existing technologies, creating significant barriers to the entry of a new technology<sup>10</sup>.

### 3.3.4 Competitors

There are a handful of important type II CNT producers. In this section we will provide an overview of them.

**CNI**<sup>11</sup> Carbon Nanotechnologies Incorporated's strongest asset is its intellectual property portfolio. It is the exclusive licensee of more than 100 patents related to the synthesis and enabling technologies of fullerenes and carbon nanotubes from the laboratories of Nobel Prize winner Richard E. Smalley at Rice University (Houston, TX). This intellectual property created great visibility, attracting many customers who were/are starting to develop applications using carbon nanotubes. They have

---

<sup>9</sup>For example, the first DRAM (Dynamic Random Access Memory) chip was released in 1970 by Intel.

<sup>10</sup>For example, current memory chips are produced in fabs (short form of "fabrication"). A new fab costs in the order of several billion dollars. It is then no surprise that Nantero has tried very hard to have its SWNT-based memory production approved for a fab [37]. Another challenge facing SWNT-based memory is its integration into circuits.

<sup>11</sup><http://www.cnanotech.com>

	Technology	Origin of Technology	Purity	Average diameter (nm)	Chirality Information	Price (US\$/g)	Capacity (kg/month)
CNI (US)	HiPco (CVD)	Rice University, Prof. Smalley	Research Grade Industry Grade	-- --	-- --	x00 's ~1	~4-40
Thomas Swan (Great Britain)	CVD	University of Cambridge	--	--	--	180 <sup>a</sup>	6
SWeNT (US)	CoMoCAT (CVD)	University of Oklahoma, Prof. Resasco	90% of carbon content is SWNTs	0.8 ± 0.1	mainly (6,5) and (7,5)	500	“competitive amount”
Carbolex (US)	Arc Discharge	University of Kentucky, Prof. Eklund	50-70 vol% <sup>b</sup>	1.4	chiral angles distributed between 0 and 30	60 <sup>c</sup>	1
Nanolege (France)	Arc Discharge	University of Montpellier	40 <sup>d</sup> 60 <sup>d</sup>	1.3 ± 0.1 1.0 ± 0.1	-- --	80 <sup>e</sup> 180 <sup>a</sup>	4 <sup>f</sup> --
Nanocyl (Belgium)	CVD	Universities of Namur and Liège	>90% carbon	2	--	255 <sup>a</sup>	--
Nanoport (China)	CVD	Chinese Academy of Science	>60% of SWNTs <sup>g</sup>	<2	--	--	a couple of kgs/month

<sup>a</sup> for quantities above 100g

<sup>b</sup> as determined by Raman spectroscopy, impurities include approximately 35w% residual catalyst (Ni, Y)

<sup>c</sup> €65/g, for quantities between 5 and 20 g

<sup>d</sup> carbon content >95% by weight

<sup>e</sup> €145/g, for quantities between 2 and 20 g

<sup>f</sup> projected capacity for the end of 2003

<sup>g</sup> >90% of CNTs

Table 5: Overview of important competitors in the type II CNT market

shipped material to over 700 customers worldwide [30]. According to Mr. Thomas Pitstick, CNI's Director of Business Development, "the majority of material is shipped to Asia and US entities. Europe seems to be somewhat behind. Most customers are using nanotubes in conductive composites, but there are many important applications in displays, electronics, fuel cells, and other composite applications that are being worked on" [30].

CNI's nanotubes are produced through the HiPco process<sup>12</sup>. CNI's carbon nanotubes are available in many different grades. According to Mr. Pitstick, "our costs are proprietary, so we really only talk about price. Price, however, depends upon many factors including the specific grade of nanotubes (quality, performance, etc.), the application it's going into, the price/performance of competitive materials if any, the strength of our patents in a given area, our current capacity vs. demand (i.e. if demand is higher than supply, price will be higher), purchase volumes, and other purchase contract terms such as duration of supply, purchase commitment levels, etc. We have applications (and associated application specific grades) that will range in price from  $\sim$ US\\$X00's/lb (hundreds of US dollars per pound  $\sim$  US\\$1/g) to US\\$100,000's/lb (US\\$X00's/g, hundreds of US dollars per gram)." CNI's capacity varies with the specific grade of nanotubes. For some of them the capacity is of grams per day, while others are several pounds per day. Asked about CNI's capacity, Mr. Pitstick says that "we have a unit that is spec'd out for 100lb/day production of one of our grades. If I had to give a cumulative weight/year number based on right now, I would say [our capacity is] a few hundred to a few thousand lb/year, but this could quickly jump up to tens of thousands of pounds per year."

CNI aims to develop "Cooperative Research" with partner companies who are working on applications that use carbon nanotubes [38]. CNI has announced partnerships with a couple of different companies to develop advanced polymer products

---

<sup>12</sup>"Each batch that is produced by Smalley's HiPco process contains about 50 different species of nanotubes, each with a characteristic diameter and chiral angle". [7]

using SWNTs: Kostak, Inc. in July 2004, Entegris Inc. in May 2004 [39], Performance Plastics Products Inc. (3P) in May 2003 [40], and DSM Venturing & Business Development (DSM V&BD) in January 2003 [41]. In July 2003 CNI announced a joint program with NanoInk to combine this company's Dip Pen Nanolithography™ (DPN™) and CNI's SWNTs to develop next-generation, nanofabricated devices [42].

CNI has also been awarded grants, such as the US\$3.96 million contract (Oct 2004) from the Office of Naval Research in Washington, DC, to develop a new class of military aircraft sealants based on SWNT technology together with Foster-Miller, Inc, and the US\$3.6 million grant from NIST (Sep 2004) to develop in conjunction with Motorola, Inc. and Johnson Matthey Fuel Cells, Inc. "free standing" carbon nanotube electrodes for micro-fuel cells [42].

Evidence of how these partnerships are working out could not be found. It might still be too early to tell how these partnerships will work out.

**Thomas Swan**<sup>13</sup> is a British manufacturer of niche performance and fine chemicals. They have worked with the Department of Chemistry at Cambridge University to devise a scalable CVD manufacturing process for SWNTs. Thomas Swan's strategy is to offer only one product under the Elicarb® brand: high-purity SWNT. They claim to be able to offer consistent quality product in commercial quantities, and to have a process that can be scaled up (currently their capacity is 6kg/month of purified SWNT [22]). In January 2005 Thomas Swan became the second (after Southwest Nanotechnologies, Inc.) carbon nanotube supplier to be certified by Zyvex's Carbon Nanotube Supply Chain Certification Program (see Section 3.3.6). Thomas Swan determines the quality of its samples by atomic absorption (percentage of catalyst in the sample), SEM, TEM, and Raman spectroscopy [35].

Unlike CNI, Thomas Swan does not seek joint development partnerships with

---

<sup>13</sup><http://www.thomas-swan.co.uk>



nanotube users, and imposes no IP constraint downstream<sup>14</sup>.

Thomas Swan currently charges US\$360/g for orders between 1g to 10g, US\$270/g for orders between 10g to 100g, and US\$180/g for orders above 100g. They expect this price to fall as they progress to higher volume production, and aim at reaching a price of US\$10's/kg for SWNTs [35].

**SWeNT**<sup>TM</sup> Southwest Nanotechnologies, Inc.<sup>15</sup> is a spin-off of the University of Oklahoma, where Prof. Resasco's research group developed the CoMoCAT<sup>TM</sup> process to produce SWNT. Their mission statement is to "be the leading producer of high quality single wall carbon nanotubes and to be an innovative partner in the continued development and application of carbon nanotubes" [17]. Prof. Resasco says that "There are many other groups in the world producing nanotubes, but we are the only group growing nanotubes in a controlled environment" [43]. Southwest Nanotechnologies was the first carbon nanotube producer to be certified by Zyvex's Carbon Nanotube Supply Chain Certification Program (see Section 3.3.6).

The company is funded by a mix of private and public resources, including investment from ConocoPhillips (the third-largest integrated U.S. energy company) and a couple of grants from the Oklahoma Center for the Advancement of Science Technology (OCAST). SWeNT also seeks strategic partnerships, such as the one announced on June 2004 with Applied Nanotech, Inc. to develop field emission displays [44].

Southwest Nanotechnologies does not disclose what their capacity is, only that it is a "competitive amount" [33]. The price of their SWNT (carbon content > 90% SWNT's) is US\$500/g. Besides offering SWNTs, they also offer some downstream products, such as "Nanotube Electrodes for Fuel Cells" and "Nanotube-based Field Emitters".

---

<sup>14</sup>However, in a company presentation they list "develop strategic collaborations" as one of their next steps [35].

<sup>15</sup><http://www.swnano.com>

**Carbolex**<sup>16</sup> is a spin-off of the Advanced Science and Technology Commercialization Center at the University of Kentucky in Lexington. It produces SWNTs through the arc discharge method. The “as produced” (AP) grade SWNT has 70 - 90 vol% (as determined by Raman spectroscopy). Prices are currently US\$100/g for orders below 50g, US\$80/g for orders between 50g to 100g, and US\$60/g for orders above 100g. Carbolex has a capacity for their AP grade SWNT of 1kg/month. Carbolex also distributes its SWNT through Sigma Aldrich, where sub-grams quantities are available.

**Nanoledge**<sup>17</sup> is a French company spun-off from the GDPC (Groupe Dynamique des Phases Condensées), a public joint lab between the University of Montpellier and the CNRS (Centre National de la Recherche Scientifique). The company uses the arc discharge method to produce SWNT, and has patents that cover nanotube synthesis (industrial process for continuous production), integration in polymer materials, and processing technologies. As evidenced by the wide coverage of their patents, Nanoledge does not want to be only a supplier of nanotubes, rather, they would like to have capabilities in all steps of the development of nanocomposite materials. In 2003 they projected that by the end of that year they would have a capacity of 1kg/month of SWNT. Currently their prices are €65/g (US\$80/g) for orders between 5 to 20g for the as produced grade, and €145/g (US\$180/g) for orders between 2 to 20g for the as high-purity grade. Nanoledge hopes to one day bring down its price to US\$10/g [45].

As a curiosity, Nanoledge has co-developed with Babolat the tennis racquet with carbon nanotubes. That series of racquets does not contain much nanotubes, but were an efficient marketing tool to create awareness to carbon nanotubes [45]. Currently these racquets are being sold for about US\$200 a piece [46].

---

<sup>16</sup><http://carbolex.com>

<sup>17</sup><http://www.nanoledge.com>

**Nanocyl**<sup>18</sup> is a spin-off from the Universities of Namur and Liège (Belgium). It announced in May 2005 the inauguration of a new industrial CVD reactor with capacity of 15kg/day (of presumably SWNT, DWNT, and MWNT), representing an investment of €2 million [47]. In Sep 2004 Nanocyl successfully raised US\$3.7 million, and it plans to invest over US\$6 million in R&D and equipment [48] before the end of 2006.

In addition to patents in nanotube synthesis technology, Nanocyl's intellectual property covers functionalization of the nanotubes, as well as utilizing nanotubes in composite polymers [49].

In March 2005 Nanocyl signed an agreement with NanoDynamics<sup>19</sup> (a manufacturer of nanomaterials) for a strategic partnership where Nanocyl's ability to manufacture carbon nanotubes will be combined with NanoDynamics experience in identifying commercial markets for nanomaterials in North America and customer contacts.

**Shenzhen Nanotech Port**<sup>20</sup>(Nanoport - NTP) was developed based on intellectual property from the Chinese Academy of Science. They use the CVD method to produce nanotubes, and claim to have low cost, high purity and good control of nanotube properties. Very little public information about NTP is available. It is probably a major supplier in Asia, producing also big quantities of MWNT (tons/year). Their capacity for SWNT is of the order of a couple of kg/month [33].

### 3.3.5 Buyers

The consumers of type II CNT can basically be divided into four different classes. Each of these classes have different resources and background. Here we will discuss the particularities of these consumers.

---

<sup>18</sup><http://www.nanocyl.com>

<sup>19</sup><http://www.nanodynamics.com>

<sup>20</sup><http://www.ntp.com.cn>

**Research groups in universities** This class of consumers is very fragmented, since there are many university-related groups doing experimental research on nanotubes. The areas of experimental research are: 1) study of CNT properties, 2) growth of CNT, and 3) development of applications using CNT. Scientists working on the properties of CNTs are currently focusing on single nanotubes, with specific characteristics, and thus are not likely customers of companies such as those described in Section 3.3.4. The groups that are trying to grow nanotubes might require small samples to use as standards, but are obviously not very frequent buyers. Finally, groups developing applications that use carbon nanotubes are the most attractive within the academic customers. However, many of these research groups have collaborations with other academic groups that produce nanotubes and can supply them with material, or they decide to grow their own nanotubes<sup>21</sup>. Samples needed for research purposes are very small, and academic research budgets are usually tight.

**Nanotechnology start-ups** These companies are usually spin-offs from academic research labs. They have a working concept for an application that uses carbon nanotubes, and are dealing with various aspect of making a commercial product. These start-ups know how they would like the nanotube to perform in their application, but they don't necessarily know what kind of nanotube would achieve that performance. They are thus testing the nanotubes from various suppliers, and their main consideration are in addition to quality of the nanotube (i.e., if it works well with their application), reproducibility, and scalability of the nanotube production process. Cost of the nanotube is usually also taken into account, but not always, since in some cases the nanotubes are only a fraction of the cost of the final product. Examples of such companies are Nantero (memory), Eikos (transparent conductive film), Nanomix (sensors), and Nanosys (novel nanostructured surface coatings).

---

<sup>21</sup>as did the researchers at the Georgia Tech Research Institute developing CNT-based supercapacitors [50]

**Technology companies** These are small R&D companies that are active in areas affected by CNT. They are in early stages of research, trying to incorporate nanotubes into their products.

Some of them have partnerships with nanotubes suppliers, such as MetaMateria Partners<sup>22</sup>, a 20 people company owned by NanoDynamics. They “develop and manufacture nanopowders and components for fuel cells, batteries, membranes, other electrochemical devices, filters, rocket nozzles, and catalyst supports”. Since NanoDynamics has an agreement with Nanocyl to distribute this Belgian company’s carbon nanotubes, MetaMateria will test Nanocyl’s nanotubes to improve the dispersion of nanoparticles in thin film batteries [51].

Others just buy nanotubes from the open market. For example, Eltron Research<sup>23</sup>, “a high technology company dedicated to basic and applied research in energy, chemical processing, environmental, and catalysis technologies” with core technologies in (among others) catalytic membranes, materials research, and electrolytic processes, is conducting research on incorporation of carbon nanotubes into nylon filaments. According to Principal Investigator Richard Bley, they buy their nanotubes from Carbolex and CNI [52]. They do not have partnerships with the suppliers to try to develop a sample of nanotubes that might perform better for their application. Mr. Bley buys as produced grades, and purifies the nanotubes himself, because the high-purity grades are too expensive.

Most of these companies do not have a target price for the carbon nanotubes, since they are still testing technical feasibility. They however state that the current price is too high for commercial feasibility of their applications [52, 53]. These companies hope to have a commercial product within five to 10 years [52, 53].

---

<sup>22</sup><http://www.metamateria.com>

<sup>23</sup><http://www.eltronresearch.com>

**Big corporations** such as Samsung, Motorola, General Electrics, DuPont, IBM, Intel, NEC ... are all known to have nanotube programs or products [54]. Their situation is similar to the situation of the “technology companies” described previously, but on a different scale. Big corporations have big resources. Mr. Susumu Katagiri, Business Manager for Nano Materials at Mitsubishi Corporation states that they would like to be a value added supplier of nanotube-based applications such as batteries, supercapacitors, various material composites, and fuel cell separators [25]. They have suppliers of nanotubes, but additional information about the nanotube producers was not disclosed. Dr. Ji Ung Lee, research scientist at GE working with carbon nanotube-based field emitters and LED says that his group buys nanotubes from (undisclosed) suppliers and also grow their own nanotubes [55]. This mode of operation (both producing nanotubes in-house and buying from suppliers) is probably common to all the big corporations who are now conducting research on nanotube-based devices [56, 57].

Dr. Lee says that his group is developing applications for niche use, and it will take additional 5 to 10 years before they are commercially available. According to him, it is now too early to tell what the target price for carbon nanotubes in their applications is. Dr. Lee adds that availability of purely semiconducting or metallic nanotubes is very desirable.

### 3.3.6 Value Chain Overseers

In addition to Porter’s traditional five forces that influence an industry, we identified one important class of players in the CNT industry, and we call them the “value chain overseers”. These companies are taking the role of value chain architects, acting as coordinators in more than one level of the value chain.

Zyvex<sup>24</sup> is a company that aims at becoming “the leading worldwide supplier

---

<sup>24</sup><http://www.zyvex.com>

of tools, products, and services that enable adaptable, affordable, and molecularly precise manufacturing” [58]. Currently they offer the NanoSolve™ Material product line, which are basically functionalized carbon nanotubes. In addition to buying raw type I and type II CNTs from suppliers, adding value by functionalizing the product, and selling the processed nanotubes under the Zyvex brand, the company is taking an active role towards the management of the value chain by providing certification to suppliers that can deliver products with consistent quality. Since Zyvex’s Carbon Nanotube Supply Chain Certification Program is the only third party quality assurance standard currently available, it is becoming quite prestigious<sup>25</sup>.

We have mentioned NanoDynamics<sup>26</sup> previously in connection with Nanocyl and with MetaMateria. Although NanoDynamics itself does not produce carbon nanotubes nor develops applications for this material, it is playing a coordination role in this industry by linking the suppliers (Nanocyl) with the buyers (such as MetaMateria) in the value chain. NanoDynamics also sells Nanocyl’s carbon nanotubes in the US. A typical lead time for a research grade CNT is 4 weeks [59].

Xintek<sup>27</sup> (formerly Applied Nanotechnologies, Inc.) is a vertically integrated company that produces type II CNT and develops CNT-based applications. Although Xintek is not trying to coordinate the activities of other companies, we included it in the list of “value chain overseers”, because as a vertically integrated company it can coordinate the efforts between the internal type II CNT producers and users more effectively. Through this coordination it might gain insights into the CNT industry that might turn out to be important sources of competitive advantage.

---

<sup>25</sup>SWeNT, Thomas Swan, and Arkema have been certified by Zyvex.

<sup>26</sup><http://www.nanodynamics.com>

<sup>27</sup><http://xintek.com>

## 4 Exercise in Predicting the Future

### 4.1 Scenario Planning

There are so many uncertainties in the future development of the type II CNT market, that any company participating in this market should never place all its bets in one description of the future, since it is almost certain that this description will be wrong.

In this section we will develop different possible scenarios, to emphasize the importance of strategic flexibility that allows companies to position themselves to take advantage of unexpected opportunities. We will follow a simplified version of the steps suggested by Schoemaker [60] for scenario development.

**I. Define Scope** We will focus our study on the global type II CNT market, with a time frame of 10 years. A relatively long time frame was chosen because of the expected long development times for some of the applications, as suggested by our survey results.

**II. Identify the Major Stakeholders** This step is important to determine whether a scenario is an equilibrium point or not. If in a given scenario a major stakeholder is in a position that it does not like, it might be able to change it, and thus the scenario is not stable. In this exercise we identify major stakeholders to be governments (financing R&D projects and ensuring the safety of public health) and large corporations.

**III. Identify Basic Trends** These are trends in the economy, society, technology and industry that can influence the development of the type II CNT market. All the scenarios that will be developed will have these trends as a background.

**Trend 1** Continuing funding of basic science in the carbon nanotube field by the (American) government [28].



**Trend 2** Transistors, memories, sensors, and other electronic components that are faster, smaller, better will always be in demand.

**IV. Identify Key Uncertainties** The uncertainties are at the heart of any scenario planning exercise, since it is the uncertainties that give rise to the different scenarios. As discussed in Section 3, the carbon nanotubes (in particular the type II material) industry is still in the fluid phase, that is, the industry is still in its formative stage, and most questions remain unanswered. We distilled all these unanswered questions into four key uncertainties:

**Uncertainty 1** Will society develop a negative perception of nanotechnology?

**Uncertainty 2** When will we have the capability to reproducibly mass-produce and characterize CNTs with high purity and a narrow diameter and/or chirality distribution?

**Uncertainty 3** How many applications will start to be commercialized before the event in U2 takes place?

**Uncertainty 4** Change in private and public funding before event in U2 takes place?

Based on the information we gathered<sup>28</sup>, we think that these key uncertainties capture the essence of the questions surrounding the future of the type II CNT industry. A negative perception of the society towards nanotechnology can develop for example if carbon nanotubes are linked to harmful health effects or dubious ethical and/or environmental issues [61, 62]. Little (and unexpected) things can make big differences and cause tipping points in the perceptions of the society<sup>29</sup>.

Uncertainty **U2** lumps together all the uncertainties in the technologies for the supply of large quantities of carbon nanotubes with controlled purity, diameter, and

---

<sup>28</sup>Through interviews, the surveys, and collection of secondary data

<sup>29</sup>Society has been wary of some technologies before, such as nuclear energy and genetically modified crops.

chirality. These technologies include capability of producing the nanotubes, of characterizing them, and also of separating them (if the production does not provide sufficient purity or sufficiently narrow diameter/chirality distribution). We chose to consider all the uncertainties related to the commercialization of the product together because, as discussed in Section 3.1, they are all interrelated, and their development will most likely occur in tandem. This development might occur through many incremental improvements, or through major breakthroughs in the technology.

Uncertainty **U3** relates to the possibility that even before we have the capability to produce carbon nanotubes with controlled diameter and chirality, commercial application(s) using type II CNT s might be available. These applications will have been developed through trial and error, by testing samples produced at different conditions (and/or from different suppliers) and seeing which gives the best result. The relationship between the characteristics of the nanotubes and the performance of the application will not be fully understood. This is how current product development occurs [63].

By conditioning the events in uncertainties **U3** and **U4** to the timing of uncertainty **U2** we are implicitly assuming that once the capability to produce and characterize large quantities of carbon nanotubes with controlled diameter and chirality distribution exists, the number of applications developed and the levels of private funding in the type II CNT industry will increase.

For each of these uncertainties, we will limit our study to a couple of possible outcomes, shown in Table 6. We have to limit the number of outcomes studied for this work to be manageable. Based on the answers to the surveys that we received and on interviews that we conducted we think that these outcomes capture a wide and reasonable range of the possible future.

Table 6: Four key uncertainties in the type II CNT industry and outcomes considered in this study

Uncertainties	Outcomes		
	Best case	Compromise	Worst case
<b>U1</b> Will society develop a negative perception of nanotechnology?	No	--	Yes
<b>U2</b> When will we have the capability to reproducibly mass-produce and characterize CNTs with high purity and a narrow diameter and/or chirality distribution?	<2010 <sup>a</sup>	2010-2015	>2015
<b>U3</b> How many applications will start to be commercialized before the event in U2 takes place?	$\geq 2$	1	0
<b>U4</b> Change in private and public funding before event in U2 takes place?	increasing	stable	decreasing

<sup>a</sup>According to Mr. Pitstick, Director of Business Development at CNI, Prof. Smalley is “about one year into what he thinks will be a 5 year project” to develop the ability to synthesize CNTs of desired diameters and chirality. Mr. Pitstick’s conservative estimate is that in 5+ years this capability will be available.

## V. Construct Initial Scenario Themes and Check for Consistency and Plausibility

Once we have identified trends and key uncertainties, we can make a list of all the combinations of the outcomes for the uncertainties. Right away we can identify some scenarios as being inconsistent. For example, if society develops a negative perception of nanotechnology, and outcomes of **U2** and **U3** fall in the worst case, it is very unlikely that private funding (**U4**) will increase. In fact, we can assume that if **U1** and **U2** fall in the worst case, the type II CNT industry is not going to take-off, or at best it is going to be short-lived. A negative public perception towards nanotechnology is certainly not in the interest of major stakeholders (government<sup>30</sup> and big corporations). They will try to avoid this outcome as best as they can, but sometimes public opinion can be tipped by little things, and once public perception is formed, it is very hard to reverse it.

<sup>30</sup>The American government alone has spent in the last eight years billions of dollars in nanotechnology already [64], and European and Asian countries have spent even more than the American government [64].

Table 7: Outcomes for each of the key uncertainties that make up the scenarios developed in this work

Uncertainties	Scenarios			
	Nanotech Feast	Nanotech Drought	Astronaut Food	Nanotech Bubble Bursts
<b>U1</b> Will society develop a negative perception of nanotechnology?	No	No	Yes	Yes
<b>U2</b> When will we have the capability to reproducibly mass-produce and characterize CNTs with high purity and a narrow diameter and/or chirality distribution?	<2010	>2015	<2010	>2015
<b>U3</b> How many applications will start to be commercialized before the event in U2 takes place?	$\geq 2$	1	$\geq 2$	0
<b>U4</b> Change in private and public funding before event in U2 takes place?	↑	→	↓	↓

Moreover, it is believed that the next five years will be crucial for the carbon nanotubes<sup>31</sup> industry. If in the next couple of years no major application for (type II to IV) carbon nanotubes reaches the commercial market (outcome of uncertainty **U3** is zero), it is very likely that governmental agencies will stop funding research on applications [28, 65]<sup>32</sup>, leading to even longer delays in the development of applications.

**VI. Develop Scenarios** From all the possible combinations of outcomes of the key uncertainties, we arrived at four consistent and plausible scenarios, that should cover a wide range of possible futures (see Table 7). Each scenario is like a story, with a title to capture its essence and make it easy to follow and remember.

**Nanotech Feast** In the most optimistic of all scenarios, carbon nanotubes fulfill all its predicted potential. Society does not develop a negative perception of

<sup>31</sup>types II to IV CNT

<sup>32</sup>Prof. Dresselhaus is quite certain however, that funding for basic science in carbon nanotubes will always be available.

nanotechnology (in particular, no harmful health effects of carbon nanotubes are proven), knowledge in carbon nanotubes advances rapidly, and in less than five years technologies for the large scale production and characterization of nanotubes with controlled diameters and chirality are developed. A couple of applications using type II CNT s reach the commercial market in less than five years from now, starting a virtuous cycle. Encouraged by these positive developments, investors continue to increase their funding to the type II CNT industry, which increases the probability of technological improvements and breakthroughs in the type II CNT-production process and in the development of applications. This is the scenario that people currently in the type II CNT industry are hoping for. For example, the future market sizes estimated by various market research groups shown in Table 8 probably apply best for this scenario.

**Nanotech Drought** Another very likely scenario is that society does not develop a negative perception of nanotechnology, however, knowledge in the carbon nanotube field develops much slower than in the “Nanotech Feast” scenario. Here we consider that only after 2015 will the capability to produce and characterize CNTs with high purity and narrow diameter and chirality distribution be available. In the meantime, one application using carbon nanotubes reaches the market, keeping hopes of a brighter future up. Obtaining funds continues to be hard, as investors approach this industry cautiously.

**Astronaut Food** In this scenario, society’s perception towards nanotechnology tips to the negative side, practically shutting out any hopes for a big market for CNT-based applications (for example, CNT are found to be a health hazard). However, before the tipping point, knowledge in the field advances rapidly, and capability for the large scale production of carbon nanotubes with controlled

properties is achieved, and a couple of applications using carbon nanotubes reach (a limited) market. Although banned from the consumer market, carbon nanotubes will still be used for very specialized applications (an hypothetical example would be super sensitive sensors for the military), where its function cannot be performed by other materials. The name from this scenario is an analogy to the niche market for “astronaut food” in the food industry.

**Nanotech Bubble Bursts** In the most pessimistic scenario, society rejects nanotechnology (or carbon nanotubes in particular), stalling research and development in this field. Funding dwindles, and no application reaches the market. The once promising field of carbon nanotubes dies away and enters history as yet another fad.

## 4.2 Future Market Sizes

Existing reports published by market research firms such as Frost & Sullivan [31], NanoMarkets [54], Cientifica [66], and Business Communications Company [67] all give estimates of future market sizes. These values are compiled in Table 8. For example, Frost & Sullivan predicts that by 2007 US\$ 200 million/year worth of SWNTs will be sold, while for the same year NanoMarkets predicts that CNT-based sensors, displays, and memories (all these applications use mainly SWNTs) will generate a market worth over US\$ 600 million/year. We think that these estimates all assume the scenario “Nanotech Feast” to hold true. However, one must be aware that this is not the only possible scenario for the future. Business Communications Company in 2000 estimated that CNT-based applications would generate a market of US\$ 400 million/year by 2004 <sup>33</sup>, a value that has not materialized.

---

<sup>33</sup>We assume that they are referring to CNTs of market segment II to IV as defined in Section 3, since they also mention that production of CNT in 2000 was estimated to range from 1 to 5 kg. It is certain that in 2000 the production of type I material was much more than 5kg.

Table 8: Future market sizes for CNT and for CNT-based applications estimated by market research companies (in millions)

Market	2001	2004	2007	2009	2010	Ref.
CNT and CNT fibers					>€3,000	[66]
New business based on CNT in electronics and semiconductor sectors				US\$3,600		[54]
CNT-based sensors			>US\$200			[54]
CNT-based displays			>US\$200			[54]
CNT-based memory			>US\$200			[54]
CNT	US\$10		US\$540			[31]
SWNT	US\$0.03		US\$200			[31]
MWNT	US\$9.97		US\$340			[31]
CNT	US\$1.5					[67]
CNT-based applications		US\$400 <sup>a</sup>				[67]

<sup>a</sup>This number refers to the potential for 2004 estimated in 2000 under the assumption that no dramatic improvements are made in nanotube production methodology that would lower the cost of nanotubes.

## 5 Strategy for Nano-C

Nano-C was founded in 2001 by Prof. Jack Howard<sup>34</sup> to explore the commercial potential of combustion synthesis of fullerenes. During his Ph.D. thesis, conducted under the supervision of Prof. Howard, Murray J. Height [68, 69] demonstrated the formation of SWNT in premixed flames after the addition of catalyst precursors. Nano-C is currently trying to enter the type II CNT market.

In this section we will first present the current situation of Nano-C's SWNTs business. Next, we will use strategy generation tables [70] to provide an overview of possible strategic alternatives and to aid in the selection of strategies consistent with the scenarios developed in Section 4.1. We suggest one strategy for the near term (2005-2010), when the scenarios discussed in Section 4.1 will still be in formation and a couple of strategies for the subsequent years, dependent on which scenario unfolds.

<sup>34</sup>Chemical Engineering Professor Emeritus at MIT.

## 5.1 Current Situation of Nano-C's type II CNT Business

Nano-C's flame based process can selectively produce SWNT<sup>35</sup>, and it might be a good technology for the production of type II CNT, because it is potentially controllable, scalable, and low cost<sup>36</sup>.

The company has currently 6 employees, working on commercialization of fullerenes, carbon nanotubes and their production technologies.

Nano-C has recently been awarded an NSF SBIR Phase II grant for the research and development of "Commercial Combustion Synthesis of Homogeneous Lots of Carbon Nanotubes"<sup>37</sup>. Nano-C plans to do empirical studies on the operation ranges of the flame, to determine the relationship between flame conditions and produced nanotube properties. The company is working in collaboration with Prof. Vander Sande's Group in the Department of Materials Science and Engineering at MIT to characterize the samples produced in the burner. Currently Nano-C is characterizing its samples through Raman spectroscopy, thermogravimetric analysis (TGA), scanning and transmission electron microscopy (SEM and TEM). Additionally, they are working in close collaboration with Dr. John Wen, a postdoctoral associate from Prof. Green's Group in the Department of Chemical Engineering at MIT, to develop a model for carbon nanotube growth in flame environment.

Nano-C has two burners, a small and a larger one, currently only the smaller burner is being operated for nanotube production. Each run of the small burner produces quantities sufficient for characterization and testing. The larger burner should produce about four times more material in each batch [71].

Nano-C's current business model is to seek partners that are developing applications based on (type II) carbon nanotubes, and to try to adjust the flame to produce

---

<sup>35</sup>It is believed that CO is an important intermediary for the production of SWNT, and flames obviously are abundant in this intermediary. It has been postulated that it is beneficial to have oxygen in the environment where nanotubes are grown because it oxidizes amorphous carbon [63, 71]

<sup>36</sup>Since it does not require energy input to heat up the reactants.

<sup>37</sup>NSF Award #0522093, start day is July 1, 2005.



nanotubes that satisfy the requirements of the partners. Nano-C is not purifying the samples, since the application developers usually have developed their own purification techniques. Nano-C is currently in early stage negotiations with two “nanotechnology start-ups” (see Section 3.3.5).

### 5.1.1 Nano-C’s Competitive Advantage

In order to create and capture value, a company must have a sustainable competitive advantage. In this section we list Nano-C’s capability-based competitive advantages<sup>38</sup>:

- Know-how of combustion process to grow SWNTs. This technology has the potential to be an enabling technology [18] for the type II CNT industry for a couple of reasons:
  - Combustion processes are in general easily scalable<sup>39</sup>.
  - Combustion process is reproducible.
  - Combustor is a continuous flow reactor<sup>40</sup>, thus with potentially much higher throughput than batch processes.
  - There are many parameters that can be adjusted in combustion (fuel, air fuel ratio, flow rates, catalysts, amount of catalyst, pressure) that could potentially influence the characteristics of the produced carbon nanotubes.
  - The raw-material used in the combustion process has a low cost (one could potentially use natural gas as the carbon source)<sup>41</sup>, and since the combustion process is exothermic, it does not require additional input of energy to heat the reactants, such as expensive electricity or lasers used in competing processes.
  - Can (theoretically<sup>42</sup>) be conducted at atmospheric pressure, eliminating safety concerns of dealing with high pressure reactors.

---

<sup>38</sup>Strategic management literature identifies two types of competitive advantage: one based on the position of the company and the other based on its capability [72]. The first is primarily based in the firm’s external context, while the second is based in the firm’s internal context. We believe that Nano-C, being such a young and small start-up company, does not possess positional competitive advantages.

<sup>39</sup>However, the scalability of the combustion process for the production of carbon nanotubes still needs to be demonstrated

<sup>40</sup>which makes it more understandable than other processes

<sup>41</sup>Price of natural gas is of the order of US\$10/million Btu [73]. 1 million Btu has approximately 43.1 lb (20 kg) of fuel [74]. Assuming that all the fuel is CH<sub>4</sub>, of which 3/4 in weight is carbon, the cost of the carbon alone (assuming 100% conversion to carbon nanotubes) is about \$0.66/kg.

<sup>42</sup>Currently Nano-C is using pressures below 1 atm to grow the carbon nanotubes.

- It is believed that CO is an important intermediary for the production of SWNT, and flames obviously are abundant in this intermediary. It has been postulated that it is beneficial to have oxygen in the environment where nanotubes are grown because it oxidizes amorphous carbon [63, 71].
- Past experience in combustion, including scale-up.
- Contacts and experience acquired through fullerene business<sup>43</sup>.
- The intellectual property of all major innovations conducted in Prof. Howard’s Group at MIT (concerning both fullerenes and carbon nanotubes growth) has been licensed to Nano-C by MIT.

### 5.1.2 Nano-C’s Weaknesses

On the other hand, Nano-C has some weaknesses, which we list here:

- A lot of the knowledge within the company is concentrated around some few key people.
- The company is betting in only one technology: combustion process for the production of fullerenes and of carbon nanotubes.
- No proprietary know-how in purification processes.
- No backing from a large company, with whom they could partner for the development of applications, for example. Or from whom they could get financial support.
- Scale-up of the combustion process for the production of carbon nanotubes has not been demonstrated yet.
- Nano-C does not yet have one paying customer for the carbon nanotube business<sup>44</sup>. One paying customer would help Nano-C bridge the “credibility gap”

---

<sup>43</sup>For example, Nano-C has licensed its fullerene technology to Frontier Carbon, a spin-off of Mitsubishi Chemicals and Mitsubishi Corporation.

<sup>44</sup>Nano-C has started work on carbon nanotubes only a year ago.

Table 9: Nano-C’s strategy generation table showing the possible choices in the R&D decision area

R&D				
Understanding of Combustion Process	Characterization	New Product Development	Sample Purification	Scale-up of Combustion Process
understand better through empiricism	be in the forefront of characterization tech	one product with consistent quality	pursue in-house	pursue in-house
understand better through modeling	do characterization to better understand combustion process	line of standard products	pursue through partnership	pursue through partnership
pursue in-house				
pursue through partnership	pursue in-house	develop products tailored for each client	do not pursue	do not pursue
do not pursue	pursue through partnership			
	do not pursue			

with potential customers<sup>45</sup> [75].

## 5.2 Generation of Strategies

Strategy generation tables allow one to have an overview of the possible alternatives under each decision area [70]. Each strategy is comprised of choices in each decision area. We identified three main decision areas for Nano-C’s strategy: Marketing, Growth, and R&D. Each of these main decision areas has been subdivided into more specific decision areas, as shown in Tables 9 and 10.

For example, under the Research and Development decision area (see Table 9), Nano-C has to decide how it will pursue the understanding of the combustion process, what level of commitment it will dedicate to the characterization of samples, what kind of new product development it will pursue, and so on. There are a couple of dif-

<sup>45</sup>Cusumano uses the term “credibility gap” to refer to the “fear among customers that the start-up - like 90% of all start-ups- will fail.[...] The easiest thing for fearful customers to do is not to make a deal with a start-up and instead go to an established vendor” [75]. In the case of an industry that is still in the fluid state like the SWNT industry, an “established vendor” would be a company like CNI or Carbolex.

Table 10: Nano-C’s strategy generation table showing the possible choices in the Marketing and Growth decision areas

Marketing		Growth			
Publicity/ Outreach	Niche/ Segment	Production Growth Rate	Human Resources	Additional Funding	Collaboration/ Partnerships
aggressive	commodity SWNT	ramp up production	hire more marketing people	governmental grants	with another producer that has different technology
moderate	tailor production to individual customer needs	expand slowly	hire more tech people	seek investors	with application developer
none	CNT production tech	maintain current capacity	do nothing		sell out to large chemical company remain independent

ferent alternatives for Nano-C to pursue the understanding of the combustion process: it can try to understand it by doing experiments, and (or) by modelling the process. Moreover, it can decide to pursue this understanding in-house, or through partnerships, or not to try to understand the combustion process at all (this is probably not a good alternative for Nano-C, but was included for completeness’ sake).

### 5.3 Near Term (2005 – 2010) Strategy

From the exercise in scenarios development (Section 4.1), we see that uncertainties **U1** and **U2** are key to the future of the SWNTs market. Since Nano-C is a player in the type II CNT industry, its actions can affect the outcome of the uncertainties described in Section 4.1, in particular of uncertainty **U2**. Thus, Nano-C’s first priority is to ensure that its combustion process is an enabling technology [18] that can consistently produce large scale quantities of (type II) CNT with high purity and narrow diameter and/or chirality distribution. Whether or not Nano-C has an enabling technology will determine how it should position itself best in the long run.

In order to determine whether its technology will be the enabling technology,

Nano-C has to gain a better understanding of its combustion process<sup>46</sup> and demonstrate its scalability. Nano-C would benefit from a partnership with a company that is developing applications based on type II CNT because the partner would give Nano-C feedback about the performance of Nano-C's material. With this feedback, Nano-C can go back and adjust its combustion process to try to address the partners requirements. Through this interactive learning process, in addition to understanding the production of carbon nanotubes in flames better, Nano-C will also gain a deeper knowledge of (a particular) customer's needs. Currently Nano-C does not have such a partner. It should thus take advantage of its recently awarded NSF SBIR II grant to pursue empirical work in-house, since the personnel at Nano-C are leading experts in combustion systems. At this early stage empirical work to understand the formation of SWNTs in combustion will be more effective, since there are still too many unknowns for the development of predictive models<sup>47</sup>.

The choice of understanding the combustion process better through empirical work implies that great emphasis should be placed in characterizing the samples that come out of the experiments. Standards for characterization have not yet been set, since the field of characterization is still evolving. Nowadays most CNT producers (including Nano-C) supply SEM and TEM images, TGA and Raman spectra<sup>48</sup> of their samples. It is agreed however that these characterization techniques are not ideal for the determination of purity, diameter and chirality distribution of bulk materials (see Section 2.3). Researchers have recently proposed other methods, such as spectrofluorimetry<sup>49</sup> [7] and Rayleigh scattering spectra<sup>50</sup> [9], for the detailed analysis of bulk nanotube samples. Nano-C would benefit from such methods in the characterization

---

<sup>46</sup>What is the maximum yield? What are the characteristics of the nanotubes produced? How can one control these characteristics? How much can be controlled?

<sup>47</sup>It is expected that the development of a predictive model for the combustion synthesis of carbon nanotubes will take at least one more year [76].

<sup>48</sup>at only one excitation wavelength.

<sup>49</sup>The absorption of one wavelength of light and the emission of a different wavelength. This method is limited to semiconducting nanotubes.

<sup>50</sup>The scattering of light by particles smaller than the wavelength of the light.

of its samples, since they can provide information regarding the distribution of the various types of SWNTs in the bulk sample, and thus give a richer feedback to the empirical understanding of the combustion process. Nano-C does not possess the expertise in characterization methods, and thus should pursue partnerships with other organizations. Being related to MIT, research labs at MIT would be obvious places to start looking for partners. Nano-C could also scout other laboratories in the many universities in the Boston area.

Currently Nano-C does not possess proprietary purification capabilities, which is ok in current market situation, since (type II) carbon nanotubes are still a specialty chemical, commanding very high prices. However, in the long term, it is expected that the prices of this material will fall, and it would be interesting to be able to offer a higher value-added material. Nano-C could try to gain some know-how in purification techniques through the partnerships that it establishes with application developers. Most of these application developers have established their own carbon nanotube material purification methods suitable for their application.

As Nano-C begins to gain a better understanding and control of the combustion for the production of SWNTs, it should also start working on the demonstration of the feasibility of scale-up of the process, since one of the requirements of the enabling technology is that it is able to provide commercial quantity of material. Although combustors are known to be scalable (for example, production of carbon black, and jet engines), as Prof. Howard pointed out, the scalability of combustors for the production of CNT can only be proven once it is demonstrated [63]. Nano-C should increase its production according to the needs of its potential partner(s). As the partnership matures, it is probable that the application developer will request larger amounts of material, Nano-C should take this opportunity to do the scale-up feasibility study. The bigger burner that the company already has should be taken advantage of.

With this work, Nano-C should be able to have an idea of whether the growth of SWNT in flames can be an enabling technology or not.

Even the greatest of the technologies does not have much value if nobody knows about it. Once it is confident of its process, Nano-C should start marketing the company and its technology aggressively to attract potential partners, preferably “Nanotechnology start-ups” as described in Section 3.3.5. From the interviews conducted in this study, we found that Nano-C’s unique combustion based process for the production of type II CNT is not well known in the carbon nanotube community. The marketing should focus on broadcasting the advantages of Nano-C’s technology. Possible actions are:

1. Update the company’s webpage.
2. Explore more actively the carbon nanotube networks around the Boston area. Nano-C should take more advantage of its connection to MIT, and of its proximity to top-notch universities in the area. Company presentations to targeted groups (such as the “Nanotube Lunches” at MIT) should increase the awareness of Nano-C’s technology, and help spread the word on the company’s capabilities.
3. Participate in technical conferences.
4. Attract the attention of market research companies, such as Frost & Sullivan<sup>51</sup> and Lux Research<sup>52</sup>.
5. Securing a partner that is developing a CNT-based application. If a company like Nantero for example, announces that Nano-C’s SWNTs are ideal for its application, Nano-C’s visibility and credibility will increase dramatically.

Regarding its product offering, initially Nano-C should focus on tailoring production to customer needs, through close collaboration with CNT-based application developers, preferably “Nanotechnology start-ups”, as described in Section 3.3.5. These companies, along with the “Big corporations” have the highest chance of near term success<sup>53</sup>. Ideally Nano-C would kill two rabbits with one bullet by gaining more

---

<sup>51</sup><http://www.frost.com/prod/servlet/frost-home.pag>

<sup>52</sup><http://www.luxresearchinc.com>

<sup>53</sup>However, “Big corporations” are harder to approach, and Nano-C’s relationship with “Big corporations” (“800 lb gorillas”) would not be very balanced.

understanding of its combustion process and testing its scalability while trying to satisfy a potential partner's needs. Nano-C should focus all its efforts in securing a partner that is developing applications based on type II CNT. In addition to providing valuable technical feedback to Nano-C's combustion process, such a partnership would increase Nano-C's awareness in the media considerably.

Currently Nano-C seems to have achieved a good human resources equilibrium. It can get all the tasks done, and nobody is idle. However, if Nano-C really adopts a more aggressive marketing and partnership strategy, it might be necessary to hire more people, both in the technical as well as in the marketing areas.

For Nano-C to increase the chances of a positive outcome for uncertainty **U2**<sup>54</sup>, i.e., to increase the chances of its combustion process being an enabling technology for the production of type II CNT, it has to work in collaboration with groups that are familiar with the forefront of characterization techniques (most likely groups in academia), and with organizations that are developing purification techniques and applications based on type II CNTs. As discussed in Section 3.1, a positive outcome for uncertainty **U2** lies on the advancement of many fields that are interdependent, and thus multidisciplinary collaborations are essential.

In Table 11 we summarize Nano-C's current strategy by showing the choices that it has made in each decision area and compare it to our suggested strategy for the near term (2005 – 2010). Although both strategies are essentially very similar, the suggested near term strategy is designed to increase the chances that Nano-C's combustion process is an enabling technology. Emphasis is put on the importance of strategic partnerships and targeted publicity.

---

<sup>54</sup>We will have the capability to reproducibly mass-produce and characterize CNTs with high purity and a narrow diameter and/or chirality distribution before 2010.



Table 11: Nano-C's current strategy and suggested strategy for the near future (2005 - 2010)

		Nano-C's Current Strategy	Suggested Strategy for 2005--2010
R & D	Understanding of Combustion Process	Understand better through empiricism AND modeling, pursue in-house	Understand better through empiricism, pursue in-house, guided by partner's needs
	Characterization	(Starting) to do characterization to better understand combustion process	Do characterization to better understand combustion process, through partnerships
	New Product Development	Develop products tailored for each client	Develop products tailored for each client
	Sample Purification	Do not pursue	Pursue through partnership
	Scale-up of Combustion Process	Currently not pursuing (but have plans to pursue in the near future)	Pursue in-house (or through partnership)
Mktg	Publicity/ Outreach	Moderate	Aggressive (but targeted) publicity of the advantages of Nano-C's technology, with the aim of developing partnerships
	Niche/ Segment	Tailor production to individual customer needs	Tailor production to individual customer needs
Growth	Production Growth Rate	Expand slowly	Expand slowly
	Human Resources	Do nothing	(Maybe) hire more marketing and/or technical people
	Additional Funding	Governmental funding	Governmental funding
	Collaboration/ Partnerships	With application developers	With application developers (influencing Nano-C's pursue understanding of the combustion process and scale-up study)

## 5.4 Longer Term (after 2010) Strategy

Longer term strategies are dependent on whether Nano-C has the enabling technology for the production of large scale quantities of type II CNT or not, and on which of the scenarios proposed in Section 4.1 materializes.

### 5.4.1 Nano-C Has Enabling Technology

**Strategy for the “Nanotech Feast” Scenario** In this most optimistic of all scenarios, Nano-C’s combustion technology is the enabling technology [18], and the SWNT industry really takes off and fulfills its predicted potential.

Once its technology is proven, Nano-C can scale down its efforts in marketing, since the company will gain a lot of free publicity from the nanotech press.

If Nano-C has the enabling technology, it is assumed that it has a reasonable understanding of the growth of carbon nanotubes in flames. In this case, tailoring the production to customer needs will be easier, and Nano-C should continue to focus in this segment, since it is the more lucrative one.

In this very optimistic scenario, Nano-C will have many good options in many of the decision areas. For example, it could even consider ramping up its production and becoming a major SWNT supplier. It will definitely have to hire many more technical people. With a proven technology, it won’t be difficult for Nano-C to attract investors eager to get a share of the pie. It will have options in the collaboration/partnerships decision area as well. Nano-C might want to try to become a value chain architect, since it would hold the strongest position in the value chain and thus could command the largest share of the pie. Another option would be to sell out the company to a large chemical corporation and retire luxuriously.

**Strategy for the “Nanotech Drought” Scenario** If the rate of past discoveries and breakthroughs in the carbon nanotube technology is extrapolated over the next

ten years, the future would look a lot like this scenario <sup>55</sup>. If however Nano-C thinks it has the enabling technology, it should try to survive the drought, because when the capability of reproducibly producing large scale quantities of type II CNT is achieved, it will be very valuable.

The most likely reason for a slow rate of discoveries and breakthroughs are unexpected technical difficulties in the integration of carbon nanotubes in the application. Vertically integrated organizations, where the producer of type II CNT and the application developer are tightly coordinated will fair better in this scenario. One option for Nano-C would be to license out its technology to a vertically integrated company.

**Strategy for the “Astronaut Food” Scenario** In this scenario, the type II CNT market will be highly specialized. The market will be small and will not accommodate many players. If Nano-C has the enabling technology, it might actually find itself in a comfortable position without many competitors. However, it will have to battle alone for the creation and maintenance of the market. Partnerships with application developers would strengthen its position by aligning Nano-C’s and the partner’s interests towards the maintenance of the market.

#### 5.4.2 Nano-C Does Not Have Enabling Technology

**Strategy for the “Nanotech Feast” Scenario** In this case the full potential of carbon nanotubes is unleashed and the industry takes off. However, another technology for the production of carbon nanotubes is the enabling technology.

Nano-C would be in a difficult situation, however, it might still be able to take a small role in the feast by identifying and entering a niche market, where the carbon nanotubes that they produce are better and/or cheaper than the standard technology.

---

<sup>55</sup>There are many technical difficulties in scaling up production processes and in developing applications using carbon nanotubes, as illustrated, for example, by Samsung having been announcing that its FED would be commercially available in the next couple of months since 1999. Currently no CNT-based FED is available yet, although many working prototypes have been exhibited.

**Strategy for the “Nanotech Drought” and “Astronaut Food” Scenarios** If the potential of carbon nanotubes is not fulfilled in the next couple of years, the greatest challenge for Nano-C will be to identify as early as possible whether it has an enabling technology or not.

If Nano-C does not have an enabling technology, they might want to try to partner with another producer that has a different technology (it could be the enabling technology or another one), to be able to offer a wider variety of products. They would have to target a niche market (of the already small type II CNT market) where the carbon nanotubes are better and/or cheaper than the standard technology.

However, the most sensible thing to do if these scenarios unfold would probably be to exit the market.

## 6 Conclusions and Final Remarks

In this capstone paper we have studied the market dynamics of the nascent carbon nanotubes industry, rounding off the technical knowledge acquired during this Ph.D. work with some experience in analyzing a business environment.

The carbon nanotube industry is still in the fluid phase<sup>56</sup>, as defined by Utterback [?], many of the technologies around carbon nanotubes (for characterization, incorporation of the nanotube into the applications) are still being developed. Relations between suppliers and buyers are still not well established, and the enabling technology(ies) for the production of this material has not been defined yet. The whole industry (science, technology, and applications) is interdependent, and thus has to evolve in tandem. In the past couple of years there has been considerable progress in the carbon nanotubes field, however, this industry has yet to deliver a truly revolutionary commercial product that lives up to its promise. The next five years or so are going to be crucial for the development of carbon nanotube applica-

---

<sup>56</sup>We are referring here to the types II to IV CNT. See Section 3.

tions. Many uncertainties will have to be resolved, leading to many possible scenarios, as described in Section 4.1. If the outcomes of the uncertainties are negative, it is very probable that funding for research and development will dry out.

In addition to an overview of the dynamics of the carbon nanotubes industry, we analyzed strategic alternative for Nano-C, a start-up company that has a technology to produce carbon nanotubes through combustion. The foremost priority for Nano-C now is to ensure that its technology can be an enabling technology to consistently produce large scale quantities of carbon nanotubes with high purity and controlled characteristics. To achieve this goal, Nano-C has to gain a better understanding of its combustion process and demonstrate its scalability. A partnership with an application developer would be extremely valuable in this endeavor. In addition to providing feedback on the performance of Nano-C's material, such a partner would increase Nano-C's awareness in the media considerably.

Longer term strategies for nano-C are dependent on whether the company has the enabling technology for the production of carbon nanotubes or not, and on the outcomes of the uncertainties discussed in Section 4.1. In any case, it is crucial for Nano-C to gain knowledge about the potential of its combustion-based technology in the next couple of years, to allow the company to position itself better for the long term.

## **7 Additional Information**

### **7.1 Interviewees**

We conducted interviews with people in academia and industry working with carbon nanotube related projects. The following is a list of the interviewees.

**Joost Bensen**, Core Officer of the MIT TinyTechnology Club, June 30, 2005.

- Anastasios John Hart** , graduate student at the MIT Mechanical Engineering Department, July 7, 2005.
- Riccardo Signorelli**, graduate student at the MIT Electrical Engineering and Computer Science Department, July 7, 2005.
- Prof. Sang-Gook Kim**, Esther & Harold Edgerton Associate Professor, MIT Department of Mechanical Engineering, July 8, 2005.
- Prof. Mildred Dresselhaus**, Institute Professor, MIT Department of Physics, July 13, 2005.
- Prof. John Preston**, Professor, MIT Sloan School of Management, July 19, 2005.
- Joe Marasco**, VP of Commercial Development, Nano-C, July 19, 2005.
- Dr. Suvankar Sengupta** (ssengupta@aol.com), Principal Investigator, MetaMateria, July 25, 2005.
- Dr. Joel Pierce** (jpierce@resodyn.com), Principal Investigator, Resodyn Corporation, July 25, 2005.
- Dr. Richard Bley** (bley@eltronresearch.com), Principal Investigator, Eltron Research, July 25, 2005.
- Dr. Henning Richter**, Director, Materials Synthesis Research, Nano-C, July 27, 2005.
- Eduardo Barros**, Graduate Student, MIT Department of Physics, July 30, 2005.
- Prof. Jack Howard**, Chairman and Founder, Nano-C, August 1, 2005.

## 7.2 Survey Questionnaires and Respondents

In this section we present the surveys sent to the researchers working both in industry, academia, and governmental laboratories, carbon nanotube producers, and to the nanotube@mit.edu list. This list is organized and maintained by graduate students at MIT, to connect people working with carbon nanotubes throughout the Institute. There are currently around 70 people in this mailing list. In total surveys were sent to about 120 people. The names of the respondents to each of the surveys are also listed in this section.

### 7.2.1 Researchers Working in Industry, Academia, and Governmental Laboratories

-----S U R V E Y-----

1. What are the main applications that you are developing that incorporate carbon nanotubes?
2. When do you think these applications will be available commercially, and what is the expected market size?
3. Do you grow your own nanotubes or do you purchase them from a supplier? If you grow your own nanotubes, what method do you use? If you purchase them, who is your supplier?
4. If you could make a "wish list" for carbon nanotubes characteristics (for example: longer, higher purity...), what would it be?
5. What is your target price for carbon nanotubes?
6. Finally, would you be available for a short follow-up interview via phone or email?

-----  
**Respondent:**

**Dr. Ji Ung Lee** (leeji@research.ge.com), scientist at General Electrics.

## 7.2.2 Carbon Nanotube Producers

-----S U R V E Y-----

1. Who are your main clients and what are they using carbon nanotubes for?
  
2. What is your company's capacity for SWNT today (in weight/year)?
  
3. What is the cost for the SWNT produced by your company?
  
4. What would be your optimistic and pessimistic lead time estimate (for example, 5 to 10 years) for the following events (please feel free to add any comments you might have regarding any of the items):
  - A) Ability to synthesize CNTs of desired diameters and chirality
  
  - B) Ability to mass-produce CNTs with high purity and a narrow diameter and/or chirality distribution
  
  - C) Availability of easy and fast characterization techniques for the high-throughput evaluation of CNT quality
  
  - D) Maturity of purification, separation, and functionalization techniques for CNT



E) Ability to substantially increase the performance of composite materials by the addition of CNTs

F) Ability to effectively incorporate CNTs into electronic devices

G) Use of CNTs in biological applications

5. Finally, would you be available for a short follow-up interview via phone or email?

-----

**Respondents:**

**Dr. Harry Swan** (hswan@thomas-swan.co.uk), Business Manager for Nanotechnology at Thomas Swan.

**Dr. Thomas Pitstick** (tpitstick@enanotech.com), Director of Business Development at CNL.

**Dr. Olivier Decroly** (odecroly@nanocyl.com), Nanocyl.

### 7.2.3 nanotube@mit.edu Mailing List

-----S U R V E Y-----

1. How is your work/interests related to carbon nanotubes?
2. What would be your optimistic and pessimistic lead time estimate (for example, 5 to 10 years) for the following events (please feel free to add any comments you might have regarding any of the items):

- A) Ability to synthesize CNTs of desired diameters and chirality
  
- B) Ability to mass-produce CNTs with high purity and a narrow diameter and/or chirality distribution
  
- C) Availability of easy and fast characterization techniques for the high-throughput evaluation of CNT quality
  
- D) Maturity of purification, separation, and functionalization techniques for CNT
  
- E) Ability to substantially increase the performance of composite materials by the addition of CNTs
  
- F) Ability to effectively incorporate CNTs into electronic devices
  
- G) Use of CNTs in biological applications

3. Finally, would you be available for a short follow-up interview via phone or email?

-----

**Respondents:**

**Gilbert Nessim**, graduate student at the MIT Department of Materials Science and Engineering.

**Anastasios John Hart**, graduate student at the MIT Mechanical Engineering Department.

### 7.3 Other Contacts

Email contact was also established with other people participating in the CNT industry:

**Chuck A. Van Fleet** (swanchem@aol.com), Swan Chemical Inc. (US subsidiary of Thomas Swan & Co Ltd.).

**Todd Cleveland** (tcleveland@nanodynamics.com), Technical Sales Engineer at NanoDynamics.

**Ken A. Smith** (smith@cnanotech.com), Vice President for Technology at CNI.

**Yongwan Jin** (ywjin@samsung.com), Samsung.

**Susumu Katagiri** (susumu.katagiri@mitsubishicorp.com), Business Manager, Nano Materials at Mitsubishi Corporation.

### 7.4 Acknowledgements

Unlike the main body of this thesis, where the chief source of data was quantum chemical calculations, the most important data collected for this capstone paper were information given by experts in the carbon nanotube field, who took the time to interview with me and/or to answer a survey. I am indebted to all of them for generously sharing their insights into this nascent field.

I would like to give special thanks to Henning Richter, for his interest, encouragement, and provision of valuable information and references; John Hart for his enthusiasm, interest, and helpfulness, Prof. Mildred Dresselhaus for making time in her busy schedule to talk to me, Prof. Sang-Gook Kim for his enthusiasm, Eduardo Barros, for his alacrity in explaining much of the basics in nanotube characterization, Riccardo Signorelli, for sharing his perspectives, Joost Bensen for providing me with a first introduction to the carbon nanotubes business, and Prof. Jack Howard, for his support in this endeavor. Mr. Chuck Van Fleet and Mr. Harry Swan from Thomas Swan & Co Ltd. and Mr. Thomas Pitstick from Carbon Nanotechnologies Inc. were also particularly helpful.

## References

- [1] S. Iijima. Helical microtubules of graphitic carbon. *Nature*, 354(6348):56-58, 1991.
- [2] E. Barros. Personal communication, July 30, 2005.
- [3] J. Hart. Carbon nanotubes: Old material, recent momentum. Deshpande IdeaStream 2005.
- [4] D. Tomanek. Carbon nanotubes - a time line. <http://www.pa.msu.edu/cmp/csc/nttimeline.html> Last update date September 7, 2001. Access date August 3, 2005.
- [5] P. G. Collins and P. Avouris. Nanotubes for electronics. *Scientific American*, 283(6):62-69, 2000.
- [6] M. S. Dresselhaus, G. Dresselhaus, and P. Avouris. *Carbon Nanotubes - Synthesis, Structure, Properties, and Applications*, volume 80 of *Topics in Applied Physics*. Springer, Berlin, 2001.
- [7] R. B. Weisman. Simplifying carbon nanotube identification. *The Industrial Physicist* <http://www.aip.org/tip/INPHFA/vol-10/iss-1/p24.html> Access date August 3, 2005.
- [8] S. M. Bachilo, M. S. Strano, C. Kittrell, R. H. Hauge, R. E. Smalley, and R. B. Weisman. Structure-assigned optical spectra of single-walled carbon nanotubes. *Science*, 298(5602):2361-2366, 2002.
- [9] M. Y. Sfeir, F. Wang, L. Huang, C. c. Chuang, J. Hone, S. P. O'Brien, T. F. Heinz, and L. E. Brus. Probing electronic transitions in individual carbon nanotubes by rayleigh scattering. *Science*, 306(5701):1540-1543, 2004.
- [10] J. Giles. Growing nanotech trade hit by questions over quality. *Nature*, 432:791, 2004.
- [11] NIST. 2<sup>nd</sup> joint workshop on measurement issues in single wall carbon nanotubes: Purity and dispersion part II. Technical report, January 26-28, 2005.
- [12] European NanoBusiness Association and Austrian Research Promotion Agency. 2<sup>nd</sup> workshop on standardization for carbon nanotubes. Technical report, 28/29 April 2005.
- [13] M. J. Height. *Flame Synthesis of Carbon Nanotubes and Metallic Nanomaterials*. Ph.D. Thesis, Massachusetts Institute of Technology, 2003.
- [14] M. Daenen, R. D. de Fouw, B. Hamers, P. G. A. Janssen, K. Schouteden, and M. A. J. Veld. The wondrous world of carbon nanotubes. Technical report, Eindhoven University of Technology, 2003.

- [15] H. Richter. SBIR/STTR Phase II: Commercial combustion synthesis of homogeneous lots of carbon nanotubes. Technical report, Nano-C, Inc., 2005.
- [16] M. J. Bronikowski, P. A. Willis, D. T. Colbert, K. A. Smith, and R. E. Smalley. Gas-phase production of carbon single-walled nanotubes from carbon monoxide via the HiPco process: A parametric study. *Journal of Vacuum Science & Technology, A*, 19(4):1800-1805, 2001.
- [17] SouthWest NanoTechnologies. <http://www.swnano.com> Access date August 4, 2005.
- [18] J. M. Utterback. *Mastering the Dynamics of Innovation: How companies can seize opportunities in the face of technological change*. Harvard Business School Press, Boston, Massachusetts, 1994.
- [19] M. E. Porter. *Competitive Strategy: Techniques for Analyzing Industries and Competitors*. Free Press, New York, 1980.
- [20] Nanotechnology kills cancer cells. <http://news.bbc.co.uk/2/hi/health/4734507.stm>, Access date August, 2 2005.
- [21] S. Harris. Nanomaterials, big opportunities. *The Fuel Cell Review*, December 2004/January 2005.
- [22] H. Swan. Survey response, July 20, 2005.
- [23] M. S. Dresselhaus, G. Dresselhaus, R. Saito, and A. Jorio. Raman spectroscopy of carbon nanotubes. *Physics Reports*, 409(2):47-99, 2005.
- [24] Arkema Press Release. Zyvex and arkema announce strategic partnership. <http://www.arkemagroup.com> Last update date February 16, 2005. Access date August 2, 2005.
- [25] S. Katagiri. The nanocarbon: Potential and practical applications with business models. In *NT05: Sixth International Conference on the Science and Application of Nanotubes*, Gothenburg, Sweden, 2005.
- [26] Showa Denko Carbon Press Release. SDK ready for mass production of vapor-grown nanofiber. <http://www.sdkc.com/documents/Nanofiber%20Production.pdf> Last update date December 6, 2001. Access date August 8, 2005.
- [27] R. S. Pindyck and D. L. Rubinfeld *Microeconomics*, 5th ed. Prentice Hall, Upper Saddle River, NJ, 2001.
- [28] M. S. Dresselhaus. Personal communication, July 13, 2005.
- [29] J. Bradbury. Beyond pills and jabs. *The Lancet*, 362:1984-1985, 2003.
- [30] T. Pitstick. Survey response, July 28, 2005.

- [31] Frost & Sullivan. An Assessment on the Future of Carbon Nanotubes -- Strategic Analysis of the Market & Potential. June 2004.
- [32] Carbon Nanotubes Inc. Online store, [http://www.cnanotech.com/pages/store/6-0\\_online\\_store.html](http://www.cnanotech.com/pages/store/6-0_online_store.html) Access date July 27, 2005.
- [33] Nanotechnology Now. Nanotube surveys, *Disruptive Technology Series*. <http://www.nanotech-now.com/nanotube-survey-april2003.htm> Last update date November 3, 2004. Access date August 3, 2005.
- [34] S. Thomke and E. von Hippel. Customers as innovators: A new way to create value. *Harvard Business Review*, 80(4):74, 2002.
- [35] Thomas Swan & Co. Ltd. Manufacturing carbon nanotubes on a commercial scale – A novel material with remarkable potential. *Company presentation*, 2005.
- [36] Nantero. <http://nantero.com/> Access date August 3, 2005.
- [37] FastCompany. 38. From lab to fab, 2005. *4<sup>th</sup> Annual Fast 50*, [http://www.fastcompany.com/fast50\\_05/winners/38.html](http://www.fastcompany.com/fast50_05/winners/38.html) Access date August 3, 2005.
- [38] Carbon Nanotechnologies Inc. About CNI - Cooperative research, 2005. [http://www.cnanotech.com/pages/about/4-3\\_cooperative.html](http://www.cnanotech.com/pages/about/4-3_cooperative.html) Access date August 4, 2005.
- [39] Entegris Inc. Carbon nanotechnologies and Entegris sign joint development agreement, May 17, 2004 2005. <http://www.entegris.com/pressroom/pr/pr2004/pr51704.html> Last update date May 17, 2004. Access date August 4, 2005.
- [40] Business Wire. Carbon nanotechnologies Inc. and 3P Inc. to develop advanced polymer products. <http://www.businesswire.com> Last update date May 28, 2003. Access date August 4, 2005.
- [41] Composites News Supersite. <http://neo.compositesnews.com/cni.asp?ArticleID=2531> Last update date Jan 28, 2003. Access date August 4, 2005.
- [42] Carbon Nanotechnologies Inc. Buckytube resources & news -- Archived press releases, Feb 15, 2005 2005. <http://www.cnanotech.com> Last update date February 15, 2005. Access date August 4, 2005.
- [43] SmallTimes. Company profile: Southwest Nanotechnologies. [http://www.smalltimes.com/document\\_display.cfm?document\\_id=9508](http://www.smalltimes.com/document_display.cfm?document_id=9508) Last update date July 13, 2005. Access date August 4, 2005.

- [44] Applied nanotech and southwest nanotechnologies partner to optimize single wall carbon nanotubes for flat panel display screens. <http://www.voyle.net/Nano%20Biz/NanoBiz-2004-0051.htm> *Last update date* June 21, 2004. *Access date* August 4, 2005.
- [45] G. Oger. French firm hopes to get pr bounce out of nanotubes in tennis rackets. [http://www.smalltimes.com/document\\_display.cfm?document\\_id=2506](http://www.smalltimes.com/document_display.cfm?document_id=2506) *Last update date* November 7, 2001. *Access date* August 4, 2005.
- [46] Tennis Warehouse. Babolat NCT nanotube racquets. <http://www.tennis-warehouse.com/BabolatRacquets.html> *Access date* August 5, 2005.
- [47] Nanocyl. Nanocyl moving from university spin-off to semi-industrial company. <http://www.nanocyl.com/press/pdf/13.pdf> *Last update date* May 4, 2005. *Access date* August 5, 2005.
- [48] Small Times. Nanocyl raises \$3.7 million. <http://www.smalltimes.com> *Last update date* Sept. 30, 2004 . *Access date* August 5, 2005.
- [49] Nanocyl. Nanocyl – Profiles – Technologies. <http://www.nanocyl.com/profiles/technologies.php> *Access date* August 5, 2005.
- [50] Azonano. Researchers produce supercapacitors from carbon nanotubes. <http://www.azonano.com/details.asp?ArticleID=848> *Last update date* Apr 13, 2004. *Access date* August 8, 2005.
- [51] S. Sengupta. Personal communication, July 25, 2005.
- [52] R. Bley. Personal communication, July 25, 2005.
- [53] J. Pierce. Personal communication, July 25, 2005.
- [54] NanoMarkets. Carbon nanotube electronics – A technology analysis and market forecast. Technical report, NanoMarkets LC, May 4, 2005.
- [55] J. U. Lee. Survey response, July 28, 2005.
- [56] Azonano. Infineon demonstrates carbon nanotube transistors for power applications. <http://www.azonano.com/details.asp?ArticleID=543> *Last update date* Feb 23, 2004. *Access date* August 8, 2005.
- [57] NEC. Tests verify carbon nanotube enable ultra high performance transistor. <http://www.nec.co.jp/press/en/0309/1901.html> *Last update date* September 19, 2003. *Access date* August 8, 2005.
- [58] Zyvex. <http://www.zyvex.com> *Access date* August 8, 2005.
- [59] T. Cleveland. Personal communication, July 25, 2005.

- [60] P. J. H. Schoemaker. Scenario planning: A tool for strategic thinking. *MIT Sloan Management Review*, Winter 1995(36):25–40, 1995.
- [61] A. Mnyusiwalla, D. A. S., and S. P. A. ‘Mind the gap’: Science and ethics in nanotechnology. *Nanotechnology*, 14(3):R9–R13, 2003.
- [62] A. Aston. Nanotech: Beyond the hype – and fear. *BusinessWeek online*, May 6, 2004.
- [63] J. B. Howard. Personal communication, Aug 1, 2005.
- [64] NanoInvestorNews. Nanoinvestornews: Nanotechnology facts and figures. [http://www.nanoinvestornews.com/modules.php?name=Facts\\_Figures](http://www.nanoinvestornews.com/modules.php?name=Facts_Figures) *Access date* August 9, 2005.
- [65] S.-G. Kim. Personal communication, July 8, 2005.
- [66] Nanotubes for the composites market. Technical report, Cientifica, 2005.
- [67] Business Communications Company, Inc. GB-245 nanotubes: Directions and technologies. [http://www.mindbranch.com/products/N2-015\\_toc.html](http://www.mindbranch.com/products/N2-015_toc.html) *Last update date* November 2000. *Access date* August 9, 2005.
- [68] M. J. Height, J. B. Howard, J. W. Tester, and J. B. Vander Sande. Flame synthesis of single-walled carbon nanotubes. *Carbon*, 42:2295–2307, 2004.
- [69] M. J. Height, J. B. Howard, J. W. Tester, and J. B. Vander Sande. Carbon nanotube formation and growth via particle-particle interaction. *Journal of Physical Chemistry B*, 109(25):12337–12346, 2005.
- [70] S. E. Bodily and S. M. Allen. A dialogue process for choosing value-creating strategies. *Interfaces*, 29(6):16–28, 1999.
- [71] H. Richter. Personal communication, 2005.
- [72] G. Saloner, A. Shepard, and J. Podolny. *Strategic Management*. John Wiley & Sons, New York, 2001.
- [73] Energy Information Administration (EIA). Natural gas weekly update, *Department of Energy, US Government*. <http://tonto.eia.doe.gov/oog/info/ngw/ngupdate.asp> *Access date* August 10, 2005.
- [74] V. Ganapathy. Simplified combustion calculations for air or gas turbine exhaust. <http://vganapathy.tripod.com/combust.html> *Access date* August 10, 2005.
- [75] M. A. Cusumano. Software entrepreneurship: Essential elements of a successful start-up. In *The Business of Software – What Every Manager, Programmer, and Entrepreneur Must Know to Thrive and Survive in Good Times and Bad*. Free Press, New York, 2004.
- [76] J. Wen. Personal communication, 2005.